이학석사 학위논문

Two new maniraptorans (Dinosauria: Theropoda) from the Nemegt Formation (early Maastrichtian) of Mongolia

몽골의 네메겟층(마스트리히트세)에서 산출된 두 마니랍토라류(공룡류: 수각아목)에 대한 보고

2018년 8월

서울대학교 대학원

지구환경과학부

이 성 진

ABSTRACT

Maniraptorans are a diverse group of highly derived theropod dinosaurs which incorporate modern birds. Despite their current high diversity, fossil records are not as numerous. Nevertheless, new maniraptoran fossils from the Mesozoic have revolutionized our understandings of this group. In the Cretaceous, as each major maniraptoran clade diversifies, numerous taxa appeared around the world. The Gobi Desert is home to various dinosaurs including maniraptorans in this period and has opened a new chapter in the study of Asian dinosaurs. In 2008, an international team of the Korea-Mongolia International Dinosaur Expedition (KID) discovered a theropod assemblage that incorporated two specimens (MPC-D 102/111 and MPC-D 100/203) of new maniraptorans from the Nemegt Formation at Altan Uul III, southern Gobi Desert in Ömnögovi Province, Mongolia. Each of these two maniraptorans was later found to represent a new oviraptorid and a new alvarezsaurid. Both the new oviraptorid, *Gobiraptor minutus* gen. et sp. nov. and the new alvarezsaurid, *Nemegtonykus citus* gen. et sp. nov. are reported in this thesis. During the past few decades, multiple oviraptorids and alvarezsaurids have occurred from the Late Cretaceous formations in Mongolia although only one alvarezsaurid taxon has been known from the Nemegt Formation. Moreover, no oviraptorid or alvarezsaurid taxon has been reported from Altan Uul III although two unnamed oviraptorid specimens have been recorded. Therefore, *Gobiraptor* and *Nemegtonykus* each represents the first oviraptorid and alvarezsaurid taxon, respectively, from Altan Uul III.

In this thesis, both *Gobirator* and *Nemegtonykus* are described and compared to other closely related taxa. The holotype specimen of *Gobiraptor minutus* (MPC-

D 102/111) is a partial skeleton that include both incomplete cranial and postcranial elements. The unique set of characters of *Gobiraptor*, primarily those of the mandible and caudal vertebrae, distinguishes it from other oviraptorids. The most prominent feature of *Gobiraptor* is its massive symphyseal shelf which extends to the weakly developed lingual shelves with small occlusal grooves and ligual ridges. This mandibular structure has not been found in any oviraptorid and therefore suggests that *Gobiraptor* probably had a dietary strategy different from those of other Nemegt oviraptorids. Particularly, *Gobiraptor* is assumed to have an adaptation for crushing hard food such as seeds or mollusks. In addition, thin sections were taken from the mid-shaft of the right femur of *Gobiraptor* specimen and observed under microscopes. The osteohistology of *Gobiraptor* indicates that it was a fast-growing individual which was in an early stage of its ontogeny. A phylogenetic analysis was also performed, and *Gobiraptor* was recovered as a derived oviraptorid that is closer to three oviraptorid taxa from the Ganzhou region in southern China than to the oviraptorids from the Nemegt region. This result supports the hypothesis of an earlier study that a sympatric radiation was not the case for oviraptorids in the Nemegt Basin. The discovery of *Gobiraptor* also debunks previous suggestions that Nemegt oviraptorids preferred dry environments. With *Gobiraptor*, at least three different oviraptorid taxa exist in the Nemegt Formation which has been regarded to be deposited in wet environments. Therefore, it is most likely that Nemegt oviraptorids did not specifically favor arid habitats. As *Gobiraptor* is added to the list of Nemegt oviraptorids by this thesis, the high oviraptorid diversity in the Nemegt Basin is further bolstered.

The holotype specimen of *Nemegtonykus citus* (MPC-D 100/203) consists of incomplete postcranial elements which are partially disarticulated. The overall

morphology of *Nemegtonykus* is comparable to that of other alvarezsaurids, especially parvicursorines. However, *Nemegtonykus* has a unique combination of characters with several autapomorphies of pelvic and hindlimb elements differentiating this taxon from other alvarezsaurids. The gracile and elongate distal hindlimb components of *Nemegtonykus* are typical for parvicursorines that have been generally thought to be able cursors. Interestingly, the femur of *Nemegtonykus* has proportions that are close to that of birds, which could be indicative of a subhorizontal femoral orientation. Together with the morphology of caudal vertebrae, ilium, and hindlimb elements, this suggests that *Nemegtonykus* possibly developed a rudimentary 'knee-driven' locomotion which might resemble that of basal avialans. A separate phylogenetic analysis was also done for *Nemegtonykus*. The result shows that *Nemegtonykus* is a derived mononykin alvarezsaurid and the sister taxon of *Linhenykus* from the Wulansuhai Formation of Inner Mongolia. The relationships among mononykins obtained by the analysis in this study are rather confusing because of the distant relationship between *Nemegtonykus* and *Mononykus*, both of which are from the Nemegt Formation and the sister-taxon relationship between *Mononykus* and *Albertonykus*, the latter of which is from North America. The occurrences of alvarezsaurids in the Nemegt Basin have been strongly biased toward eolian deposits such as the Baruungoyot and Djadochta formations, with only one taxon and specimen from the mesic Nemegt Formation. The presence of *Nemegtonykus*, however, indicates that alvarezsaurids could be as abundant in wet environments as in dry ones. With the addition of *Nemegtonykus*, the number of alvarezsaurid taxa in the Nemegt Basin has become six which is the highest alvarezsaurid diversity in the world.

Keywords: dinosaurs, Maniraptora, Oviraptoridae, Alvarezsauridae, Cretaceous, Nemegt Formation, Gobi Desert, Mongolia

Student Number: 2016-29125

TABLE OF CONTENTS

LIST OF FIGURES

LIST OF TABLES

CHAPTER I

INTRODUCTION

I-1. MANIRAPTORANS FROM THE NEMEGT FORMATION

Maniraptorans are a group of highly derived theropods and include the only extant dinosaur lineage, birds (Fig. 1.1; Gauthier, 1986; Holtz and Osmólska, 2004; Sereno, 2005; Turner et al., 2007). They are generally characterized by having ossified sternal plates, semilunate carpal bones, and backward-pointing pubes (Holtz and Osmólska, 2004) although some extinct clades show the plesiomorphic propubic condition (Holtz and Osmólska, 2004; Osmólska et al., 2004). Maniraptorans, as their name implies, also have specialized hands with varying morphology among clades eventually becoming wings for flight in birds. Compared to modern birds which are represented by at least 9,993 living species (Jetz et al., 2012) or much more 15,845 to 20,470 species (Barrowclough et al., 2016), fossil maniraptorans, especially those of Mesozoic, are very scarce. However, these fossil species are still important because they present a great deal of information on the early evolution of maniraptorans and their biology. In this context, the Cretaceous period deserves profound attention it has been receiving because most of the Mesozoic maniraptoran fossils are from this time frame as a result of diversification of major maniraptoran clades into numerous taxa (Brusatte et al., 2015; Lü and Brusatte, 2015; Lü et al., 2016, 2017).

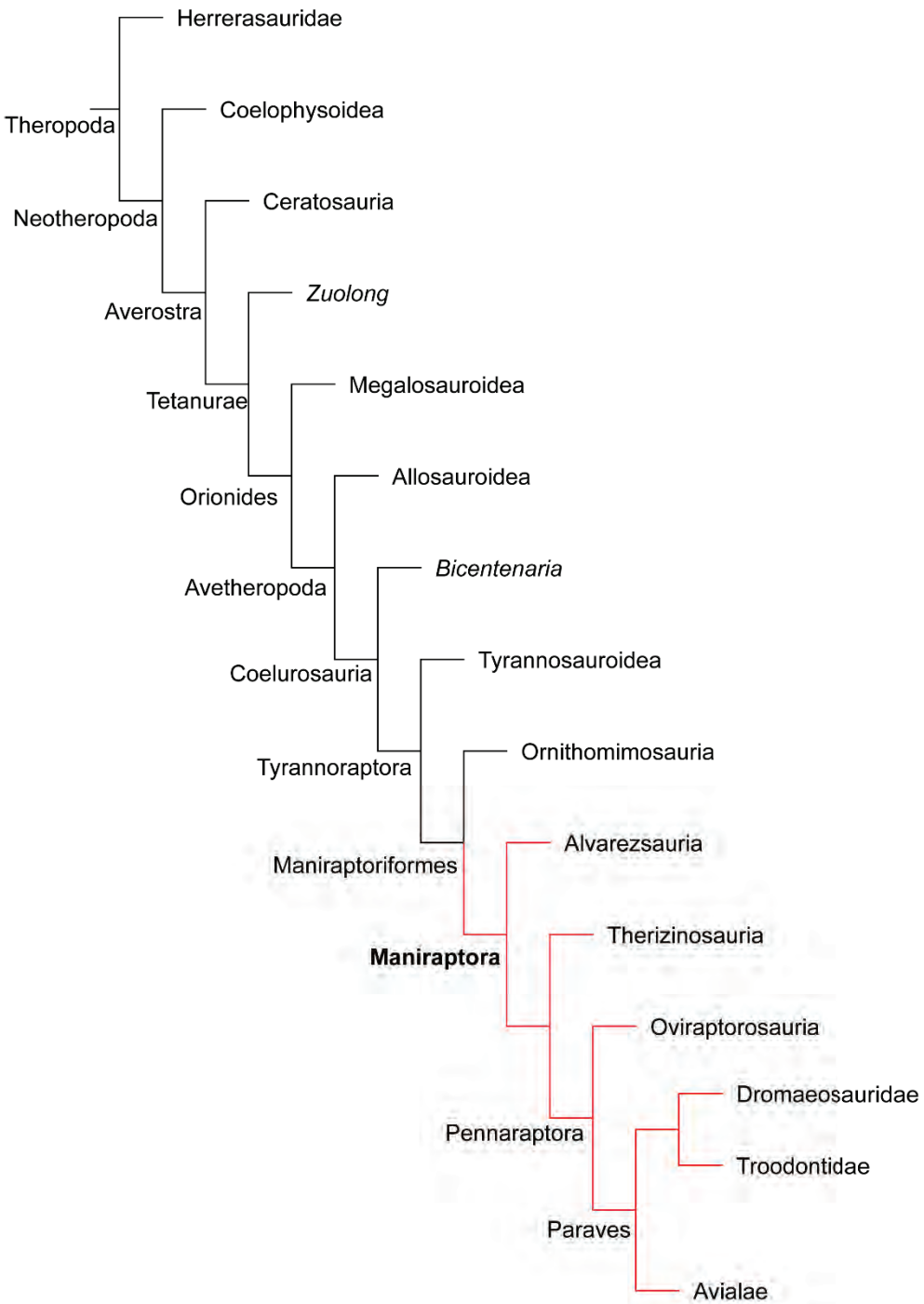

FIGURE 1.1. Simplified phylogenetic tree of Theropoda. Maniraptoran branches are in red.

The Nemegt Formation of Mongolia is an Upper Cretaceous sedimentary formation (see Chapter I-2 for geological setting) which has yielded 16 maniraptorans taxa (Table 1.1). Seventy-five percents of these taxa are non-avialans, and a half of the number of non-avialan taxa are oviraptorosaurs, possibly reflecting their high diversity. *Mononykus olecranus* (Perle et al., 1993) is the sole alvarezsaur from the Nemegt Formation as *Therizinosaurus cheloniformis* (Maleev, 1954; Barsbold, 1976b) is the only therizinosaur in this formation. Among the 6 oviraptorosaurs, two are the species of *Avimimus* (Kurzanov, 1981; Funston et al., 2018a, 2018b). *Elmisaurus rarus* (Osmólska, 1981) is the only caenagnathid if *Nomingia gobiensis* (Barsbold et al., 2000) is an oviraptorid. Definitive oviraptorids from the Nemegt Formation are *Rinchenia mongoliensis* (Barsbold, 1986) and *Nemegtomaia barsboldi* (Lü et al., 2004; Fanti et al., 2012). The number of oviraptorid taxa will increase if the unnamed Guriliin Tsav oviraptorid is indeed a new taxon (Funston et al., 2018a). Dromaeosaurids are scarce in the Nemegt Formation. The one and only dromaeosaurid taxon from this formation is *Adasaurus mongoliensis* (Barsbold, 1983). In contrast, troodontids are relatively diverse with three taxa which are second to oviraptorosaurs in diversity. The troodontids from the Nemegt Formation are *Borogovia gracilicrus* (Osmólska, 1987), *Tochisaurus nemegtensis* (Kurzanov and Osmólska, 1991), and *Zanabazar junior* (Barsbold, 1974; Norell et al., 2009). The rest four maniraptorans are all avialans. Among these birds, *Gurilynia nessovi* (Kurochkin, 1999) is the only enantiornithine. The rest three belong to the clade Ornithurae, but two are hesperornithines and the other is an anseriform being the sole neornithine taxon. The hesperornithines from the Nemegt Formation include *Brodavis mongoliensis*

(Martin et al., 2012) and *Judinornis nogontsavensis* (Nessov and Borkin, 1983; Kurochkin, 2000), the former also being a member of the family Brodavidae. The anseriform bird is *Teviornis gobiensis* (Kurochkin et al., 2002) which has been further classified as a presbyornithid.

The primary purpose of this thesis is to provide detailed descriptions of two new maniraptorans from the Nemegt Formation. These two novel taxa are an oviraptorid and an alvarezsaurid, both of which were found and collected from the Nemegt Formation in Altan Uul III, southern Gobi Desert, Mongolia during the Korea-Mongolia International Dinosaur Expedition (KID) in 2008 (Fig. 1.2). They were associated with each other and with other oviraptorid and alvarezsaurid specimens of different individuals at the same site. However, as a result of extensive preparation work, it was revealed that only two specimens preserved enough anatomical traits to be properly diagnosed as new taxa. These two specimens were examined and analyzed with other taxa via a computer program to investigate their phylogenetic positions. In case of the oviraptorid specimen, the osteohistology of femoral growth was studied in order to ascertain its ontogenetic stage. Based on their osteology and results of phylogenetic analyses, the functional morphology, paleobiology, paleoecology, and systematics are discussed for each new taxon in two separate chapters (see Chapters II and III). As this thesis adds two new maniraptorans, the diversity of the clade Maniraptora in the Nemegt Formation is increased to 18 total taxa.

TABLE 1.1. List of the maniraptorans from the Nemegt Formation.

Taxon	Affinity	Locality	References
Mononykus olecranus	Alvarezsauridae	Bugiin Tsav	Perle et al., 1993
Therizinosaurus cheloniformis	Therizinosauridae	White Beds of Hermiin Tsav	Maleev, 1954; Barsbold, 1976b
Avimimus portentosus	Avimimidae	Bugiin Tsav, Altan Uul II, and Nemegt	Kurzanov, 1981; Funston et al., 2018a
Avimumus nemegtensis			
Elmisaurus rarus	Caenagnathidae	Hermiin Tsav, Altan Uul II, and Nemegt	Osmólska, 1981
Nemegtomaia barsboldi	Oviraptoridae	Nemegt	Lü et al., 2004; Fanti et al., 2012
Rinchenia mongoliensis	Oviraptoridae	Altan Uul II	Barsbold, 1986
Nomingia gobiensis	Oviraptoridae or Caenagnathidae	Bugiin Tsav and Nemegt	Barsbold et al., 2000
Adasaurus mongoliensis	Dromaeosauridae	Bugiin Tsav	Barsbold, 1983
Borogovia gracilicrus	Troodontidae	Altan Uul IV	Osmólska, 1987
Tochisaurus nemegtensis	Troodontidae	Nemegt	Kurzanov and Osmólska, 1991
Zanabazar junior	Troodontidae	Bugiin Tsav	Barsbold, 1974; Norell et al., 2009
Gurilynia nessovi	Enantiornithes	Guriliin Tsav	Kurochkin, 1999
Brodavis mongoliensis	Brodavidae	Bugiin Tsav	Martin et al., 2012
Judinornis nogontsavensis	Hesperornithes	Nogoon Tsav	Nessov and Borkin, 1983; Kurochkin, 2000
Teviornis gobiensis	Presbyornithidae	Guriliin Tsav	Kurochkin et al., 2002
Gobiraptor minutus gen. et sp. nov.	Oviraptoridae	Altan Uul III	This study
Nemegtonykus citus gen. et sp. nov.	Alvarezsauridae	Altan Uul III	This study

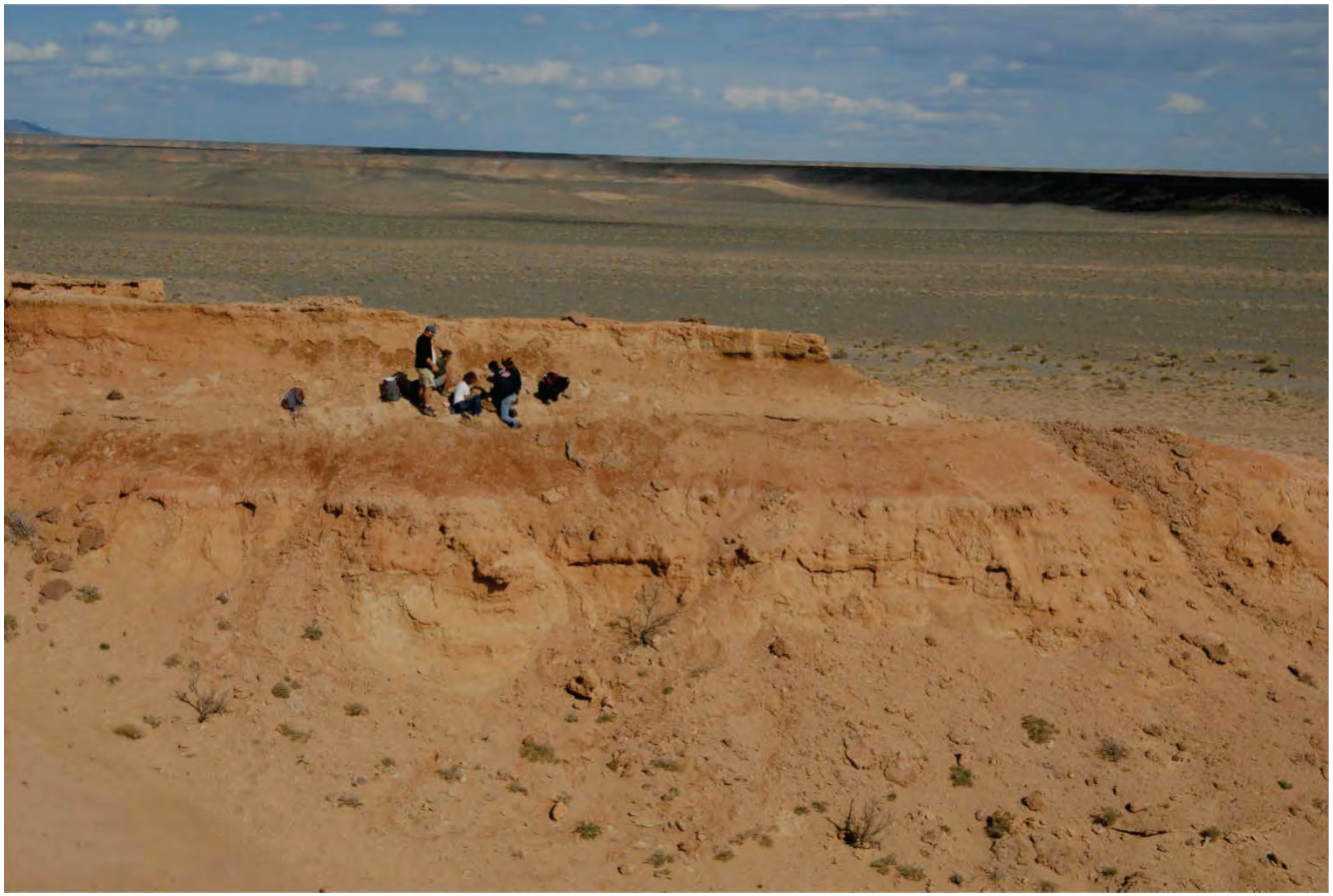

FIGURE 1.2. Photograph of the site where the two specimens (MPC-D 102/111 and MPC-D 100/203) in this study were found and collected.

I-2. GEOLOGICAL SETTING

The Gobi Desert is the largest desert in Asia and covers the southern part of Mongolia and northernmost part of China (Fig. 1.3). The Gobi Desert is also known as one of the dinosaur-rich places in the world. The locality where the two specimens described in this thesis are also from the Gobi, specifically Altan Uul III in the southern part of this desert. There are many sedimentary formations in the Gobi Desert including Upper Cretaceous ones with a great number of vertebrate fossils. The Nemegt Formation is the uppermost one of the three major Upper Cretaceous formations located in the Nemegt Basin, southern Gobi Desert in Ömnögovi Province, Mongolia (Gradzínski et al., 1968, 1977; Gradzínski, 1970). One of the other two formations in the Nemegt Basin is the Baruungoyot Formation which underlies or sometimes interfingers with the Nemegt Formation (Gradzínski and Jerzykiewicz, 1974a, 1974b; Gradzínski et al., 1977; Jerzykiewicz, 2000; Eberth, Badamgarav, et al., 2009; Fanti et al., 2012; Eberth, 2018). The age of the Nemegt Formation has been estimated to be Campanian to early Maastrichtian (Gradzínski et al., 1968, 1977; Gradzínski, 1970), but the Maastrichtian age is generally accepted (Jerzykiewicz and Russell, 1991; Khand et al., 2000; Eberth, 2018). Another Upper Cretaceous formation in the southern Gobi Desert, the Djadochta Formation, lies east to the other two formations and has been considered slightly older than the other two formations (Gradzínski et al., 1968, 1977; Lefeld, 1971; Jerzykiewicz and Russell, 1991; Dashzeveg et al., 2005; Dingus et al., 2008). The Nemegt Formation was formed by alluvial plain deposits dominated by river channel sediments and thus represents a mesic environment

with seasonally wet-dry conditions in the lower part (Gradzínski, 1970; Gradzínski et al., 1977; Eberth, Badamgarav, et al., 2009; Eberth, 2018). The Nemegt Formation is therefore different from the closely located Baruungoyot and Djadochhta formations both of which have been interpreted to represent xeric environments (Lefeld, 1971; Gradzínski and Jerzykiewicz, 1974a, 1974b; Gradzínski et al., 1977; Dashzeveg et al., 2005; Eberth, Badamgarav, et al., 2009; Eberth, 2018). In previous studies, each locality of the Nemegt Formation has been described (Gradzínski et al., 1968, 1977; Gradzínski, 1970; Eberth et al., 2009a; Watabe et al., 2010; Eberth, 2018) and correlated (Eberth, Badamgarav, et al., 2009; Eberth, 2018) in detail. Altan Uul (also called Altan Ula) III is a part of the Altan Uul area and bounds Altan Uul II and IV to the east and west, respectively (Gradzínski et al., 1968, 1977; Gradzínski, 1970; Watabe et al., 2010; Eberth, 2018). According to Eberth (2018), the Altan Uul area is exclusively composed of the Nemegt Formation, not showing any exposure of the Baruungoyot Formation but covers most of the stratigraphic zones of the Nemegt Formation. The sedimentation of the Altan Uul area consists of sand- and mudstone layers that are, for the most part, lightly colored with red and brown (Watabe et al., 2010; Eberth, 2018). Altan Uul III is much less exposed than Altan Uul II or IV and corresponds to the lowermost part of the middle Nemegt Formation and the upper section of the lower Nemegt Formation (Eberth, 2018). Altan Uul III also correlates with the lower beds of Altan Uul II and the upper beds of Altan Uul IV, bridging the two beds (Eberth, 2018). Relatively few dinosaur fossils have been reported from Altan Uul III: two oviraptorosaurs; one ankylosaur; six tyrannosaurs; one hadrosaur; five ornithomimids; and two sauropods (Funston et al., 2018b). The two new

maniraptorans and associated other fragmentary specimens indicate that the dinosaur fauna in Altan Uul III were diverse and less biased against small-sized dinosaurs.

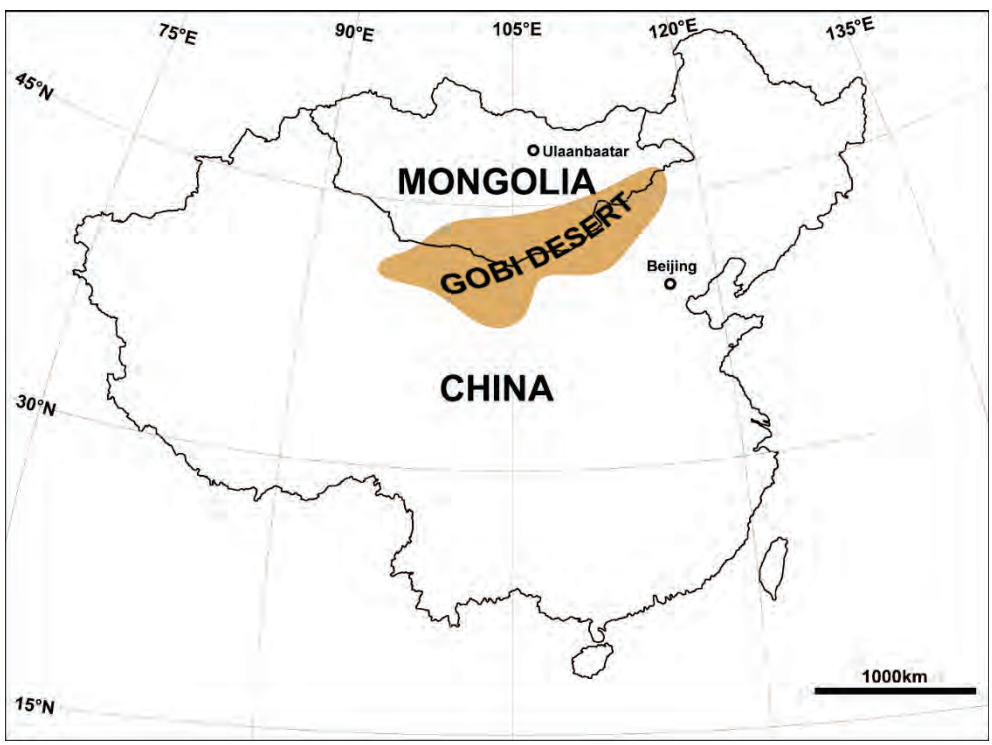

FIGURE 1.3. Map of Mongolia and China depicting the location of the Gobi Desert.

CHAPTER II

A NEW OVIRAPTORID DINOSAUR *GOBIRAPTOR MINUTUS* GEN. ET SP. NOV.

II-1. INTRODUCTION

Oviraptorosauria is an unusual group of maniraptoran theropods with distinctive anatomical characters such as a deep and short skull, edentulous jaws in derived forms, a short tail, and pneumatized proximal caudal vertebrae (Barsbold, 1976a; Barsbold et al., 2000; Maryańska et al., 2002; Osmólska et al., 2004). The origin of oviraptorosaurs is generally assumed to be from Asia based on their earliest records from the Lower Cretaceous Yixian Formation of China (Ji et al., 1998, 2012; Xu et al., 2002). Derived forms mostly appeared in the Late Cretaceous (Osmólska et al., 2004; Funston and Currie, 2016) when they dispersed throughout Asia and North America (Makovicky and Sues, 1998; Funston et al., 2018a). Within the clade Oviraptorosauria, three derived families have been recognized: the Avimimidae (Kurzanov, 1981), Caenagnathidae (Sternberg, 1940), and Oviraptoridae (Barsbold, 1976a). Avimimids are comprised of a single genus that includes two species from the Nemegt Formation of Mongolia (Kurzanov, 1981; Funston, Currie, Eberth, et al., 2016; Funston et al., 2018a) while caenagnathids and oviraptorids show high level of diversity that has especially been bolstered by recent discoveries from the Nanxiong Formation of the Ganzhou region in southern China (Xu and Han, 2010; Lü, Yi, et al., 2013; Wang et al.,

2013; Wei et al., 2013; Lü et al., 2015, 2016, 2017). Interestingly, oviraptorids are restricted to Asia although they are more diverse than caenagnathids which are reported from both Asia and North America (Funston and Currie, 2016; Funston et al., 2018a; see also Table 2.1 for the full list of oviraptorid taxa). However, most of the caenagnathids are represented by fragmentary materials (Gilmore, 1924; Sternberg, 1940; Currie, 1989; Currie et al., 1993, 2016; Zanno and Sampson, 2005; Sullivan et al., 2011; Longrich et al., 2013; Funston and Currie, 2014; Bell et al., 2015; Funston et al., 2015; Tsuihiji et al., 2015, 2016; Yao et al., 2015; Funston, Currie and Burns, 2016; Yu et al., 2018) with only a few exceptions (Makovicky and Sues, 1998; Xu et al., 2007; Lamanna et al., 2014; Funston and Currie, 2016) compared to the numerous nearly complete skeletons of oviraptorids (Clark et al., 2001; Lü, 2002; Osmólska et al., 2004; Lü, Currie, et al., 2013; Xu, Tan, et al., 2013; Lü et al., 2016, 2017; Norell et al., 2018).

Although the Nanxiong Formation is the most productive formation with regard to the number of oviraptorid taxa (Lü et al., 2017), the Gobi Desert of Mongolia, including the classic Nemegt locality, has also yielded abundant oviraptorids (Osborn, 1924; Barsbold, 1976a, 1981, 1983, 1986; Norell et al., 1994, 1995, 2018; Barsbold et al., 2000; Clark et al., 2001; Lü et al., 2004; Osmólska et al., 2004; Weishampel et al., 2008; Fanti et al., 2012). Despite this high diversity, oviraptorid occurrences have been relatively rare in the Altan Uul area (Funston et al., 2018a, 2018b). In 2008, an oviraptorid specimen was found along with other theropod skeletons during the Korea-Mongolia International Dinosaur Expedition (KID) from the Nemegt Formation of Altan Uul III, Mongolia (Fig. 2.1). The specimen is described here as a new oviraptorid taxon, *Gobiraptor minutus* gen. et sp. nov., which

TABLE 2.1. List of oviraptorids.

Taxon	Country	Formation	Locality	Age	References
Machairasaurus leptonychus	China	Wulansuhai (Bayan Mandahu) Formation	Bayan Mandahu	Campanian	Longrich and Currie, 2010
Wulatelong gobiensis	China	Wulansuhai (Bayan Mandahu) Formation	Bayan Mandahu	Campanian	Xu, Tan, et al., 2013
Yulong mini	China	Qiupa Formation	Qiupa Town, Luanchuan County, Henan Province	Late Cretaceous	Lü, Currie, et al., 2013
Nankangia jiangxiensis	China	Nanxiong Formation	Longling, Nankang District, Ganzhou City, Jiangxi Province	Campanian-Maastrichtian	Lü, Yi, et al., 2013
Jiangxisaurus ganzhouensis	China	Nanxiong Formation	Longling, Nankang District, Ganzhou City, Jiangxi Province	Campanian-Maastrichtian	Wei et al., 2013

Taxon	Country	Formation	Locality	Age	References
Huanansaurus ganzhouensis	China	Nanxiong Formation	Vicinity of the Ganzhou Railway Station, Ganzhou City, Jiangxi Province	Campanian-Maastrichtian	Lü et al., 2015
Corythoraptor jacobsi	China	Nanxiong Formation	Vicinity of the Ganzhou Railway Station, Ganzhou City, Jiangxi Province	Campanian-Maastrichtian	Lü et al., 2017
Banji long	China	Nanxiong Formation	Hongcheng Basin, near Ganzhou City, Jiangxi Province	Campanian-Maastrichtian	Xu and Han, 2010
Tongtianlong limosus	China	Nanxiong Formation	The building site of the No. 3 high school of Ganxian District, Ganzhou City, Jiangxi Province	Campanian-Maastrichtian	Lü et al., 2016
Ganzhousaurus nankangensis	China	Nanxiong Formation	Nankang District, Ganzhou City, Jiangxi Province	Campanian-Maastrichtian	Wang et al., 2013
Shixinggia oblita	China	Pingling Formation	Luyuan, Shixing County, Guangdong Province	Maastrichtian	Lü and Zhang, 2005

Taxon	Country	Formation	Locality	Age	References
Heyuannia huangi	China	Dalangshan Formation	Huangsha village, Heyuan City, Guangdong Province	?Maastrichtian	Lü, 2002
Oviraptor philoceratops	Mongolia	Djadochta Formation	Bayn Dzak	Campanian	Osborn, 1924
Khaan mckennai	Mongolia	Djadochta Formation	Ukhaa Tolgod	Campanian	Clark et al., 2001
Citipati osmolskae	Mongolia	Djadochta Formation	Ukhaa Tolgod	Campanian	Clark et al., 2001
Zamyn Khondt oviraptorid (*Citipati* sp.)	Mongolia	Djadochta Formation	Zamyn Khondt	Campanian	Osmólska et al., 2004
Heyuannia yanshini (= "*Ingenia*" *yanshini*)	Mongolia	Baruungoyot Formation	Red Beds of Hermiin Tsav	Campanian-Maastrichtian	Barsbold, 1981

Taxon	Country	Formation	Locality	Age	References
Conchoraptor gracilis	Mongolia	Baruungoyot Formation	Red Beds of Hermiin Tsav	Campanian-Maastrichtian	Barsbold, 1986
cf. Conchoraptor	Mongolia	Baruungoyot Formation	Khulsan	Campanian-Maastrichtian	Longrich and Currie, 2010
Nemegtomaia barsboldi	Mongolia	Baruungoyot and Nemegt Formations	Nemegt	Campanian-Maastrichtian	Lü et al., 2004, 2005
Nomingia gobiensis	Mongolia	Nemegt Formation	Bugiin Tsav	Maastrichtian	Barsbold et al., 2000
Unnamed Guriliin Tsav oviraptorid	Mongolia	Nemegt Formation	Guriliin Tsav	Maastrichtian	Funston et al., 2018a
Rinchenia mongoliensis	Mongolia	Nemegt Formation	Altan Uul II	Maastrichtian	Barsbold, 1986
Gobiraptor minutus gen. et sp. nov.	Mongolia	Nemegt Formation	Altan Uul III	Maastrichtian	This study

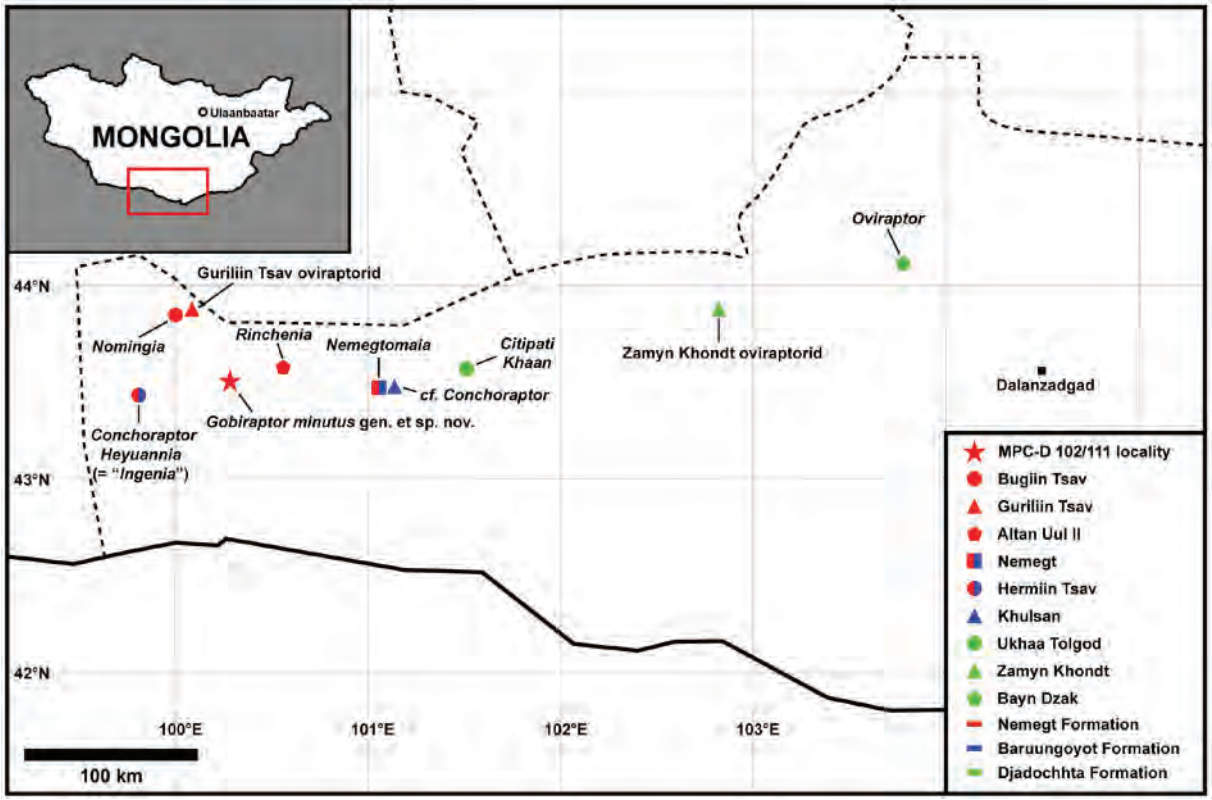

FIGURE 2.1. Map showing the occurrences of oviraptorids in the southern Gobi Desert of Mongolia. The magnified map was generated using Simplemappr (www.simplemappr.net) before modified.

is mainly characterized by its peculiar mandibular morphology. *Gobiraptor minutus* increases the diversity of oviraptorids in the Nemegt Formation and together with the unnamed Guriliin Tsav oviraptorid (Funston et al., 2018a) that may represent a new taxon, shows that oviraptorids were exceptionally diverse in this region. Additionally, the discovery of *Gobiraptor minutus* provides valuable insight into the evolution and dietary adaptations of the Nemegt oviraptorids and their abundance in a mesic environment.

II-2. METHODS

Fossil Preparation and Image Creation

The holotype specimen of *Gobiraptor minutus* gen. et sp. nov. (MPC-D 102/111) was in and around two massive blocks of matrix separated from the sandstone layer (see Chapter I-2 for geological setting) when they were excavated. The two blocks were wrapped with plaster bandages (Gypsona®) before transportation. One of the blocks was partially prepared in a fossil prepatarion laboratory of Hwaseong City, Gyeonggi Province, Korea. It and the other block were later transferred to Seoul National University (SNU) for additional preparation. From the earlier preparation, the rostral part of the lower jaw, sacral and caudal vertebrae, fragments of ilia, right femur, and left tarsometatarsus as well as other theropod skeletons were recovered, and some of them were further prepared in the Paleontological Laboratory of SNU. The rest of the elements of MPC-D 102/111 were discovered through the later preparation which also involved preparation of all the materials of the two specimens (MPC-D 102/111 and MPC-D 100/203). This later process required almost a year to be finished. Several preparation tools (Fig. 2.2) and adhesives (Fig. 2.3) were utilized during the preparation. These include an air compressor (S30-40-3 from Seowon Compressor), airscribes (ME-9100 from PaleoTools® and Micro Jack 6 with short and long styli from PaleoTools®), fossil preparation adhesive (PB 40 from PaleoBOND®), fossil repair epoxy putty (PaleoPoxy from PaleoBOND®), acetone (from Kanto Chemical), polyvinyl acetate (PVA B-15 beads from Black Hills Institute of Geological Research), instant adhesive (Loctite 401 from Henkel), and

wood glue (Carpenter's Wood Glue Max® from Elmer's). The matrix was removed from each fossil element (Micro Jack 6 was used for delicate work while removal of thick matrix was done with ME-9100), and broken pieces were assembled and glued when possible. Fragile elements were reinforced by polyvinyl acetate. The epoxy putty was applied to stabilize fossils which were missing too much of their parts to maintain firmness. The earlier preparation work was carried out in a similar fashion.

Nikon D300 digital camera was used for taking photographs of specimens. Adobe Photoshop CC 2018 and Adobe Illustrator CC 2018 were utilized for image creation.

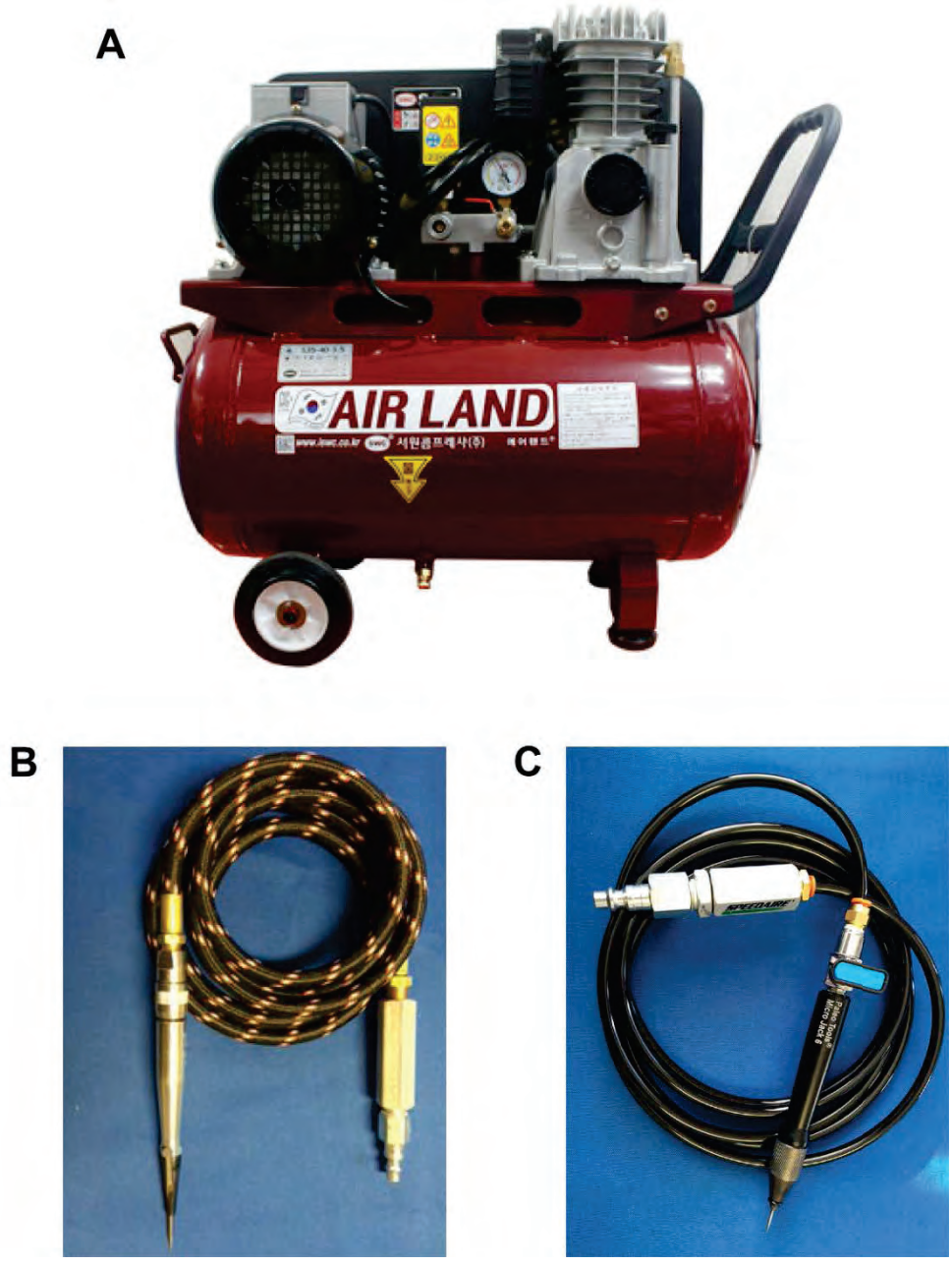

FIGURE 2.2. Tools used for preparation of the two specimens (MPC-D 102/111 and MPC-D 100/203) in this study. **A**, S30-40-3 from Seowon Compressor; **B**, ME-9100 from PaleoTools®; **C**, Micro Jack 6 from PaleoTools®. Not to scale.

FIGURE 2.3. Adhesives and chemicals used for preparation of the two specimens (MPC-D 102/111 and MPC-D 100/203) in this study. **A**, PB 40 from PaleoBOND®; **B**, PaleoPoxy from PaleoBOND®; **C**, acetone from Kanto Chemical; **D**, PVA B-15 beads from Black Hills Institute of Geological Research; **E**, Loctite 401 from Henkel; **F**, Carpenter's Wood Glue Max® from Elmer's. Not to scale.

Phylogenetic Analysis

A phylogenetic analysis was performed to obtain the position of *Gobiraptor minutus* within the clade Oviraptorosauria. The character list and data matrix used in this study were modified from that of Lü et al. (2017). The modifications include the following: unordering five ordered characters (82, 89, 183, 196, and 207) as suggested by Funston and Currie (2016); correcting an error in the data matrix of *Yulong mini* (character state 102:2 to 102:1); changing the name of *Ingenia yanshini* to *Heyuannia yanshini* following Funston et al. (2018a); changing the character states of *Gigantoraptor erlianensis* (195:0 to 195:1) and *H. yanshini* (94:1 to 94:0) based on the anatomical descriptions of each of these two species in Ma et al. (2017) and Funston et al. (2018a), respectively; combining *Caenagnathus sternbergi*, *Macrophalangia canadensis*, and *Chirostenotes pergracilis* as well as Alberta dentary morph 3 and *Leptorhynchos elegans* replacing *Elmisaurus elegans* following Funston and Currie (2016); removal of *Ojoraptorsaurus boerei* also following Funston and Currie (2016); adapting the updated data matrices of *Caenagnathus collinsi*, *Caenagnathasia martinsoni*, *Elmisaurus rarus*, and *L. elegans* in Funston and Currie (2016); incorporation of *G. minutus* to the data matrix. Including *G. minutus*, 42 taxa with 257 characters were analyzed in TNT version 1.5 (Goloboff and Catalano, 2016). An identical traditional search with the one in Lü et al. (2017) (Wagner trees; swapping algorithm: tree bisection-reconnection; random seeds: 1,000; replicates: 1,000; trees to save per replication: 10) was run, and 24 most parsimonious trees (MPTs) with 652 steps were produced (consistency index [CI]: 0.448, retention index [RI]: 0.647). The 'Bremer.run' script was used in TNT (Goloboff and Catalano, 2016) to calculate the Bremer support values on each node

of the strict consensus tree of the 24 MPTs. The tree data were then transferred to Winclada version 1.00.08 (Nixon, 2002) to generate the tree image.

Osteohistological Examination

A piece from the mid-shaft of the right femur was sampled and embedded in a polyester resin. Two histological thin sections (30 microns and 25 microns) were prepared following standard petrographic techniques (Chinsamy-Turan, 2005). The thin sections were studied under a Nikon E200 and a Zeis AXIO petrographic microscope, Photomicrographs were taken with a Nikon camera using NIS elements (version 4). Terminology used for the histological descriptions are *sensu* Chinsamy-Turan (2005).

II-3. RESULTS

SYSTEMATIC PALEONTOLOGY

DINOSAURIA Owen, 1842

THEROPODA Marsh, 1881

MANIRAPTORA Gauthier, 1986

OVIRAPTOROSAURIA Barsbold, 1976

OVIRAPTORIDAE Barsbold, 1976

GOBIRAPTOR MINUTUS GEN. ET SP. NOV.

(Figs. 2.4-22)

Holotype—MPC-D 102/111, incomplete cranial and postcranial elements including both partial premaxillae and maxillae, fragmentary right jugal, fused vomer, incomplete both pterygoids and ectopterygoids, incomplete right palatine, partial left postorbital, partial right quadrate and quadratojugal, incomplete lower jaw, the last sacral vertebra which is articulated with the two proximalmost caudal vertebrae, articulated but incomplete proximal caudal vertebrae, fragmentary chevrons, partial right scapula and humerus, incomplete pelvic girdles, nearly complete both femora, complete left metatarsus with distal tarsals 3 and 4, incomplete left pedal digits I, III, and IV, and several unidentified fragmentary elements. MPC-D 102/111 was also found with other theropod skeletons including postcranial elements of alvarezsaurids and larger oviraptorid remains.

Type locality and horizon—Altan Uul III (Gradziński et al., 1968, 1977;

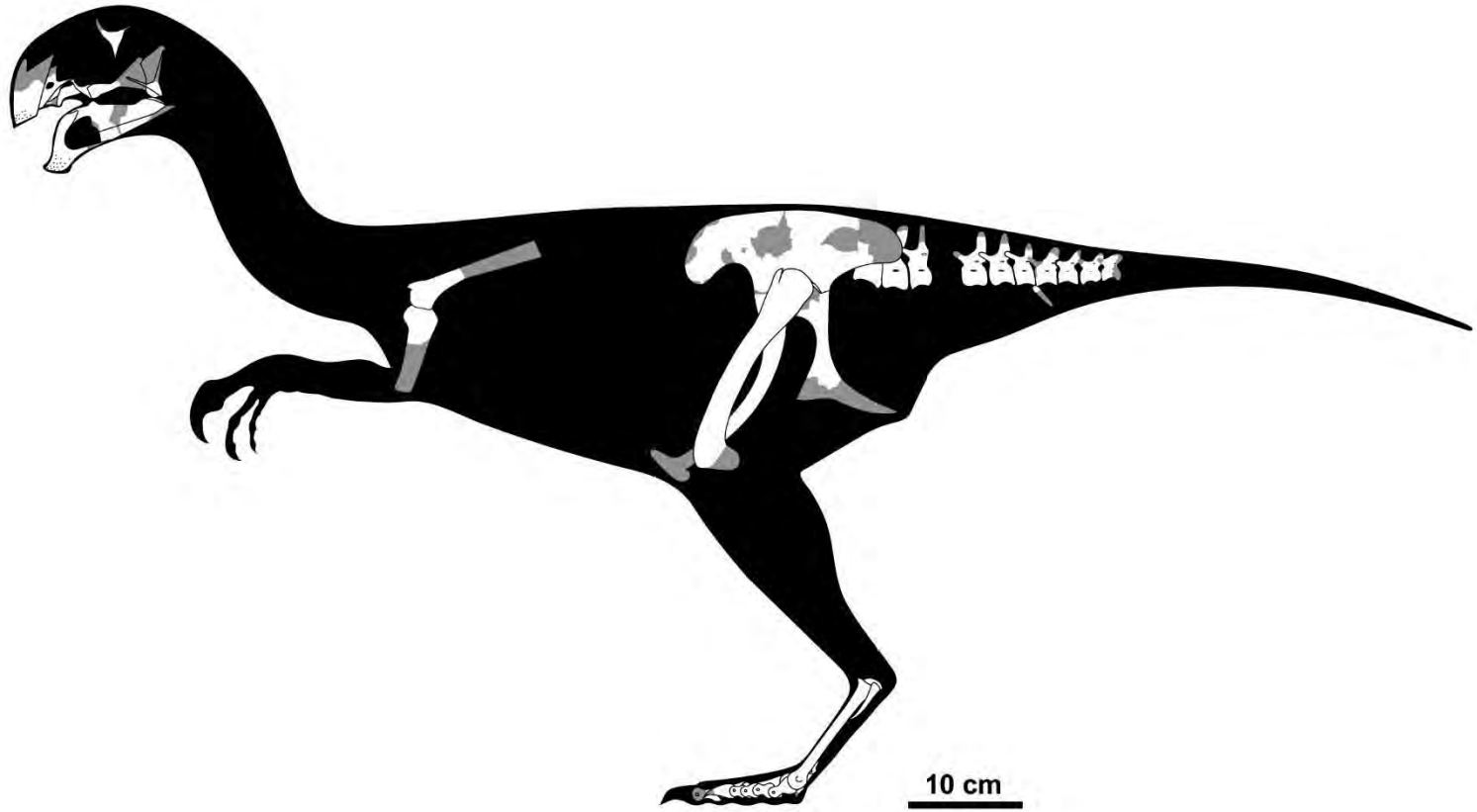

FIGURE 2.4. Skeletal and silhouette reconstruction of *Gobiraptor minutus* gen. et sp. nov. Missing parts in gray.

Gradziński, 1970; Watabe et al., 2010; Eberth, 2018), Ömnögovi Province, Mongolia (Fig. 2.1). Upper Cretaceous Nemegt Formation (Gradziński et al., 1968, 1977; Gradziński, 1970; Jerzykiewicz and Russell, 1991; Khand et al., 2000; Eberth, 2018).

Etymology—The generic name *Gobiraptor* is a combination of 'Gobi' which refers to the Gobi Desert where the holotype specimen was found and 'raptor' which is Latin for thief. The specific name '*minutus'* is Latin for small and refers to the small size of the holotype specimen.

Diagnosis—*Gobiraptor minutus* is an oviraptorid dinosaur diagnosed by the following unique set of characteristics (autapomorphies are marked with an asterisk): a flat articular surface for the quadratojugal on the quadrate*; rostrocaudally elongate dentary rostral to the external mandibular fenestra; the dentary that becomes extremely thin and sharp caudally at the rostral margin of the external mandibular fenestra; a massive symphyseal shelf of the mandible*; a rudimentary lingual triturating shelf on each dentary bearing occlusal grooves; weakly developed lingual ridges on each lingual shelf; absence of the prominent symphyseal ventral process of the dentary*; coronoid bone present; the rostral end of the coronoid bone wedging into the ventral surface of the dorsal ramus of the dentary*; more than one infraprezygapophyseal fossa on the proximal caudal vertebrae including at least one caudal vertebra with three infraprezygapophyseal fossae*.

Differential Diagnosis—*Gobiraptor minutus* differs from *Nemegtomaia barsboldi* (Lü et al., 2004, 2005; Funston et al., 2018a) in that there is a non-mobile joint between the quadrate and quadratojugal, the symphyseal shelf is massive, there are weakly developed lingual shelves and ridges, the dentary shows no deflection at

the rostral margin of the external mandibular fenestra, and surangular and articular are unfused with a clear suture between them.

Gobiraptor minutus is different from *Heyuannia* ("*Ingenia*") *yanshini* (Barsbold, 1981; Funston et al., 2018a) in that the last sacral vertebra bears a pleurocoel on each lateral surface of the centrum, the scapula has a ventrally directed glenoid, the finger-like cranial trochanter of the femur is well developed and separated from the greater trochanter, and the distal shaft of the metatarsal IV is laterally deflected.

Gobiraptor minutus is differentiated from *Conchoraptor gracilis* (Barsbold, 1986; Funston et al., 2018a) by the maxilla being more steeply inclined, the quadrate lacking the lateral cotyle for the quadratojugal, the vomer with a caudal process between the two pterygoids, and no fusion between the palatine and pterygoid.

Gobiraptor minutus primarily differs from *Rinchenia mongoliensis* (= *Oviraptor mongoliensis*) (Barsbold, 1986, 1997; Osmólska et al., 2004; Funston et al., 2018a) in that the premaxilla has a relatively elongate tomial margin, the symphyseal shelf of the dentary is more massive, the mandibular symphysis does not have a prominent ventral process, the ilium has a straight dorsal margin, the cranioventral margin of the preacetabular process is rounded, and the cranial trochanter of the femur is not fused with the greater trochanter.

Gobiraptor minutus is distinguished from *Citipati osmolskae* (Clark et al., 2001, 2002) mainly by the well-developed caudal process of the quadratojugal, the dentary with the rostrocaudally elongate symphyseal region, the coronoid bone whose rostral end is ventrally placed to the caudodorsal ramus of the dentary, and the lateral surface of the articular that is not completely covered by the surangular.

Gobiraptor minutus also differs from *Nomingia gobiensis* (Barsbold et al., 2000;

Funston et al., 2018a) in that the preacetabular process of the ilium does not have a convex dorsal margin, the cuppedicus fossa is not visible in lateral view, the pubic shaft is more concave cranially, and there is no fusion between the cranial trochanter and the greater trochanter on the femur.

DESCRIPTION

Cranial Elements

The cranial elements (Figs. 2.5-9, see Table 2.2 for measurements) of the holotype specimen of *Gobiraptor* are incompletely preserved and most of them are distorted or crushed by compression from the lateral side. A fragment of the right maxilla, the vomer, and the right palate bones are caught in between the mandibular branches detached from the skull. The cranial elements generally show a clear suture at each border between individual bones. Except for the partially preserved postorbital, the upper and middle regions of the skull are missing in the holotype.

Premaxilla—The premaxilla (Fig. 2.5) is rostrocaudally elongate in lateral view and the rostral margin is vertical as in *Citipati osmolskae* (Clark et al., 2002) or *Conchoraptor* (Osmólska et al., 2004; Funston et al., 2018a). Whether the premaxillae are fused with each other is not certain since their rostral end is distorted. This distortion made a triangular gap at the tip of the rostrum. The premaxilla is also edentulous and has an oblique tomial margin whose crenulation is obscured by weathering. The upper region of both premaxillae is missing, thus the exact location of the external nares or the location of the border between the premaxilla and nasal cannot be inferred. There are irregularly placed small nutrient foramina on the lateral surface of the premaxilla above the tomial margin. The maxillary process of the premaxilla caudodorsally extends to probably meet the nasal at the dorsal end. The palatal surface of the premaxilla is concave and U-shaped in ventral view. Along the tomial margin, there is a row of small foramina

TABLE 2.2. Selected measurements (in mm) of the holotype specimen of *Gobiraptor minutus* gen. et sp. nov. (MPC-D 102/111).

Element	Length	Width	Height	Circumference
Tomial margin of the premaxilla	23.2 (left), 24.2 (right)	-	-	-
Premaxilla-maxilla boundary (left)	-	23.7 (compressed)	-	-
Mandibular articulation surface of the quadrate (right)	15	23.9	-	-
Dentary	58 (right, from the rostral tip to the caudal end of the caudodorsal ramus)	27 (compressed)	20.6 (symphysis), 38.7 (near the posterior end)	-
Symphyseal shelf	15.1	27 (same as the dentary)	16.4	-
External mandibular fenestra	27.7 (estimation)	-	26.3	-
Articular (right)	19.8	20.7	-	-
Last sacral	25.51	-	-	-
1st caudal	23.06	-	-	-
2nd caudal	24.27	-	-	-
Caudal A	22.8	-	-	-
Caudal B	24.23	-	-	-
Caudal C	23.6	-	-	-
Caudal D	23.59	-	-	-
Caudal E	23.17	-	-	-
Caudal F	21.44	-	-	-
Acetabulum (left)	45	-	-	-

Element	Length	Width	Height	Circumference
Femur	195.1 (left, proximal surface damaged), 195.7 (right)	-	-	70 (left), 68 (right)
Metatarsal I (left)	28.8	-	-	-
Metatarsal II (left)	108.2	-	-	-
Metatarsal III (left)	123	-	-	-
Metatarsal IV (left)	112.4	-	-	-
Metatarsal V (left)	4.2	-	-	-
Pedal digit I-1 (left)	23.1	-	-	-
Pedal digit III-1 (left)	36.3	-	-	-
Pedal digit III-2 (left)	29	-	-	-
Pedal digit IV-1 (left)	20.5	-	-	-
Pedal digit IV-2 (left)	18.6	-	-	-
Pedal digit IV-3 (left)	16.2	-	-	-
Pedal digit IV-4 (left)	12.2	-	-	-

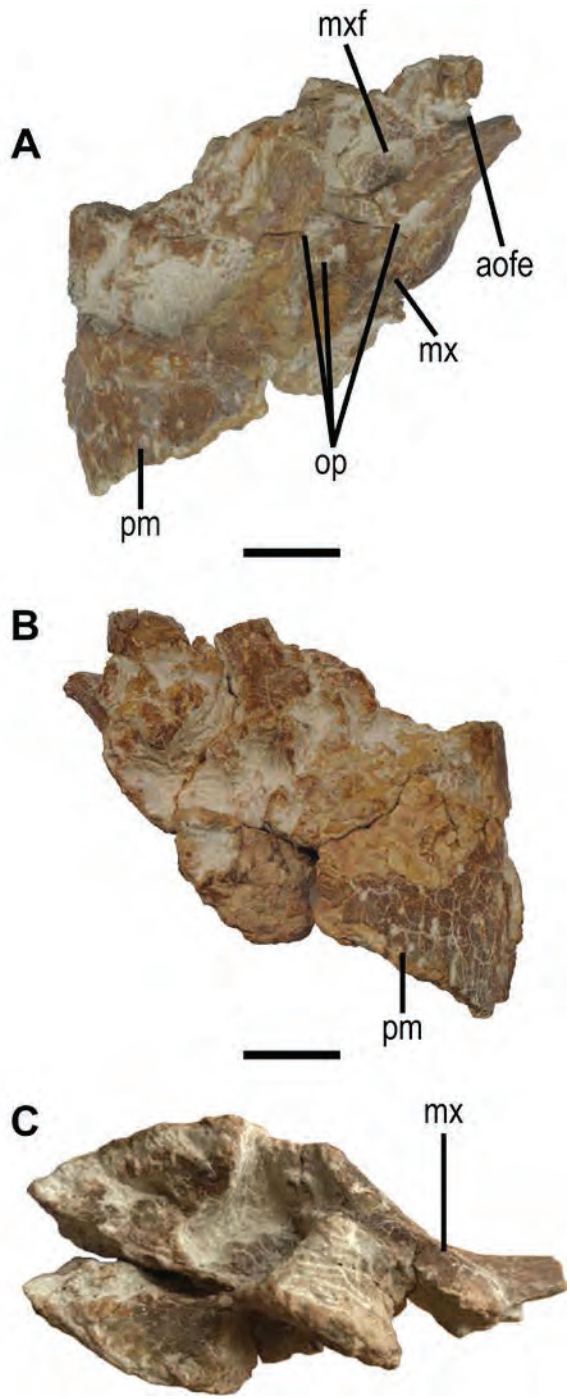

FIGURE 2.5. Premaxillae and maxillae of the holotype specimen of *Gobiraptor minutus* gen. et sp. nov. (MPC-D 102/111). **A**, left lateral view; **B**, right lateral view; **C**, ventral view. Abbreviations in Appendix 1. Scale bars equal 1 cm.

FIGURE 2.6. Left postorbital of the holotype specimen of *Gobiraptor minutus* gen. et sp. nov. (MPC-D 102/111). **A**, lateral view; **B**; medial view. Abbreviations in Appendix 1. Scale bar equals 1 cm.

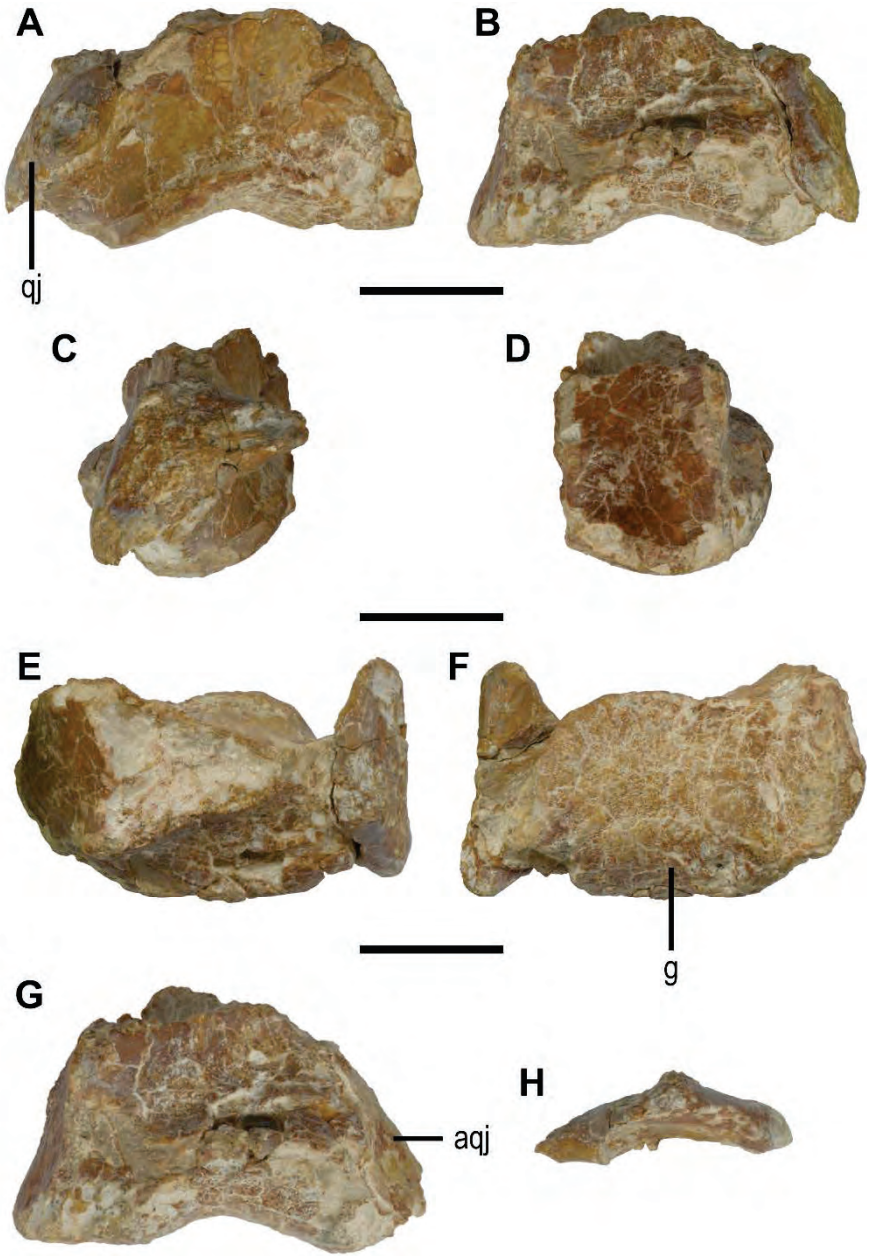

FIGURE 2.7 Right quadratojugal and quadrate of the holotype specimen of *Gobiraptor minutus* gen. et sp. nov. (MPC-D 102/111). **A**, rostral view; **B**, caudal view; **C**, lateral view; **D**, medial view; **E**, dorsal view; **F**, ventral view; **G**, quadrate in caudal view; **H**, quadratojugal in dorsal view. Abbreviations in Appendix 1. Scale bars equal 1 cm.

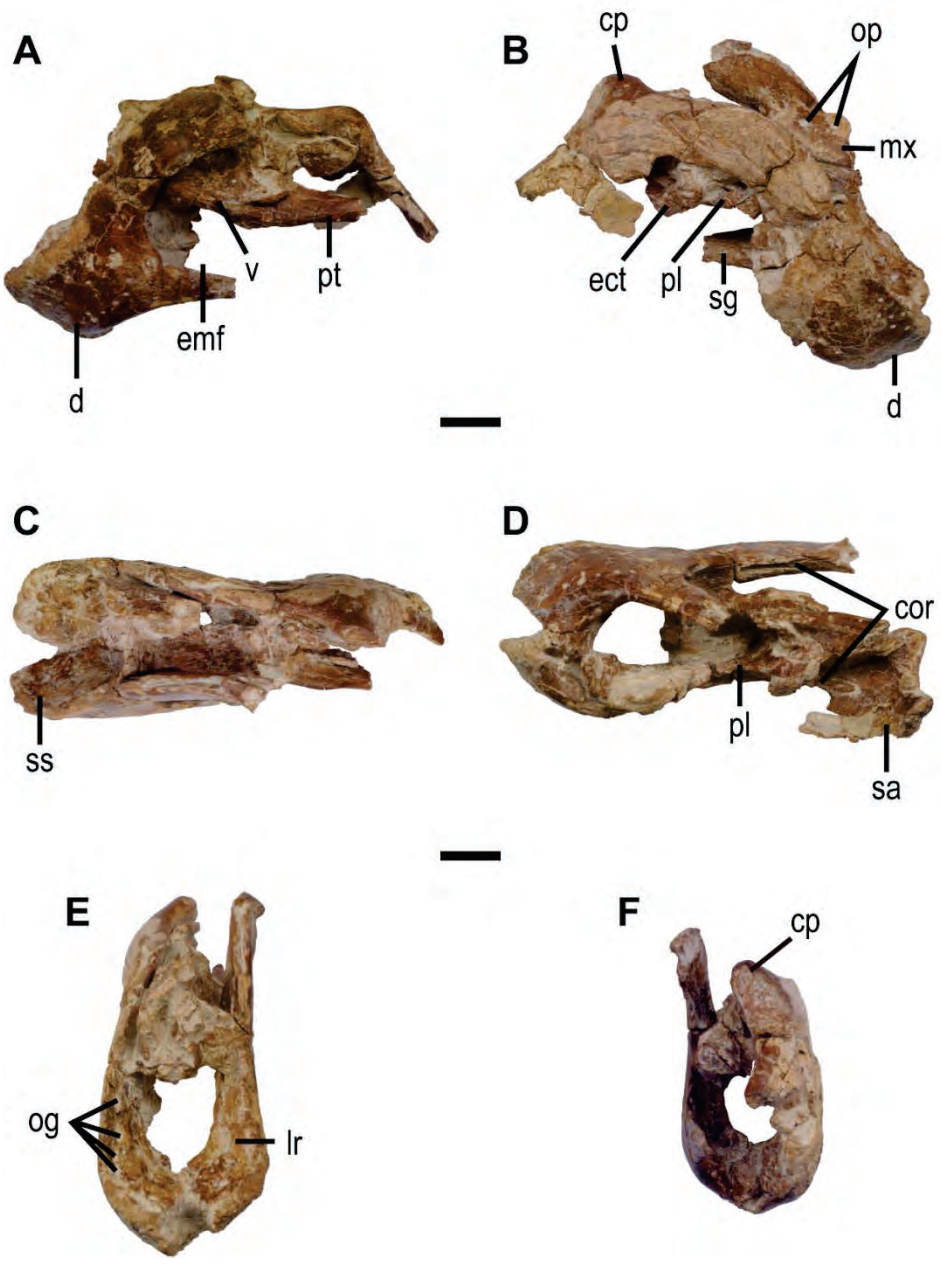

FIGURE 2.8. Mandible (right maxilla and palatal elements caught in the middle) of the holotype specimen of *Gobiraptor minutus* gen. et sp. nov. (MPC-D 102/111). **A**, left lateral view; **B**, right lateral view; **C**, dorsal view; **D**, oblique ventral view; **E**, rostral view; **F**, caudal view. Abbreviations in Appendix 1. Scale bars equal 1 cm.

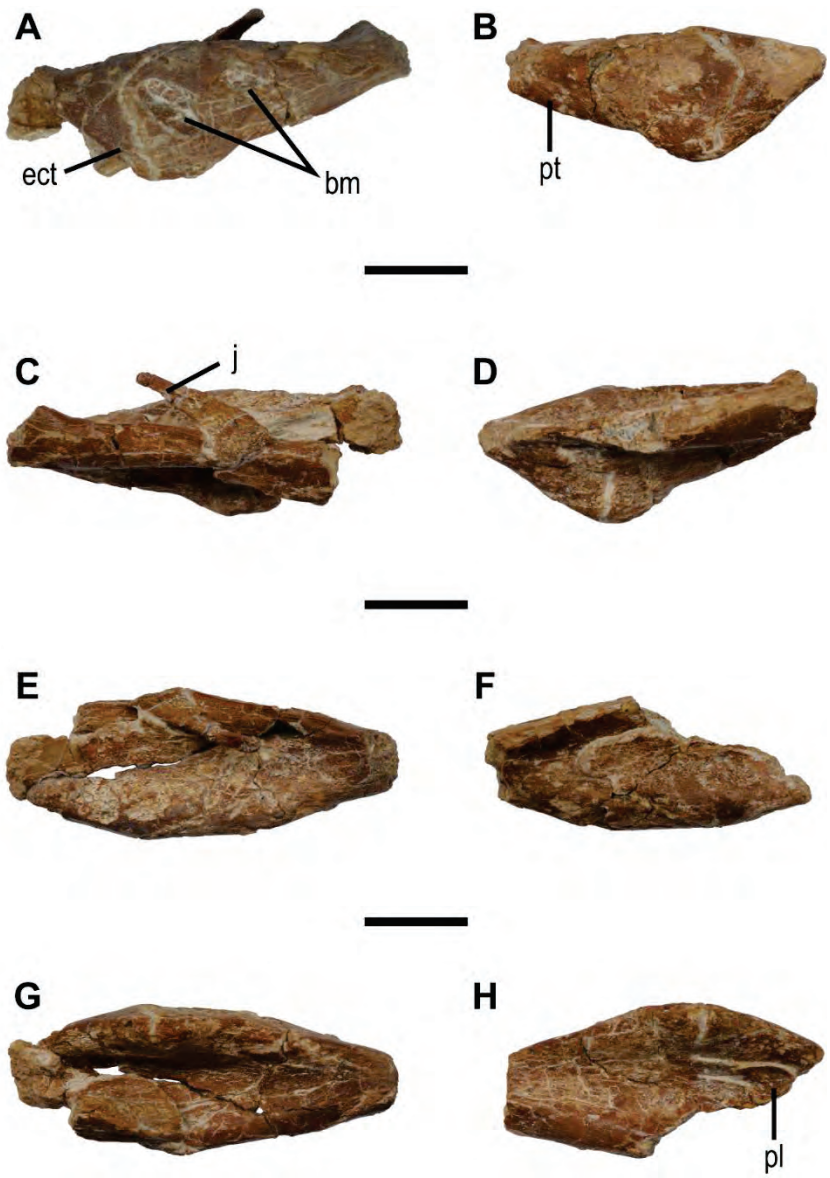

FIGURE 2.9. Pterygoids and ectopterygoids of the holotype specimen of *Gobiraptor minutus* gen. et sp. nov. (MPC-D 102/111). **A**, left elements in lateral view; **B**, right elements in lateral view; **C**, left elements in medial view; **D**, right elements in medial view; **E**, left elements in dorsal view; **F**, right elements in dorsal view; **G**, left elements in ventral view; **H**, right elements in ventral view. Abbreviations in Appendix 1. Scale bars equal 1 cm.

which would have met the occlusal grooves on the dentary when the beak was closed (Fig. 2.5C).

Maxilla—The rostrocaudally short maxilla (Figs. 2.5, 2.8) is edentulous as the premaxilla. The right maxilla is fragmentary and the more complete left one has a crushed lateral surface. The lateral surface of the maxilla contacts the premaxilla rostrally but it is broken along the border. The antorbital fossa is not recognizable because of the crushed surface. The maxilla does not form a continuous ventral margin with the tomial margin of the premaxilla but ascends in a greater angle in lateral view. A maxillary fenestra is present on the lateral surface rostral to the antorbital fenestra but its rim is lost except for the caudoventral margin. The caudal border of the maxillary fenestra is comprised of the interfenestral bar which also constitutes the rostral margin of the antorbital fenestra. Caudal to the interfenestral bar, the maxilla extends caudally as a narrow splint to make up the ventral margin of the antorbital fenestra. There are two openings on the lateral surface of the right maxilla (Fig. 2.8B) and three on the left (Fig. 2.5A). The openings on the right maxilla are circular and smaller than the ones on the left. Between the two openings on the right maxilla, the caudal one is larger than the rostral one. The openings on the left maxilla are similar in size and shape being subtriangular. Two of them are very close to each other and located near the rostral margin of the maxilla while the third one is right beneath the maxillary fenestra. These five openings show broken margins and inwardly compressed surface which are indicative of punctuation marks but they have different appearances from the bite marks on the left pterygoid. On the palatal surface of each maxilla is a rostrocaudally elongate ridge that must have bordered the premaxilla rostrally.

Postorbital—The partially preserved postorbital (Fig. 2.6) is a triradiate bone but none of the three processes is complete. The frontal process of the postorbital is broken at its base although it shows a rostrodorsal orientation, which is typical of oviraptorids. The mediolaterally thin squamosal process extends caudodorsally but its tip is missing. The rostral margin of the postorbital forms the caudodorsal orbital rim. It is caudally concave and caudomedially slanted. The jugal process of the postorbital is rostrocaudally narrow but mediolaterally long having a subrectangular cross section.

Quadratojugal—The quadratojugal (Fig. 2.7A-E, H) tightly adheres to the quadrate without a distinct suture. The dorsal and rostral processes of the quadratojugal are perpendicular to each other. They are broken off near the quadratojugal body while the caudal process is well preserved and extends caudoventrally beyond the quadrate. The medial articular surface of the quadratojugal for the quadrate is distinctly concave.

Quadrate—The quadrate (Fig. 2.7A-G) is missing its dorsal part of the shaft. The quadrate becomes narrower dorsally while it widens medially. The mandibular articular surface of the quadrate is saddle-shaped and divided into two distinct condyles by a longitudinal groove at the center. The lateral condyle extends slightly further ventrally than the medial condyle. Dorsolateral to the lateral condyle is the articular surface for the quadratojugal. It is flat lacking a concavity described by Maryańska and Osmólska (1997) or a convex surface in *Nemegtomaia* (Lü et al., 2004). The caudal surface of the quadrate is prominently concave and the broad medial surface is nearly flattened.

Vomer—The palate (Figs. 2.8, 2.9) of *Gobiraptor* generally shows a typical

oviraptorid morphology described by Elzanowski (1999) and Osmólska et al. (2004). The fused vomer (Fig. 2.8A, D) forms a round ventral process at its rostral end but the rostral tip is obscured by the dentary and matrix. The vomer has a dorsal expansion which meets the maxilla although the border is worn off. Each lateral surface of the ventral process of the vomer is concave and steeply slanted bordering a round ridge caudodorsally. Caudal to these ridges, the vomer has a medially concave lateral surface which gradually expands dorsoventrally in lateral view. The ventral surface of the vomer becomes flat caudally. At its caudal end, the vomer is tightly wedged by the pterygoids and separates them with a short caudal process. The vomer also contacts the palatine laterally together forming the choana. The preserved specimen only shows the right choana whose rostral border is not visible because of matrix.

Palatine—The left palatine is entirely missing while the right palatine (Fig. 2.8B, D) is preserved articulating with the pterygoid and the ectopterygoid although it is heavily eroded. The exposed part of the palatine is a thin lateral ramus which is visible in lateral and ventral views. The lateral ramus extends to probably meet the maxilla and dorsomedially to meet the vomer. The contact between the palatine and the maxilla, however, is obscured by the dentary and matrix. The palatine also contacts the pterygoid and the ectopterygoid caudodorsally but it is not fused to them showing a clear suture at the border. The suborbital fenestra that is present in *Citipati* (Clark et al., 2002) and *Conchoraptor* (Elzanowski, 1999) is not visible.

Pterygoid—The pterygoid (Figs. 2.8, 2.9) shows a typical morphology of oviraptorids. The palatal ramus of the pterygoid has concave dorsal and ventral

surfaces, the latter being deeper. The pterygoid contacts the ectopterygoid rostrally and dorsally forming a rostrocaudally elongate pterygoid-ectopterygoid bar. The suture between the pterygoid and the ectopterygoid is distinct and V-shaped in dorsal and lateral views. Rostrally, the pterygoid-ectopterygoid bar has a deep ventral flange which is mainly formed by the pterygoid. Caudal to the flange the pterygoid becomes slender. The rod-like caudal tip of the right jugal is broken off and adheres to the medial surface of the left pterygoid. There are two elliptical bite marks on the lateral surface of the left pterygoid (Fig. 2.9A). Between the two bite marks, the rostral one is much larger and deeper. The bite marks do not show any sign of healing suggesting that either the animal died as a result of predation or it was scavenged after death.

Ectopterygoid—The ectopterygoid (Figs. 2.8, 2.9) extends rostrodorsally to meet the maxilla and jugal although these contacts are not preserved. Caudal to this ascending process, the ectopterygoid dorsoventrally expands and contacts the pterygoid caudally in lateral view. The thin dorsal surface of the ectopterygoid is concave and overlies the palatine and the pterygoid.

Mandible

The mandible (Figs. 2.8, 2.10) is severely distorted and broken into several pieces although the rostral region is relatively well preserved. The preserved mandibular elements are mostly incomplete including both dentaries, surangulars, coronoid bones, angulars, splenials, prearticulars, and the right articular. The morphology of the mandible shows oviraptorid features, namely the large external mandibular fenestra and the distinct coronoid processes on each surangular.

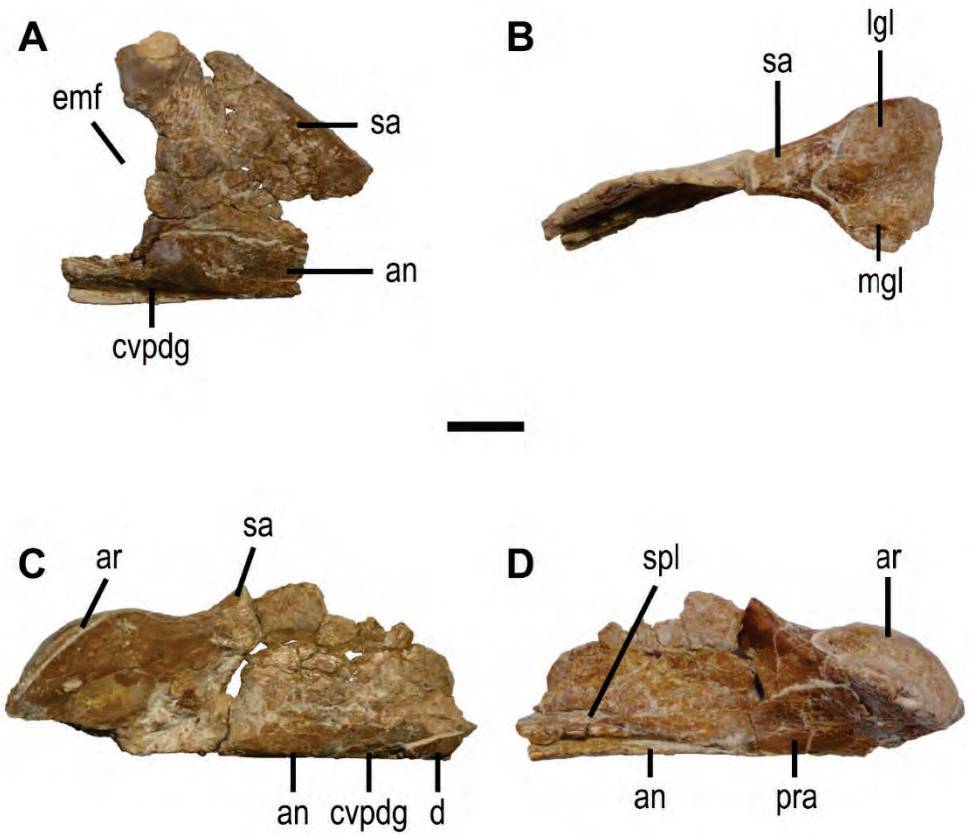

FIGURE 2.10. Mandibular elements of the holotype specimen of *Gobiraptor minutus* gen. et sp. nov. (MPC-D 102/111). **A**, left surangular and angular in lateral view; **B-D**, caudal region of the right mandibular ramus in **B**, dorsal; **C**, lateral; and **D**, medial views. Abbreviations in Appendix 1. Scale bar equals 1 cm.

Dentary—The unfused dentary (Figs. 2.8, 2.10C) is edentulous, deep and marked by numerous small nutrient foramina on the rostral and lateral surfaces. Like the premaxilla, the two dentaries are compressed in the same direction and as a result, they are distorted and broken having a V-shaped gap at the rostral tip (Fig. 2.8C-E). The symphyseal region of the dentary is greatly downturned at an angle of approximately 32° to the ventral ramus when measured as done in Ma et al. (2017) and its rostrodorsal tip is only slightly upturned. The rostrocaudally short symphyseal shelf (Fig. 2.8C, E) is unique among oviraptorids being massive and thick at the tip of the beak. The dentary also has a weakly developed lingual ridge on each rudimentary lingual shelf that extends caudally from the symphyseal shelf. These ridges do not meet each other at the middle and they are not well developed like those in derived caenagnathids (Lamanna et al., 2014). Each lingual shelf bears at least four elliptical occlusal grooves between the dorsal margin of the dentary and the lingual ridge (Fig. 2.8C, E). The caudal margin of the symphyseal shelf, together with that of the lingual shelves, forms a U-shaped ridge. Caudal to this ridge, a slightly concave surface that is nearly perpendicular to the symphyseal shelf slopes down to the ventral margin at the middle (Fig. 2.8F). Lateral to this surface is a large fossa near the rostral end of the splenial in case of the left dentary. Caudally, there is also a deep fossa on the ventral surface of the lingual shelf. There are likely to be another pair of fossae on the right dentary but this region is covered by matrix. The large external mandibular fenestra is semicircular with smoothly curved rostrodorsal margin and mostly formed by the dentary and surangular (Figs. 2.8A, B, 2.10A). The dentary strongly thins towards the rostral margin of the external mandibular fenestra not having a deflection known in *Nemegtomaia* (Lü et

al., 2004). The external mandibular fenestra divides the dentary into two rami. The mediolaterally thicker caudodorsal ramus ascends making a weak S-shape in lateral view until it is bifurcated by the surangular into lateral and medial branches. At their borders, the dentary and surangular are tightly joined together making a zig-zagged suture. The thin and splint-like coronoid bone which has been known only in *Citipati* (Clark et al., 2002) dorsally wedges into the ventral surface of the caudodorsal ramus of the dentary at its rostral end (Fig. 2.8D). However, this is unlike in *Citipati* where it is on the medial surface of the caudodorsal ramus (Clark et al., 2002). The coronoid bone twists as it extends to the medial surface of the surangular along a shallow groove which is below the coronoid process. The mediolaterally thin caudoventral ramus of the dentary is elongate and must have extended caudally beyond the caudal margin of the external mandibular fenestra like *Rinchenia* (Funston et al., 2018a) along the shallow groove on the lateral surface of the angular. On the medial surface of the caudoventral ramus, there is a shallow groove for the splenial.

Splenial—The thin splenial (Fig. 2.10D) is poorly preserved. Both left and right splenials are missing their rostral parts, but the groove on the medial surface of the left dentary indicates that their rostral ends must have reached below the symphyseal shelf. This groove for the splenial extends along the caudodorsal ramus of the dentary to the medial surface of the angular where the splenial overlies the prearticular. The splenial tapers caudally forming a pointed end at which the prearticular twists so that its broad surface faces medially.

Surangular—Both surangulars are preserved in the holotype specimen of *Gobiraptor minutus* although the left surangular (Fig. 2.10A) is fragmentary. The

broken but better preserved right surangular (Fig. 2.10B-D) is relatively thick along the dorsal margin until it meets the articular although it is broken and missing its middle region. The prominent coronoid process is dorsomedially oriented and ventrally forms a ridge on the medial surface. Below the coronoid process is the convex lateral surface caudal to which is a low ridge in contrast to the concave medial surface. The surangular gently descends caudally from the coronoid process to meet the articular but does not completely cover it in lateral view having a distinct suture along the border unlike *Citipati* (Clark et al., 2002). As in other oviraptorids, there is a thin process which protrudes into the external mandibular fenestra but it is broken at its base. Ventral to the dorsal margin, the surangular becomes thin and contacts the angular on the lateral surface and the prearticular on the medial surface ventrally also with clear sutures. The surangular is not fused with the articular and does not contribute to the mandibular articulation surface. In dorsal view (Fig. 2.10B), the suture between the surangular and articular is V-shape. The lateral surface which incompletely covers the articular is flat but has a minute bump near the caudal end of the surangular-articular suture (Fig. 2.10C). There is no visible adductor fossa or a foramen on the surangular but it could be due to poor preservation.

Angular—The preserved angulars (Fig. 2.10A, C, D) are fragmentary but much of the morphological information is not lost. The angular is well exposed in lateral view and generally thin but on its lateral surface has a small mound right below the rostral end of the border with the surangular. Ventrally the angular also has a shallow depression on the lateral surface for the caudoventral ramus of the dentary. On the medial surface, a groove for the prearticular lies under the splenial

and its associated groove. The ventral surface of the angular is flat, maintaining almost constant mediolateral width until it is invaded by the prearticular.

Articular—The rostrocaudally elongate mandibular articulation surface is entirely formed by the articular and its shape is semicircular in dorsal view (Fig. 2.10B). Around the midline of the articulation surface, there is a low longitudinal ridge which must have articulated with the groove between the two condyles of the quadrate. This ridge divides the articulation surface into two glenoids which are dorsally convex and probably allowed propalinal movement at the jaw joint. The medial glenoid is slender and nearly flat in contrast to the massive lateral glenoid which does not laterally extend beyond the level of the lateral surface of the surangular. Below the mandibular articulation, the medial surface of the articular is partially covered by the surangular and prearticular.

Prearticular—The prearticular (Fig. 2.10D) is rod-like rostrally but soon twists before it dorsoventrally expands near the articular to become a major element of the caudal region of the mandibular ramus. It meets the surangular dorsally below the mandibular articulation and probably sends the retroarticular process but this region is broken off and missing.

Postcranial Elements

Preserved postcranial elements (Figs. 2.11-22, see Table 2.2 for measurements) are partially disarticulated and some are fragmentary. Most of the axial skeletons are missing except for the last sacral vertebra and nine proximal caudal vertebrae with mostly disarticulated chevrons. The last sacral is articulated with the two proximalmost caudals but disarticulated from the other seven caudals. These seven

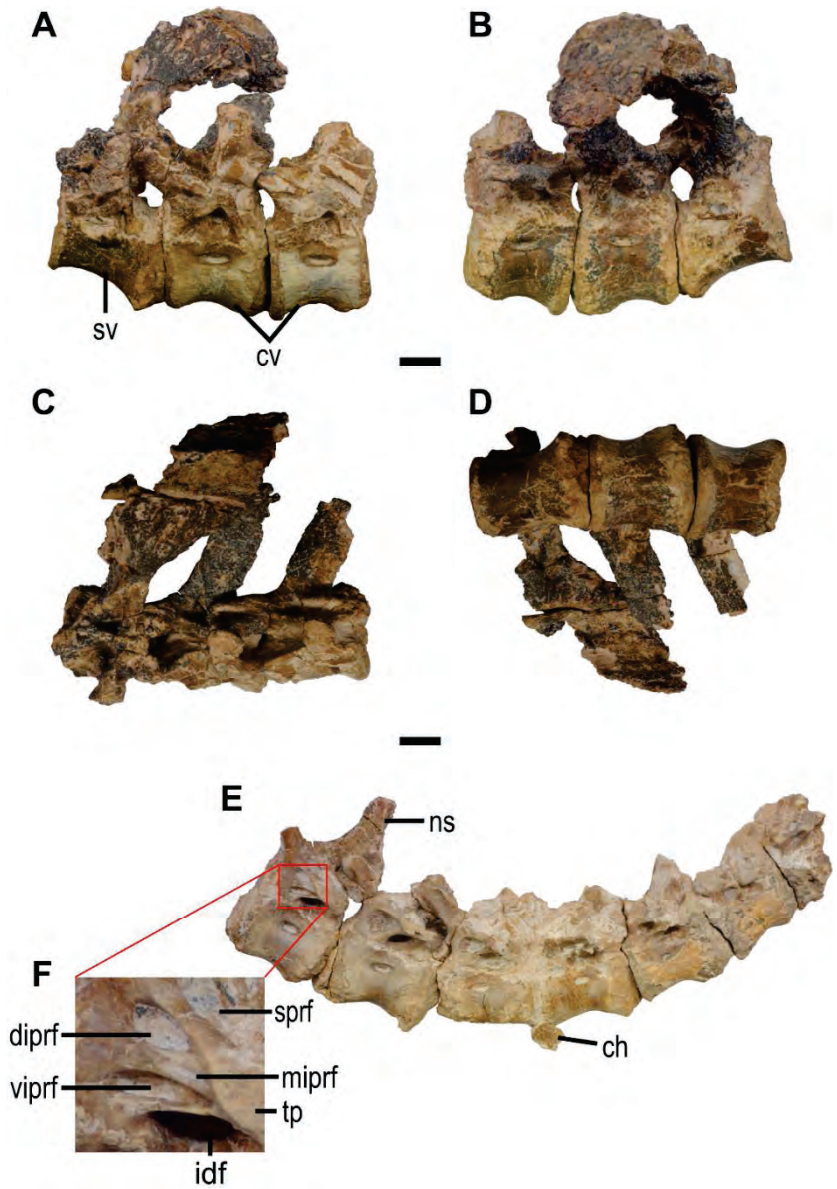

FIGURE 2.11. Last sacral vertebra and proximal caudal vertebrae of the holotype specimen of *Gobiraptor minutus* gen. et sp. nov. (MPC-D 102/111). **A**-**D**, last sacral vertebra and two proximalmost caudal vertebrae in **A**, left lateral; **B**, right lateral; **C**, dorsal; and **D**, ventral views; **E**, proximal caudal vertebrae (caudal A to G) in left lateral view; **F**, magnified view of the infraprezygapophyses in **E**. Abbreviations in Appendix 1. Scale bars equal 1 cm.

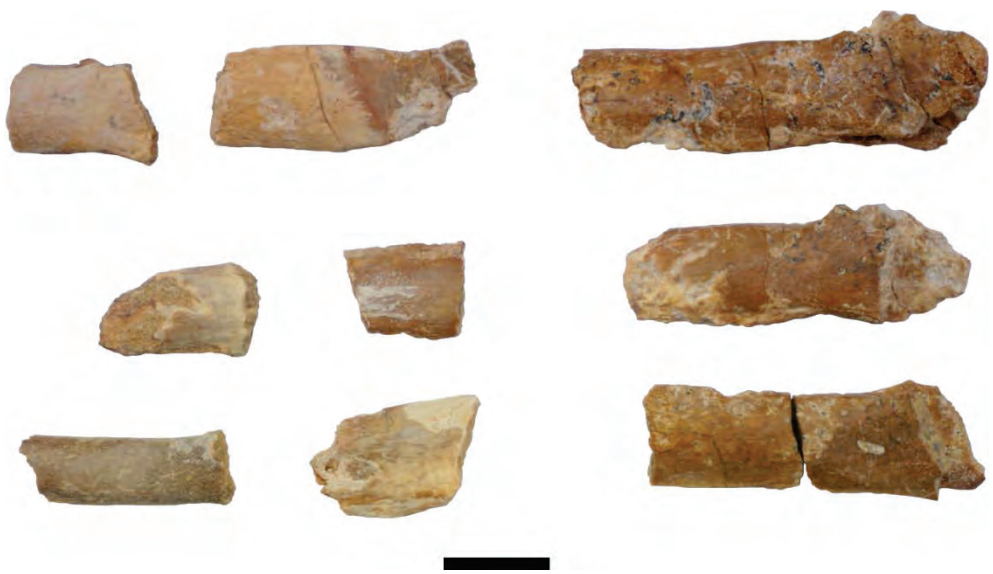

FIGURE 2.12. Chevrons of the holotype specimen of *Gobiraptor minutus* gen. et sp. nov. (MPC-D 102/111). Scale bar equals 1 cm.

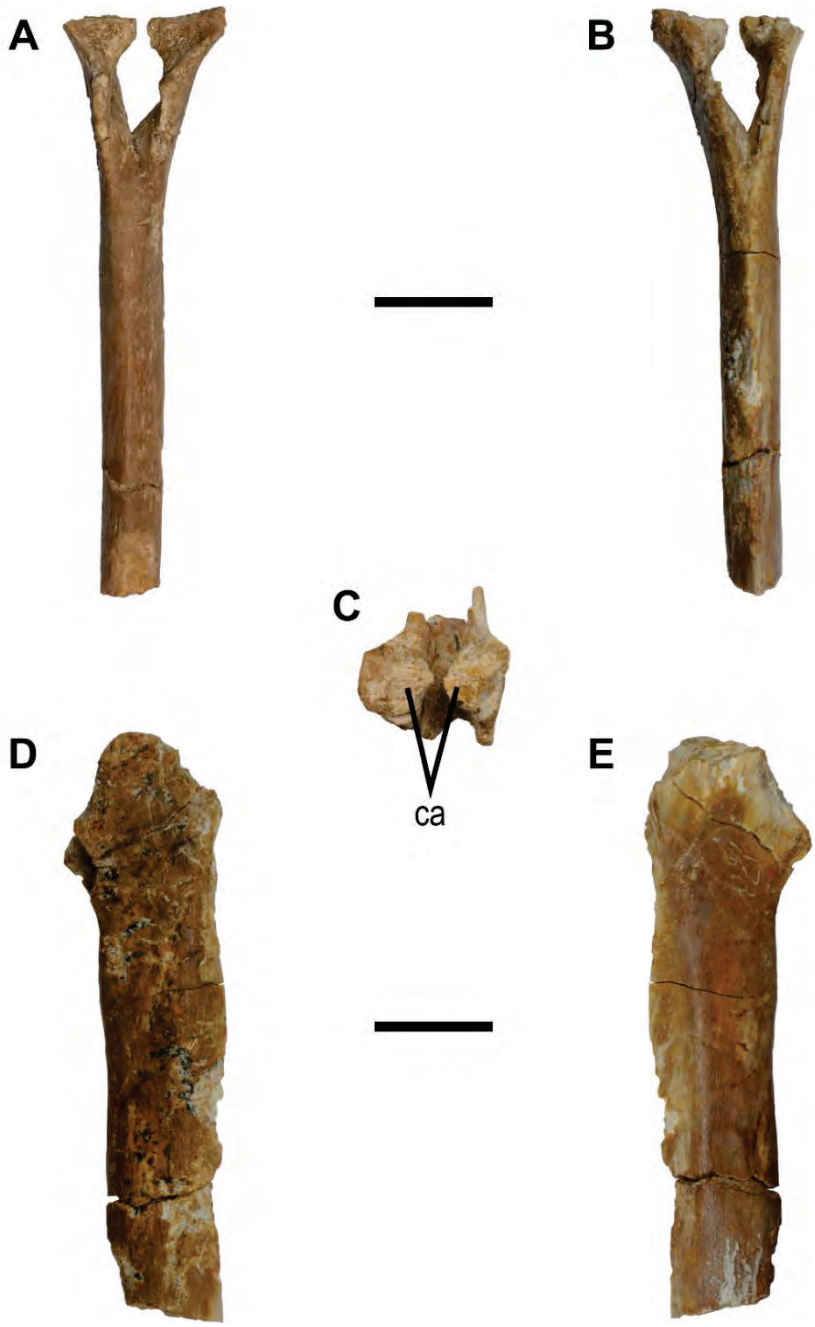

FIGURE 2.13. Proximal chevron of the holotype specimen of *Gobiraptor minutus* gen. et sp. nov. (MPC-D 102/111). **A**, cranial view; **B**, caudal view; **C**, proximal view; **D**, left lateral view; **E**, right lateral view. Abbreviation in Appendix 1. Scale bars equal 1 cm.

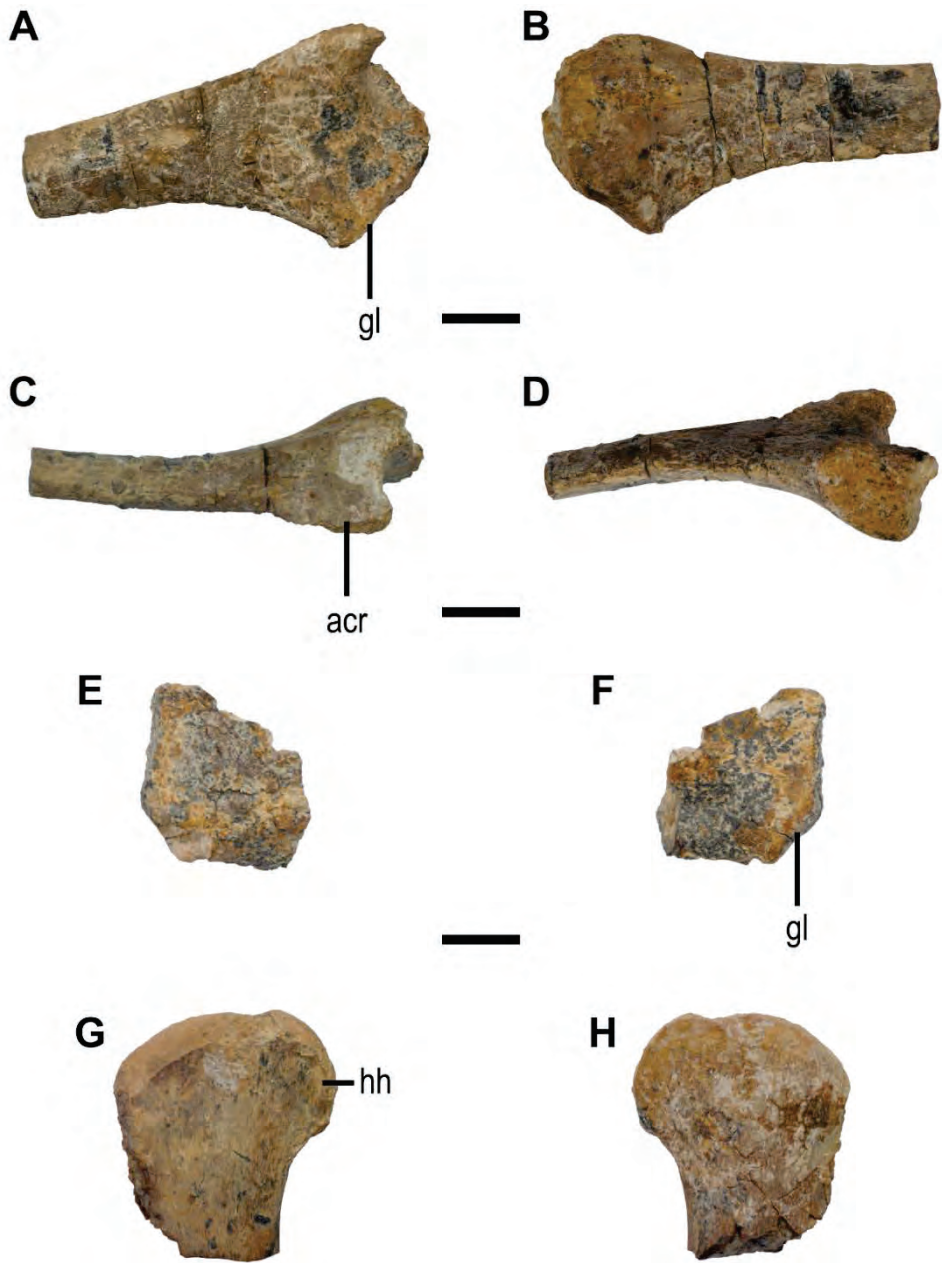

FIGURE 2.14. Right pectoral girdle and forearm of the holotype specimen of *Gobiraptor minutus* gen. et sp. nov. (MPC-D 102/111). **A-D**, right scapula in **A**, lateral; **B**, medial; **C**, dorsal; and **D**, ventral views; **E-F**, right coracoid in **E**, lateral; and **F**, medial views; **G-H**, right humerus in **G**, cranial; and **H**, caudal views. Abbreviations in Appendix 1. Scale bars equal 1 cm.

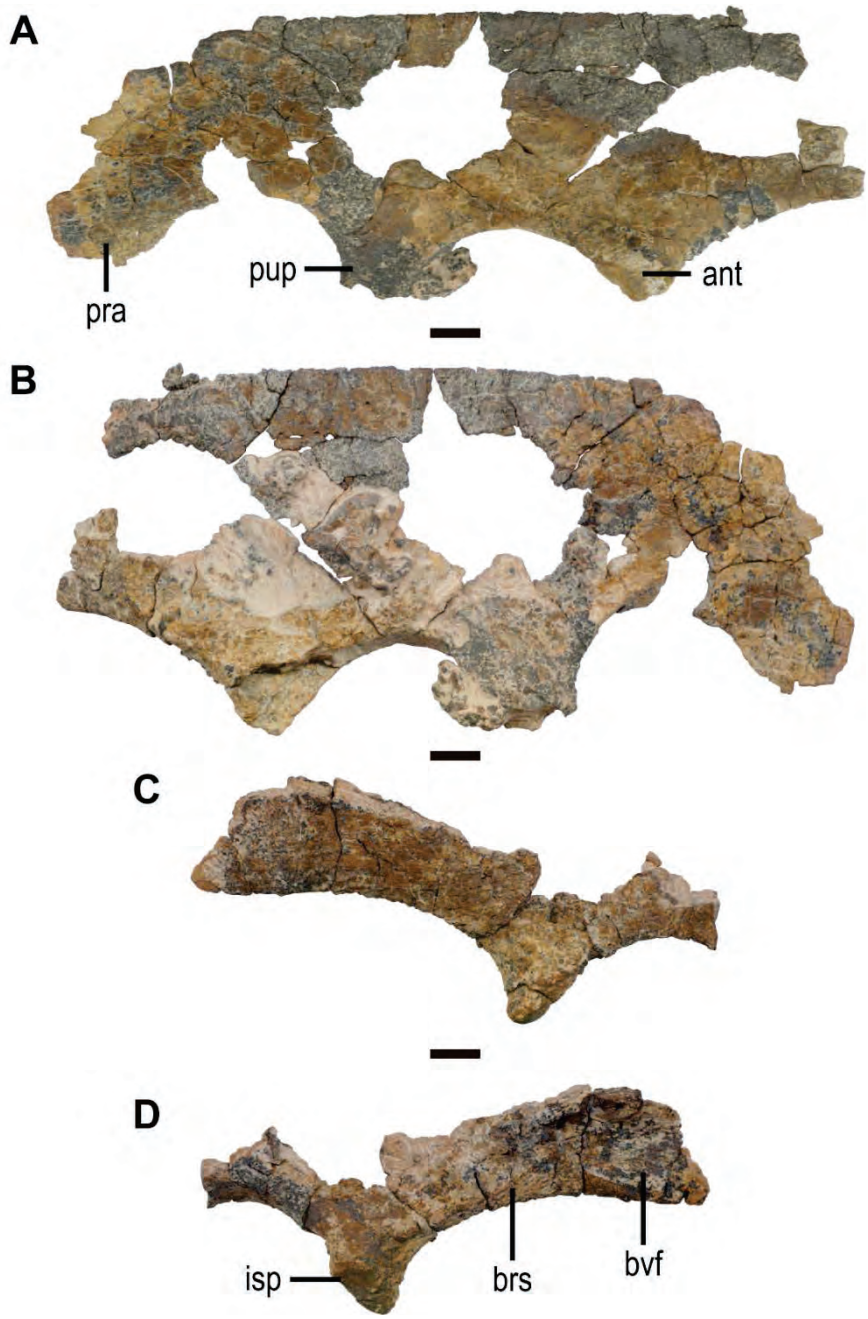

FIGURE 2.15. Ilia of the holotype specimen of *Gobiraptor minutus* gen. et sp. nov. (MPC-D 102/111). **A**-**B**, left ilium in **A**, lateral; and **B**, medial views; **C**-**D**, right ilium in **C**, lateral; and **D**, medial views. Abbreviations in Appendix 1. Scale bars equal 1 cm.

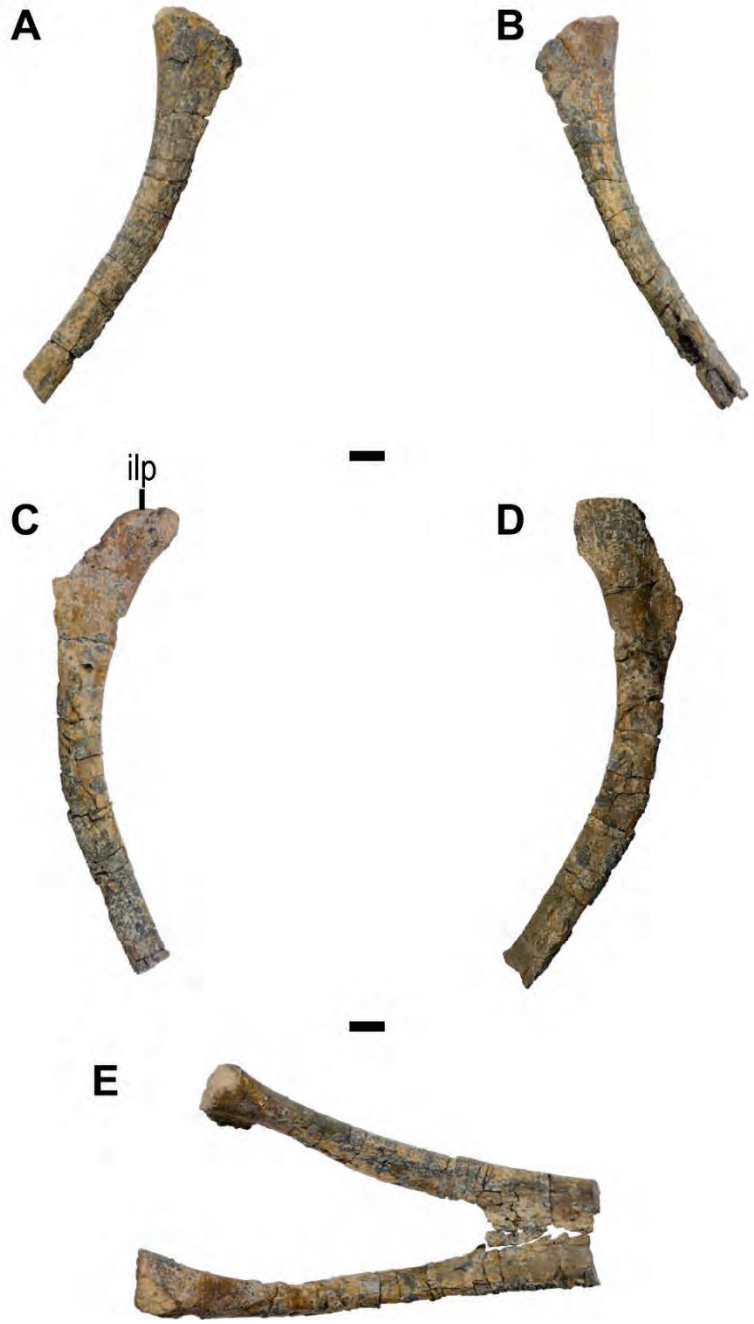

FIGURE 2.16. Pubes of the holotype specimen of *Gobiraptor minutus* gen. et sp. nov. (MPC-D 102/111). **A-B**, left pubis in **A**, lateral; and **B**, medial views; **C-D**, right pubis in **C**, lateral; and **D**, medial views; **E**, pubes in cranial view. Abbreviation in Appendix 1. Scale bars equal 1 cm.

FIGURE 2.17. Ischia of the holotype specimen of *Gobiraptor minutus* gen. et sp. nov. (MPC-D 102/111). **A-B**, left ischium in **A**, lateral; and **B**, medial views; **C-D**, right ischium in **C**, lateral; and **D**, medial views. Abbreviation in Appendix 1. Scale bar equals 1 cm.

FIGURE 2.18. Left femur of the holotype specimen of *Gobiraptor minutus* gen. et sp. nov. (MPC-D 102/111). **A**, cranial view; **B**, caudal view; **C**, lateral view; **D**, medial view. Abbreviations in Appendix 1. Scale bar equals 1 cm.

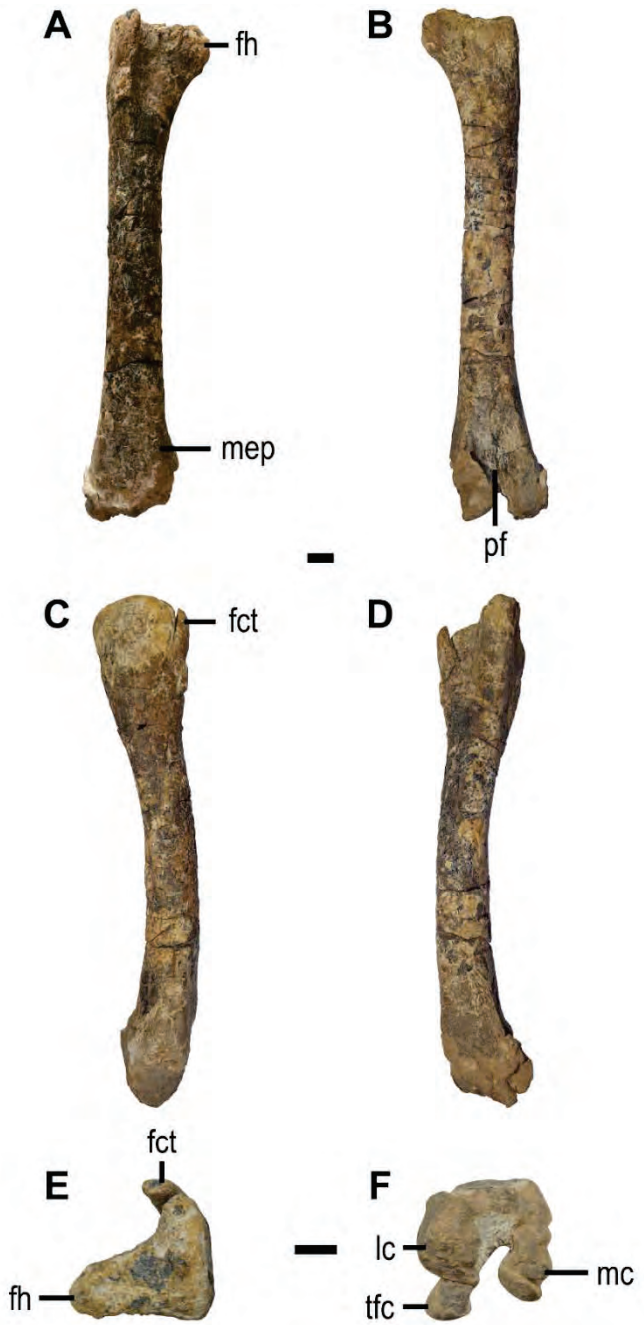

FIGURE 2.19. Right femur of the holotype specimen of *Gobiraptor minutus* gen. et sp. nov. (MPC-D 102/111). **A**, cranial view; **B**, caudal view; **C**, lateral view; **D**, medial view; **E**, proximal view; **F**, distal view. Abbreviations in Appendix 1. Scale bars equal 1 cm.

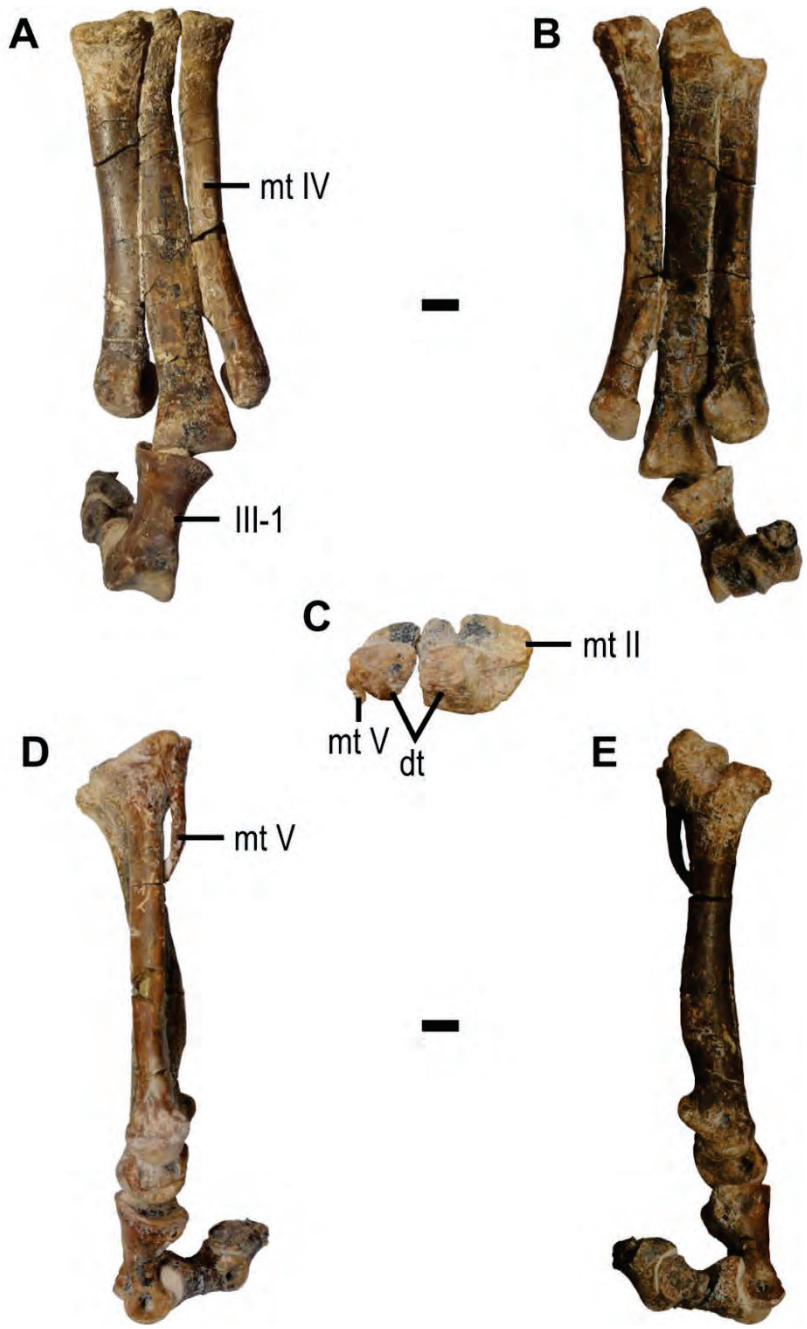

FIGURE 2.20. Left distal tarsals with metatarsus and pedal digit III of the holotype specimen of *Gobiraptor minutus* gen. et sp. nov. (MPC-D 102/111). **A**, dorsal view; **B**, plantar view; **C**, proximal view; **D**, lateral view; **E**, medial view. Abbreviations in Appendix 1. Scale bars equal 1 cm.

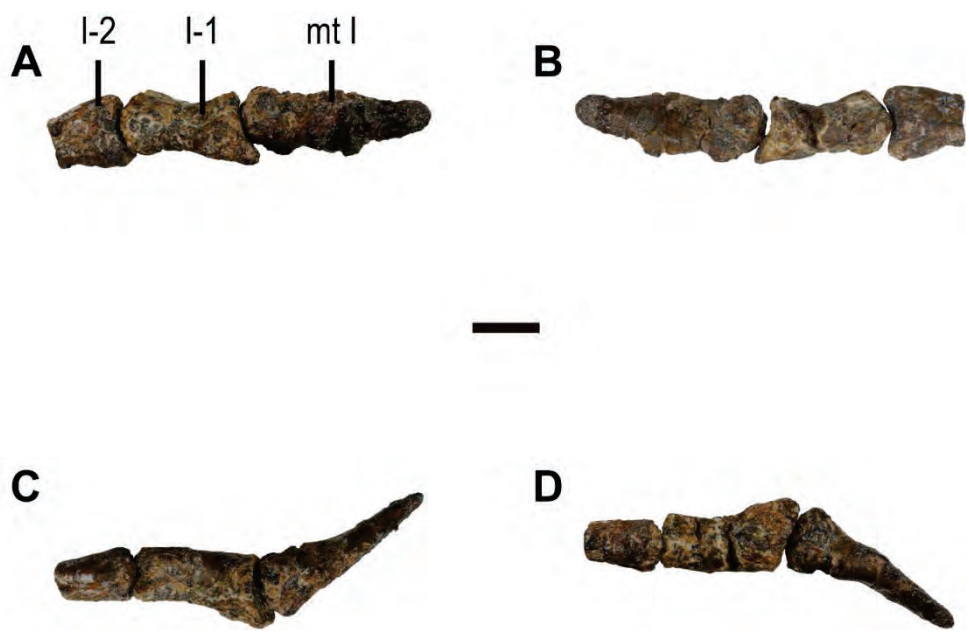

FIGURE 2.21. Left metatarsal I and pedal digit I of the holotype specimen of *Gobiraptor minutus* gen. et sp. nov. (MPC-D 102/111). **A**, lateral view; **B**, medial view; **C**, dorsal view; **D**, plantar view. Abbreviations in Appendix 1. Scale bar equals 1 cm.

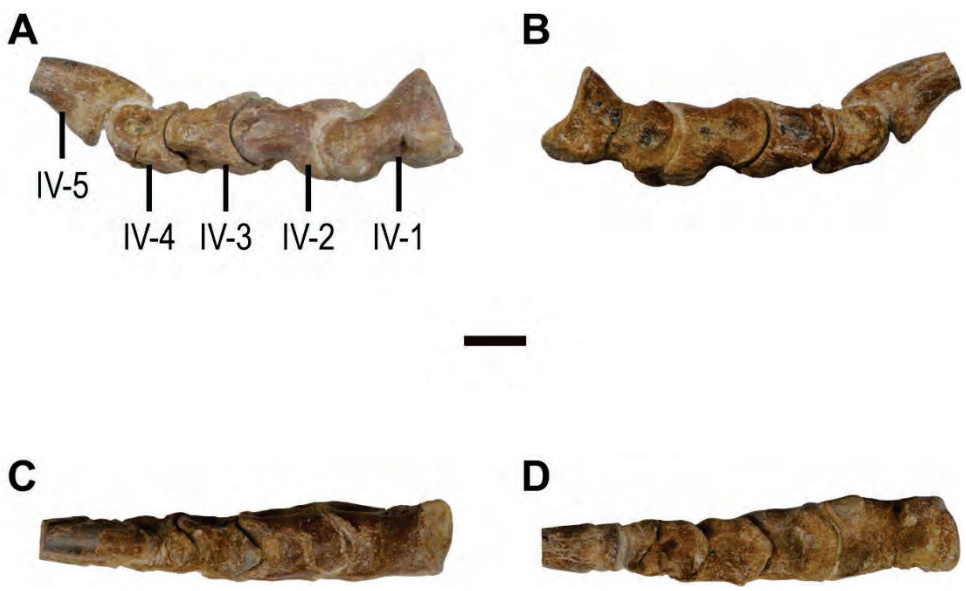

FIGURE 2.22. Left pedal digit IV of the holotype specimen of *Gobiraptor minutus* gen. et sp. nov. (MPC-D 102/111). **A**, lateral view; **B**, medial view; **C**, dorsal view; **D**, plantar view. Abbreviations in Appendix 1. Scale bar equals 1 cm.

caudals are not the third to ninth caudals, but considering their size and shape it is likely that they are proximal caudals. The pectoral girdle and forearms are almost entirely missing except for the right scapula and humerus both of which are only partially preserved. There is also a small fragment of bone which might be a part of coracoid. The pelvic girdle is relatively well preserved, and although there are no missing elements, they are generally incomplete and some are only represented by small fragments. The preserved hind limb elements include both femora, left metatarsus with distal tarsals, partial digit I, III, and IV. The distal portions of the unguals are missing in the first and fourth digits whereas the third digit has only two proximal phalanges (III-1 and III-2) with the proximal half of the phalanx III-3.

Sacral Vertebra—Only the last sacral vertebra is preserved and articulated with the first and second caudal vertebrae (Fig. 2.11A-D). All of the preserved vertebrae retain unclosed neurocentral sutures. The centrum of the sacral vertebra has a large pleurocoel and shows caudal expansion increasing the height to meet the first caudal vertebra. There is a shallow craniocaudally elongate and groove-like depression on the ventral surface of the centrum. This depression covers the entire craniocaudal length of the centrum and is narrow at the cranial end and becomes wider caudally. On each side, there is one infraprezygapophyseal fossa and a slightly larger and triangular supraprezygapophyseal fossa, which respectively corresponds to the centroprezygapophyseal and spinoprezygapophyseal fossa of sauropods (Wilson et al., 2011). They are also separated from each other by a prominent lamina. In the case of sauropods, this lamina is known as prezygodiapophyseal lamina (Wilson, 1999). The robust sacral

rib broadens before it meets the ilium. The length of the sacral rib is more than 1.5 times that of the centrum. The neural spine is almost missing but there is a pair of small fossae near the base.

Caudal Vertebrae—The spool-shaped first caudal vertebra (Fig. 2.11) has a cranial articular end that is smaller than the caudal end. The centrum of the first caudal has a pleurocoel that is slightly more elongate but less circular. The prezygapophyses face medially and extend to a half the length of the last sacral. There are elliptical dorsal and ventral infraprezygapophyseal fossae, but the thin lamina between them is poorly preserved so that it is not possible to recognize any additional fossa on this lamina. In oviraptorids, the presence of an infraprezygapophyseal fossa on caudal vertebrae has only been reported for *Nankangia* but this taxon does not have more than one infrazygapophyseal fossa per side (Lü, Yi, et al., 2013). Dorsal to the infrazygapophyseal fossae, there is a deep supraprezygapophyseal fossa which is triangle-shaped as the one on the last sacral but larger. The transverse process is long and oriented caudolaterally but also shows slight dorsal orientation. Ventral to the transverse process is a large and triangular infradiapophyseal fossa which is also known in *Nankangia* (Lü, Yi, et al., 2013). The supraprezygapophyseal fossa and infradiapophyseal fossa get smaller in the following vertebrae but presents on every preserved caudal. There is a small protuberance with two low ridges on the caudoventral surface of the centrum. The second caudal vertebra has a concave cranial articular surface and flat caudal articular surface but the latter is poorly preserved. The craniocaudal length of the centrum is slightly shorter than that of the first caudal. The prezygapophyses extend over the mid length of the preceding centrum, but the cranial tip of the left

prezygapophysis is missing. The second caudal also has dorsal and ventral infraprezygapophyseal fossae, but the lamina between them is not preserved on the right side and it is barely visible on the left. It is not certain whether there is a middle infraprezygapophyseal fossa. The transverse process of the second caudal is sub-horizontal unlike that of the first caudal which is oriented caudolaterally. The two ridges on the ventral surface of the centrum are almost invisible. The third caudal vertebra is not preserved except for the prezygapophyses that reach the mid length of the centrum of the second caudal. The remaining seven caudal vertebrae (Fig. 2.11E, F) that are disarticulated with the proximalmost three caudals are articulated with each other. For convenience, these seven caudals are each designated here as caudal A to caudal G in a proximal to distal sequence. Although we do not know their exact positions, they are likely to be proximal caudals judging by their sizes and shape although three distalmost caudals may represent transitional or mid-caudals because the pleurocoels become substantially smaller than those of preceding caudals. Most of the seven caudals are heavily eroded on the right side in contrast to the relatively well preserved left side. Caudal A has three infraprezygapophyseal fossae. The middle infraprezygapophyseal fossa is slit-like and much smaller than the dorsal and ventral infraprezygapophyseal fossae. The neural spine is similar in morphology to that of the first caudal although it is missing its dorsal tip as well. As the second caudal the two ridges on the ventral surface of the centrum are extremely low and this is also the case for caudal B. Caudals B to G have only one infraprezygapophyseal fossa except for caudal E which has two infraprezygapophyseal fossae on the right side, so it is most likely that the thin lamina that divides the infraprezygapophyseal fossa was

lost for the other caudals due to poor preservation. Caudal B, in particular, has broken remnants of this lamina as a small bump and a ridge. Caudal B is generally similar in morphology to caudal A but the shape of its pleurocoel is more elliptical. Caudals C and D have a somewhat smaller infraprezygapophyseal fossa and pleurocoel compared to caudal B. The ventral surface of caudal C is obliterated, but caudal D has the two ventral ridges that are more prominent than those of preceding caudals on its centrum. These ridges become more pronounced in the following caudals. In caudal E, the centrum becomes low but its craniocaudal length is nearly the same as that of caudal D. The cranial articular surface is concave and the caudal one is obscured by matrix. Each pleurocoel is greatly reduced in size compared to that of preceding caudals. Caudal F has a pair of pleurocoels which are especially minute and almost indistinguishable. The caudal half of caudal G is missing. On each side, the centrum bears an elliptical pleurocoel, which is larger than that of caudals E and F. The infraprezygapophyseal fossae of caudal G are asymmetrical in size, the right one being much larger.

Chevrons—Fragmentary chevrons are preserved but are disarticulated from the caudal vertebrae (Figs. 2.12, 2.13) except for a small fragment which is articulated with caudals C and D (Fig. 2.11E). However, it does not provide much information in terms of its morphology. The preserved chevrons are craniocaudally narrow and proximodistally elongate. The most complete chevron (Fig. 2.13) is also the largest. The proximal articular surfaces are concave and separated from each other proximally (Fig. 2.13A-C) although it is possible that they were connected in life. The distal end this chevron is missing.

Pectoral Girdle and Forearm—The scapula (Fig. 2.14A-D) is not fused with

the coracoid and has a laterally everted acromion process whose dorsal surface is flat. The distal part of the scapular blade is missing, so the exact length of the scapula or whether there is a distal expansion is uncertain. The cross section of the preserved scapular blade is reversed tear shaped due to the relatively thick dorsal region. The glenoid is nearly flat and directed ventrally. A thick subtrapezoidal bone was nearly articulated with the scapula (Fig. 2.14E, F). It is interpreted as a coracoid in this thesis. The articular surface for the scapula is almost flat with a shallow depression. The glenoid fossa is poorly preserved, but it is slightly concave near the scapula. There are two ridges, each of which is on the opposite surface of the coracoid body and runs diagonally from the caudoventral margin. The humerus (Fig. 2.14G, H) has a round head which is medially expanded. The deltopectoral crest is broken off and the distal humerus is entirely missing.

Ilium—The ilium is dolichoiliac and has a straight dorsal margin (Fig. 2.15A, B). The right ilium is fragmentary preserving only the acetabular area and ventral region of the postacetabular process (Fig. 2.15C, D). The left ilium, however, is more complete but missing the caudal end of the postacetabular process. The preacetabular process has a round ventral margin and extends ventrally to the level below the dorsal margin of the acetabulum. A shallow cuppedicus fossa is present but not visible in lateral view. There is no supracetabular crest and an antitrochanter is weakly developed. The straight brevis shelf faces ventrally, which is not visible in lateral view. At its caudal end is the brevis fossa which is shallow but broad. The pubic peduncle is craniocaudally longer than the ichiadic peduncle unlike that of *Rinchenia mongoliensis* or *Heyuannia yanshini*.

Pubis—The pubis (Fig. 2.16) is greatly concave cranially and the articular

surface for the ilium is slightly depressed. Unfortunately, the pubic boot is missing in both pubes. The cross section of the pubic shaft is sub-triangular. The pubic apron is thin and narrow (Fig. 2.16E).

Ischium—The caudally concave ischium (Fig. 2.17) is similar in morphology to other oviraptorids (Osmólska et al., 2004; Balanoff and Norell, 2012; Norell et al., 2018). The medial surface of the ischium is flat in contrast to the lateral surface that has a concavity due to the obturator process. The thin obturator process is well developed but incomplete, so its exact shape is not inferable.

Femur—Both femora (Figs. 2.18, 2.19) are almost completely preserved. The femoral head is nearly perpendicular to the shaft, and the femoral neck is not distinct. A shallow depression separates the femoral head from the large greater trochanter which is also detached from the finger-like cranial trochanter by a prominent furrow. The shaft of the femur is moderately concave caudally and there is no sign of a fourth trochanter. The two distal condyles are well separated from each other by the large popliteal fossa. The lateral condyle extends ventrally below the level of the medial condyle. The tibiofibular crest is well developed and extends caudally beyond the caudal margin of the medial condyle (Fig. 2.19F). A weakly developed medial epicondyle is present on the craniomedial surface (Figs. 2.18D, 2.19A).

Distal Tarsals—The distal tarsal 3 and 4 are not fused with the metatarsals but closely attached to them (Fig. 2.20B-E). These tarsals are deeper at the plantar extremity and each has a flat proximal surface. The size of the two tarsals are comparable but the distal tarsal 3 is deeper than the distal tarsal 4. The distal tarsal 3 covers the metatarsals II and III, but the distal tarsal 4 only covers the metatarsal

IV.

Metatarsus—The metatarsals (Figs. 2.20, 2.21) do not show the arctometatarsalian condition and every metatarsal has a pair of ligament pits. Metatarsal I (Fig. 2.21) is strongly reduced and not articulated with the rest of the metatarsals. It has a dorsoplantar expansion at the middle. Its articular surface for the phalanx I-1 is triangular in distal view. The medial ligament pit is larger and deeper than the lateral one which is just a shallow depression. Metatarsal II is straight and slightly shorter than metatarsal IV. In proximal view, the articular surface of metatarsal II is the widest. Metatarsal II becomes proximally wider in dorsal view but the reverse is true in plantar view. It has a distinct ridge on the plantar surface of its shaft. The distal articular condyle for phalanx II-1 is larger than that of metatarsal IV, and the lateral ligament pit of metatarsal II is larger than the medial one unlike the rest of the metatarsals. Metatarsal III is the longest and visible along its entire length although its mediolateral width becomes narrower proximally in dorsal view. At the proximoplantar end of the shaft, metatarsal III has a prominent mound whose plantar surface is flat. The distal condyle of metatarsal III bears two ridges on its plantar surface. The medial ridge is more prominent than the lateral one. Metatarsal IV is straight proximally but the distal shaft is laterally deflected to a small degree. The shaft of metatarsal IV displays a rather continuous mediolateral width. It has a mound-like process on the proximoplantar end similar to that of metatarsal III but it is much smaller. The distal condyle is smaller than those of the metatarsals II and III and subtriangular in distal view. Metatarsal V (Fig. 2.20B-E) is thin and slightly curved dorsally at the distal end so it almost touches the metatarsal IV. It also meets metatarsal IV and the distal tarsal 4.

Pedal Digits—The digits I and IV are nearly completely preserved only without their distal ends of the unguals (Figs. 2.21, 2.22). The preserved pedal phalanges have symmetrical and ginglymoid interphalangeal joints. The pedal phalanx I-1 (Fig. 2.21) is asymmetrical having a distinct medial projection on the proximal end. It has a pair of shallow ligament pits that are similar in size and shape. The ungual of the pedal digit I has a minute tubercle right ventral to the proximal articular surface. The pedal digit II is not preserved. The pedal digit III preserves complete proximal two phalanges and the proximal part of phalanx III-3 (Fig. 2.20A, B, D, E). The phalanges of the digits III and IV have a pit on the dorsal surface right proximal to the distal end for the flexor muscles. A pair of similar-sized deep ligament pits are present on the medial and lateral surfaces of the distal condyles of the phalanges III-1 and III-2. The pedal digit IV has five phalanges including an ungual (Fig. 2.22). They have asymmetrical ligament pits, medial ones being larger and deeper than the lateral ones. The distal tip of the ungual is missing. The ungual is slightly curved ventrally with two distinct grooves on the medial and lateral surfaces (Fig. 2.22A, B). A short dorsal lip at the proximal end extends over the phalanx IV-4 (Fig. 2.22A-C).

PHYLOGENETIC ANALYSIS

The topology of the strict consensus tree (Fig. 2.23) is generally similar to that of Lü et al. (2017) with the better-resolved Caenagnathidae. The Mongolian oviraptorids are scattered across the subclades of the Oviraptoridae, some of them being closer to those from geographically far regions than other Mongolian species. This is also the case for the oviraptorid taxa from the Nanxiong Formation of Ganzhou in southern China (Lü et al., 2015, 2016, 2017). In addition, the strict consensus tree shows that *Gobiraptor minutus* belongs to the Oviraptoridae being the sister taxon to a clade composed of three Ganzhou oviraptorids: *Jiangxisaurus ganzhouensis* (Wei et al., 2013), *Banji long* (Xu and Han, 2010), and *Tongtianlong limosus* (Lü et al., 2016). These three Ganzhou taxa and *Gobiraptor* also form a small clade which is supported by the following three synapomorphies: premaxillae that have a significant ventral projection below the ventral margin of the maxillae (character 7, state 1), a vomer that is level with other palatal elements (character 222, state 0), and the same pattern of the distal ends of the shafts of metatarsals II and IV with a straight metatarsal II and a laterally deflected metatarsal IV (character 252, state 2).

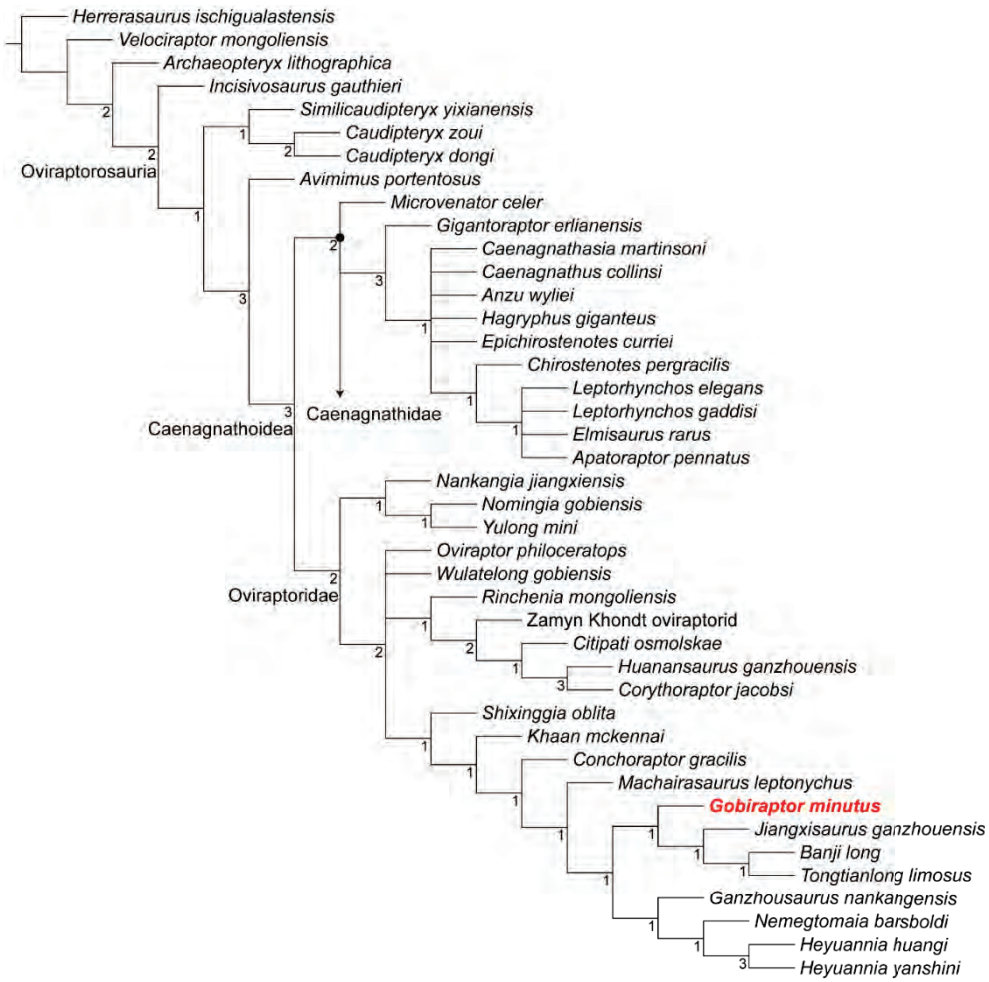

FIGURE 2.23. Strict consensus (CI: 0.448, RI: 0.647) of the 24 most parsimonious trees of 652 steps obtained by TNT based on the data matrix of 42 taxa and 257 characters. Numbers at each node indicate Bremer support values.

OSTEOHISTOLOGY OF *GOBIRAPTOR MINUTUS*

Although there are some diagenetic alterations in the bone tissue, the histological structure is still reasonably well preserved (Fig. 2.24). The maximum cross sectional width of the bone is about 2 cm. A narrow compact bone wall (~4 mm) surrounds a large vacant medullary cavity. The bone wall comprises essentially of fibrolamellar bone tissue (Fig. 2.24B), and there is a distinctive large nutrient foramen evident (Fig. 2.24A, B) in the compacta. The foramen is lined by a narrow band of lamellar bone tissue. The woven bone matrix of the bone wall is inundated by many canals (that house vascular tissue, as well as other connective tissue) (Starck and Chinsamy, 2002). Many well-formed primary osteons are present in the cortex, but many of the canals of the primary osteons formed during earlier stages of ontogeny (nearest the medullary cavity) are enlarged due to resorption, which give the bone a rather cancellous texture (Fig. 2.24A). The canals tend to have variable orientations that range from longitudinal to circumferential, as well as some with more radial arrangements (relative to the long axis of the bone). In some areas of the more recently formed periosteal bone (nearest the peripheral margin), there appears to be a transition to a more laminar arrangement, which is indicative of a localized change to a slower rate of bone deposition. In a small section of the lateral bone wall the vascular canals appear to follow a radial transect from the endosteal region towards the outside (although the outermost part of the bone wall is not preserved). This arrangement most likely corresponds to a muscle attachment site (Chinsamy-Turan, 2005).

The medullary cavity is large, and it has a distinctive uneven, resorptive

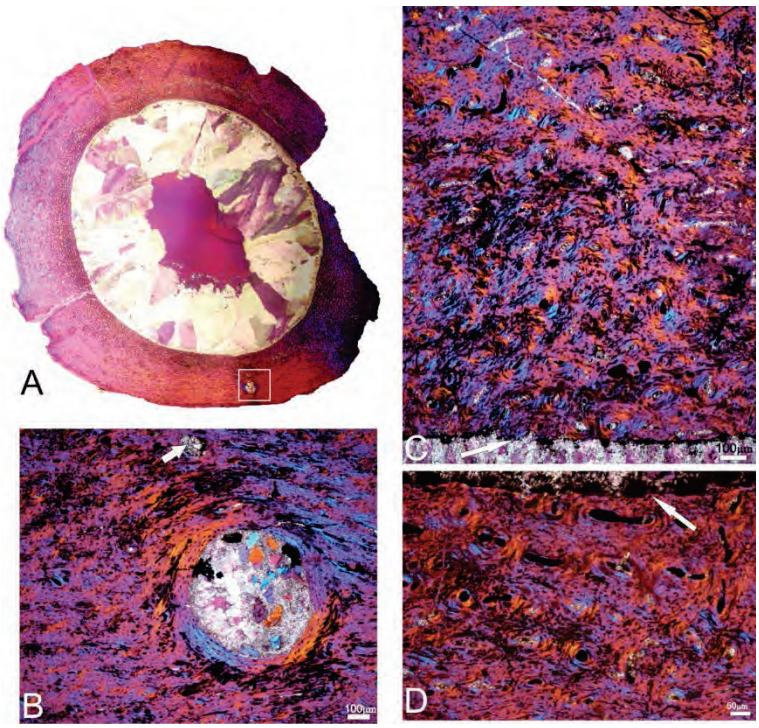

FIGURE 2.24. Femoral osteohistology of the holotype specimen of *Gobiraptor minutus* gen. et sp. nov. (MPC-D 102/111). **A**, Transverse section from the mid-shaft of the right femur. The maximum diameter of the cross section is 2 cm. A distinctive layer of compact bone surrounds the large medullary cavity. Note the large number of open spaces in the bone wall, which are the vacant canals that become infilled with lamellar bone to form primary osteons during later stages of ontogeny. **B**, A higher magnification of the framed region in **A** showing the large nutrient foramen in the bone wall. The white arrow points to a large erosion cavity. **C**, Endosteal region of the bone matrix. This section shows the endosteal margin (white arrow) of the bone wall, showing its resorptive nature. **D**, Peripheral region of the bone matrix. The white arrow points to the peripheral margin of the bone wall, which shows that osteogenesis is still ongoing. Well-developed primary osteons are clearly visible in this region.

margin (Fig. 2.24A, C), suggesting that medullary expansion was still underway. Although the periosteal surface of the bone is not well preserved across the entire section, it is evident that rapid appositional bone deposition was still underway in this individual. It is noteworthy that secondary reconstruction is at a very early stage of development with many canals secondarily enlarged although no secondary osteons are present in the compacta (Chinsamy-Turan, 2005). One of the larger resorption cavities occurs near the large nutrient foramen (Fig. 2.24B). No growth marks (annuli or lines of arrested growth) are present in the compacta.

II-4. DISCUSSION

Implications of the Unique Mandibular Morphology of *Gobiraptor minutus*

The mandible of *Gobiraptor* (Figs. 2.8, 2.10) has typical oviraptorid characters such as a short and deep dentary, a tall external mandibular fenestra, a prominent coronoid process, and a rostroventral process of surangular protruding into the external mandibular fenestra. However, the symphyseal shelf of *Gobiraptor* is very unusual in that it is thick along its entire rostroocaudal length. This peculiar morphology of the symphyseal shelf and the presence of lingual shelves and ridges are not known in other oviraptorids, but similar structures exist in derived caenagnathids (Osmólska et al., 2004; Longrich et al., 2013; Funston and Currie, 2014; Lamanna et al., 2014; Sues and Averianov, 2015; Tsuihiji et al., 2016; Ma et al., 2017). This resemblance between *Gobiraptor* and the derived caenagnathids may be a result of convergence. Nevertheless, the symphyseal region of *Gobiraptor* is certainly distinguished from that of caenagnathids namely by its strongly downturned form, the absence of occlusal grooves on the symphyseal shelf, unfused mandibular symphysis, the rostrodorsally directed rostral tip, the continuous surface of the symphyseal shelf, not as extensively developed lingual shelves, and much shallower lingual ridges although some of these could be subject to ontogenetic changes. Thus, the mandibular structure of *Gobiraptor* may represent an intermediate state between that of other oviraptorids and derived caenagnathids as in case of *Gigantoraptor* which, however, does not have a thick symphyseal shelf and lacks lingual ridges or occlusal grooves (Ma et al., 2017). This distinct jaw morphology of *Gobiraptor* could be related to its specialized

diets. While the diets of oviraptorosaurs are still puzzling, it has been suggested that oviraptorids were likely to be durophagous, eating eggs or mollusks (Osborn, 1924; Barsbold, 1977, 1983, 1986; Currie et al., 1993) or they might be herbivores (Smith, 1992; Longrich et al., 2010; Zanno and Makovicky, 2011; Lü, Yi, et al., 2013; Lü, Currie, et al., 2013) and could be specialized for eating nuts and seeds like extant psittaciform birds (Funston et al., 2018a) although Longrich et al. (2010) argued that oviraptorid jaws were more suitable for shearing plants rather than crushing hard shells. Herbivory has been proposed for caenagnathids as well (Zanno and Makovicky, 2011; Longrich et al., 2013), but Lamanna et al. (2014) concluded that it is most appropriate to view caenagnathids as ecological generalists. Furthermore, Funston and Currie (2014) noted that *Chirostenotes*, a derived caenagnathid, was probably an omnivore capable of processing meat as well as plant leaves with the sharp edges of rhamphothecae. Caenagnathids also possess hind limbs that are suited for a cursorial lifestyle (Currie, 1990; Funston, Currie and Burns, 2016) that could have been helpful in chasing prey. On the contrary, the non-arctometatarsalian foot of *Gobiraptor* is not effective in fast running (Holtz, 1995), meaning that active hunting is highly doubtful for this taxon. Instead, durophagy or granivory or possibly both modes of feeding would have been suitable for *Gobiraptor* judging by the unusual structure of the dentary. Hard food items could be crushed by its massive symphyseal shelf with assistance from the lateral occlusal grooves on the lingual shelves and the propalinal movement of the jaw joint. Consequently, *Gobiraptor* probably had different diets and occupied a different specific dietary niche from derived caenagnathids or other Nemegt oviraptorids. The unique morphology of the mandible and accordingly

inferred specialized diets of *Gobiraptor* also indicate that different dietary strategies may be one of important factors linked with the remarkably high diversity of oviraptorids in the Nemegt Basin. Future discoveries and works on more oviraptorid specimens will be of great help in estimating their exact feeding habits.

Insights from the Femoral Osteohistology of *Gobiraptor minutus*

The overall primary nature of the bone compacta with abundant fibrolamellar bone tissue, the uneven, osteogenic periosteal margin and the resorptive endosteal margin of the bone wall, as well as the early onset of secondary reconstruction without any secondary osteons are features that all suggest that the holotype specimen of *Gobiraptor minutus* was at an early stage of ontogeny (see Fig. 2.24). This histological finding is congruent with the anatomical observations of closed neurocentral sutures of the preserved vertebrae.

Phylogenetic Position of *Gobiraptor minutus*

The position of *Gobiraptor* on the strict consensus tree (Fig. 2.23) indicates that *Gobiraptor* is a derived oviraptorid and closer to three Ganzhou oviraptorids *Jianxisaurus*, *Banji*, and *Tongtianlong* than to others from the Nemegt or Baruungoyot formations such as *Nemegtomaia* or *Conchoraptor*. This kind of discordance between the geographical and phylogenetic distances is prevalent among oviraptorids from Mongolia or southern China as shown by the strict consensus tree as well as in recent studies (Lü et al., 2015, 2016, 2017; Funston and Currie, 2016), implying that sympatric speciation was not a major factor in the

evolution of oviraptorids in these regions (Funston et al., 2018a). Although they form a distinct subclade, *Gobiraptor* is clearly distinguished from *Jianxisaurus*, *Banji*, and *Tongtianlong* which together form another subclade. Most notably, the morphology of the mandible, especially of the dentary, of *Gobiraptor* is distinctively different from those of the other three taxa. One of the most prominent differences is the extent to which the symphyseal region of the dentary is downturned. *Gobiraptor* has a greatly downturned symphyseal region but in case of *Jianxisaurus*, it is marginally downturned (Wei et al., 2013) and it is nearly straight in *Banji* and *Tongtianlong* (Xu and Han, 2010; Lü et al., 2016). The femoral osteohistology of the holotype specimen of *Gobiraptor minutus* also suggests that it did not reach maturity before death. Therefore, it is highly unlikely that the morphological differences between *Gobiraptor* and its three closest relatives represent ontogenetic variation but are best explained by a rapid adaptive radiation of the Ganzhou oviraptorids (Lü et al., 2016). However, the low Bremer support value of this subclade implies that it is weakly supported, and future studies may find alternative phylogenetic relationships among these four taxa. *Gobiraptor* also represents the first oviraptorid taxon from Altan Uul III. The absence of *Gobiraptor* specimens from other localities might be a result of sampling bias, but it has been noted that each species of Nemegt oviraptorids has occurred only in one locality in spite of high diversity (Longrich et al., 2010; Funston et al., 2018a). Thus, it appears to be reasonable to assume that most oviraptorid taxa, if not all, from the Nemegt Formation were separated from each other spatially or temporally as Funston et al. (2018a) indicated. The reason behind this is uncertain although niche partitioning (Lyson and Longrich, 2011; Mallon et

al., 2013; Mallon and Anderson, 2014, 2015) or high species turnover in a short time interval (Alfaro et al., 2009; Mallon et al., 2012) might have played a role (Funston et al., 2018a). The distant phylogenetic relationships among Nemegt oviraptorids, therefore, imply that the evolutionary history of this diverse family in the Nemegt region might be more complicated.

Paleoecology and Diversity of Oviraptorids in the Nemegt Basin

The Nemegt and Baruungoyot formations in the Nemegt Basin are rich with oviraptorids (Barsbold, 1976a, 1981, 1983, 1986; Barsbold et al., 2000; Lü et al., 2004; Osmólska et al., 2004; Weishampel et al., 2008; Fanti et al., 2012) as well as other dinosaur taxa (Funston et al., 2018b). Whereas the Nemegt Formation was mostly formed by fluvial, alluvial plain, paludal, and lacustrine deposits indicating mesic environments (Gradziński, 1970; Gradziński et al., 1977; Eberth, 2018), the Baruungoyot Formation includes eolian deposits in addition to those mentioned above and has been interpreted to represent drier environments (Gradziński and Jerzykiewicz, 1974a, 1974b; Eberth, 2018). Previous works showed that these two formations interfinger at Hermiin Tsav and Nemegt area forming successive stratifications (Gradziński et al., 1977; Jerzykiewicz and Russell, 1991; Eberth, Badamgarav, et al., 2009; Eberth, 2018), the latter locality producing *Nemegtomaia* from the beds of both formations (Fanti et al., 2012). The distribution of oviraptorids in the Nemegt Basin is thus different from those of avimimids or Nemegt caenagnathids, which are known only from the Nemegt Formation (Kurzanov, 1981; Osmólska, 1981; Funston, Currie, Eberth, et al., 2016; Tsuihiji et al., 2016, 2017; Funston et al., 2018a). Although it was suggested that oviraptorids

preferred xeric environments because of their abundance in the Baruungoyot and Djadochta formations (Longrich et al., 2010; Tsuihiji et al., 2016; Funston et al., 2018a), the presence of multiple oviraptorid taxa in the Nemegt Formation showed that they were also well adapted to wet environments (Funston et al., 2018a). The discovery of *Gobiraptor* and associated fragmentary oviraptorid specimens confirms this notion. In addition, oviraptorid diversity in the Nemegt Basin is increased by *Gobiraptor* to six taxa not including the unnamed Guriliin Tsav oviraptorid (Funston et al., 2018a) although *Nomingia* has been thought to be a possible caenagnathid in several previous studies (Barsbold et al., 2000; Osmólska et al., 2004; Funston et al., 2018a) despite its phylogenetic position in the results of many others (Lamanna et al., 2014; Lü et al., 2015, 2016, 2017; Funston and Currie, 2016). The reason behind this remarkable diversity of oviraptorids is still a mystery, although it is apparent that they diversified in a short time span and prospered in both dry and wet environments.

II-5. CONCLUSIONS

Gobiraptor minutus gen. et sp. nov. is a new derived oviraptorid represented by an incomplete skeleton including both cranial and postcranial elements. *Gobiraptor* is primarily distinguished from other oviraptorids by its dentary with the massive symphyseal shelf and accessory lingual shelves bearing occlusal grooves. The unique morphology of the mandible of *Gobiraptor* is probably closely related to a crushing-related feeding style and a specialized diet, which may have incorporated hard seeds or shelled organisms. Although *Gobiraptor* was recovered from the Nemegt Formation, its phylogenetic position showed a close relationship with three Ganzhou oviraptorids. The distant relationships among the Nemegt oviraptorids on the phylogenetic tree were reaffirmed in this study. Therefore, it is highly unlikely that the evolution of these unusually diverse animals was facilitated by a simple sympatric speciation. The presence of *Gobiraptor* in the Nemegt Formation, together with occurrences of other oviraptorids, also indicates that abundant oviraptorids lived in mesic environments and they were one of the most diverse and successful groups of dinosaurs in the Nemegt region.

CHAPTER III

A NEW ALVAREZSAURID DINOSAUR

NEMEGTONYKUS CITUS GEN. ET SP. NOV.

III-1. INTRODUCTION

Alvarezsaurids are an extraordinary group of animals characterized mainly by greatly reduced lengths of forelimbs with the enlarged medialmost manual digit and contrastingly elongate distal hindlimbs with specialized arctometatarsal conditon in derived forms (Perle et al., 1993, 1994; Novas, 1996; Chiappe et al., 2002; Longrich and Currie, 2009; Xu et al., 2010, 2011; Agnolin et al., 2012; Xu, Upchurch, et al., 2013). They occur on nearly every continent, but most taxa are from either Asia or South America with fragmentary specimens from North America and Europe (Table 3.1; Bonaparte, 1991; Perle et al., 1993; Karhu and Rautian, 1996; Novas, 1996; Chiappe et al., 1998; Chiappe and Coria, 2003; Naish and Dyke, 2004; Martinelli and Vera, 2007; Alifanov and Barsbold, 2009; Longrich and Currie, 2009; Salgado et al., 2009; Turner et al., 2009; Xu et al., 2010, 2011; Nesbitt et al., 2011; Agnolin et al., 2012; Hone et al., 2013; Pittman et al., 2015; Averianov and Sues, 2017). Despite their wide distribution across the globe, no complete alvarezsaurid remain has been reported, contributing to the difficulty in interpretation of their ecology and phylogenetic relationships. The origin of alvarezsaurids has also been rather confusing. It was thought that they originated from South America (Novas, 1996; Hutchinson and Chiappe, 1998; Longrich and

TABLE 3.1. List of alvarezsaurids.

Taxon	Country	Formation	Locality	Age	References
Albertonykus borealis	Canada	Horseshoe Canyon Formation	Dry Island, Buffalo Jump Provincial Park, Alberta	Maastrichtian	Longrich and Currie, 2009
Alvarezsauridae indet.	USA	Hell Creek Formation	UCMP locality V80092, known as the Sandstone Basin, eastern Montana	Maastrichtian	Hutchinson and Chiappe, 1998
Bonapartenykus ultimus	Argentina	Allen Formation	Salitral Ojo de Agua, Río Negro Province	Campanian-Maastrichtian	Agnolin et al., 2012
Alvarezsaurus calvoi	Argentina	Bajo de la Carpa Formation	Neuquén City, Neuquén Province	Santonian	Bonaparte, 1991
Achillesaurus manazzonei	Argentina	Bajo de la Carpa Formation	Paso Córdova locality, Río Negro Province	Santonian	Martinelli and Vera, 2007
Patagonykus puertai	Argentina	Portezuelo Formation	Sierra del Portezuelo, Neuquén Province	Turonian	Novas, 1996; Chiappe and Coria, 2003
Alnashetri cerropoliciensis	Argentina	Candeleros Formation	La Buitrera, Río Negro Province	Cenomanian-Turonian	Makovicky et al., 2012

Taxon	Country	Formation	Locality	Age	References
Alvarezsauridae indet.	Romania	Sânpetru Formation	Haţeg, Transylvania	Maastrichtian	Harrison and Walker, 1975; Naish and Dyke, 2004
Alvarezsauridae indet.	Uzbekistan	Bissekty Formation	Dzharakuduk, central Kyzylkum Desert	Turonian	Averianov and Sues, 2017
Xixianykus zhangi	China	Majiacun Formation	Zhoujiagou, Yangcheng, Xixia County, Henan Province	Coniacian-Santonian	Xu et al., 2010
Linhenykus monodactylus	China	Wulansuhai (Bayan Mandahu) Formation	'Gate Locality', Bayan Mandahu	Campanian	Xu et al., 2011
Parvicursorinae indet.	China	Wulansuhai (Bayan Mandahu) Formation	Bayan Mandahu	Campanian	Pittman et al., 2015
Shuvuuia deserti	Mongolia	Djadochta Formation	Ukhaa Tolgod and Tugrikin-Shire	Campanian	Chiappe et al., 1998, 2002; Suzuki et al., 2002
Kol ghuva	Mongolia	Djadochta Formation	Ukhaa Tolgod	Campanian	Turner et al., 2009

Taxon	Country	Formation	Locality	Age	References
Parvicursor remotus	Mongolia	Baruungoyot Formation	Khulsan	Campanian-Maastrichtian	Karhu and Rautian, 1996
Ceratonykus oculatus	Mongolia	Baruungoyot Formation	Hermiin Tsav	Campanian-Maastrichtian	Alifanov and Barsbold, 2009
Albinykus baatar	Mongolia	Javkhlant Formation	Shine Us Khudag redbeds at Khugenetslavkant	?Santonian–Campanian	Nesbitt et al., 2011
Mononykus olecranus	Mongolia	Nemegt Formation	Bugiin Tsav	Maastrichtian	Perle et al., 1993
Nemegtonykus citus gen. et sp. nov.	Mongolia	Nemegt Formation	Altan Uul III	Maastrichtian	This study

Currie, 2009). However, the discovery of *Haplocheirus sollers* has cast doubt on the Gondwanan origin of alvarezsaurids (Choiniere et al., 2010).

Their somewhat peculiar morphology, which is strikingly similar to that of birds, has caused extensive debate regarding their place on the tree of life (Perle et al., 1993, 1994; Chiappe, 1995; Zhou, 1995; Chiappe et al., 1996, 1997, 1998, 2002; Forster et al., 1996; Ji et al., 1998; Sereno, 1999a, 1999b; Novas and Pol, 2002; Suzuki et al., 2002; Padian, 2004; Longrich and Currie, 2009; Turner et al., 2009; Choiniere et al., 2010, 2014; Xu et al., 2010, 2011; Agnolin et al., 2012; Xu, Upchurch, et al., 2013). Even ornithomimid affinity of alvarezsaurids has been proposed (Sereno, 1999a, 1999b, 2001) and refuted (Suzuki et al., 2002). As more specimens are included in analyses, especially that of the basalmost alvarezsaur *Haplocheirus*, they are generally thought to be the most basal maniraptans in recent studies (Choiniere et al., 2010, 2014; Xu et al., 2010, 2011; Agnolin et al., 2012; Xu, Upchurch, et al., 2013; Lee et al., 2014; Cau et al., 2015; Hendrickx et al., 2015; Cau, 2018; Cau and Madzia, 2018).

The highly modified forelimbs in alvarezsaurids have been as much puzzling as their origin and relationships. In alvarezsaurids, the humerus is greatly reduced in length, but instead it is stout and robust with a well-developed deltopectoral crest (Perle et al., 1994; Chiappe et al., 2002). The ulna is also very exceptional in alvarezsaurids, characterized by a hypertrophied olecranon process (Perle et al., 1994; Chiappe et al., 2002). One of the most conspicuous specializations of alvarezsaurids is observed in hands. The carpometacarpus is fused in varying degrees among taxa, and the medialmost manual phalanges including the claw became massive whereas the lateral digits were reduced in size and sometimes lost

entirely (Perle et al., 1994, Chiappe et al., 2002; Xu et al., 2011). Consequently, alvarezsuarids have been depicted with an extremely short forelimbs and one functional digit with a large claw (Perle et al., 1993; Chiappe et al., 1996; Novas, 1997; Longrich and Currie, 2009; Xu et al., 2011; Xu, Upchurch, et al., 2013). The function of the stout forearms and hands have been a subject of heated debate, and digging is generally accepted as their primary role (Perle et al., 1993, 1994; Zhou, 1995; Chiappe et al., 2002; Senter, 2005; Longrich and Currie, 2009).

From the Nemegt Formation, only one specimen of an alvarezsaurid has been reported (Perle et al., 1993). In contrast, the nearby Baruungoyot and Djadochta formations, both of which are exposed in the Nemegt Basin as is the Nemegt Formation, have yielded four alvarezsaurid taxa in total, and some of them are even represented by multiple specimens (Fig. 3.1; Karhu and Rautian, 1996; Chiappe et al., 1998, 2002; Suzuki et al., 2002; Turner et al., 2009). Similarly, oviraptorids are more abundant in Baruungoyot and Djadochta formations which have been regarded to be comprised of eolian deposits (Gradziński and Jerzykiewicz, 1974a, 1974b; Eberth 2018) than in the fluvial Nemegt Formation (Gradziński 1970; Gradziński et al., 1977; Eberth 2018; Funston et al., 2018a). As an explanation, it was suggested that oviraptorids preferred dry environments to wet ones (Longrich et al., 2010; Tsuihiji et al., 2016; Funston et al., 2018a). If this logic could be applied to alvarezsaurids, they could have a similar taste in habitats. However, oviraptorids are also plentiful in the Nemegt Formation (Funston et al., 2018a; see also Chapter II-4), and there are too few specimens of alvarezsaurids to determine their habitat preference. In addition, more than one individuals of alvarezsaurid specimens have been found from the same site in Altan Uul III (Nemegt

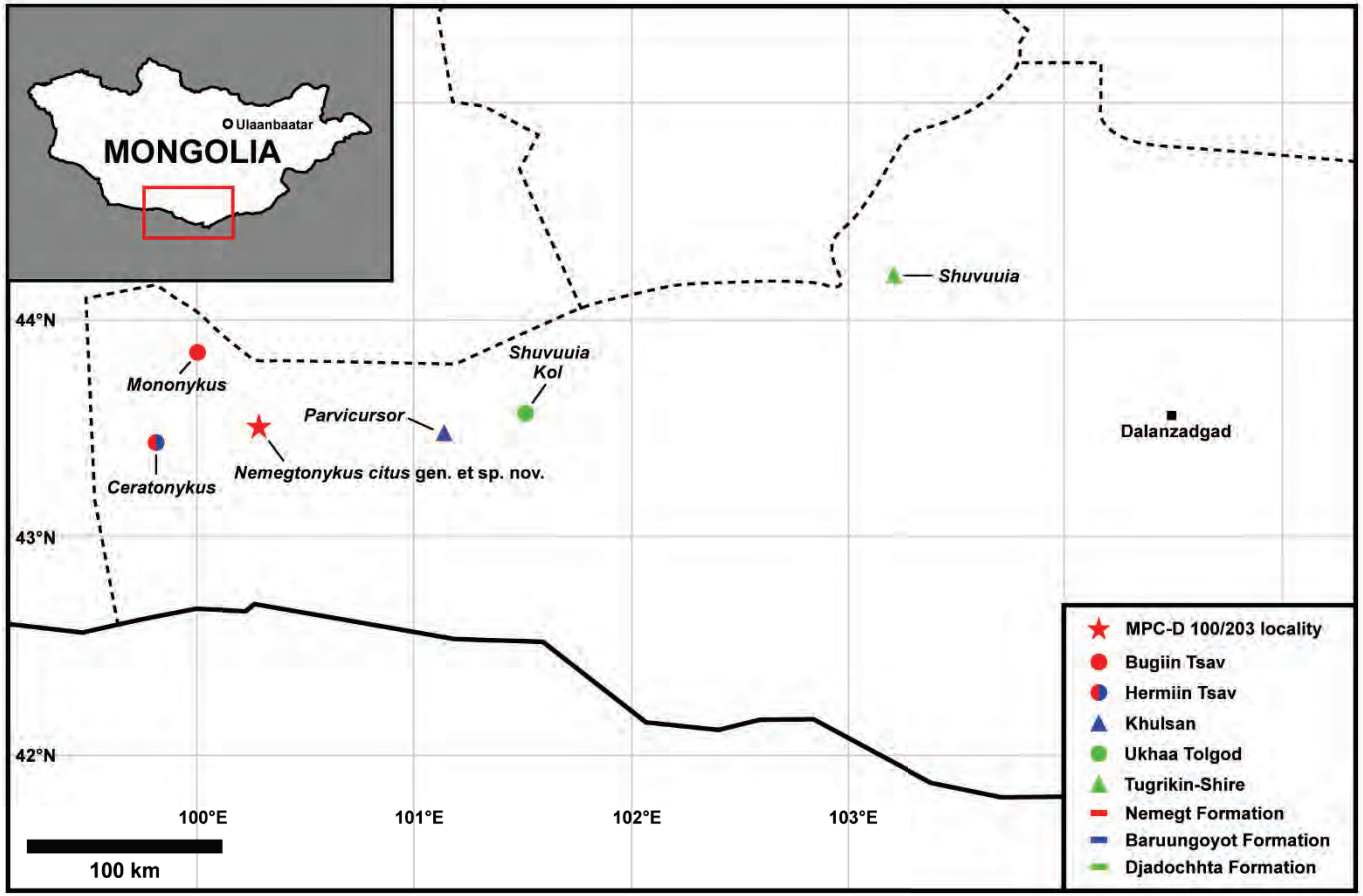

FIGURE 3.1. Map showing the occurrences of alvarezsaurids in the southern Gobi Desert of Mongolia. The magnified map was generated using Simplemappr (www.simplemappr.net) before modified.

Formation) during the KID in 2008 (see Chapter I-1) although the presence of alvarezsaurids in the excavated matrix was recognized later. They were associated with oviraptorid specimens (see Chapter II), and one alvarezsaurid specimen represents a novel taxon having a distinctive combination of characters including several autapomorphies. This new alvarezsaurid, *Nemegtonykus citus* gen. et sp. nov., is here described and analyzed in the phylogenetic and morphological contexts.

III-2. METHODS

Fossil Preparation and Image Creation

The alvarezsaurid specimen MPC-D 100/203 was prepared with the same instruments which were also used for the preparation of MPC-D 102/111, the holotype specimen of *Gobiraptor minutus*. The places where the preparation was conducted and the manners of preparation were also identical (see chapter II-2 for detailed preparation methods).

Images in this chapter were also created in the same way as done in the Chapter II.

Phylogenetic Analysis

In order to obtain the phylogenetic relationship of *Nemegtonykus citus*, a phylogenetic analysis was performed. The terminal taxa, character lists, and data matrix used in the analysis were from those of Agnolin et al. (2012) whose dataset was also based on that of Choiniere et al. (2010), and they were not modified except for the inclusion of *Nemegtonykus citus* to the data matrix (see Appendices 3, 4 for the full character list and data matrix). A total of 104 taxa with 423 unordered characters of an equal weight were included in the data matrix and analyzed by using TNT version 1.5 (Goloboff and Catalano, 2016). A traditional search (Wagner trees with 1000 random seeds and 10 random-addition-sequence replications, Tree bisection and reconnection (TBR) algorithm for the swapping algorithm, and 100 trees to save per replication) was implemented to produce 300 most parsimonious trees with 1915 steps. The consistency index (CI) was 0.272

and the retention index (RI) was 0.645. A consensus tree was then generated, and the Bremer support values for each node of the consensus tree was acquired by utilization of the 'Bremer.run' script as done for *Gobiraptor minutus* in chapter II. Winclada version 1.00.08 (Nixon, 2002) and Adobe Illustrator CC 2018 were also used to create the image of the phylogenetic tree.

III-3. RESULTS

SYSTEMATIC PALEONTOLOGY

DINOSAURIA Owen, 1842

THEROPODA Marsh, 1881

MANIRAPTORA Gauthier, 1986

ALVAREZSAURIA Bonaparte, 1991

ALVAREZSAURIDAE Bonaparte, 1991

PARVICURSORINAE Karhu and Rautian, 1996

MONONYKINI Chiappe, Norell, and Clark, 1998

NEMEGTONYKUS CITUS, gen. et sp. nov.

(Figs. 3.2-11)

Holotype—MPC-D 100/203, incomplete and partially disarticulated postcranial elements with two caudalmost dorsal vertebrae in articulation with two cranialmost sacral vertebrae, a partial caudal series including twenty-one consecutive vertebrae which are articulated with fragmentary chevrons, four dorsal ribs, two nearly complete chevrons, a nearly complete left scapulocoracoid, a nearly complete left ilium, a partial left pubis, fragmentary pelvic girdle elements, a complete left femur, a complete left tibiotarsus, a nearly complete left tarsometatarsus which is comprised of a distal tarsal fused with metatarsals II and IV.

Locality and Horizon—Altan Uul III (Gradziński et al., 1968, 1977;

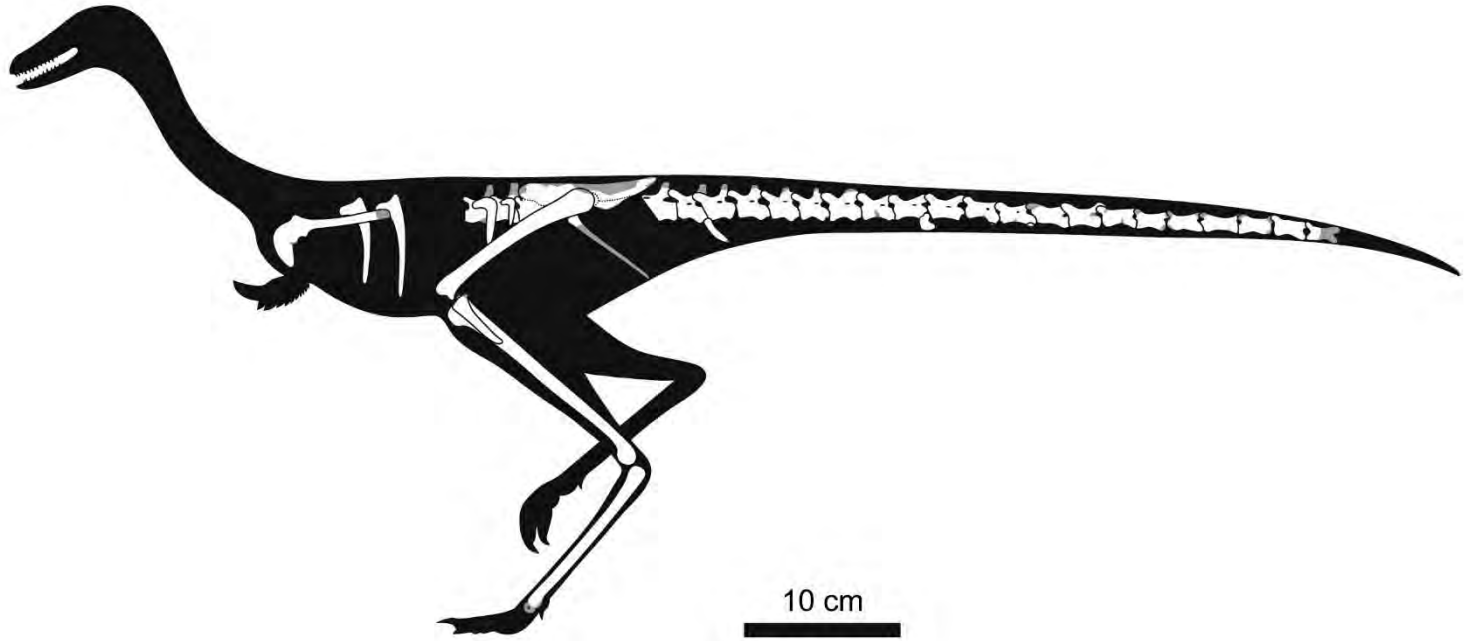

FIGURE 3.2. Skeletal and silhouette reconstruction of *Nemegtonykus citus* gen. et sp. nov. Missing parts in gray.

Gradziński, 1970; Watabe et al., 2010; Eberth, 2018), Ömnögovi Province, Mongolia (Fig. 3.1). Upper Cretaceous Nemegt Formation (Gradziński et al., 1968, 1977; Gradziński, 1970; Jerzykiewicz and Russell, 1991; Khand et al., 2000; Eberth, 2018).

Etymology—The generic name refers to the Nemegt Formation (the origin of the holotype specimen) and onyx ('claw' in Greek); specific name means 'swift' in Latin, referring to the hypothesized cursorial lifestyle of this taxon.

Diagnosis—Mononykin alvarezsaurid of moderate size distinguished by the following unique set of characters (autapomorphies with asterisk): completely fused first and second sacral vertebrae; first sacral vertebra with a craniocaudally elongate and semi-trapezoidal lamina formed by the transvere process-sacral rib complex and neural arch, which is fused to the preacetabular part of the ilium* (similar to *Xixianykus*); fusion between the second sacral centrum and preacetabular part of the ilium without visible sacral rib*; fused scapulocoracoid (also present in *Linhenykus*); cranially reduced pubic peduncle; caudodorsally oriented postacetabular process of the ilium*; a distinct fossa on the dorsal surface of the ilium near the antitrochanter (also present in *Xixianykus*); greatly reduced medial and lateral condyles at the distal end of the femur*; coossification between distal tarsal and the metatarsus (also present in *Xixianykus* and *Albinykus*); partial fusion of the metatarsals II and IV at the plantar surface of the distal shafts without any suture*.

Differential Diagnosis—*Nemegtonykus citus* is different from *Mononykus olecranus* (Perle et al., 1993, 1994) in that scapula and coracoid are fused together, acromion process of scapula is more symmetrical in lateral view, pubic peduncle of

the ilium is more reduced and tubercle-like, medial and lateral condyles at the distal end of the femur are reduced to a large extent, popliteal fossa is completely open and less prominent, the distal tarsal is fused with the metatarsus, and there is no collateral ligament fossa on the distal articular end of the metatarsal IV.

Nemegtonykus citus differs from *Shuvuuia deserti* (Chiappe et al., 2002; Suzuki et al., 2002) in that *Nemegtonykus* has fused scapula and coracoid, first sacral vertebra with a semi-trapezoidal lamina which is fused with the preacetabular process of ilium, and second sacral centrum fused with the ilium. In addition, postacetabular process of the ilium is more dorsally oriented, tibial shaft is straight, there is a deeper excavation at the medial margin of the ascending process of the astragalus, ascending process of the astragalus reaches the medial end of the medial condyle of tibiotarsus at its base, tibia and astragalocalcaneum are broadly coossified, a thin spine at the distal end of the fibula is absent, and the distal tarsal metatarsus are coossified.

Nemegtonykus citus is mainly differentiated from *Parvicursor remotus* (Karhu and Rautian, 1996; Chiappe et al., 2002) by dorsally extending postacetabular process of the ilium, less cranial curvature of the femoral shaft, weak fourth trochanter of the femur (absent in *Parvicursor*), straight shaft of tibiotarsus, prominent ridge on the distolateral end of the tibial shaft, deeply excavated medial margin of the ascending process of the astragalus, and fusion between the distal tarsal and metatarsus.

Nemegtonykus citus is distinguished from *Ceratonykus oculatus* (Alifanov and Barsbold, 2009) by absence of any crest on the dorsal surface of the postacetabular process of the ilium, less bowed femoral shaft, relatively much longer femur

compared to the tibiotarsus or tarsometatarsus, not curved proximal shaft of the tibiotarsus, partial fusion between the shafts of metatarsals II and IV near the distal divergence, and the slightly deflected distal end of the metatarsal IV in lateral direction.

Nemegtonykus citus primarily differs from *Albinykus baatar* (Nesbitt et al., 2011) in that the shaft of the tibiotarsus is straight, there is a prominent ridge on the distolateral end of the tibial shaft, tibia and astragalocalcaneum are coossified to a lesser degree, there is no groove on the ascending process of the astragalus, the crest on the lateral surface of the fibula for the attachment of M. iliofibularis is proportionally less developed, the shafts of metatarsals II and IV are straight in contrast to slightly bowed ones of *Albinykus*, and the distal shafts of metatarsals II and IV are partially coossified.

Nemegtonykus citus differs from *Xixianykus zhangi* (Xu et al., 2010) in that the second sacral vertebra does not contribute to the lamina formed by transverse process-sacral rib complex and neural arch in the first sacral, second sacral centrum is directly fused with the ilium, postacetabular process of the ilium shows caudodorsal orientation, pubic peduncle of the ilium is greatly reduced, femoral shaft is curved to a lesser degree, femur bears a completely open popliteal fossa, distal condyles of the femur are much reduced, medial condyle on the proximal end of the tibiotarsus proximally protrudes beyond the level of the cnemial crest, there is no lateral tuber on the lateral condyle of the femur, ectocondylar tuber is less prominent, distal end of the tibial shaft lacks lateral protrusion, and the fibula is straight.

Nemegtonykus citus is also distinguished from *Linhenykus monodactylus* (Xu

et al., 2011; Xu, Upchurch, et al., 2013) by subcircular articular surfaces of dorsal centra (subtriangular in *Linhenykus*), opisthocoelous penultimate dorsal centrum (biconvex in *Linhenykus*), convex cranial articular surface of the last dorsal centrum (concave in *Linhenykus*), less prominent ventral keel of the last dorsal centrum, no ventral groove on the preserved sacral centra, prominently developed glenoid lip, lateral ridge bordering the popliteal fossa on the caudal surface of the distal femoral shaft being more prominent than the medial ridge (reverse in *Linhenykus*), greatly reduced medial and lateral condyles at the distal end of the femur, no accessory crest on the fibular condyle of the tibiotarsus, coossified distal tarsal and metatarsus, and partially fused the metatarsals II and IV at the plantar surface of the distal shafts.

DESCRIPTION

The holotype specimen of *Nemegtonykus citus* (MPC-D 100/203) is generally smaller than that of *Mononykus* (Perle et al., 1994), but larger than specimens of *Parvicursor* (Karhu and Rautian, 1996) and *Shuvuuia* (Suzuki et al., 2002). The estimated body weight of MPC-D 100/203 inferred from the mid-shaft circumference of the femur based on the equation of Campione et al. (2014) is approximately 2.9 kg.

Axial Skeleton

The total number of preserved vertebrae is 25 or 26 if the caudalmost portion of the third last dorsal vertebra is included (Figs. 3.3, 3.4; see Table 3.2 for measurements). Among these, four vertebrae form the dorsal-sacral succession and the rest make up the caudal series. The two sacral vertebrae are fused together forming a cranial part of a synsacrum. However, the caudal vertebrae are not articulated with the synsacrum. None of the preserved vertebrae shows any neurocentral suture although closure of neurocentral sutures may not indicate the exact ontogenetic stage of an individual in derived archosaurs (Irmis, 2007). The cervical vertebrae are entirely missing. Four dorsal ribs and two complete chevrons are preserved (Figs. 3.5, 3.6). Each dorsal rib is isolated, but the chevrons are articulated with the caudal vertebrae.

Dorsal Vertebrae—The preserved two dorsal vertebrae are the penultimate and last dorsals, respectively (Fig. 3.3). They are articulated with each other and with the sacral vertebrae. None of the preserved dorsal vertebrae show any

TABLE 3.2. Selected measurements (in mm) of the holotype specimen of *Nemegtonykus citus* gen. et sp. nov. (MPC-D 100/203).

Element	Length	Width	Height	Circumference (mid-shaft)
Penultimate dorsal vertebra	14.8	-	-	-
Last dorsal vertebra	17.35	-	-	-
First sacral vertebra	14	-	-	-
Second sacral vertebra	14.27	-	-	-
Caudal A	16.84	-	-	-
Caudal B	15.12	-	-	-
Caudal C	15.37	-	-	-
Caudal D	14.78	-	-	-
Caudal E	13.97	-	-	-
Caudal F	14.14	-	-	-
Caudal G	14.24	-	-	-
Caudal H	16.02 (distorted)	-	-	-
Caudal I	15.68	-	-	-

Element	Length	Width	Height	Circumference (mid-shaft)
Caudal J	15.86	-	-	-
Caudal K	16.2	-	-	-
Caudal L	16.24	-		-
Caudal M	16.66	-	-	-
Caudal N	14.31	-	-	-
Caudal O	15.69	-	-	-
Caudal P	15.27	-	-	-
Caudal Q	16.23	-	-	-
Caudal R	15.54		-	-
Caudal S	13.55	-	-	-
Caudal T	12.58	-	-	-
Acetabulum (left)	16.92	-	-	-
Femur (left)	116.52	9.59 (craniocaudal diameter)	-	32
Tibiotarsus (left)	152.72	-	-	30

Element	Length	Width	Height	Circumference (mid-shaft)
Fibula (left)	38.91	-	-	-
Metatarsal II (left)	112.94	9.11 (proximal, transverse) 9.55 (proximal, dorsoplantar) 8.17 (distal, transverse)	-	-
Metatarsal IV (left)	113.59	8.61 (proximal, transverse) 9.5 (proximal, dorsoplantar) 6.9 (distal, transverse)	-	-

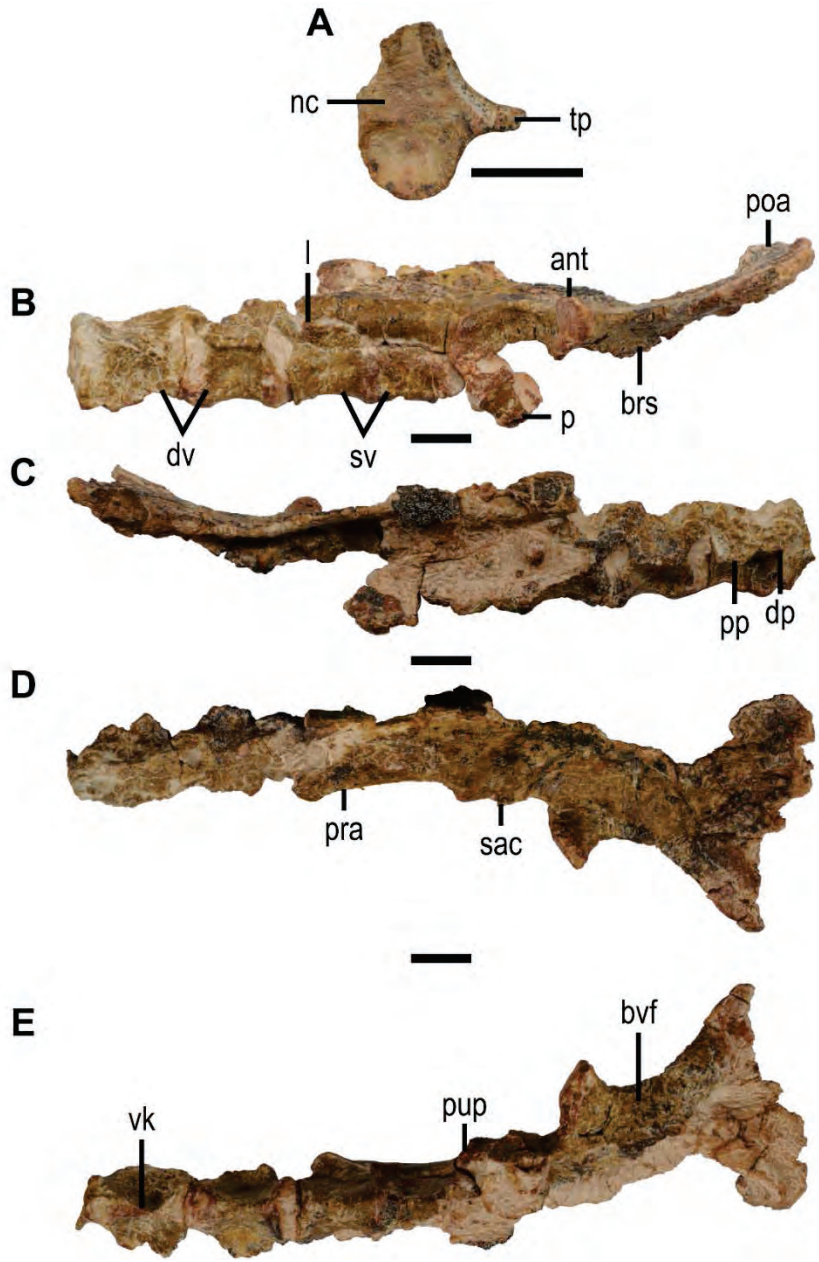

FIGURE 3.3. Dorsal and sacral vertebrae with left ilium and pubis of the holotype specimen of *Nemegtonykus citus* gen. et sp. nov. (MPC-D 100/203). **A**, penultimate dorsal vertebra in caudal view; **B**-**E**, dorsal and sacral vertebrae with left ilium and pubis in **B**, left lateral; **C**, right lateral; **D**, dorsal; and **E**, ventral views. Abbreviations in Appendix 1. Scale bars equal 1 cm.

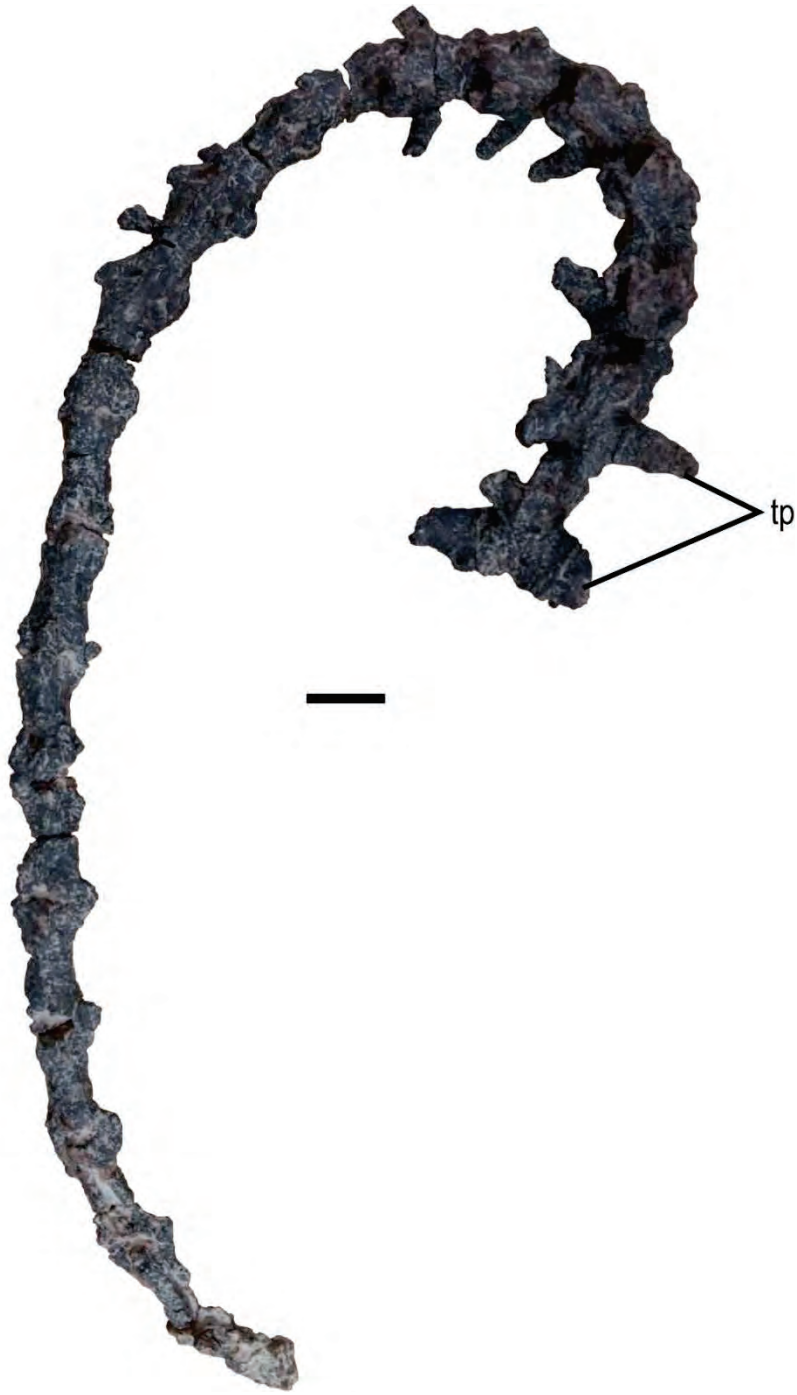

FIGURE 3.4. Caudal series of the holotype specimen of *Nemegtonykus citus* gen. et sp. nov. (MPC-D 100/203) in dorsal view. Abbreviation in Appendix 1. Scale bar equals 1 cm.

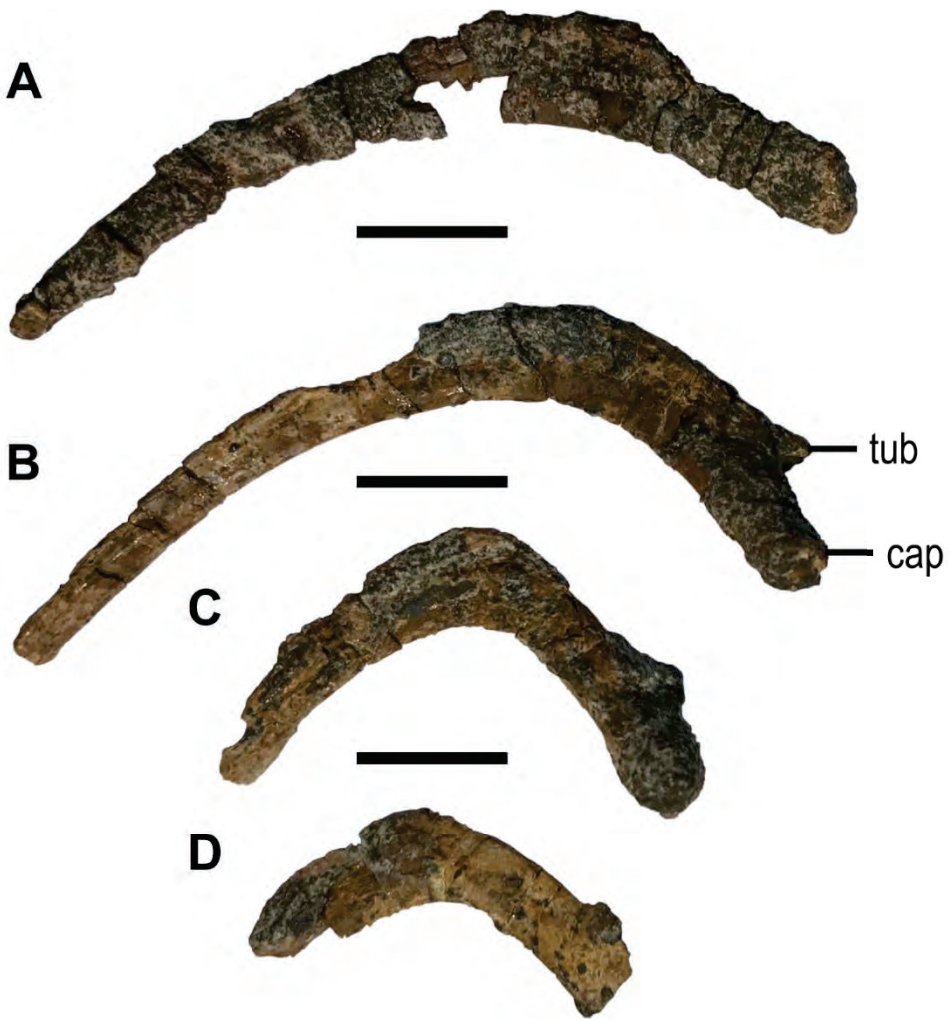

FIGURE 3.5. Dorsal ribs of the holotype specimen of *Nemegtonykus citus* gen. et sp. nov. (MPC-D 100/203). **A**, right dorsal rib (long) in cranial view; **B**, left dorsal rib (long) in caudal view; **C**, left dorsal rib (short) in caudal view; **D**, right dorsal rib (short) in cranial view. Abbreviations in Appendix 1. Scale bars equal 1 cm.

FIGURE 3.6. Chevrons of the holotype specimen of *Nemegtonykus citus* gen. et sp. nov. (MPC-D 100/203). **A-E**, proximal chevron in **A**, left lateral; **B**, right lateral; **C**, cranial; **D**, proximal; and **E**, caudal views; **F-G**, distal chevron in **F**, left lateral; and **G**, right lateral views. Scale bars equal 1 cm.

hyposphene-hypantrum articulation which is also absent in other parvicursorines (Chiappe et al., 2002; Longrich and Currie, 2009; Xu, Upchurch, et al., 2013), but present in more basal *Patagonykus puertai* (Novas, 1997). There is no pleurocoel on the preserved dorsal vertebrae. The penultimate dorsal is also articulated with the third last dorsal, but the latter is broken and missing most of its neural arch and centrum. The centrum of the penultimate dorsal is opisthocoelous and craniocaudally longer than dorsoventrally high or transversely wide. The cranial articular surface is obscured by the preceding vertebra so it is difficult to infer its exact shape. However, the caudal articular surface was observable when it was broken off (Fig. 3.3A). It is subcircular with decreasing in transverse width from dorsal to ventral direction. The centrum is also laterally compressed and thins ventrally forming a prominent keel as in *Mononykus* or *Linhenykus* (Perle et al., 1994; Xu, Upchurch, et al., 2013). This ventral keel is pinched at the middle, having an hourglass shape in ventral view (Fig. 3.3E). Each transverse process is broken off but the diapophysis and parapophysis are still visible on the right side lying on the cranial and caudal end of the transverse process, respectively. The prezygapophyses are craniodorsally oriented. They are very short and barely extends to the level of the caudal end of the preceding centrum. A midline ridge is developed caudal to the prezygapophyses. It leads to the base of the neural spine. The neural spine is largely broken so its dimension or shape is uncertain. The postzygapophyses faces ventrolaterally. The last dorsal vertebra has a convex cranial articular surface. The condyle is ball-shaped and well fits into the caudal articular surface of the preceding centrum. The caudal articular surface of the last dorsal is, however, not clearly observable due to tight articulation with the first

sacral vertebra although it seems either convex or flat. In *Mononykus* and *Shuvuuia*, the last dorsal is biconvex (Chiappe et al., 2002), but in *Linhenykus*, it has a concave cranial articular surface (Xu, Upchurch, et al., 2013). The centrum of the last dorsal is slightly longer than the preceding centrum in craniocaudal length. It is also dorsoventrally higher than transversely wide. The last dorsal centrum maintains a laterally compressed condition, but to a lesser degree than that of the penultimate dorsal. As a result, the ventral keel is not as sharp but it is rather blunt. The caudal end of the centrum is transversely much wider than the cranial end. The transverse processes are directed caudolaterally. The pre- and postzygapophyses are similar in morphology to those of the preceding vertebra, and a midline ridge is present on the dorsal surface of the neural arch. The neural spine of the last dorsal is also broken off.

Sacral Vertebrae—The two preserved sacral vertebrae represent the first and second sacrals, respectively (Fig. 3.3B-E). The right side of them are substantially damaged in contrast to the left side which only exhibits minor breakage. They are completely fused to each other without any contribution of zygapophyses or sacral ribs. However, it is uncertain if the rest of the sacral centra were all fused to one another in life due to the lack of these elements. The exact number of the sacrals cannot be determined as well although it is highly unlikely that there were more than seven scarals, considering the craniocaudal lengths of the two sacrals. The sacral counts in *Shuvuuia* and *Xixianykus* are seven (Chiappe et al., 2002; Xu et al., 2010), and four sacral vertebrae are known in *Alvarezsaurus calvoi* and *Patagonykus puertai* although they might have five or more sacrals (Novas, 1997; Chiappe et al., 2002). The centra of preserved sacrals show lateral compression as

in dorsal centra, but it is not as extensive. Ventrally, the first sacral vertebra has a slightly pinched surface whereas the ventral surface of the second sacral is almost flat. The first sacral centrum is transversely expanded at the cranial end to articulate with the last dorsal vertebra. The first and second sacral centra are more or less the same in craniocaudal length as well as in the dorsoventral heights. The prezygapophyses of the first sacral are short and craniodorsally oriented, similar to those of the dorsal vertebrae. Just right caudal to the base of the prezygapophyses, there is a dorsolaterally oriented lamina formed by transverse process-sacral rib complex and neural arch. It is fused to the preacetabular process of the ilium. This structure is comparable to the anterior lamina of *Xixianykus* (Xu et al., 2010). It is, however, different from that of *Xixianykus* being present only on the first sacral vertebra. In *Xixianykus*, the cranial three sacral vertebrae contribute to the development of the anterior lamina (Xu et al., 2010). The lamina in *Nemegtonykus* is semi-trapezoidal in shape, decreasing in dorsoventral height from cranial to caudal direction. It is also craniocaudally elongate and reaches the level of the caudal end of the centrum. The second sacral centrum is directly fused to the preacetabular part of the ilium, which is unique among alvarezsaurids although this portion is not known in most Mongolian taxa such as *Mononykus*, *Parvicursor*, *Ceratonykus*, and *Albinykus* (Perle et al., 1993, 1994; Karhu and Rautian, 1996; Alifanov and Barsbold, 2009; Nesbitt et al., 2011). There is no zygapophysis or sacral rib on the second sacral vertebra, and presence of a neural spine is uncertain because of poor preservation of the right side. The caudal end of the second sacral centrum is also damaged so the articulation surface is not visible.

Caudal Vertebrae—The preserved caudal series includes 21 consecutive

vertebrae all of which are procoelous (Fig. 3.4). They are nearly complete although the most distal one is missing its distal half. In general, the caudals have similar morphology to those of other alvarezsaurids, especially to caudals of *Shuvuuia* (Chiappe et al., 2002; Suzuki et al., 2002). The craniocaudal length of each centrum does not show a gradual decrease although the distalmost preserved caudals are much shorter than preceding ones unlike in *Alvarezsaurus* where distal caudals are craniocaudally longer (Chiappe et al., 2002), or *Linhenykus* which has a gradually shorter caudals (Xu, Upchurch, et al., 2013). In *Shuvuuia*, the distal caudals are gradually shortened craniocaudally (Suzuki et al., 2002), but incomplete distal part of the caudal series in *Nemegtonykus* hampers comparison in this region between these two taxa. The exact position of the preserved caudals among the entire axial column is not certain, but the distinctly different morpholgy of the proximalmost caudal vertebra from the following ones suggests that it is from among the most proximal caudals if not the first. For convenience, the caudal vertebrae are designated here as caudal 1 to 21 in a proximal to distal sequence.

The preserved caudal vertebrae can be divided into three different groups based on their morphology. The first group includes only caudal 1 which is distinguished from the rest of the caudals by the caudoventrally inclined cranial articulation surface, presence of a ventral keel instead of a furrow on the centrum, a lack of prezygapophyses, and the shape of the transverse processes. The centrum of caudal 1 is laterally compressed, but only to a small extent. It develops a ventral keel which is reversed V-shaped in lateral view. The cranial articular surface is distinctly concave and subcircular. Ventral to the cranial articulation surface, there is a flat and triangular surface whose ventral tip becomes a ventral keel. The ventral

keel disappears caudally as it is transversely expanded. The elliptical neural canal is half the size of the cranial articulation surface at the proximal end and becomes distally smaller. The neural arch pedicles are located cranially, and the cranial margin of the transverse processes are flush with the cranial end of the centrum. Cranially positioned neural arch pedicles are also known in other alvarezsaurids (Chiappe et al., 2002; Xu, Upchurch, et al., 2013). The transverse processes of caudal 1 are craniocaudally more elongate than those of the following caudals, but mediolaterally shorter than those of caudal 2. There is a very short midline ridge on the dorsal surface of caudal 1 leading to the neural spine which is broken off. The neural spine and postzygapophyses are located at the level of the mid-length of the centrum.

The second group consists of caudals 2 to 10, and among them, two or three distalmost ones could be transitional caudal vertebrae. They are distinguished from the more distal caudals by presence of transverse processes and relatively high dorsoventral height/craniocaudal length ratios. The caudals in the second group shares general morphology, but distally, the centra become lower and rectangular in shape in lateral views. All of the centra exhibit a small degree of lateral compression having a reversed V-shaped ventral margin in lateral view and a ventral furrow bordered by two longitudinal ridges. The neural arch pedicles are positioned cranially in caudals 2-5, but transverse processes in these caudals are located more caudally than those of caudal 1. From caudal 5, the positions of transverse processes are near the level of mid-centrum due to the caudal positioning of the neural arch pedicles. In the second group, the transverse processes are more gracile than those of caudal 1. Caudal 2 have transverse

processes that are the longest in mediolateral length and also perpendicular to the prezygapophyses whereas the rest of the caudals have progressively smaller and caudolaterally oriented transverse processes. Caudolateral orientation of transverse processes is also shown in *Linhenykus* (Xu, Upchurch, et al., 2013), *Shuvuuia*, and *Alvarezsaurus* (Chiappe et al., 2002), but in *Parvicursor* they are craniolaterally oriented (Karhu and Rautian, 1996). The axes of the transverse processes are dorsally inclined in all caudals of the second group. The morphology of zygapophyses is rather conservative except the shortening tendency of prezygapophyses which have craniodorsal orientation as in *Haplocheirus* (Choiniere et al., 2010) as well as other alvarezsaurids (Chiappe et al., 2002; Xu, Upchurch, et al., 2013; Averianov and Sues, 2017). The midline ridges are more prominent in this group, and although none of the caudal vertebrae retains a complete neural spine, the triangular cross section at the base is observable. It is also clear that neural spines become thinner and ridge-like in more distal caudals even in the second group. Consequently, from caudal 8, the neural spines are reduced into a low ridge.

The rest of the caudal vertebrae belong to the third group, and they may represent distal caudals. They are conspicuously longer craniocaudally than dorsoventrally high with a greatly reduced neural arch. Including caudal 21, all the centra in the third group exhibits lateral compression and a ventral furrow. A ventral furrow in distal caudal vertebrae is also known in alvarezsaurid specimens from Uzbekistan (Averianov and Sues, 2017). Distal caudal vertebrae are not well known in alvarezsaurids except for *Shuvuuia* whose caudals are slightly different in morphology having lateral grooves and small neural canals. None of the caudals in

third group has any groove on the lateral surface, and the neural canal in each vertebra is relatively large as in proximal caudals. The neural spines are inconspicuously low ridges. The craniodorsally oriented prezygapophyses are very short not extending beyond one fourth of the length of each preceding centrum. The postzygapophyses of the preserved distalmost caudals are greatly reduced in size being almost invisible in dorsal view.

Dorsal Ribs and Chevrons—Among the isolated four dorsal ribs (Fig. 3.5), two are much longer than the other two. The longer two are likely from mid-dorsal vertebrae while the rest are probably from those that are close to sacrum. The dorsal ribs have a pronounced capitulum and much smaller tuberculum although the second longest rib is missing its tuberculum and both attachment points of the shortest rib are broken off. The shape of the dorsal ribs suggests that parapophyses of mid-dorsals are more ventrally located than the diapophyses. The dorsal ribs have a general crescentic curvature, but the two shorter ribs are curved more abruptly to form a right angle being boomerang-shaped. There is no uncinate process on any preserved ribs, but the longer two have an elongate depression on the dorsal surface of their shafts.

The two complete chevrons are each from between caudal 2 and 3 and between caudal 9 and 10 (Fig. 3.6). They are similar to those of *Linhenykus* (Xu, Upchurch, et al., 2013), *Shuvuuia*, and *Alvarezsaurus* (Chiappe et al., 2002) in morphology. Between the two, the more proximal chevron is proximodistally elongate and caudoventrally oriented (Fig. 3.6A-E). At the proximal end, a bony bridge connects the left and right articular surfaces as in *Linhenykus* (Xu, Upchurch, et al., 2013). The vertically long hemal canal is right ventral to this

bridge. Distally the proximal chevron becomes thinner and slightly curves caudally. The more distal chevron is flat distal to the articular surface. It is also craniocaudally elongate, and the proximodorsally length is reduced compared to the proximal chevron (Fig. 3.6F, G). As a result, the distal chevron is L-shaped with a small cranial protrusion. This is slightly different from the inverted T-shaped distal chevrons of *Shuvuuia* and *Alvarezsaurus* (Chiappe et al., 2002). Other fragmentary chevrons are articulated with the caudal series. The preserved parts of these chevrons are proximal ends which have dorsally convex lateral surfaces.

Appendicular Skeleton

The preserved appendicular skeleton includes incomplete pectoral and pelvic girdles and left hindlimb elements (Figs. 3.7-11; see Table 3.2 for measurements). Although forelimbs are missing in the holotype specimen, the elongate and slender tibiotarsus and tarsometatarsus are indicative of a relatively long and gracile hindlimb which is typical in alvarezsaurids (Xu et al., 2010; Xu, Upchurch, et al., 2013).

Scapulocoracoid—The scapula and coracoid are fused to form scapulocoracoid (Fig. 3.7) as in *Linhenykus* (Xu et al., 2011; Xu, Upchurch, et al., 2013), but unlike those of *Mononykus* (Perle et al., 1994), *Patagonykus* (Novas, 1997), *Shuvuuia*, and *Alvarezsaurus* (Chiappe et al., 2002). The scapular blade is missing its caudal end, but otherwise it is complete. It is nearly straight like that of *Mononykus* and *Shuvuuia* (Perle et al., 1994; Chiappe et al., 2002) although the dorsal margin has a slight medial deflection in the middle. In more basal alvarezsaurids, the scapular blade is distinctly curved in medial direction

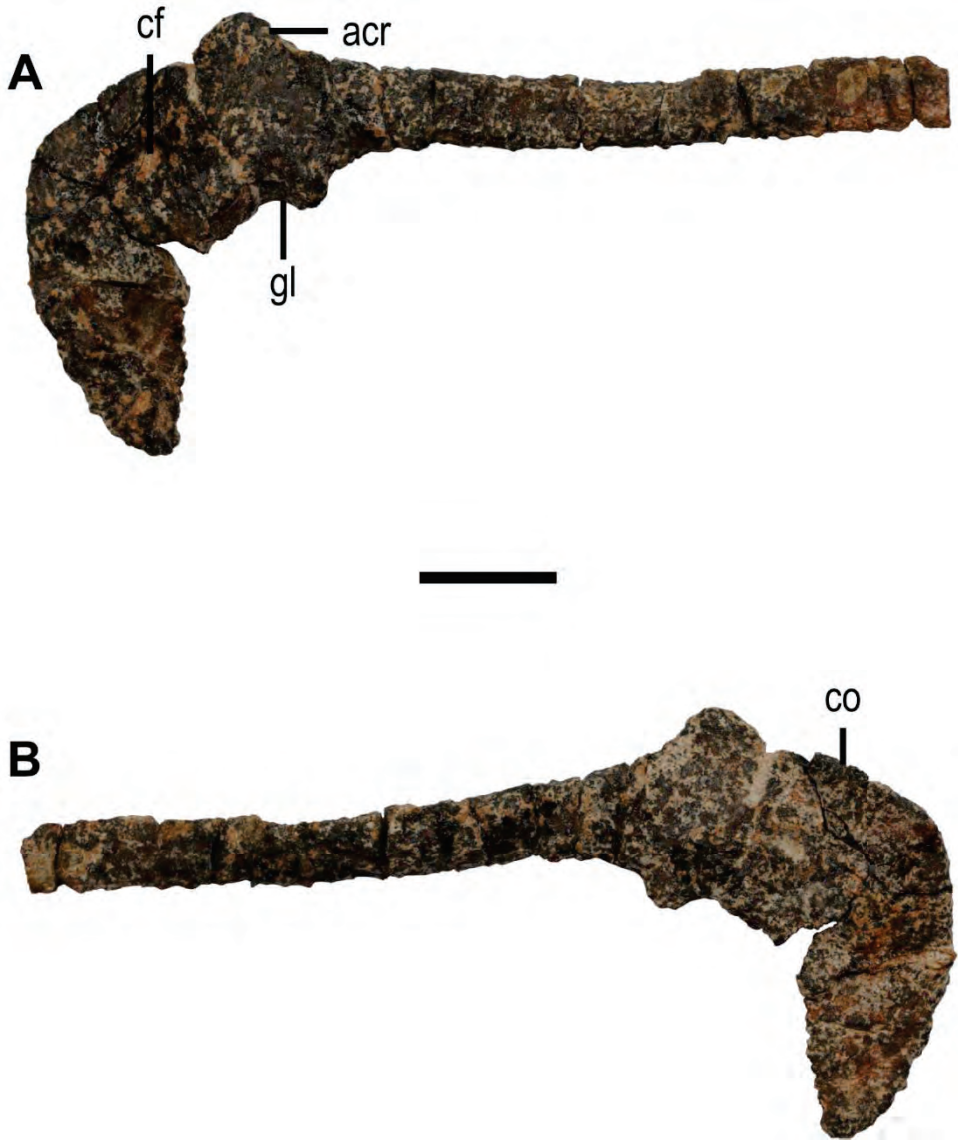

FIGURE 3.7. Left scapulocoracoid of the holotype specimen of *Nemegtonykus citus* gen. et sp. nov. (MPC-D 100/203). **A**, lateral view; **B**, medial view. Abbreviations in Appendix 1. Scale bar equals 1 cm.

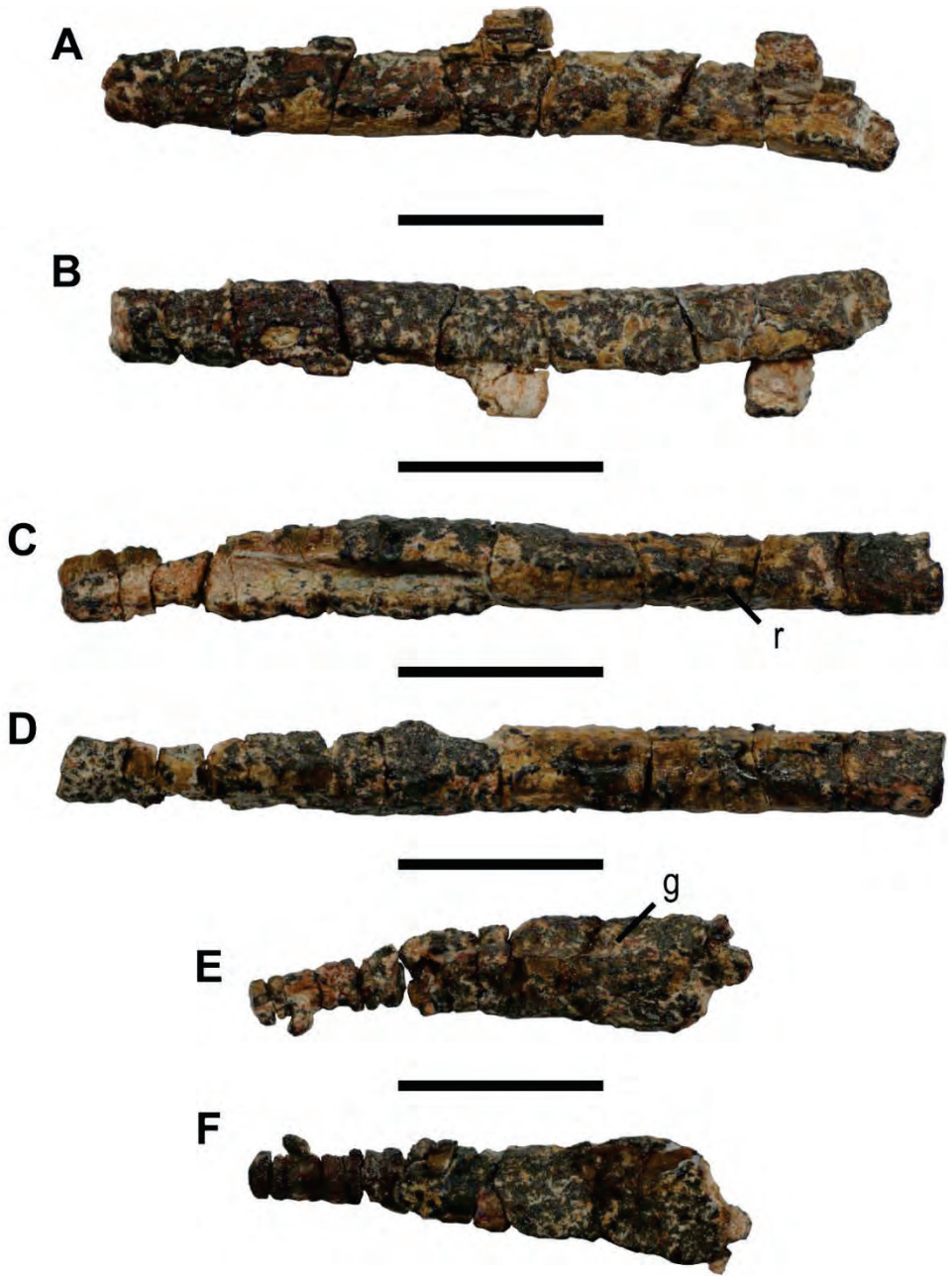

FIGURE 3.8. Other pelvic elements (pubis or ischium) of the holotype specimen of *Nemegtonykus citus* gen. et sp. nov. (MPC-D 100/203). **A**-**B**, second longest element in opposite views; **C**-**D**, longest element in opposite views; **E**-**F**, shortest element in opposite views. Abbreviations in Appendix 1. Scale bars equal 1 cm.

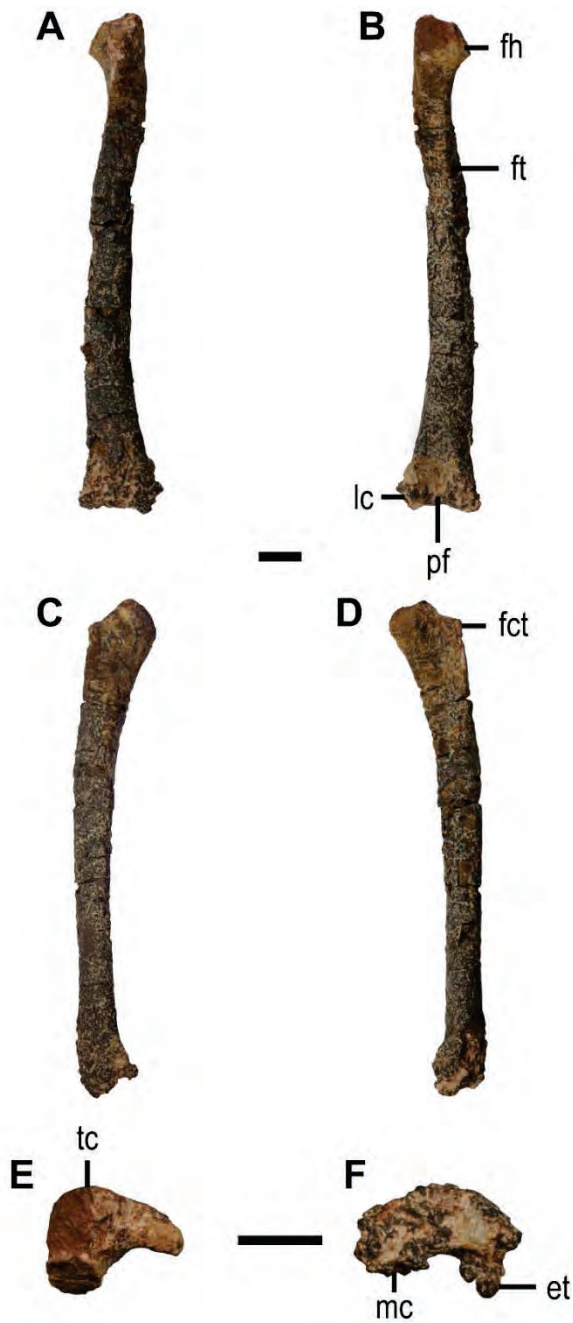

FIGURE 3.9. Left femur of the holotype specimen of *Nemegtonykus citus* gen. et sp. nov. (MPC-D 100/203). **A**, cranial view; **B**, caudal view; **C**, lateral view; **D**, medial view; **E**, proximal view; **F**, distal view. Abbreviations in Appendix 1. Scale bars equal 1 cm.

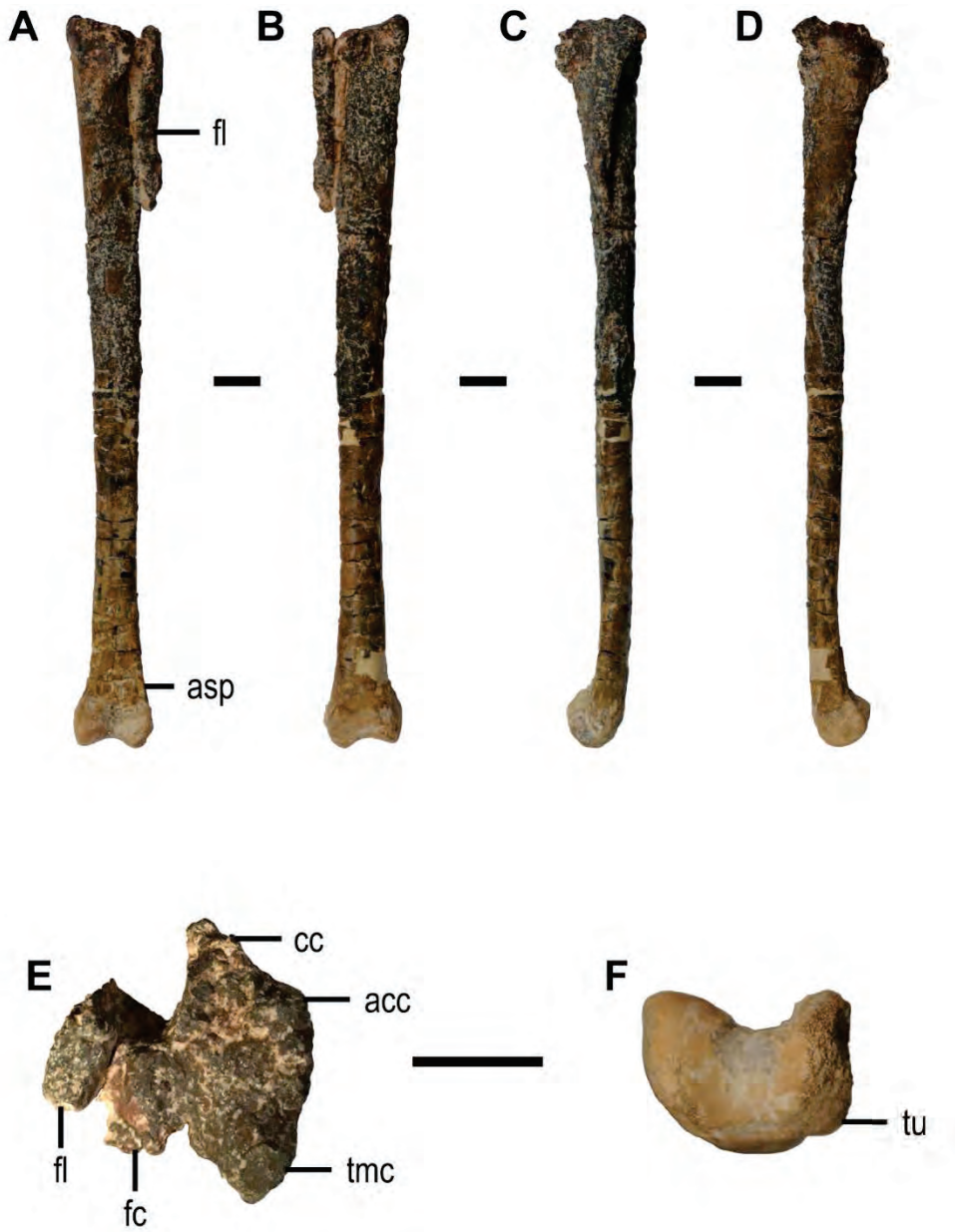

FIGURE 3.10. Left tibiotarsus of the holotype specimen of *Nemegtonykus citus* gen. et sp. nov. (MPC-D 100/203). **A**, cranial view; **B**, caudal view; **C**, lateral view; **D**, medial view; **E**, proximal view; **F**, distal view. Abbreviations in Appendix 1. Scale bars equal 1 cm.

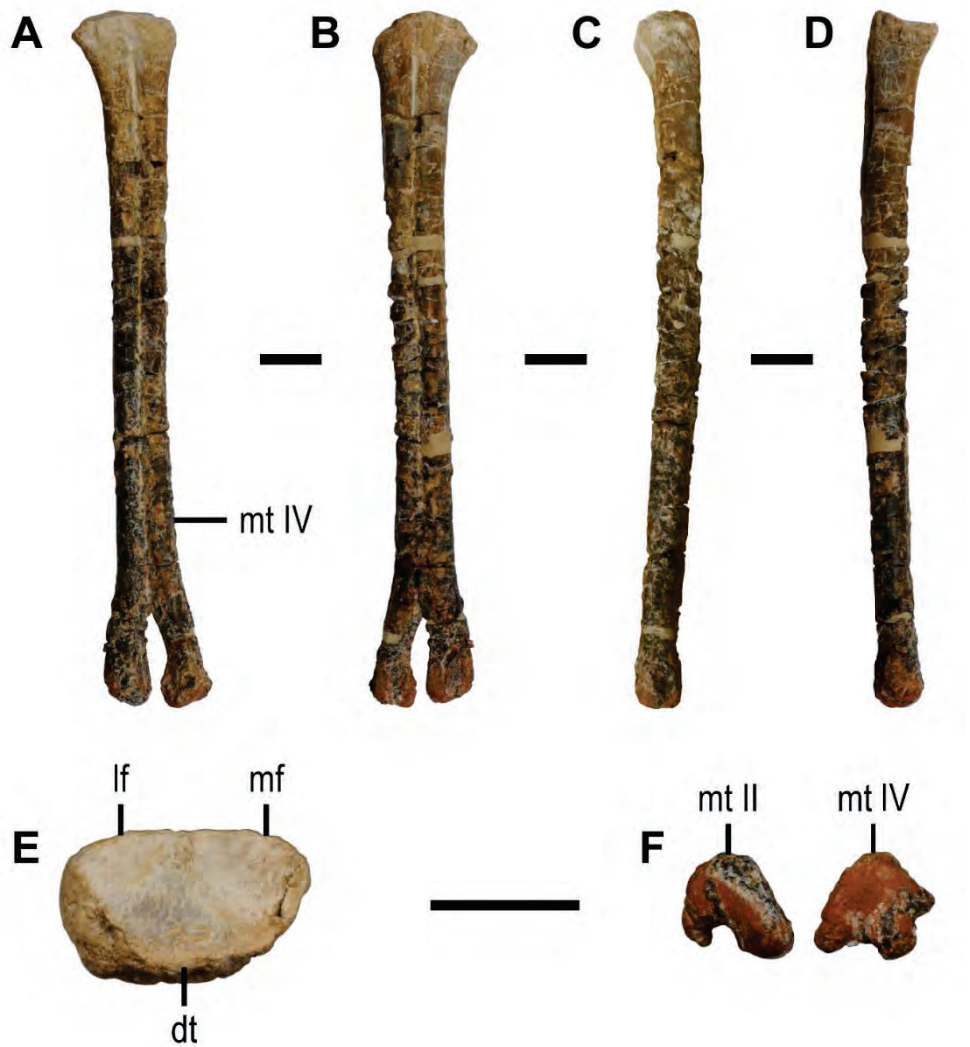

FIGURE 3.11. Left tarsometatarsus of the holotype specimen of *Nemegtonykus citus* gen. et sp. nov. (MPC-D 100/203). **A**, dorsal view; **B**, plantar view; **C**, lateral view; **D**, medial view; **E**, proximal view; **F**, distal view. Abbreviations in Appendix 1. Scale bars equal 1 cm.

(Bonaparte, 1991; Agnolin et al., 2012). The scapular blade of *Nemegtonykus* is also mediolaterally compressed and thickens towards the cranial end resulting in dorsoventrally expanded region. This region has a symmetrical acromion process at the dorsal end and the glenoid fossa at the ventral end. The glenoid fossa is ventrolaterally oriented, and the glenoid lip is well developed as in other parvicursorines (Chiappe et al., 2002) except *Linhenykus* which has a weak glenoid lip (Xu, Upchurch, et al., 2013). The coracoid is a crescent-shaped thin plate apart from the relatively thick region near the scapula. The medial and lateral surfaces of the coracoid is straight and smooth without any ridge. This flat and smooth condition is also seen in *Mononykus* (Perle et al., 1994), *Alvarezsaurus* (Bonaparte, 1991), and *Shuvuuia* (Chiappe et al., 2002). However, in *Ceratonykus*, a small crest is present near the caudoventral margin of the coracoid (Alifanov and Barsbold, 2009). Basal alvarezsaurids such as *Patagonykus puertai* and *Bonapartenykus ultimus* has a distinct ridge on the lateral surface of the coracoid which is also medially curved and has a relatively thick dorsal margin (Novas, 1997; Agnolin et al., 2012). There must have been a glenoid lip on the coracoid as well, but it is broken off in the specimen. The coracoid foramen is subcircular and located at the center of the coracoidal shaft. Biceps tubercle is absent as in other alvarezsaurids (Perle et al., 1994; Chiappe et al., 2002; Agnolin et al., 2012). The dorsoventrally elongate ventral blade is triangular in shape tapering ventrally.

Ilium—The preserved left ilium is fused with the first and second sacral vertebrae (Fig. 3.3B-E). It is low and medially inclined to a large extent being nearly horizontal as in *Parvicursor* (Karhu and Rautian, 1996), *Shuvuuia* (Chiappe et al., 2002), *Xixianykus* (Xu et al., 2010), and perhaps *Linhenykus* (Xu, Upchurch,

et al., 2013). The pre- and postacetabular processes are partially preserved so it is difficult to determine the exact craniocaudal length of the ilium. The preacetabular process has a vertical region which is fused to the second sacral near the acetabulum. Aside from this region, it is flat and faces dorsolaterally. The cranial end of the preacetabular process is broken off, but given that the preserved cranial end is near the neural spine of the last dorsal vertebra, the craniocaudal length of the preacetabular process is unlikely to exceed that of the postacetabular process. The postacetabular process expands laterally toward the caudal end, so the lateral margin displays a wide curvature in dorsal view like that of other parvicursorines (Karhu and Rautian, 1996; Chiappe et al., 2002; Xu et al., 2010). In these taxa, the postacetabular process is also horizontal being on the approximately same level of the antitrochanter in lateral view (Xu et al., 2010). However, in *Nemegtonykus*, it is caudodorsally deflected forming a distinct fossa on its dorsal surface near the antitrochanter. This fossa might have had a function similar to the one for M. iliofibularis in other non-avian theropods accommodating more muscle mass (Carrano and Hutchinson, 2002). A similar fossa is also known in *Xixianykus* (Xu et al., 2010). On the ventral surface of the postactabular process, the longitudinal brevis shelf demarcates the shallow brevis fossa. Cranial to the brevis shelf is a medially facing subrectangular fossa that might be an articular facet for the synsacrum as in *Xixianykus* (Xu et al., 2010). The acetabulum is overhanged by the supracetabular crest which caudally diminishes to completely disappear after the mid-length of the acetabulum, which is also seen in *Mononykus* (Perle et al., 1994). In *Xixianykus*, the supracetabular crest is also more prominent cranially, but it extends far caudally (Xu et al., 2010). Origin of the supracetabular crest is at the

level of center of the pubic peduncle as in other parvicursorines (Perle et al., 1994; Xu et al., 2010), but unlike in more basal *Patagonykus* where it is more caudally located (Novas, 1997) although it is broken so the exact shape of the supracetabular crest is not observable. The acetabulum has a well-developed concave lateral wall that bridges the pubic and ischiadic peduncles. The pubic peduncle is greatly reduced compared to craniocaudally elongate one of other alvarezsaurids (Perle et al., 1994; Novas, 1997; Chiappe et al., 2002; Xu et al., 2010; Xu, Upchurch, et al., 2013) and barely visible as a cranial protrusion. Its ventral and medial surfaces are obscured by matrix so the articular surface is not visible in this specimen. As in other parvicursorines, the ischiadic peduncle is small and transversely oriented (Xu et al., 2010). It is also craniocaudally narrow and ridge-like forming a convex ventral margin. At the caudal end of the acetabulum, a massive antitrochanter is developed in a nearly horizontal orientation. It laterally extends as in other parvicursorines (Perle et al., 1994; Chiappe et al., 2002; Xu et al., 2010), and the articular surface for the femur faces craniolaterally like that of *Mononykus* (Perle et al., 1994) differing from *Xixianykus* where it faces cranially (Xu et al., 2010). The dorsal margin of the antitrochanter is above the level of the supracetabular crest.

Pubis—The preserved left pubis is fragmentary proximal part and slightly offset from the pubic peduncle (Fig. 3.3B). The articular surface for the ilium is not visible and neither is the one for the ischium. At the proximal end, the pubis is craniocaudally elongate but soon it becomes narrower. The lateral surface is flat and smooth without any fossa. The orientation of the preserved part of the pubis suggests an opisthopubic condition as in other parvicursorines (Chiappe et al., 2002).

Other Pelvic Elements—Three isolated partial pelvic elements each of which is either pubis or ischium are preserved (Fig. 3.8) although they are too fragmentary to determine their identities. Each of them has a slightly different morphology. The longer two are rod-like (Fig. 3.8A-D) and likely to be pubic or ischiadic shafts, and the shortest one is transversely compressed and has a robust head with a longitudinal groove extending to the narrow shaft (Fig. 3.8 E, F) indicating that it may be from the proximal part of pubis or ischium. The longest one (Fig. 3.8C, D) is subtriangular in cross section, and a distinct diagonal ridge is developed along the entire longitudinal length. The center of this bone is hollow, but it is uncertain if this is a natural condition. The slightly shorter elongate element (Fig. 3.8 A, B) is compressed at one end and circular in cross section at the opposite end. At one longitudinal side, it is tightly adjoined by another fragmentary bone along the less compressed region. The two bones become separated from each other toward the compressed end.

Femur—The left femur is completely preserved except for the broken femoral head and cranial half of the trochanteric crest (Fig. 3.9). The base of the femoral head is dorsomedially oriented, but the exact orientation of the femoral head is uncertain. The femoral head is medially directed in other parvicursorines (Perle et al., 1994; Chiappe et al., 2002; Xu et al., 2010; Xu, Upchurch, et al., 2013). The trochanteric crest seems to be well developed, but it is unclear whether the greater and cranial trochanters are completely fused as in *Mononykus* (Perle et al., 1994), *Parvicursor* (Karhu and Rautian, 1996), and *Xixianykus* (Xu et al., 2010), or separated as in *Alvarezsaurus* (Bonaparte, 1991), *Patagonykus* (Novas, 1997), *Achillesaurus manazzonei* (Martinelli and Vera, 2007), and *Bonapartenykus*

(Agnolin et al., 2012). It is also separated from the femoral head by a shallow groove. The cranial trochanter medially is curved to make a distinct fossa which is located cranial to the femoral head. This fossa is also known in *Mononykus* (Perle et al., 1994) and *Xixianykus* (Xu et al., 2010). A sigmoidal ridge is developed on the cranial margin of the proximal part of the femur, descending from the thin anterior margin of the cranial trochanter to near the mid-shaft. The femoral shaft is cranially bowed like that of other alvarezsaurids (Chiappe et al., 2002; Alifanov and Barsbold, 2009; Xu et al., 2010; Xu, Upchurch, et al., 2013), but to a lesser extent than in *Parvicursor* (Karhu and Rautian, 1996), *Ceratonykus* (Alifanov and Barsbold, 2009), or *Xixianykus* (Xu et al., 2010). An incipient fourth trochanter is present on the caudomedial margin of the proximal third of the femoral shaft as a sharp ridge. A weak fourth trochanter is also present in *Mononykus*, *Patagonykus*, *Alvarezsaurus*, *Shuvuuia*, and *Xixianykus* (Chiappe et al., 2002; Xu et al., 2010; Xu, Upchurch, et al., 2013). In contrast, there is no fourth trochanter in *Parvicursor* (Karhu and Rautian, 1996) and *Linhenykus* (Xu, Upchurch, et al., 2013). The femoral shaft is also subtriangular in cross section proximally, but the distal shaft is craniocaudally compressed distally being elliptical in cross section. There is also a distinct ridge along the entire caudolateral margin of the femur. It is most prominent around the mid-shaft and distally confluent with the ectocondylar tuber. This is similar to the caudolateral ridge of *Xixianykus* (Xu et al., 2010). On the distal end of the shaft, the femur has a distally open popliteal fossa which is bordered by two shallow ridges (Fig. 3.9B, E). Among alvarezsaurids in which distal region of the femur is known, *Parvicursor*, *Patagonykus*, and *Linhenykus* (Chiappe et al., 2002; Xu et al., 2011; Xu, Upchurch, et al., 2013) also have a

completely open popliteal fossa whereas *Mononykus* has a closed one (Perle et al., 1994; Chiappe et al., 2002), and in *Xixianykus* it is partially open (Xu et al., 2010). The medial and lateral condyles of the femur are significantly reduced in *Nemegtonykus*. The medial condyle is subtriangular in caudal view and has a nearly flat caudal surface. The lateral condyle has a knob-like projection on the distal end comparable to, but relatively more reduced than that of other alvarezsaurids. It also caudally produces a well-developed ectocondylar tuber which thins towards the caudal margin. Additionally, the lateral condyle has a small tubercle on its lateral surface, similar to the lateral protrusion in *Linhenykus* (Xu, Upchurch, et al., 2013).

Tibiotarsus—The left tibiotarsus is completely preserved (Fig. 3.10). The tibia and astragalocalcaneum is fused together, but not as completely as in *Albinykus* (Nesbitt et al., 2011). The tibiotarsus is straight along its entire length unlike in *Parvicursor* (Karhu and Rautian, 1996) or *Shuvuuia* (Chiappe et al., 2002). The proximodistal length of the tibiotarsus is 1.3 times as long as that of the femur. The proximal surface of the tibiotarsus is craniolaterally and cranioventrally as the medial condyle projects proximally like in other parvicursorines (Chiappe et al., 2002; Xu, Upchurch, et al., 2013) except for *Xixianykus*, where the medial condyle is on the same level as the cnemial crest (Xu et al., 2010). The cnemial crest is proximodistally short and craniolaterally deflected to a small extent (Fig. 3.10A, E). Medial to the cnemial crest is a nearly flat surface which forms the cranial margin of an accessory condyle, also known in other parvicursorines (Chiappe et al., 2002; Xu et al., 2010) but not in more basal *Patagonykus* (Novas, 1997). The medial condyle has a pointed caudal end and round proximal surface. It is separated from the fibular condyle by a deep notch on the caudal surface. The

fibular condyle is rectangular in proximal view and larger than the medial condyle. The articulation surface for the fibula is mainly obscured, but it seems to be either flat or slightly convex. The cnemial crest and fibular condyle together define a wide depression. The fibular crest is unconnected from the fibular condyle and dramatically reduced as in *Albertonykus* (Longrich and Currie, 2009), not like the less reduced one in *Mononykus* (Perle et al., 1994). It distally extends slightly beyond the level of the distal end of the fibula. The proximal part of the tibial shaft is subtriangular in cross section, and it becomes suboval and elliptical distally. Along the proximal third of the tibiotarsus, a blunt ridge is developed along the craniomedial margin. Distal to the midshaft, additional shallow ridge is also present on the cranial surface of the tibial shaft. This ridge is medially located and becomes a sharp craniomedial margin of the distal end which is mediolaterally expanded. The distalmost region of the tibial shaft has a flat cranial surface and a convex caudal surface. Near the distal end of the tibiotarsus, a prominent tubercle is present on the caudolateral margin (Fig. 3.10F). The astragalocalcaneum is completely coossified without any trace of sutures. The laminar ascending process is missing its proximal part, but it is clear that there is a distinct notch at the medial margin near its base so it only occupies the lateral half of the cranial surface of the tibia as in other parvicursorines (Perle et al., 1994; Chiappe et al., 2002; Xu et al., 2010; Xu, Upchurch, et al., 2013). A comparable morphology of the astragalocalcaneum is known in a Romanian specimen BMNH A4359 which was suggested to be from an alvarezsaurid (Naish and Dyke, 2004). The ascending process also arises from the medial margin of the astragalocalcaneum as in *Mononykus* and *Parvicursor* (Chiappe et al., 2002) in contrast to the more lateral

origin in *Shuvuuia* (Chiappe et al., 2002) and *Linhenykus* (Xu, Upchurch, et al., 2013). In addition, there is a circular excavation at the center of the base of the ascending process similar to *Mononykus* (Perle et al., 1994) and *Xixianykus* (Xu et al., 2010). As in other parvicursorines, the medial condyle is more robust than the lateral one (Chiappe et al., 2002). The medial condyle has its cranial peak on the medial end and it gradually descends laterally while the lateral condyle is almost perpendicular to the cranial surface of the astragalocalcaneum (Fig. 3.10F). Between the medial and lateral condyles is a deep groove that extends to the caudal surface of the distal end of the tibiotarsus.

Fibula—The proximodistally short fibula is nearly completely preserved (Fig. 3.10A-C, E). It is generally similar to that of other parvicursorines in morphology being thin and craniocaudally expanded at the proximal end as well as having a distinct crest on the lateral surface of the distal shaft for attachment of M. iliofibularis (Chiappe et al., 2002; Xu et al., 2010; Nesbitt et al., 2011). The proximal surface of the fibula is moderately concave. The anterior margin of the fibula near the proximal end is a sharp and proximodistally short ridge. On the opposite side to this ridge, the caudal margin also forms a short ridge which is not as sharp. The fibular shaft becomes craniocaudally short towards its distal extremity where it tapers to produce a pointed end. It is straight unlike the caudally deflected fibula in *Xixianykus* (Xu et al., 2010). The medial surface of the fibula is obscured by matrix and tibiotarsus, and the lateral surface is flat. The distal crest is not as robust as that of *Albinykus* (Nesbitt et al., 2011).

Tarsometatarsus—The left tarsometatarsus is almost complete missing the metatarsals I, III, and V (Fig. 3.11). The distal tarsals are fused with the proximal

end of the metatarsus. The metatarsals II and IV are also partially coossified together at their proximal extremities. The proximal articular surface is subrectangular in proximal view (Fig. 3.11F). At the center of the articular surface is a subtriangular elevation which is interpreted here as the fused distal tarsals. It borders two triangular fossae medially and laterally, respectively. On the plantolateral corner, there is also a small depression which may be the articular facet for metatarsal V. This configuration of the proximal articular surface of the tarsometatarsus is also found in *Xixianykus* (Xu et al., 2010). Despite its absence, the metatarsal III was likely to be very short forming a highly modified arctometatarsal condition like that of other parvicursorines (Chiappe et al., 2002; Alifanov and Barsbold, 2009; Xu et al., 2010, 2011; Xu, Upchurch, et al., 2013) judging by the tightly adjoined metatarsals II and IV. The metatarsal IV is only marginally longer than the metatarsal II and approximately 3 mm shorter than the femur. However, with metatarsal III, the whole proximodistal length of the tarsometatarsus would have exceeded that of the femur as in other parvicursorines (Chiappe et al., 2002; Longrich and Currie, 2009; Xu et al., 2010, 2011; Xu, Upchurch, et al., 2013). The proximal ends of the metatarsals II and IV are medially and laterally deflected respectively, but the deflection of the metatarsal IV is inconspicuous. The rest of the two metatarsal shafts are rather straight until they diverge near the distal end. Each of the two metatarsals has dorsal and plantar ridges which are proximodorsally elongate. The dorsal ridges are prominent along the two thirds of each shaft while the plantar ones are developed only near the mid-length of each shaft. The mid-shaft of the metatarsal II is dorsoplantarly higher than other parts of the shaft, having a convex plantar margin in medial view (Fig.

3.11D). In case of the metatarsal IV, the dorsoplantar height is nearly consistent along the shaft except for the lower distal third. Unlike in other parvicursorines, the distal shafts of the metatarsals II and IV are fused together at their plantar surfaces before the divergence without any visible line of contact between them (Fig. 3.11B). Distal to the divergence, the metatarsal II is more or less strraight whereas the metatarsal IV is laterally deflected. The articulation surfaces of the metatarsals II and IV for the metatarsal III is flat and restricted laterally and medially, respectively indicating that the metatarsal III was not much expanded mediolaterally. The non-ginglymoid distal articular ends of the metatarsals II and IV are similar to those of *Mononykus* (Perle et al., 1994) or *Shuvuuia* (Chiappe et al., 2002) in morphology. The trochleae of the metatarsals II and IV are subtriangular in distal view (Fig. 3.11E). The metatarsal II has a robust lateral rim and a small medial rim at its distal end. However, the metatarsal IV has a nearly symmetrical medial and lateral rims although the lateral one is slightly larger. The trochlea of the metatarsal IV also has a small notch on its lateral surface forming a sharp crest. There is no collateral ligament fossa on both trochleae of the metatarsals II and IV, whilst in *Mononykus*, a lateral fossa is present on the trochlea of the metatarsal IV (Perle et al., 1994).

PHYLOGENETIC ANALYSIS

The consensus tree recovered Alvarezsauria (*sensu* Agnolin et al., 2012) as the most basal maniraptoran clade (Figs. 3.12). It exhibits most of the major clades in Theropoda although positions of several taxa and clades vary from those in the most recent study (Cau, 2018). The most striking example is the position of the family Troodontidae which was found to be a sister clade to another paravian family Dromaeosauridae in this study, but the result of Cau (2018) suggests that the Troodontidae is a sister clade of Avialae, not that of the Dromaeosauridae. However, the position of Alvarezsauria is not different between the trees in this study and Cau (2018). Other previous studies also indicated the same phylogenetic position of Alvarezsauria as the basalmost clade in Maniraptora (Choiniere et al., 2010, 2014; Xu et al., 2010, 2011; Agnolin et al., 2012; Xu, Upchurch, et al., 2013; Lee et al., 2014; Cau et al., 2015; Hendrickx et al., 2015; Cau and Madzia, 2018) although avian, or sometimes ornithomimid, affinity of alvarezsaurids was heavily disputed earlier (Perle et al., 1993, 1994; Chiappe, 1995; Zhou, 1995; Chiappe et al., 1996, 1997, 1998, 2002; Forster et al., 1996; Ji et al., 1998; Sereno, 1999a, 1999b, 2001; Novas and Pol, 2002; Suzuki et al., 2002; Padian, 2004; Turner et al., 2009). The general topology of Alvarezsauria in the consensus tree is very similar to the result of Agnolin et al. (2012), only differing in relationships among three mononykins due to the inclusion of *Nemegtonykus* (Fig. 3.13). *Nemegtonykus* is placed at one of the most derived positions among alvarezsaurids and also as a sister taxon of *Linhenykus* in the consensus tree. *Mononykus,* another alvarezsaurid from the Nemegt Formation, was recovered as a sister taxon of *Albertonykus* which

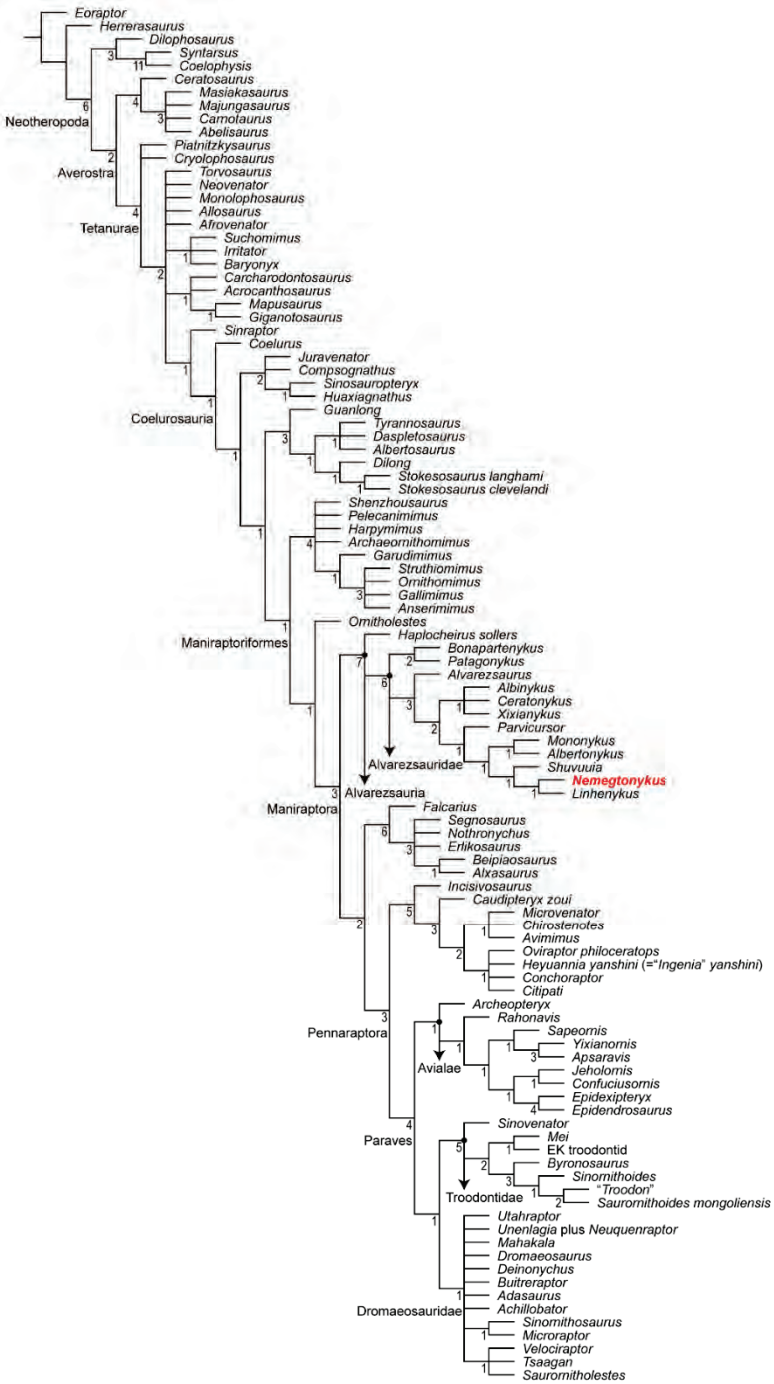

FIGURE 3.12. Strict consensus (CI: 0.272, RI: 0.645) of the 300 most parsimonious trees of 1915 steps obtained by TNT based on the data matrix of 104 taxa and 423 characters. Numbers at each node indicate Bremer support values.

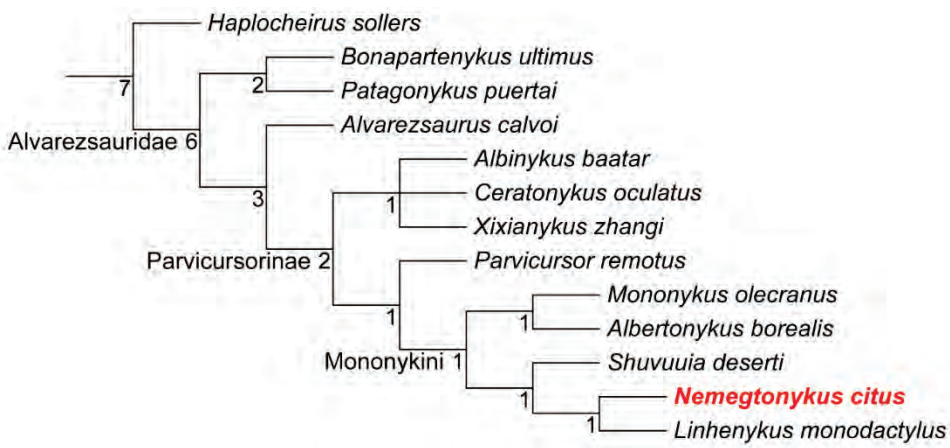

FIGURE 3.13. Alvarezsauria part of the strict consensus tree in the figure 3.12.

is from North America. Mongolian alvarezsaurids included in the phylogenetic analysis were all placed in the subfamily Parvicursorinae, and three of them (*Mononykus*, *Shuvuuia*, and *Nemegtonykus*) in the less inclusive clade Mononykini. The other two taxa (*Albinykus* and *Ceratonykus*), with *Xixianykus*, form a distinct clade Ceratonykini which was defined and named by Agnolin et al. (2012). *Alvarezsaurus* was recovered as a sister taxon to the subfamily parvicursorinae while the other two South American taxa (*Bonapartenykus* and *Patagonykus*) formed another subfamily Patagonykinae that was also defined and named by Agnolin et al. (2012). *Haplocheirus*, which is from the Late Jurassic of China, was recovered as the most basal alvarezsaur as in previous studies (Choiniere et al., 2010, 2014; Xu et al., 2011; Agnolin et al., 2012; Xu, Upchurch, et al., 2013).

III-4. DISCUSSION

Morphological Implications of *Nemegtonykus citus*

The hindlimbs of alvarezsaurids have not been investigated as much as the extremely modified forelimbs (Perle et al., 1993, 1994; Zhou, 1995; Chiappe et al., 2002; Senter, 2005; Longrich and Currie, 2009; Xu et al., 2010; Xu, Upchurch, et al., 2013) although a few recent studies discussed significance of alvarezsaurid hindlimb morphology which was compared to that of other theropods (Xu et al., 2010; Xu, Upchurch, et al., 2013). They regarded the generally slender hindlimbs and elongated distal hindlimb elements (tibiotarus and tarsometatarsus) relative to the proximal one (femur) of parvicursorines as indicators of a highly cursorial lifestyle for this group (Xu et al., 2010; Xu, Upchurch, et al., 2013). The relatively long tibiotarsus and tarsometatarsus of *Nemegtonykus* also well correlate with the morphology of other parvicursorines (Table 3.3). The tibiotarsal length of the holotype specimen of *Nemegtonykus citus* is approximately 1.3 times as long as the femoral length, which is also the case for *Xixianykus* (Xu et al., 2010). The tarsometatarsus is also elongate in *Nemegtonykus*, being only slightly shorter than the femur even without the metatarsal III. Therefore, the tarsometatarsus was likely to be longer than the femur in this individual if the metatarsal III had a proportion similar to that of other parvicursorines. As a useful tool for locomotion analysis, ternary diagrams have been utilized for theropods (Gatesy and Middleton, 1997). This was adopted by Xu et al. (2010) for *Xixianykus* which was just outside the range of the non-avialan theropod morphospace and comparable to some neornithine birds. *Nemegetonykus* and other parvicursorines also occupy almost the

TABLE 3.3. Ratios among the lengths of hindlimb elements in parvicursorines.

Lengths are estimated where the exact measurements were not obtainable.

Taxon	Tibiotarsus/Femur	Tarsometatarsus/Femur	Tarsometatarsus/Tibiotarsus
Linhenykus	1.4	1.04	0.74
Nemegtonykus	1.3	1.02	0.78
Xixianykus	1.3	1.06	0.81
Mononykus	1.26	-	-
Parvicursor	1.4	1.1	0.77
Shuvuuia	1.5	1.13	0.83

same morphospace as does *Xixianykus*, probably reflecting a similar locomotion style. The gracile hindlimbs and their proportions in parvicursorines resemble those of birds as supported by ternary diagrams (Xu et al., 2010). However, it was also suggested that parvicursorines were not likely to adopt the 'knee-driven' locomotion in birds because they lack some of the specializations in the latter group for the cranial displacement of the center of gravity such as extreme shortening of the tail (Xu et al., 2010). Instead, Xu et al. (2010) assumed that the elongated distal hindlimbs in parvicursorines were more likely to represent cursoriality.

While the hindlimb proportions and specialized arctometatarsalian condition indicate parvicursorines were capable cursors (Xu et al., 2010; Xu, Upchurch, et al., 2013), it cannot be easily disregarded that they might also had a kind of locomotion akin to that of birds. In this matter, the morphology of *Nemegtonykus* provides with several pieces of information that may be useful. Although missing most distal and possibly proximal vertebrae, the caudal series of *Nemegtonykus* suggests the morphological transition of caudals occurs quite proximally. Based on the general morphology of caudal vertebrae, shape of the chevrons, and the estimation of caudal 1 being one of the proximalmost caudals, it seems reasonable to assume that the transition point from proximal caudals to distal ones are around the tenth caudal vertebra. This trend is prevalent in other maniraptorans as well (Ostrom, 1976; Ji et al., 1998; Barsbold et al., 2000; Makovicky et al., 2005; Hu et al., 2009; Xu et al., 2009; Allen et al., 2013; Godefroit et al., 2013; Lamanna et al., 2014; Pei et al., 2017), but it is not the case in most of more basal theropods (Gilmore, 1920; Welles, 1954; Brochu, 2003). Among parvicursorines, morphology

of caudal vertebrae is not well known with only *Shuvuuia*, *Linhenykus* and *Nemegtonykus* preserving more than 10 caudals (Chiappe et al., 2002; Suzuki et al., 2002; Xu, Upchurch, et al., 2013). For *Shuvuuia*, 35 or more were estimated as the number of caudal vertebrae (Suzuki et al., 2002), which is not few compared to avialans. It is, however, highly unlikely that *Nemegtonykus* had that many caudals because the proximal transition point apparent and the distalmost preserved caudals show sudden decrease in length (Table 3.2). Therefore, it is most probable that *Nemegtonykus* had much fewer caudal vertebrae than non-maniraptorans did. In addition, the transverse processes of caudals are generally slender and short and present on a few caudals. Together with the substantially reduced fourth trochanter of femur, these characters of the tail indicate that *Nemegtonykus* did not have much developed M. caudofemoralis which is the prime muscle group for propulsion in many non-maniraptorans as well as extant crocodilians and lepidosaurs, but reduced in the avian lineage (George and Berger, 1966; Gatesy, 1990; Gatesy and Dial, 1996; Hutchinson, 2002).

In extant birds, femur is subhorizontally oriented with the distal end pointing forward and thus placing the center of body mass more cranially as they acquired the 'knee-driven' locomotion which has been thought to be unique in this particular group of animals (Gatesy, 1990, 1991; Carrano, 1998; Carrano and Biewener, 1999; Farlow et al., 2000; Hutchinson and Gatesy, 2000; Jones et al., 2000; Hutchinson, 2001a; Rubenson et al., 2007). Non-avian theropods, on the other hand, maintained the more vertical femoral orientation for the 'hip-driven' locomotion (Gatesy, 1990, 1991; Carrano, 1998; Carrano and Biewener, 1999; Farlow et al., 2000; Hutchinson and Gatesy, 2000; Jones et al., 2000; Hutchinson,

2001a). The femoral morphology between these two groups also differ from each other as non-avian theropods mainly have slender femora whereas those of birds are robust, so they can be well differentiated quantatively based on the relationship of length and craniocaudal mid-shaft diameter in log-scale (Gatesy, 1991). The relatively short and robust femur of *Nemegtonykus* places it in line with birds on the regression line in Gatesy (1991). The relationship between the natural logarithm of femoral circumference and length have been shown to be different between non-avian theropods and birds (Christiansen and Bonde, 2002). Again, *Nemegtonykus* lies near the birds on the regression line in Christiansen and Bonde (2002). Therefore, the proportions among femur length and mid-shaft diameter, and circumference demonstrate compelling similarity in femoral morphology between *Nemegtonykus* and birds. Although they were not articulated, the dorsolaterally directed antitrochanter of the ilium also indicates that the orientation of the femur was closer to subhorizontal than vertical in *Nemegtonykus* (Fig. 3.3B). A strong medial inclination of the ilium further suggests that the pelvic anatomy of *Nemegtonykus* is similar to that of modern birds (Rezk, 2015). However, other osteological characters such as extreme fusion between the preacetabular region and sacrum and dorsal deflection of the postacetabular process with a large fossa are unique in *Nemegtonykus* and clearly distinguished from the general morphology of avian ilia (Hutchinson, 2001b). These two features of *Nemegtonykus* are suitable to provide extra rigidity to the hip for resisting torsion and to accommodate more muscle mass (most probably M. iliofibularis and M. iliotibialis lateralis), respectively, which are advantageous when running fast.

The relatively large number of caudal vertebrae in *Nemegtonykus* suggests that

it might not have adopted the fully 'knee-driven' locomotion that is present in modern birds, but many similarities in pelvic and hindlimb morphology between them cannot be ignored. With present evidence, therefore, it appears to be most plausible that *Nemegtonykus* used the knee joint more than the hip joint as a primary source of motion during locomotion, but not as extensively as in modern birds. This might be similar to rudimentary avian locomotion which must have been present in basal avialans with a comparatively long tail if the avian limb posture was developed in a stepwise manner (Allen et al., 2013). However, it is still uncertain if other parvicursorines had a similar manner of locomotion. Future biomechanical studies on parvicursorines and more parvicursorine specimens that preserve a complete sacrum and caudal series as well as pelvis will be helpful to more accurately reconstruct their locomotion.

Phylogenetic Position of *Nemegtonykus citus*

The phylogenetic analysis recovered *Nemegtonykus citus* as one of the most derived alvarezsaurids and sister taxon of *Linhenykus* (Fig. 3.12, 13). These two taxa are united by the following two synapomorphies: scapula and coracoid fused into scapulocoracoid and distally open popliteal fossa on the distal end of femur. They also form a clade with *Shuvuuia* which was recovered as a sister taxon to *Linhenykus* in Agnolin et al. (2012). On the opposite branch of this clade *Mononykus* and *Albertonykus* establish another clade, all of which are members of the more inclusive Mononykini. Phylogenetic relationships among non-mononykin alvarezsaurids on the consensus tree is the same with those in Agnolin et al. (2012). The position of *Nemegtonykus* on the cladogram suggests it is closer to *Linhenykus*

which is from the older Wulansuhai Formation (= Bayan Mandahu Formation) in Inner Mongolia than to *Mononykus* which is from the Nemegt Formation as is *Nemegtonykus*. Additionally, *Nemegtonykus* has a closer relationship with *Shuvuuia* than with *Mononykus*. Considering *Shuvuuia* is from the Djadochta Formation which has been regarded similar to the Wulansuhai Formation in age (Jerzykiewicz et al., 1993), a rather distant relationship between *Nemegtonykus* and *Mononykus* is puzzling. It is possible that basal mononykin alvarezsaurids diverged into two lineages earlier than Campanian which has been generally assumed to be the age of the Djadochta and Wulansuhai Formations (Jerzykiewicz et al., 1993; Dashzeveg et al., 2005; Dingus et al., 2008) although Coniacian or Santonian age has also been proposed for Djadochta Formation (Lefeld, 1971). The sister-taxon relationship between *Mononykus* and *Albertonykus* adds further complexity to the intrarelationships among mononykins. A possible explanation is a dispersion event from Asia to North America or vice versa as suggested for other vertebrates (Jerzykiewicz and Russell, 1991; Russell, 1993; Cifelli et al., 1997; Makovicky and Sues, 1998; Farke et al., 2014; Funston et al., 2018a) including alvarezsaurids (Longrich and Currie, 2009; Xu et al., 2010, 2011; Xu, Upchurch, et al., 2013). For alvarezsaurids, South American origin has been suggested (Novas, 1996) and this correlates well with basal positions of South American alvarezsaurids on phylogenetic trees (Chiappe et al., 2002; Choiniere et al., 2010, 2014; Xu et al., 2010, 2011; Agnolin et al., 2012; Xu, Upchurch, et al., 2013) although basalmost alvarezsaur *Haplocheirus* suggests a possible Asian origin of Alvarezsauria (Choiniere et al., 2010). The most recent phylogenetic analysis on alvarezsaurids (Xu, Upchurch, et al., 2013), however, produced slightly different cladograms from

that of Agnolin et al. (2012) or this study. The phylogenetic position of *Albertonykus* and *Linhenykus* in the cladograms of Xu, Upchurch, et al. (2013) are more basal than other parvicursorines. This disparity between results are in part due to inclusion/exclusion of specific taxa or specimens such as *Achillesaurus*, *Ceratonykus*, *Albinykus*, and unnamed North American and Asian specimens. In order to resolve the phylogenetic relationships among alvarezsaurs, more well-preserved specimens are needed especially those from North America or Europe where only fragmentary materials have been reported (Hutchinson and Chiappe, 1998; Naish and Dyke, 2004; Longrich and Currie, 2009).

Palaeoecology and Diversity of Alvarezsaurids in the Nemegt Basin

The extremely short and robust forelimbs of alvarezsaurids attracted much attention, with various studies attempting to explain their purpose (Perle et al., 1993, 1994; Zhou, 1995; Chiappe et al., 2002; Senter, 2005; Longrich and Currie, 2009; Agnolin et al., 2012). Most of these studies concluded that the primary usage of the highly modified forelimbs is likely to be digging (Perle et al., 1993, 1994; Zhou, 1995; Chiappe et al., 2002; Senter, 2005; Longrich and Currie, 2009), and they might have preyed upon termites (Chiappe et al., 2002; Senter, 2005; Longrich and Currie, 2009) whereas Agnolin et al. (2012) argued that the evidence for alvarezsaurids being myrmecophages is too weak. Because no forelimb element was preserved in the holotype specimen of *Nemegtonykus* it does not contribute much to the argument except that its fused scapulocoracoid may be indicative of a structure for enduring force when digging.

In the Nemegt Basin, alvarezsaurids have mostly been found from eolian

deposits such as Baruungoyot and Djadochta Formations (Fig. 3.1; Karhu and Rautian, 1996; Chiappe et al., 1998; Suzuki et al., 2002; Alifanov and Barsbold, 2009; Turner et al., 2009; see also Table 3.1). The only alvarezsaurid from the mesic Nemegt Formation has been *Mononykus* which is represented only by the holotype specimen (Perle et al., 1993). A similar tendency has been observed in oviraptorids but they are also abundant in the Nemegt Formation (Longrich et al., 2010; Tsuihiji et al., 2016; Funston et al., 2018a; see also Chapter II-4). The discovery of *Nemegtonykus* may suggest that Mongolian alvarezsaurids did not specifically prefer dry environments. The occurrence of associated alvarezsaurid specimens with *Nemegtonykus* may even indicate that rich alvarezsaurid fauna were present in the Nemegt Formation. In the eastern Gobi Desert, presence of *Albinykus* in the Javkhlant Formation (Nesbitt et al., 2011) which has been interpreted as alluvial to alluvial fan deposits (Eberth, Kobayashi, et al., 2009) further supports that alvarezsaurids were unlikely to favor xeric habitats. Fragmentary alvarezsaurid specimens found in Uzbekistan also suggest that they lived in a fluvial environment (Averianov and Sues, 2017). Therefore, relative abundance of alvarezsaurids in the eolian deposits in the Nemegt Basin could be an artifact of a preservational or sampling bias or both. In addition, *Nemegtonykus* increases the diversity of alvarezsaurids in the Nemegt Formation to two taxa which are the same with the number of alvarezsaurid taxa from the Baruungoyot or Djadochta Formations. With *Nemegtonykus*, the Nemegt Basin becomes a region with the highest alvarezsaurid diversity worldwide with 6 taxa, followed by Argentinian Patagonia with 5 alvarezsaurid taxa (see Table 3.1). However, despite their global distribution, alvarezsaurids are relatively rare in a typical dinosaur

fauna possibly due to their small size. It is also notable that alvarezsaurids, despite their wide distribution and the presence of the basalmost alvarezsaur *Haplocheirus* (Choiniere et al., 2010), have been extremely rare in China with only two taxa (Xu et al., 2010, 2011) and a specimen which may be a new taxon (Pittman et al., 2015). Excluding those from the Gobi Desert, Chinese alvarezsaurids are represented only by *Xixianykus*. This scarcity contrasts the remarkable high diversity of Chinese oviraptorids (Lü, 2002; Lü and Zhang, 2005; Longrich et al., 2010; Xu and Han, 2010; Lü, Currie, et al., 2013; Lü, Yi, et al., 2013; Lü et al., 2015, 2016, 2017; Wang et al., 2013; Wei et al., 2013; see also Chapter II-1) which are also fairly small although not as alvarezsaurids in general. It is likely, however, that future discoveries of alvarezsaurids will provide additional clue to their true diversity in China as a number of Chinese oviraptorids have been reported in very short intervals.

III-5. CONCLUSIONS

A new alvarezsaurid *Nemegtonykus citus* gen. et sp. nov. from the Nemegt Formation of Mongolia is distinguished from other alvarezsaurids by a unique set of characters with autapomorphies in pelvic and hindlimb elements. The most prominent feature of *Nemegtonykus* is extreme fusion between the sacrum and ilium at the preacetabular region. This unique pelvic morphology was probably helpful for withstanding force during fast locomotion. The hindlimb proportions, possibly reduced number of caudals, and drastic medial inclination of ilium with a robust antitrochanter which is laterally expanded indicate that *Nemegtonykus* might have developed a rudimentary style of the 'knee-driven' locomotion, which might be similar to the mode of locomotion in basal alvialans although this is not clear in case of other parvicursorines. The phylogenetic analysis recovered *Nemegtonykus* as a derived parvicursorine and a sister taxon of *Linhenykus* from the Wulansuhai Formation and showed that *Nemegtonykus* is not very close to *Mononykus* in the clade Mononykini. The relatively distant relationship between these latter two taxa as well as the sister-taxon relationship between *Mononykus* and *Albertonykus* render the intrarelationships among mononykins more difficult to resolve. The presence of *Nemegtonykus* in the Nemegt Formation suggests that alvarezsaurids well adapted to both dry and wet environments. The alvarezsaurid diversity in the Nemegt Basin is also increased to 6 taxa, which is the greatest number of taxa from this group in the world.

CHAPTER IV

CONCLUSIONS

Maniraptorans from the Nemegt Formation, even with their relative rarity compared to larger non-maniraptorans (Funston et al., 2018b), have provided novel features previously unknown or unconfirmed especially in alvarezsaurids and oviraptorosaurs (e.g., Perle et al., 1993; Funston, Currie, Eberth, et al., 2016). Many aspects of these two groups are still mysterious despite extensive previous studies partially due to insufficient amounts of specimens. The two new maniraptorans described in this thesis offer important clues about their ecology and phylogenetic relationships.

One of the two new maniraptorans named and described in this thesis is *Gobiraptor minutus* gen. et sp. nov. which is a highly derived oviraptorid dinosaur. The specimen is smaller than its relatives in the same Nemegt Formation, probably because of its early ontogenetic stage as the osteohistology data suggest. *Gobiraptor* is different from all other oviraptorids having a flat articular surface for quadratojugal on the quadrate, a massive symphyseal shelf of dentary, rudimentary lingual shelves and ridges, small occlusal grooves on each lingual shelf, a coronoid bone with a ventral position at the rostral end, and proximal caudal vertebrae with more than one infraprezygapophyseal fossae. Among its unique characters, the most noteworthy is its dentary structure. None of the previously reported oviraptorid had this kind of massive symphyseal shelf as well as lingual shelves with occlusal grooves. More importantly, these peculiar features imply that

Gobiraptor had a beak which was suited to crush hard materials. As other oviraptorids do not show this morphology, it is likely that *Gobiraptor* evolved a separate dietary strategy which could be a result of niche partitioning. Further, it may indicate that different diets among oviraptorids were connected to their extremely high diversity. The phylogenetic position of *Gobiraptor*, being closer to several Ganzhou oviraptorids than geographically nearby taxa, supports previous results about the distant relationships among Nemegt oviraptorids (Lü et al., 2015, 2016, 2017; Funston and Currie, 2016) which could reflect their complicated evolutionary history. The discovery of *Gobiraptor* in the Nemegt Formation confirms that oviraptorids did not prefer xeric environments. It is also clear that they achieved high diversity in the Nemegt Basin, being comparable to the oviraptorid diversity in the Ganzhou region of southern China.

The other new maniraptoran, *Nemegtonykus citus* gen. et sp. nov. is a novel alvarezsaurid. *Nemegtonykus* is distinguished from other alvarezsaurids by an extreme fusion between the sacrum and ilium, fused scapulocoracoid, much reduced pubic peduncle of ilium, dorsally deflected postacetabular process of ilium with a large fossa near the antitrochanter, greatly reduced distal condyles of femur, proximally fused tarsometatarsus, and distal fusion between metararsals II and IV. Some of the characters are present only in *Nemegtonykus*, among which the most significant is the extreme fusion between the sacrum and ilium. Although only the cranial two sacrals are preserved, the sacral vertebrae apparently lack distinct sacral ribs. Instead, the first sacral has a dorsolaterally projected subtrapezoidal lamina which is fused to the preacetabular process of ilium. The second sacral shows a more dramatic condition, the centrum being directly fused to the preacetabular

region of ilium. This remarkable pelvic morphology and elongate distal hinlimb elements as well as hindlimb proportions suggest *Nemegtonykus* was likely to be an able cursor with a nascent avian locomotion which could be similar to that of basal avialans. The phylogenetic analysis of *Nemegtonykus* in this study recovered this taxon as a derived mononykin parvicursorine, sister to *Linhenykus* from Inner Mongolia. However, the phylogenetic relationships among alvarezsaurids differ from the results of some recent studies (Xu et al., 2010, 2011; Xu, Upchurch, et al., 2013) so more specimens and data are needed to resolve the contradictions. As the second alvarezsaurid taxon from the Nemegt Formation and the sixth from the Nemegt Basin, *Nemegtonykus* is crucial in recognition of alvarezsaurid diversity and paleoecology in this region. The skewed occurrences of alvarezsaurids in the Nemegt Basin has possibly been affected by preservational bias, judging by their small size and the fact that holotype specimen of *Nemegtonykus* was associated with other alvarezsaurid remains. Additionally, presence of *Nemegtonykus* in the Nemegt Formation may indicate that alvarezsaurids in the Nemegt Basin probably flourished in mesic environments as well.

Although detailed descriptions of the two new maniraptorans are included in this thesis, paleobiology and evolution of alvarezsaurids and oviraptorids are yet to be fully resolved. Additional specimens and more elaborate studies on a particular question about their biology or systematics will be of great help in revealing how these animals lived. This thesis will serve as a basis of such work since it presents a vast amount of information on the anatomy of these novel taxa.

LITERATURE CITED

Agnolin, F. L., J. E. Powell, F. E. Novas, and M. Kundrát. 2012. New alvarezsaurid (Dinosauria, Theropoda) from uppermost Cretaceous of north-western Patagonia with associated eggs. Cretaceous Research 35:33-56.

Alfaro, M. E., F. Santini, C. Brock, H. Alamillo, A. Dornburg, D. L. Rabosky, G. Carnevale, and L. J. Harmon. 2009. Nine exceptional radiations plus high turnover explain species diversity in jawed vertebrates. Proceedings of the National Academy of Sciences 106:13410-13414.

Alifanov, V. R., and R. Barsbold. 2009. *Ceratonykus oculatus* gen. et sp. nov., a new dinosaur (?Theropoda, Alvarezsauria) from the Late Cretaceous of Mongolia. Paleontological Journal 43:94-106.

Allen, V., K. T. Bates, Z. Li, and J. R. Hutchinson. 2013. Linking the evolution of body shape and locomotor biomechanics in bird-line archosaurs. Nature 497:104-107.

Averianov, A., and H.-D. Sues. 2017. The oldest record of Alvarezsauridae (Dinosauria: Theropoda) in the Northern Hemisphere. PLoS ONE 12:e0186254.

Balanoff, A. M., and M. A. Norell. 2012. Osteology of *Khaan mckennai* (Oviraptorosauria: Theropoda). Bulletin of the American Museum of Natural History 372:1-77.

Barrowclough, G. F., J. Cracraft, J. Klicka, and R. M. Zink. 2016. How many kinds of birds are there and why does it matter? PLoS ONE 11:e0166307.

Barsbold, R. 1974. Saurornithoididae, a new family of small theropod dinosaurs

from Central Asia and North America. Palaeontologia Polonica 30:5-22.

Barsbold, R. 1976a. On a new Late Cretaceous family of small theropods (Oviraptoridae fam. n.) of Mongolia. Doklady Akademia Nauk SSSR 226:685-688.

Barsbold, R. 1976b. New data on *Therizinosaurus* (Therizinosauridae, Theropoda). Transactions, Joint Soviet–Mongolian Paleontological Expedition 3:76-92.

Barsbold, R. 1977. Kinetizi i osobennosti stroeniy chelyustnogo apparata u oviraptorov (Theropoda, Saurischia). Transactions of the Joint Soviet-Mongolian Paleontological Expedition 4:37-47.

Barsbold, R. 1981. Toothless dinosaurs of Mongolia. Transactions of the Joint Soviet-Mongolian Paleontological Expedition 15:28-39.

Barsbold, R. 1983. Carnivorous dinosaurs from the Cretaceous of Mongolia. Transactions of the Joint Soviet-Mongolian Paleontological Expedition 19:5-117.

Barsbold, R. 1986. Raubdinosaurier Oviraptoren; pp. 210-223 in O. I. Vorob'eva (ed.), Gerpetologičeskie issledovaniâ v Mongol'skoj Narodnoj Respublike. Institut èvolûcionnoj morfologii i èkologii životnyh im. A.N. Severcova, Akademiâ nauk SSSR, Moscow, Russia.

Barsbold, R. 1997. Oviraptorosauria; pp. 505-508 in P. J. Currie, and K. Padian (eds.), Encyclopedia of Dinosaurs. Academic Press, Oxford, U.K.

Barsbold, R., H. Osmólska, M. Watabe, P. J. Currie, and K. Tsogtbaatar. 2000. A new oviraptorosaur (Dinosauria, Theropoda) from Mongolia: the first dinosaur with a pygostyle. Acta Palaeontologica Polonica 45:97-106.

Bell, P. R., P. J. Currie, and D. A. Russell. 2015. Large caenagnathids (Dinosauria,

Oviraptorosauria) from the uppermost Cretaceous of western Canada. Cretaceous Research 52:101-107.

Bonaparte, J. F. 1991. Los vertebrados fósiles de la Formación Río Colorado, de la ciudad de Neuquén y cercanías, Cretácico superior, Argentina. Revista del Museo Argentino de Ciencias Naturales "Bernardino Rivadavia." Paleontología 4:17-123.

Brochu, C. A. 2003. Osteology of *Tyrannosaurus rex*: insights from a nearly complete skeleton and high-resolution computed tomographic analysis of the skull. Journal of Vertebrate Paleontology 22:1-138.

Brusatte, S. L., J. K. O'Connor, and E. D. Jarvis. 2015. The origin and diversification of birds. Current Biology 25:R888-R898.

Campione, N. E., D. C. Evans, C. M. Brown, and M. T. Carrano. 2014. Body mass estimation in non-avian bipeds using a theoretical conversion to quadruped stylopodial proportions. Methods in Ecology and Evolution 5:913-923.

Carrano, M. T. 1998. Locomotion in non-avian dinosaurs: integrating data from hindlimb kinematics, in vivo strains, and bone morphology. Paleobiology 24:450-469.

Carrano, M. T., and A. A. Biewener. 1999. Experimental alteration of limb posture in the chicken (*Gallus gallus*) and its bearing on the use of birds as analogs for dinosaur locomotion. Journal of Morphology 240:237-249.

Carrano, M. T., and J. R. Hutchinson. 2002. Pelvic and hindlimb musculature of *Tyrannosaurus rex* (Dinosauria: Theropoda). Journal of Morphology 253:207-228.

Cau, A. 2018. The assembly of the avian body plan: a 160-million-year long

process. Bollettino della Società Paleontologica Italiana 57:1-25.

Cau, A., and D. Madzia. 2018. Redescription and affinities of *Hulsanpes perlei* (Dinosauria, Theropoda) from the Upper Cretaceous of Mongolia. PeerJ 6:e4868.

Cau, A., T. Brougham, and D. Naish. 2015. The phylogenetic affinities of the bizarre Late Cretaceous Romanian theropod *Balaur bondoc* (Dinosauria, Maniraptora): dromaeosaurid or flightless bird? PeerJ 3:e1032.

Chiappe, L. M. 1995. The first 85 million years of avian evolution. Nature 378:349-355.

Chiappe, L. M., and R. A. Coria. 2003. A new specimen of *Patagonykus puertai* (Theropoda: Alvarezsauridae) from the Late Cretaceous of Patagonia. Ameghiniana 40:119-122.

Chiappe, L. M., M. A. Norell, and J. M. Clark. 1996. Phylogenetic position of *Mononykus* (Aves: Alvarezsauridae) from the Late Cretaceous of the Gobi Desert. Memoirs of the Queensland Museum 39:557-582.

Chiappe, L. M., M. A. Norell, and J. M. Clark. 1997. *Mononykus* and birds: methods and evidence. The Auk 114:300-302.

Chiappe, L. M., M. A. Norell, and J. M. Clark. 1998. The skull of a relative of the stem-group bird *Mononykus*. Nature 392:275-278.

Chiappe, L. M., M. A. Norell, and J. M. Clark. 2002. The Cretaceous, short-armed Alvarezsauridae: *Mononykus* and its kin; pp. 87-120 in L. M. Chiappe, and L. M. Witmer (eds.), Mesozoic Birds: Above the Heads of Dinosaurs. University of California Press, Berkeley.

Chinsamy-Turan, A. 2005. The Microstructure of Dinosaur Bone: Deciphering

Biology with Fine-Scale Techniques. Johns Hopkins University Press, Baltimore, 216 pp.

Choiniere, J. N., J. M. Clark, M. A. Norell, and X. Xu. 2014. Cranial osteology of *Haplocheirus sollers* Choiniere et al., 2010 (Theropoda: Alvarezsauroidea). American Museum Novitates 3816:1-44.

Choiniere, J. N., X. Xu, J. M. Clark, C. A. Forster, Y. Guo, and F. Han. 2010. A basal alvarezsauroid theropod from the early Late Jurassic of Xinjiang, China. Science 327:571-574.

Christiansen, P., and N. Bonde. 2002. Limb proportions and avian terrestrial locomotion. Journal für Ornithologie 143:356-371.

Cifelli, R. L., J. I. Kirkland, A. Weil, A. L. Deino, and B. J. Kowallis. 1997. High-precision $^{40}Ar/^{39}Ar$ geochronology and the advent of North America's Late Cretaceous terrestrial fauna. Proceedings of the National Academy of Sciences 94:11163-11167.

Clark, J. M., M. A. Norell, and R. Barsbold. 2001. Two new oviraptorids (Theropoda: Oviraptorosauria), Upper Cretaceous Djadokhta Formation, Ukhaa Tolgod, Mongolia. Journal of Vertebrate Paleontology 21:209-213.

Clark, J. M., M. A. Norell, and T. Rowe. 2002. Cranial anatomy of *Citipati osmolskae* (Theropoda, Oviraptorosauria), and a reinterpretation of the holotype of *Oviraptor philoceratops*. American Museum Novitates 3364:1-24.

Currie, P. J. 1989. The first records of *Elmisaurus* (Saurischia, Theropoda) from North America. Canadian Journal of Earth Sciences 26:1319-1324.

Currie, P. J. 1990. The Elmisauridae; pp. 245-248 in D. B. Weishampel, P. Dodson,

and H. Osmólska (eds.), The Dinosauria. University of California Press, Berkeley.

Currie, P. J., G. F. Funston, and H. Osmólska. 2016. New specimens of the crested theropod dinosaur *Elmisaurus rarus* from Mongolia. Acta Palaeontologica Polonica 61:143-157.

Currie, P. J., S. J. Godfrey, and L. Nessov. 1993. New caenagnathid (Dinosauria: Theropoda) specimens from the Upper Cretaceous of North America and Asia. Canadian Journal of Earth Sciences 30:2255-2272.

Dashzeveg, D., L. Dingus, D. B. Loope, C. C. Swisher, T. Dulam, and M. R. Sweeney. 2005. New stratigraphic subdivision, depositional environment, and age estimate for the Upper Cretaceous Djadokhta Formation, southern Ulan Nur Basin, Mongolia. American Museum Novitates 3498:1-31.

Dingus, L., D. B. Loope, D. Dashzeveg, C. C. Swisher, C. Minjin, M. J. Novacek, and M. A. Norell. 2008. The geology of Ukhaa Tolgod (Djadokhta Formation, Upper Cretaceous, Nemegt Basin, Mongolia). American Museum Novitates 3616:1-40.

Eberth, D. A. 2018. Stratigraphy and paleoenvironmental evolution of the dinosaur-rich Baruungoyot-Nemegt succession (Upper Cretaceous), Nemegt Basin, southern Mongolia. Palaeogeography, Palaeoclimatology, Palaeoecology 494:29-50.

Eberth, D. A., D. Badamgarav, and P. J. Currie. 2009. The Baruungoyot-Nemegt transition (Upper Cretaceous) at the Nemegt type area, Nemegt Basin, south central Mongolia. Journal of the Paleontological Society of Korea 25:1-15.

Eberth, D. A., Y. Kobayashi, Y.-N. Lee, O. Mateus, F. Therrien, D. K. Zelenitsky, and M. A. Norell. 2009. Assignment of *Yamaceratops dorngobiensis* and associated redbeds at Shine Us Khudag (eastern Gobi, Dorngobi Province, Mongolia) to the redescribed Javkhlant Formation (Upper Cretaceous). Journal of Vertebrate Paleontology 29:295-302.

Elzanowski, A. 1999. A comparison of the jaw skeleton in theropods and birds, with a description of the palate in the Oviraptoridae. Smithsonian Contributions to Paleobiology 89:311–323.

Fanti, F., P. J. Currie, and D. Badamgarav. 2012. New specimens of *Nemegtomaia* from the Baruungoyot and Nemegt Formations (Late Cretaceous) of Mongolia. PLoS ONE 7:e31330.

Farke, A. A., W. D. Maxwell, R. L. Cifelli, and M. J. Wedel. 2014. A ceratopsian dinosaur from the Lower Cretaceous of western North America, and the biogeography of Neoceratopsia. PLoS ONE 9:e112055.

Farlow, J. O., S. M. Gatesy, T. R. Holtz, Jr., J. R. Hutchinson, and J. M. Robinson. 2000. Theropod locomotion. American Zoologist 40:640-663.

Forster, C. A., L. M. Chiappe, D. W. Krause, and S. D. Sampson. 1996. The first Cretaceous bird from Madagascar. Nature 382:532-534.

Funston, G. F., and P. J. Currie. 2014. A previously undescribed caenagnathid mandible from the late Campanian of Alberta, and insights into the diet of *Chirostenotes pergracilis* (Dinosauria: Oviraptorosauria). Canadian Journal of Earth Sciences 51:156-165.

Funston, G. F., and P. J. Currie. 2016. A new caenagnathid (Dinosauria: Oviraptorosauria) from the Horseshoe Canyon Formation of Alberta,

Canada, and a reevaluation of the relationships of Caenagnathidae. Journal of Vertebrate Paleontology 36:e1160910.

Funston, G. F., P. J. Currie, and M. E. Burns. 2016. New elmisaurine specimens from North America and their relationship to the Mongolian *Elmisaurus rarus*. Acta Palaeontologica Polonica 61:159-173.

Funston, G. F., S. E. Mendonca, P. J. Currie, and R. Barsbold. 2018a. Oviraptorosaur anatomy, diversity and ecology in the Nemegt Basin. Palaeogeography, Palaeoclimatology, Palaeoecology 494:101-120.

Funston, G. F., S. E. Mendonca, P. J. Currie, and R. Barsbold. 2018b. A dinosaur community composition dataset for the Late Cretaceous Nemegt Basin of Mongolia. Data in Brief 16:660-666.

Funston, G. F., W. S. Persons, G. J. Bradley, and P. J. Currie. 2015. New material of the large-bodied caenagnathid *Caenagnathus collinsi* from the Dinosaur Park Formation of Alberta, Canada. Cretaceous Research 54:179-187.

Funston, G. F., P. J. Currie, D. A. Eberth, M. J. Ryan, T. Chinzorig, D. Badamgarav, and N. R. Longrich. 2016. The first oviraptorosaur (Dinosauria: Theropoda) bonebed: evidence of gregarious behaviour in a maniraptoran theropod. Scientific Reports 6:35782.

Gatesy, S. M. 1990. Caudofemoral musculature and the evolution of theropod locomotion. Paleobiology 16:170-186.

Gatesy, S. M. 1991. Hind limb scaling in birds and other theropods: implications for terrestrial locomotion. Journal of Morphology 209:83-96.

Gatesy, S. M., and K. P. Dial. 1996. Locomotor modules and the evolution of avian flight. Evolution 50:331-340.

Gatesy, S. M., and K. M. Middleton. 1997. Bipedalism, flight, and the evolution of theropod locomotor diversity. Journal of Vertebrate Paleontology 17:308-329.

Gauthier, J. 1986. Saurischian monophyly and the origin of birds. Memoirs of the California Academy of Sciences 8:1-55.

George, J. C., and A. J. Berger. 1966. Avian Myology. Academic Press, New York, 500 pp.

Gilmore, C. W. 1920. Osteology of the carnivorous Dinosauria in the United States National Museum: with special reference to the genera *Antrodemus* (*Allosaurus*) and *Ceratosaurus*. Bulletin of the United States National Museum 110:1-154.

Gilmore, C. W. 1924. Contributions to vertebrate palaeontology. Geological Survey of Canada, Bulletin 38:1-89.

Godefroit, P., A. Cau, H. Dong-Yu, F. Escuillié, W. Wenhao, and G. Dyke. 2013. A Jurassic avialan dinosaur from China resolves the early phylogenetic history of birds. Nature 498:359-362.

Goloboff, P. A., and S. A. Catalano. 2016. TNT version 1.5, including a full implementation of phylogenetic morphometrics. Cladistics 32:221-238.

Gradziński, R. 1970. Sedimentation of dinosaur-bearing Upper Cretaceous deposits of the Nemegt Basin, Gobi Desert. Palaeontologia Polonica 21:147-229.

Gradziński, R., and T. Jerzykiewicz. 1974a. Dinosaur-and mammal-bearing aeolian and associated deposits of the Upper Cretaceous in the Gobi Desert (Mongolia). Sedimentary Geology 12:249-278.

Gradziński, R., and T. Jerzykiewicz. 1974b. Sedimentation of the Barun Goyot

formation. Palaeontologica Polonica 30:111-146.

Gradziński, R., J. Kazmierczak, and J. Lefeld. 1968. Geographical and geological data from the Polish-Mongolian Palaeontological Expeditions. Palaeontologia Polonica 19:3-82.

Gradziński, R., Z. Kielan-Jaworowska, and T. Maryańska. 1977. Upper Cretaceous Djadokhta, Barun Goyot and Nemegt formations of Mongolia, including remarks on previous subdivisions. Acta Geologica Polonica 27:281-318.

Harrison, C. J. O., and C. A. Walker. 1975. The Bradycnemidae, a new family of owls from the Upper Cretaceous of Romania. Palaeontology 18:563-570.

Hendrickx, C., S. A. Hartman, and O. Mateus. 2015. An overview of non-avian theropod discoveries and classification. PalArch's Journal of Vertebrate Palaeontology 12:1-73.

Holtz, T. R., Jr. 1995. The arctometatarsalian pes, an unusual structure of the metatarsus of Cretaceous Theropoda (Dinosauria: Saurischia). Journal of Vertebrate Paleontology 14:480-519.

Holtz, T. R., Jr., and H. Osmólska. 2004. Saurischia; pp. 21-24 in D. B. Weishampel, P. Dodson, and H. Osmólska (eds.), The Dinosauria, second edition. University of California Press, Berkely.

Hone, D. W. E., J. N. Choiniere, Q. Tan, and X. Xu. 2013. An articulated pes from a small parvicursorine alvarezsauroid dinosaur from Inner Mongolia, China. Acta Palaeontologica Polonica 58:453-458.

Hu, D., L. Hou, L. Zhang, and X. Xu. 2009. A pre-*Archaeopteryx* troodontid theropod from China with long feathers on the metatarsus. Nature 461:640-643.

Hutchinson, J. R. 2001a. The evolution of femoral osteology and soft tissues on the line to extant birds (Neornithes). Zoological Journal of the Linnean Society 131:169-197.

Hutchinson, J. R. 2001b. The evolution of pelvic osteology and soft tissues on the line to extant birds (Neornithes). Zoological Journal of the Linnean Society 131:123-168.

Hutchinson, J. R. 2002. The evolution of hindlimb tendons and muscles on the line to crown-group birds. Comparative Biochemistry and Physiology Part A: Molecular & Integrative Physiology 133:1051-1086.

Hutchinson, J. R., and L. M. Chiappe. 1998. The first known alvarezsaurid (Theropoda: Aves) from North America. Journal of Vertebrate Paleontology 18:447-450.

Hutchinson, J. R., and S. M. Gatesy. 2000. Adductors, abductors, and the evolution of archosaur locomotion. Paleobiology 26:734-751.

Irmis, R. B. 2007. Axial skeleton ontogeny in the Parasuchia (Archosauria: Pseudosuchia) and its implications for ontogenetic determination in archosaurs. Journal of Vertebrate Paleontology 27:350-361.

Jerzykiewicz, T. 2000. Lithostratigraphy and sedimentary settings of the Cretaceous dinosaur beds of Mongolia; pp. 279-296 in M. J. Benton, M. A. Shishkin, D. M. Unwin, and E. N. Kurochkin (eds.), The Age of Dinosaurs in Russia and Mongolia. Cambridge University Press, Cambridge, U.K.

Jerzykiewicz, T., and D. A. Russell. 1991. Late Mesozoic stratigraphy and vertebrates of the Gobi Basin. Cretaceous Research 12:345-377.

Jerzykiewicz, T., P. Currie, D. Eberth, P. Johnston, E. Koster, and J.-J. Zheng. 1993.

Djadokhta Formation correlative strata in Chinese Inner Mongolia: an overview of the stratigraphy, sedimentary geology, and paleontology and comparisons with the type locality in the pre-Altai Gobi. Canadian Journal of Earth Sciences 30:2180-2195.

Jetz, W., G. H. Thomas, J. B. Joy, K. Hartmann, and A. O. Mooers. 2012. The global diversity of birds in space and time. Nature 491:444-448.

Ji, Q., P. J. Currie, M. A. Norell, and S.-A. Ji. 1998. Two feathered dinosaurs from northeastern China. Nature 393:753–761.

Ji, Q., J. Lü, X.-F. Wei, and X.-R. Wang. 2012. A new oviraptorosaur from the Yixian Formation of Jianchang, western Liaoning Province, China. Geological Bulletin of China 31:2102-2107.

Jones, T. D., J. O. Farlow, J. A. Ruben, D. M. Henderson, and W. J. Hillenius. 2000. Cursoriality in bipedal archosaurs. Nature 406:716-718.

Karhu, A. A., and A. S. Rautian. 1996. A new family of Maniraptora (Dinosauria: Saurischia) from the Late Cretaceous of Mongolia. Paleontological Journal 30:583-592.

Khand, Y., D. Badamgarav, Y. Ariunchimeg, and R. Barsbold. 2000. Cretaceous system in Mongolia and its depositional environments; pp. 49-79 in H. Okada, and N. J. Mateer (eds.), Cretaceous Environments of Asia. Elsevier, Amsterdam.

Kurochkin, E. N. 1999. A new large enantiornithid from the Late Cretaceous of Mongolia; pp. 132-147 in I. Darevskii, and A. Averianov (eds.), Materials on the History of Fauna of Eurasia. Zoological Institute of the Russian Academy of Sciences, Saint-Petersburg, Russia.

Kurochkin, E. N. 2000. Mesozoic birds of Mongolia and the former USSR; pp. 533-559 in M. J. Benton, M. A. Shishkin, D. M. Unwin, and E. N. Kurochkin (eds.), The Age of Dinosaurs in Russia and Mongolia. Cambridge University Press, Cambridge, U.K.

Kurochkin, E. N., G. J. Dyke, and A. A. Karhu. 2002. A new presbyornithid bird (Aves, Anseriformes) from the Late Cretaceous of southern Mongolia. American Museum Novitates 3386:1-11.

Kurzanov, S. M. 1981. An unusual theropod from the Upper Cretaceous of Mongolia. Joint Soviet-Mongolian Paleontological Expedition 15:39-49.

Kurzanov, S. M., and H. Osmólska. 1991. *Tochisaurus nemegtensis* gen. et sp. n., a new troodontid (Dinosauria, Theropoda) from Mongolia. Acta Palaeontologica Polonica 36:69-76.

Lamanna, M. C., H.-D. Sues, E. R. Schachner, and T. R. Lyson. 2014. A new large-bodied oviraptorosaurian theropod dinosaur from the latest Cretaceous of western North America. PLoS ONE 9:e92022.

Lee, Y.-N., R. Barsbold, P. J. Currie, Y. Kobayashi, H.-J. Lee, P. Godefroit, F. Escuillié, and T. Chinzorig. 2014. Resolving the long-standing enigmas of a giant ornithomimosaur *Deinocheirus mirificus*. Nature 515:257-260.

Lefeld, J. 1971. Geology of the Djadokhta Formation at Bayn Dzak (Mongolia). Palaeontologia Polonica 25:101-127.

Longrich, N. R., and P. J. Currie. 2009. *Albertonykus borealis*, a new alvarezsaur (Dinosauria: Theropoda) from the Early Maastrichtian of Alberta, Canada: implications for the systematics and ecology of the Alvarezsauridae. Cretaceous Research 30:239-252.

Longrich, N. R., P. J. Currie, and Z. M. Dong. 2010. A new oviraptorid (Dinosauria: Theropoda) from the Upper Cretaceous of Bayan Mandahu, Inner Mongolia. Palaeontology 53:945-960.

Longrich, N. R., K. Barnes, S. Clark, and L. Millar. 2013. Caenagnathidae from the Upper Campanian Aguja Formation of West Texas, and a revision of the Caenagnathinae. Bulletin of the Peabody Museum of Natural History 54:23-49.

Lü, J. 2002. A new oviraptorosaurid (Theropoda: Oviraptorosauria) from the Late Cretaceous of southern China. Journal of Vertebrate Paleontology 22:871-875.

Lü, J., and S. L. Brusatte. 2015. A large, short-armed, winged dromaeosaurid (Dinosauria: Theropoda) from the Early Cretaceous of China and its implications for feather evolution. Scientific Reports 5:11775.

Lü, J., and B.-K. Zhang. 2005. A new oviraptorid (Theropod: Oviraptorosauria) from the Upper Cretaceous of the Nanxiong Basin, Guangdong Province of southern China. Acta Palaeontologica Sinica 44:412-422.

Lü, J., L. Yi, H. Zhong, and X. Wei. 2013. A new oviraptorosaur (Dinosauria: Oviraptorosauria) from the Late Cretaceous of southern China and its paleoecological implications. PLoS ONE 8:e80557.

Lü, J., R. Chen, S. L. Brusatte, Y. Zhu, and C. Shen. 2016. A Late Cretaceous diversification of Asian oviraptorid dinosaurs: evidence from a new species preserved in an unusual posture. Scientific Reports 6:35780.

Lü, J., Y. Tomida, Y. Azuma, Z. Dong, and Y.-N. Lee. 2004. New oviraptorid dinosaur (Dinosauria: Oviraptorosauria) from the Nemegt Formation of

southwestern Mongolia. Bulletin of National Science Museum, Tokyo, Series C 30:95-130.

Lü, J., Y. Tomida, Y. Azuma, Z. Dong, and Y.-N. Lee. 2005. *Nemegtomaia* gen. nov., a replacement name for the oviraptorosaurian dinosaur *Nemegtia* Lü et al., 2004, a preoccupied name. Bulletin of National Science Museum, Tokyo, Series C 31:51.

Lü, J., P. J. Currie, L. Xu, X. Zhang, H. Pu, and S. Jia. 2013. Chicken-sized oviraptorid dinosaurs from central China and their ontogenetic implications. Naturwissenschaften 100:165-175.

Lü, J., G. Li, M. Kundrat, Y.-N. Lee, Z. Sun, Y. Kobayashi, C. Shen, F. Teng, and H. Liu. 2017. High diversity of the Ganzhou Oviraptorid Fauna increased by a new "cassowary-like" crested species. Scientific Reports 7:6393.

Lü, J., H. Pu, Y. Kobayashi, L. Xu, H. Chang, Y. Shang, D. Liu, Y.-N. Lee, M. Kundrat, and C. Shen. 2015. A new oviraptorid dinosaur (Dinosauria: Oviraptorosauria) from the Late Cretaceous of southern China and its paleobiogeographical implications. Scientific Reports 5:11490.

Lyson, T. R., and N. R. Longrich. 2011. Spatial niche partitioning in dinosaurs from the latest Cretaceous (Maastrichtian) of North America. Proceedings of the Royal Society of London B: Biological Sciences 278:1158-1164.

Ma, W., J. Wang, M. Pittman, Q. Tan, L. Tan, B. Guo, and X. Xu. 2017. Functional anatomy of a giant toothless mandible from a bird-like dinosaur: *Gigantoraptor* and the evolution of the oviraptorosaurian jaw. Scientific Reports 7:16247.

Makovicky, P. J., and H.-D. Sues. 1998. Anatomy and phylogenetic relationships of

the theropod dinosaur *Microvenator celer* from the Lower Cretaceous of Montana. American Museum Novitates 3240:1-27.

Makovicky, P. J., S. Apesteguía, and F. L. Agnolin. 2005. The earliest dromaeosaurid theropod from South America. Nature 437:1007-1011.

Makovicky, P. J., S. Apesteguía, and F. A. Gianechini. 2012. A new coelurosaurian theropod from the La Buitrera Fossil Locality of Río Negro, Argentina. Fieldiana Life and Earth Sciences 5:90-98.

Maleev, E. A. 1954. New turtle-like reptile in Mongolia. Priroda 3:106-108.

Mallon, J. C., and J. S. Anderson. 2014. Implications of beak morphology for the evolutionary paleoecology of the megaherbivorous dinosaurs from the Dinosaur Park Formation (upper Campanian) of Alberta, Canada. Palaeogeography, Palaeoclimatology, Palaeoecology 394:29-41.

Mallon, J. C., and J. S. Anderson. 2015. Jaw mechanics and evolutionary paleoecology of the megaherbivorous dinosaurs from the Dinosaur Park Formation (upper Campanian) of Alberta, Canada. Journal of Vertebrate Paleontology 35:e904323.

Mallon, J. C., D. C. Evans, M. J. Ryan, and J. S. Anderson. 2012. Megaherbivorous dinosaur turnover in the Dinosaur Park Formation (upper Campanian) of Alberta, Canada. Palaeogeography, Palaeoclimatology, Palaeoecology 350-352:124-138.

Mallon, J. C., D. C. Evans, M. J. Ryan, and J. S. Anderson. 2013. Feeding height stratification among the herbivorous dinosaurs from the Dinosaur Park Formation (upper Campanian) of Alberta, Canada. BMC Ecology 13:14.

Marsh, O. C. 1881. Classification of the Dinosauria. American Journal of Science

(Series 3) 23:81-86.

Martin, L. D., E. N. Kurochkin, and T. T. Tokaryk. 2012. A new evolutionary lineage of diving birds from the Late Cretaceous of North America and Asia. Palaeoworld 21:59-63.

Martinelli, A. G., and E. I. Vera. 2007. *Achillesaurus manazzonei*, a new alvarezsaurid theropod (Dinosauria) from the Late Cretaceous Bajo de la Carpa Formation, Río Negro Province, Argentina. Zootaxa 1582:1-17.

Maryańska, T., and H. Osmólska. 1997. The quadrate of oviraptorid dinosaurs. Acta Palaeontologica Polonica 42:361-371.

Maryańska, T., H. Osmólska, and M. Wolsan. 2002. Avialan status for Oviraptorosauria. Acta Palaeontologica Polonica 47:97-116.

Naish, D., and G. J. Dyke. 2004. *Heptasteornis* was no ornithomimid, troodontid, dromaeosaurid or owl: the first alvarezsaurid (Dinosauria: Theropoda) from Europe. Neues Jahrbuch für Geologie und Paläontologie 7:385-401.

Nesbitt, S. J., J. A. Clarke, A. H. Turner, and M. A. Norell. 2011. A small alvarezsaurid from the eastern Gobi Desert offers insight into evolutionary patterns in the Alvarezsauroidea. Journal of Vertebrate Paleontology 31:144-153.

Nessov, L. A., and L. J. Borkin. 1983. New records of bird bones from the Cretaceous of Mongolia and Soviet Middle Asia. Trudy Zoologicheskogo Instituta Akademii Nauk SSSR 116:108-110.

Nixon, K. C. 2002. WinClada ver. 1.00. 08. Published by the author, Ithaca, NY.

Norell, M. A., A. M. Balanoff, D. E. Barta, and G. M. Erickson. 2018. A second specimen of *Citipati osmolskae* associated with a nest of eggs from Ukhaa

Tolgod, Omnogov Aimag, Mongolia. American Museum Novitates 3899:1-44.

Norell, M. A., J. M. Clark, L. M. Chiappe, and D. Dashzeveg. 1995. A nesting dinosaur. Nature 378:774-776.

Norell, M. A., P. J. Makovicky, G. S. Bever, A. M. Balanoff, J. M. Clark, R. Barsbold, and T. Rowe. 2009. A review of the Mongolian Cretaceous dinosaur *Saurornithoides* (Troodontidae: Theropoda). American Museum Novitates 3654:1-63.

Norell, M. A., J. M. Clark, D. Demberelyin, B. Rhinchen, L. M. Chiappe, A. R. Davidson, M. C. McKenna, P. Altangerel, and M. J. Novacek. 1994. A theropod dinosaur embryo and the affinities of the Flaming Cliffs dinosaur eggs. Science 266:779-782.

Novas, F. E. 1996. Alvarezsauridae, Cretaceous basal birds from Patagonia and Mongolia. Memoirs of the Queensland Museum 39:675-702.

Novas, F. E. 1997. Anatomy of *Patagonykus puertai* (Theropoda, Avialae, Alvarezsauridae), from the Late Cretaceous of Patagonia. Journal of Vertebrate Paleontology 17:137-166.

Novas, F. E., and D. Pol. 2002. Alvarezsaurid relationships reconsidered; pp. 121-125 in L. M. Chiappe, and L. M. Witmer (eds.), Mesozoic Birds: Above the Heads of Dinosaurs. University of California Press, Berkeley.

Osborn, H. F. 1924. Three new Theropoda, *Protoceratops* zone, central Mongolia. American Museum Novitates 144:1-12.

Osmólska, H. 1981. Coossified tarsometatarsi in theropod dinosaurs and their bearing on the problem of bird origins. Palaeontologia Polonica 42:79-95.

Osmólska, H. 1987. *Borogovia gracilicrus* gen. et sp. n., a new troodontid dinosaur from the Late Cretaceous of Mongolia. Acta Palaeontologica Polonica 32:133-150.

Osmólska, H., P. J. Currie, and R. Barsbold. 2004. Oviraptorosauria; pp. 165-183 in D. B. Weishampel, P. Dodson, and H. Osmólska (eds.), The Dinosauria, second edition. University of California Press, Berkeley.

Ostrom, J. H. 1976. On a new specimen of the Lower Cretaceous theropod dinosaur *Deinonychus antirrhopus*. Breviora 439:1-21.

Owen, R. 1842. Report on British fossil reptiles. Part II. Report for the British Association for the Advancement of Science 11:60-204.

Padian, K. 2004. Basal avialae; pp. 210-231 in D. B. Weishampel, P. Dodson, and H. Osmólska (eds.), The Dinosauria, second edition. University of California Press, Berkeley.

Pei, R., Q. Li, Q. Meng, M. A. Norell, and K.-Q. Gao. 2017. New specimens of *Anchiornis huxleyi* (Theropoda: Paraves) from the Late Jurassic of northeastern China. Bulletin of the American Museum of Natural History 411:1-67.

Perle, A., M. A. Norell, L. M. Chiappe, and J. M. Clark. 1993. Flightless bird from the Cretaceous of Mongolia. Nature 362:623-626.

Perle, A., L. M. Chiappe, B. Rinchen, J. M. Clark, and M. Norell. 1994. Skeletal morphology of *Mononykus olecranus* (Theropoda, Avialae) from the Late Cretaceous of Mongolia. American Museum Novitates 3105:1-29.

Pittman, M., X. Xu, and J. B. Stiegler. 2015. The taxonomy of a new parvicursorine alvarezsauroid specimen IVPP V20341 (Dinosauria: Theropoda) from the

Upper Cretaceous Wulansuhai Formation of Bayan Mandahu, Inner Mongolia, China. PeerJ 3:e986.

Rezk, H. M. 2015. Anatomical investigation on the appendicular skeleton of the cattle egret (*Bubulcus ibis*). Journal of Experimental and Clinical Anatomy 14:5-12.

Russell, D. A. 1993. The role of Central Asia in dinosaurian biogeography. Canadian Journal of Earth Sciences 30:2002-2012.

Salgado, L., R. A. Coria, A. B. Arcucci, and L. M. Chiappe. 2009. Restos de Alvarezsauridae (Theropoda, Coelurosauria) en la Formación Allen (Campaniano-Maastrichtiano), en Salitral Ojo de Agua, Provincia de Río Negro, Argentina. Andean Geology 36:67-80.

Senter, P. 2005. Function in the stunted forelimbs of *Mononykus olecranus* (Theropoda), a dinosaurian anteater. Paleobiology 31:373-381.

Sereno, P. C. 1999a. A rationale for dinosaurian taxonomy. Journal of Vertebrate Paleontology 19:788-790.

Sereno, P. C. 1999b. The evolution of dinosaurs. Science 284:2137-2147.

Sereno, P. C. 2001. Alvarezsaurids: birds or ornithomimosaurs?; pp. 69-98 in J. Gauthier, and L. F. Gall (eds.), New Perspectives on the Origin and Early Evolution of Birds: Proceedings of the International Symposium in Honor of John H. Ostrom. Peabody Museum of Natural History, New Haven, Connecticut.

Sereno, P. C. 2005. The logical basis of phylogenetic taxonomy. Systematic Biology 54:595-619.

Smith, D. 1992. The type specimen of *Oviraptor philoceratops*, a theropod

dinosaur from the Upper Cretaceous of Mongolia. Neues Jahrbuch für Geologie und Paläontologie Abhandlungen 186:365-388.

Starck, J. M., and A. Chinsamy. 2002. Bone microstructure and developmental plasticity in birds and other dinosaurs. Journal of Morphology 254:232-246.

Sternberg, R. 1940. A toothless bird from the Cretaceous of Alberta. Journal of Paleontology 14:81-85.

Sues, H.-D., and A. Averianov. 2015. New material of *Caenagnathasia martinsoni* (Dinosauria: Theropoda: Oviraptorosauria) from the Bissekty Formation (Upper Cretaceous: Turonian) of Uzbekistan. Cretaceous Research 54:50-59.

Sullivan, R. M, S. E. Jasinski, and M. P. A. van Tomme. 2011. A new caenagnathid *Ojoraptorsaurus boerei* n. gen., n. sp. (Dinosauria, Oviraptorosauria), from the Upper Cretaceous Ojo Alamo Formation (Naashoibito Member), San Juan Basin, New Mexico. Fossil Record 3, New Mexico Museum of Natural History and Science Bulletin 53:418-428.

Suzuki, S., L. M. Chiappe, G. J. Dyke, M. Watabe, R. Barsbold, and K. Tsogtbaatar. 2002. A new specimen of *Shuvuuia deserti* Chiappe et al., 1998 from the Mongolian Late Cretaceous with a discussion of the relationships of alvarezsaurids to other theropod dinosaurs. Contributions in Science 494:1-18.

Tsuihiji, T., M. Watabe, R. Barsbold, and K. Tsogtbaatar. 2015. A gigantic caenagnathid oviraptorosaurian (Dinosauria: Theropoda) from the Upper Cretaceous of the Gobi Desert, Mongolia. Cretaceous Research 56:60-65.

Tsuihiji, T., M. Watabe, K. Tsogtbaatar, and R. Barsbold. 2016. Dentaries of a caenagnathid (Dinosauria: Theropoda) from the Nemegt Formation of the Gobi Desert in Mongolia. Cretaceous Research 63:148-153.

Tsuihiji, T., L. M. Witmer, M. Watabe, R. Barsbold, K. Tsogtbaatar, S. Suzuki, and P. Khatanbaatar. 2017. New information on the cranial morphology of *Avimimus* (Theropoda: Oviraptorosauria). Journal of Vertebrate Paleontology 37:e1347177.

Turner, A. H., S. J. Nesbitt, and M. A. Norell. 2009. A large alvarezsaurid from the Late Cretaceous of Mongolia. American Museum Novitates 3648:1-14.

Turner, A. H., D. Pol, J. A. Clarke, G. M. Erickson, and M. A. Norell. 2007. A basal dromaeosaurid and size evolution preceding avian flight. Science 317:1378-1381.

Wang, S., C. Sun, C. Sullivan, and X. Xu. 2013. A new oviraptorid (Dinosauria: Theropoda) from the Upper Cretaceous of southern China. Zootaxa 3640:242-257.

Watabe, M., K. Tsogtbaatar, S. Suzuki, and M. Saneyoshi. 2010. Geology of dinosaur-fossil-bearing localities (Jurassic and Cretaceous: Mesozoic) in the Gobi Desert: Results of the HMNS-MPC Joint Paleontological Expedition. Hayashibara Museum of Natural Sciences Research Bulletin 3:41-118.

Wei, X., H. Pu, L. Xu, D. Liu, and J. Lü. 2013. A new oviraptorid dinosaur (Theropoda: Oviraptorosauria) from the Late Cretaceous of Jiangxi Province, southern China. Acta Geologica Sinica 87:899-904.

Weishampel, D. B., D. E. Fastovsky, M. Watabe, D. Varricchio, F. Jackson, K.

Tsogtbaatar, and R. Barsbold. 2008. New oviraptorid embryos from Bugin-Tsav, Nemegt Formation (Upper Cretaceous), Mongolia, with insights into their habitat and growth. Journal of Vertebrate Paleontology 28:1110-1119.

Welles, S. P. 1954. New Jurassic dinosaur from the Kayenta Formation of Arizona. Geological Society of America Bulletin 65:591-598.

Wilson, J. A. 1999. A nomenclature for vertebral laminae in sauropods and other saurischian dinosaurs. Journal of Vertebrate Paleontology 19:639-653.

Wilson, J. A., M. D. D'Emic, T. Ikejiri, E. M. Moacdieh, and J. A. Whitlock. 2011. A nomenclature for vertebral fossae in sauropods and other saurischian dinosaurs. PLoS ONE 6:e17114.

Xu, X., and F. Han. 2010. A new oviraptorid dinosaur (Theropoda: Oviraptorosauria) from the Upper Cretaceous of China. Vertebrata PalAsiatica 48:11-18.

Xu, X., Y.-N. Cheng, X.-L. Wang, and C.-H. Chang. 2002. An unusual oviraptorosaurian dinosaur from China. Nature 419:291–293.

Xu, X., Q. Tan, J. Wang, X. Zhao, and L. Tan. 2007. A gigantic bird-like dinosaur from the Late Cretaceous of China. Nature 447:844–847.

Xu, X., D.-Y. Wang, C. Sullivan, D. W. Hone, F.-L. Han, R.-H. Yan, and F.-M. Du. 2010. A basal parvicursorine (Theropoda: Alvarezsauridae) from the Upper Cretaceous of China. Zootaxa 2413:1-19.

Xu, X., Q.-W. Tan, S. Wang, C. Sullivan, D. W. E. Hone, F.-L. Han, Q.-Y. Ma, L. Tan, and X. Dong. 2013. A new oviraptorid from the Upper Cretaceous of Nei Mongol, China, and its stratigraphic implications. Vertebrata PalAsiatica 51:85-101.

Xu, X., Q. Zhao, M. Norell, C. Sullivan, D. Hone, G. Erickson, X. Wang, F. Han, and Y. Guo. 2009. A new feathered maniraptoran dinosaur fossil that fills a morphological gap in avian origin. Chinese Science Bulletin 54:430-435.

Xu, X., C. Sullivan, M. Pittman, J. N. Choiniere, D. Hone, P. Upchurch, Q. Tan, D. Xiao, L. Tan, and F. Han. 2011. A monodactyl nonavian dinosaur and the complex evolution of the alvarezsauroid hand. Proceedings of the National Academy of Sciences 108:2338-2342.

Xu, X., P. Upchurch, Q. Ma, M. Pittman, J. Choiniere, C. Sullivan, D. W. E. Hone, Q. Tan, L. Tan, D. Xiao, and F. Han. 2013. Osteology of the Late Cretaceous alvarezsauroid *Linhenykus monodactylus* from China and comments on alvarezsauroid biogeography. Acta Palaeontologica Polonica 58:25-46.

Yao, X., X.-L. Wang, C. Sullivan, S. Wang, T. Stidham, and X. Xu. 2015. Caenagnathasia sp. (Theropoda: Oviraptorosauria) from the Iren Dabasu Formation (Upper Cretaceous: Campanian) of Erenhot, Nei Mongol, China. Vertebrata PalAsiatica 53:291-298.

Yu, Y., K. Wang, S. Chen, C. Sullivan, S. Wang, P. Wang, and X. Xu. 2018. A new caenagnathid dinosaur from the Upper Cretaceous Wangshi Group of Shandong, China, with comments on size variation among oviraptorosaurs. Scientific Reports 8:5030.

Zanno, L. E., and P. J. Makovicky. 2011. Herbivorous ecomorphology and specialization patterns in theropod dinosaur evolution. Proceedings of the National Academy of Sciences 108:232-237.

Zanno, L. E., and S. D. Sampson. 2005. A new oviraptorosaur (Theropoda,

Maniraptora) from the Late Cretaceous (Campanian) of Utah. Journal of Vertebrate Paleontology 25:897-904.

Zhou, Z. 1995. Is *Mononykus* a bird? The Auk 112:958-963.

APPENDIX 1. Abbreviations

Institutional Abbreviations

MPC Institute of Paleontology and Geology, Mongolian Academy of Sciences, Ulaanbaatar, Mongolia.

SNU Seoul National University, Seoul, Repulic of Korea.

Anatomical Abbreviations

Cranial Elements

an angular

aofe antorbital fenestra

aqj articular surface for quadratojugal

ar articular

bm bite mark(s)

cor coronoid bone

cp coronoid process

cvpdg groove for caudoventral process of dentary

d dentary

ect ectopterygoid

emf external mandibular fenestra

fp frontal process of postorbital

g groove

j jugal

jp	jugal process of postorbital
lgl	lateral glenoid
lr	lingual ridge
mgl	medial glenoid
mx	maxilla
mxf	maxillary fenestra
og	occlusal groove(s)
op	opening(s)
pl	palatine
pm	premaxilla
pra	prearticular
pt	pterygoid
qj	quadratojugal
sa	surangular
sg	groove for splenial
spl	splenial
ss	symphyseal shelf
v	vomer

Postcranial Elements

acc	accessory condyle (= medial cnemial crest)
acr	acromion process
ant	antitrochanter
asp	ascending process

brs	brevis shelf
bvf	brevis fossa
ca	articular facet for caudal vertebrae
cap	capitulum
cc	cnemial crest
cf	coracoid foramen
ch	chevron
co	coracoid
cv	caudal vertebra(e)
diprf	dorsal infraprezygapophyseal fossa
dp	diapophysis
dt	distal tarsal(s)
dv	dorsal vertebra(e)
et	ectocondylar tuber
fc	fibular condyle
fct	cranial trochanter of femur
fh	femoral head
fl	fibula
ft	fourth trochanter
g	groove
gl	glenoid fossa
hh	humeral head
idf	infradiapophyseal fossa
ilp	iliac peduncle of pubis

isp	ischiadic peduncle of ilium
l	lamina
lc	lateral condyle of femur
lf	lateral fossa
mc	medial condyle of femur
mep	medial epicondyle
mf	medial fossa
miprf	middle infraprezygapophyseal fossa
mt I	metatarsal I
mt II	metatarsal II
mt IV	metatarsal IV
mt V	metatarsal V
nc	neural canal
ns	neural spine
obp	obturator process
p	pubis
pf	popliteal fossa
poa	postacetabular process
pp	parapophysis
pra	preacetabular process
pup	pubic peduncle of ilium
r	ridge
sac	supracetabular crest
sprf	supraprezygapophyseal fossa

sv	sacral vertebra(e)
tc	trochanteric crest
tfc	tibiofibular crest
tmc	medial condyle of tibiotarsus
tp	transverse process
tu	tubercle
tub	tuberculum
viprf	ventral infraprezygapophyseal fossa
vk	ventral keel
I-IV	first to fourth pedal digits
1-5	first to fifth pedal phalanges

APPENDIX 2. Character List for the Phylogenetic Analysis of *Gobiraptor minutus* gen. et sp. nov.

1. Ratio of the preorbital skull length to the basal skull length: 0.6 or more (0); less than 0.6 (1) (Lü et al., 2013b).

2. Pneumatized crest-like prominence on the skull roof: absent (0); present (1).

3. Ratio of the width (across premaxilla–maxilla suture) of the snout to its length: less than 0.3 (0); 0.3–0.4 (1); more than 0.4 (2) (Lü et al., 2013b). (ORDERED)

4. Ratio of the length of the tomial margin of the premaxilla to the premaxilla height (ventral to the external naris): 0.7 or less (0); 1.0–1.4 (1); more than 1.7 (2). (ORDERED)

5. Inclination of the anteroventral margin of the premaxilla relative to the horizontally positioned ventral margin of the jugal: vertical (0); posterodorsal (1); anterodorsal (2).

6. Ventral projection of the premaxilla below the ventral margin of the maxilla: absent (0); present (1).

7. Ventral projection of the premaxilla below the ventral margin of the maxilla: small (0); significant (1)

8. Share of the premaxilla (ventral) in the basal skull length: 0.10 or less (0); 0.12 or more (1).

9. Pneumatization of the premaxilla: absent (0); present (1).

10. Ratio of the length of the maxilla (in lateral view) to the basal skull length: 0.4–0.7 (0); less than 0.4 (1) (Lü et al., 2013b).

11. Subantorbital portion of the maxilla: not inset medially (0); inset medially (1).

12. Palatal shelf of the maxilla with two longitudinal ridges and a tooth-like ventral process: absent (0); present (1).

13. Ventral margins of maxilla and jugal: margins form a straight line (0); the ventral margin of the maxilla slopes anteroventrally, its longitudinal axis at an angle of ca. 120° to the longitudinal axis of the jugal (1).

14. Rim around antorbital fossa: well pronounced (0); poorly delimited (1).

15. Antorbital fossa: bordered anteriorly by the maxilla (0); bordered anteriorly by the premaxilla (1).

16. Accessory maxillary fenestrae: absent (0); at least one accessory fenestra present (1).

17. Nasal along midline: longer than frontal (0); shorter than or as long as the frontal (1).

18. Nasals: separate (0); fused (1).

19. Subnarial process of the nasal: long (0); short (1).

20. Shape of the narial opening: longitudinally oval (0); teardrop-shaped, slightly longer than wide (1); much longer than wide (2). (ORDERED)

21. Nasal recesses: absent (0); present (1).

22. External naris position relative to the antorbital fossa: naris and fossa widely separated (0); posterior margin of the naris reaching the fossa (1); overlapping anterodorsally most of the fossa (2). (ORDERED)

23. Ventral margin of the external naris: at the level of the maxilla (0); dorsal to the maxilla (1).

24. Prefrontal: present (0); absent or fused with the lacrimal (1).

25. Lacrimal shaft: not projecting outward beyond the orbital plane and lateral surface of the snout (0); the middle part of the shaft projecting laterally to form a flattened transverse bar in front of the eye (1).

26. Lacrimal recesses: absent (0); present (1).

27. Ratio of the length of the orbit to the length of the antorbital fossa: 0.7–0.9 (0); 1.2 or more (1).

28. Ratio of the length of the parietal to the length of the frontal: 0.6 or less (0); 1.0 or more (1).

29. Pneumatization of skull roof bones: absent (0); present (1).

30. Sagittal crest along the interparietal contact: absent (0); present (1).

31. Supratemporal fossa: invading the frontal (0); not invading the frontal (1).

32.Infratemporal fenestra: dorsoventrally elongate, narrow anteroposteriorly (0); subquadrate, its anteroposterior length comparable to the orbital length (1).

33. Pneumatization of the squamosal: absent (0); present (1).

34. Cotyle-like incision on the ventrolateral margin of the squamosal (for reception of the dorsal end of the ascending process of the quadratojugal): absent (0); present (1).

35. Ventral ramus of the jugal: deep dorsoventrally and flattened mediolaterally (0); shallow dorsoventrally or rod-shaped (1).

36. Jugal process of the postorbital: not extending ventrally below two-thirds of the orbit height (0); long, extending ventrally close to the base of the postorbital process of the jugal (1).

37. Postorbital process of the jugal: posterodorsally inclined (0); perpendicular to the ventral ramus of the jugal (1).

38. Postorbital process of the jugal: present (0); absent (1).

39. Jugal–postorbital contact: present (0); absent (1).

40. Quadratojugal process of the jugal in lateral view: forked (0); not forked (1); fused with the quadratojugal (2).

41. Quadratojugal–squamosal contact: absent (0); present (1).

42. Ascending (squamosal) process of the quadratojugal: bordering ca. the ventral half, or less, of the infratemporal fenestra (0); bordering the ventral two-thirds or more of the infratemporal fenestra (1).

43. Ascending (squamosal) process of the quadratojugal: present (0); absent (1).

44. Angle between the ascending and jugal processes of the quadratojugal: ca. 90° (0); less than 90° (1).

45. Quadrate process of the quadratojugal: well developed, extending posteriorly or posteroventrally beyond the posterior margin of the ascending process (0); not extending beyond the posterior margin of the ascending process (1).

46. Dorsal part of the quadrate: erect (0); bent backward (1).

47. Otic process of the quadrate: articulating only with the squamosal (0); articulating with the squamosal and the lateral wall of the braincase (1).

48. Pneumatization of the quadrate: absent (0); present (1).

49. Lateral accessory process on the distal end of the quadrate for articulation with the quadratojugal: absent (0); present (1).

50. Lateral cotyle for the quadratojugal on the quadrate: absent (0); present (1).

51. Mandibular condyles of quadrate: posterior to the occipital condyle (0); in the same vertical plane as the occipital condyle (1); anterior to the occipital condyle (2). (ORDERED)

52. Nuchal transverse crest: pronounced (0); not pronounced (1).

53. Occiput position in relation to the ventral margin of the jugal–quadratojugal bar: about perpendicular (0); inclined anterodorsally (1).

54. Paroccipital process: directed laterally (0); directed ventrally (1).

55. Foramen magnum: smaller than or equal in size to the occipital condyle (0); larger than the occipital condyle (1).

56. Basal tubera: modestly pronounced (0); well developed, widely separated (1).

57. Pneumatization of the basisphenoid: weak or absent (0); extensive (1).

58. Basipterygoid processes: well developed (0); strongly reduced (1).

59. Basipterygoid processes:present (0); absent (1).

60. Parasphenoid rostrum: horizontal or anterodorsally directed (0); sloping anteroventrally (1).

61. Depression in the periotic region: absent (0); present (1).

62. Pneumatization of the periotic region: absent or weak (0); extensive (1).

63. Quadrate ramus of the pterygoid: distant from the braincase wall (0); overlapping the braincase (1).

64. Pterygoid basal process for contact with the basisphenoid: absent (0); present (1).

65. Ectopterygoid position: lateral to the pterygoid (0); anterior to the pterygoid (1).

66. Ectopterygoid contacts with the maxilla and lacrimal: absent (0); present (1).

67. Ectopterygoid: short anteroposteriorly with a hook-like jugal process (0); elongate, shaped like a Viking ship, without a hook-like process (1).

68. Massive pterygoid–ectopterygoid longitudinal bar: absent (0); present (1).

69. Palate extending below the cheek margin: absent (0); present (1).

70. Palatine: tetraradiate or trapezoidal (0); triradiate, without a jugal process (1); developed in horizontal, longitudinal, and transverse planes perpendicular to each other (2).

71. Pterygoid wing of the palatine: dorsal to the pterygoid (0); ventral to the pterygoid (1).

72. Maxillary process of the palatine: shorter than the vomeral process (0); longer than the vomeral process (1).

73. Vomer: distant from the parasphenoid rostrum (0); approaching or in contact with the parasphenoid rostrum (1).

74. Suborbital (ectopterygoid–palatine) fenestra: well developed (0); closed or reduced (1).

75. Jaw joint: distant from the midline of the skull (0); close to the skull midline (1).

76. Movable intramandibular joint: present (0); suppressed (1).

77. Mandibular symphysis: loose (0); tightly sutured (1); fused (2). (ORDERED)

78. Extended symphyseal shelf at the mandibular symphysis: absent (0); present (1).

79. Downturned symphyseal portion of the dentary: absent (0); present (1).

80. U-shaped mandibular symphysis: absent (0); present (1).

81. Ratio of the length of the retroarticular process to the total mandibular length: less than 0.05 or the process absent (0); ca. 0.10 (1).

82. Dentary: elongate (0); proportionately short and deep, with maximum depth of dentary between 25% and 50% of dentary length (with length measured from the

tip of the jaw to the end of the posterodorsal process) (1); extremely short and deep, with maximum depth 50% or more of dentary length (2).

83. Ratio of the height of the external mandibular fenestra to the length of the fenestra: 0.2–0.5 (0); 0.7–1.0 (1).

84. External mandibular fenestra: present (0); absent (1).

85. Ratio of the length of the external mandibular fenestra to total mandibular length: absent or not more than 0.10 (0); between 0.15 and 0.20 (1), greater than 0.25 (2). (ORDERED)

86. Process of the surangular dividing the external mandibular fenestra: absent (0); short and broad (1); elongate and spike-like (2) (ORDERED) (Longrich et al., 2010).

87. Coossification of the articular with the surangular: absent (0); present (1).

88. Mandibular rami in dorsal view: straight (0); laterally bowed at midlength (1).

89. Anterodorsal margin of dentary in lateral view: straight (0); concave (1); broadly concave (2).

90. Posterior margin of the dentary: incised, producing two posterior processes (0); oblique (1).

91. Posterodorsal process of the dentary long and shallow: present (0); absent (1).

92. Posteroventral process of the dentary shallow and long, extending posteriorly at least to the posterior border of the external mandibular fenestra: absent (0); present (1).

93. Coronoid process: posteriorly positioned and vertically projected (0); anteriorly positioned, near the midpoint of the jaw, with a medially hooked apex (1) (Longrich et al., 2013).

94. Surangular foramen: present (0); absent (1).

95. Mandibular articular facet for the quadrate: comprising the surangular and the articular (0); formed exclusively of the articular (1).

96. Mandibular articular facet for the quadrate: with one or two cotyles (0); convex in lateral view, transversely wide (1).

97. Position of the quadrate articular surface relative to the level of the adjoining dorsal margin of the mandibular ramus: ventral (0); moderately elevated, quadrate articulation grades smoothly into remainder of mandible (1); highly elevated, anterior and posterior margins of quadrate articulation at nearly right angles to remainder of mandible (2) (ORDERED) (Lamanna et al., 2014).

98. Anterior part of the prearticular: deep, approaching the dorsal margin of the mandible (0); shallow, strap-like, not approaching the dorsal mandibular margin (1).

99. Splenial: subtriangular, approaching the dorsal mandibular margin (0); strap-like, shallow, not approaching the margin (1).

100. Mandibular adductor fossa: anteriorly delimited, occupying the posterior part of the mandible (0); large, anteriorly and dorsally extended, not delimited anteriorly (1).

101. Coronoid bone: well developed (0); strongly reduced (1).

102. Coronoid bone: present (0); absent (1).

103. Premaxillary teeth: present (0); absent (1).

104. Maxillary tooth row: extends at least to the level of the preorbital bar (0); does not reach the level of the preorbital bar (1); maxillary teeth absent (2). (ORDERED)

105. Dentary teeth: present (0); absent from tip of jaw but present posteriorly (1); absent (2) (ORDERED) (Longrich et al., 2013).

106. Number of cervicals (excluding cervicodorsal): not more than 10 (0); more than 10 (1).

107. Anterior articular facets of the centra in the anterior postaxial cervicals: not inclined or only slightly inclined (0); strongly inclined posteroventrally, almost continuous with the ventral surfaces of the centra (1).

108. Centra of the anterior cervicals: not extending posteriorly beyond their respective neural arches (0); extending posteriorly beyond their respective neural arches (1).

109. Epipophyses on the postaxial cervicals: in the form of a low crest or rugosity (0); prong-shaped (1).

110. Cervical ribs in adults: loosely attached to vertebrae (0); firmly attached (1); fused (2). (ORDERED)

111. Shafts of cervical ribs: longer than their respective centra (0); not longer than their respective centra (1).

112. Lateral pneumatic fossae (‘pleurocoels’) on the dorsal centra: absent (0); present (1).

113. Ossified uncinate processes on the dorsal ribs: absent (0); present (1).

114. Number of vertebrae included in the synsacrum in adults: not more than 5 (0); 6 (1); 7–8 (2). (ORDERED)

115. Sacral spines in adults: unfused (0); fused (1).

116. Lateral pneumatic fossae on the sacral centra: absent (0); present (1).

117. Transition point on the caudals: absent (0); present (1).

118. Number of caudals with transverse processes: 15 or more (0); fewer than 15 (1).

119. Lateral pneumatic fossae on the caudal centra: absent (0); present at least in the anterior part of the tail (1).

120. Neural spines confined to: at least 23 anterior caudals (0); at most 16 anterior caudals (1).

121. Number of caudals: more than 35 (0); 30 or fewer (1).

122. Posterior caudal prezygapophyses: overlapping less than half of the centrum of the preceding vertebra (0); overlapping at least half of the centrum of the preceding vertebra (1).

123 Hypapophyses in the cervicodorsal vertebral region: absent (0); small (1); prominent (2). (ORDERED)

124. Posterior hemal arches: deeper than long (0); longer than deep (1).

125. Ratio of the length of the scapula to the length of the humerus: 0.7 or less (0); 0.8-1.1 (1), 1.2 or more (2). (ORDERED)

126. Acromion: projecting dorsally (0); projecting anteriorly (1); everted laterally (2).

127. Posteroventral process of the coracoid: absent or short, not extending beyond the glenoid diameter (0); long, posteroventrally extending beyond the glenoid (1).

128. Orientation of the glenoid on the pectoral girdle: posteroventral (0); lateral (1).

129. Deltopectoral crest: low, its width equal to, or smaller than, the shaft diameter (0); expanded, wider than the shaft diameter (1).

130. Extent of the deltopectoral crest (measured from the humeral head to the apex of the crest): about the proximal third of the humerus length or less (0); ca. 40%–

50% of the humerus length (1).

131. Shaft of the ulna: straight (0); bowed, convex posteriorly (1).

132. Ratio of the length of the radius to the length of the humerus: 0.80 or less (0); 0.85 or more (1).

133. Combined lengths of manual phalanges III-1 and III-2: greater than the length of phalanx III-3 (0); less than or equal to the length of phalanx III-3 (1).

134. Ratio of the length of metacarpal I to the length of metacarpal II: 0.5 or more (0); less than 0.5 (1).

135. Proximal margin of metacarpal I in dorsal view: straight, horizontal (0); angled due to a medial extent of the carpal trochlea (1).

136. Metacarpal II relative to metacarpal III: shorter (0); subequal (1); longer (2). (ORDERED)

137. Ratio of the length of metacarpal II to the length of the humerus: 0.4 or less (0); more than 0.4 (1).

138. Ratio of the length of the manus to the length of the humerus plus the radius: less than 0.50 (0), between 0.50 and 0.65 (1), greater than 0.65 (2). (ORDERED)

139. Ratio of the length of the manus to the length of the femur: 0.3–0.6 (0); more than 0.7 (1).

140. Ratio of the length of the humerus to the length of the femur: 0.50–0.69 (0); 0.70 or more (1) (Lü et al., 2013b).

141. Dorsal margins of opposite iliac blades: well separated from each other (0); close to or contacting each other along their medial sections (1).

142. Dorsal margin of the ilium along the central portion of the blade: straight (0); arched (1); concave (2) [modified based on *Nomingia*]

143. Preacetabular process of the ilium relative to the postacetabular process (lengths measured from the center of the acetabulum): shorter or equal (0); longer (1).

144. Preacetabular process: not expanded or weakly expanded ventrally below the level of the dorsal acetabular margin (0); expanded ventrally well below the level of the dorsal acetabular margin (1).

145. Morphology of the ventral margin of the preacetabular process: cuppedicus fossa absent, margin transversely narrow (0); cuppedicus fossa or a wide shelf present (1); margin flat, wide at least close to the pubic peduncle (2).

146. Anteroventral extension of the preacetabular process: absent (0); present (1).

147. Anteroventral extension of the preacetabular process: with rounded tip (0); hook-like (1).

148. Posterior end of the postacetabular process: truncated or broadly rounded (0); narrowed or acuminate (1).

149. Anteroposterior length of the pubic peduncle: about the same as that of the ischial peduncle (0); distinctly greater than that of the ischial peduncle (1).

150. Dorsoventral extension of the pubic peduncle: level with the ischial peduncle (0); deeper than the ischial peduncle (1).

151. Ratio of the length of the ilium to the length of the femur: 0.50–0.79 (0); 0.80 or more (1) (Lü et al., 2013b).

152. Pelvis: propubic (0); mesopubic (1); opisthopubic (2). (ORDERED)

153. Pubic shaft: straight (0); concave anteriorly (1).

154. Pubic foot: anterior process absent or shorter than posterior process (0); two processes equally long (1); anterior process longer than posterior process (2).

(ORDERED)

155. Posterior margin of the ischial shaft: straight or almost straight (0); distinctly concave (1).

156. Greater trochanter of the femur: weakly separated, or not separated, from the femoral head (0); distinctly separated from the femoral head (1).

157. Anterior and greater trochanters: separated (0); contacting (1).

158. Dorsal extremity of the anterior trochanter: well below the greater trochanter (0); about level with the greater trochanter (1).

159. Fourth trochanter: well developed (0); weakly developed or absent (1).

160. Adductor fossa and the associated anteromedial crest on the distal femur: weak or absent (0); well developed (1).

161. Distal projection of the fibular condyle of the femur beyond the tibial condyle: absent (0); present (1).

162. Ascending process of the astragalus: as tall as wide across the base (0); taller than wide (1).

163. Distal tarsals: not fused with the metatarsus (0); fused with the metatarsus (1).

164. Proximal coossification of metatarsals II–IV: absent (0); present (1).

165. Arctometatarsus: absent (0); present, but only proximalmost extreme of metatarsal III obscured from anterior view in articulated metatarsus (1); present, proximal ~half of metatarsal III obscured from anterior view in articulated metatarsus (2) (Lamanna et al., 2014). (ORDERED)

166. Length of metatarsal I constituting: more than 50% of metatarsal II length (0); less than 50% of metatarsal II length (1); metatarsal I absent (2). (ORDERED)

167. Ratio of the maximum length of the metatarsus to the length of the femur: less

than 0.3 (0), between 0.4 and 0.6 (1), 0.7-0.8 (2). (ORDERED)

168. Crenulated tomial margin of the premaxilla: absent (0); present (1).

169. Frontals: flat or weakly arched, not strongly projecting above orbit in lateral view (0); strongly arched, projecting well above orbit in lateral view to contribute to nasal–frontal crest (1).

170. Exoccipital: short, weakly projecting (0); strongly projects ventrally beyond squamosal in lateral view, approaching ventral end of quadrate (1).

171. Dentary posterodorsal ramus: straight or weakly curved (0); strongly bowed dorsally (1).

172. Dentary symphyseal ventral process: absent (0); prominent process present on posteroventral surface of symphysis (1).

173. Dentary anteroventral margin in lateral view: straight or weakly downturned (0); strongly downturned (1).

174. Lateral surface of dentary: smooth (0); bearing a deep fossa, sometimes with associated pneumatopore (1).

175. Angular: contributes extensively to the border of the external mandibular fenestra (0); largely excluded by surangular (1).

176. Surangular with an anteroposteriorly elongate flange on the ventral edge: absent (0); present (1).

177. External mandibular fenestra: elongate (0); height subequal to length (1).

178. Dentary contribution to external mandibular fenestra relative to length of dentary: no more than 50% (0); exceeds 50% (1).

179. Metacarpal I expanded ventrally to cover ventral surface of metacarpal II: absent (0); present (1).

180. Unguals of manual digits II and III: strongly curved (0); weakly curved (1).

181. Manual phalanx I-1: slender (0); more robust than II-1 (1); more than 200% diameter of II-1 (2) (ORDERED).

182. Manual phalanx III-3: longer than phalanx III-2 (0); shorter than or equal in length to III-2 (1).

183. Manual phalanx II-2: longer than II-1 (0); subequal to or slightly shorter than II-1 (1); distinctly shorter than II-1 (2).

184. Manual digit II: elongate, with combined lengths of manual phalanges II-1 and II-2 longer than metacarpal II (0); combined lengths of manual phalanges II-1 and II-2 subequal to metacarpal II (1) (Lamanna et al., 2014).

185. Ischium strongly bent posteriorly at midshaft, distal end forms an angle of at least 60º with proximal end: absent (0); present (1).

186. Metatarsus: elongate (0); short, length does not exceed 300% of proximal width (1).

187. Ilium: tall (0); low and anteroposteriorly elongate, height less than 25% of length (1).

188. Anterior blade of ilium shallower than posterior blade: absent (0); present (1).

189. External naris: placed anteriorly (0); extends posteriorly, with posterior end lying above antorbital fenestra (1).

190. Premaxillae, nasal processes anteroposteriorly expanded and mediolaterally compressed to form a bladelike internarial bar: absent (0); present (1).

191. Dentary, anterodorsal tip of beak: projecting upwards (0); projecting anterodorsally, tip of beak projecting at an angle of 45° or less relative to the ventral margin of the symphysis (1).

192. Dentary symphysis with interior surface bearing vascular grooves and associated foramina: absent (0); present (1).

193. Dentary symphysis bearing an hourglass-shaped ventral depression: absent (0); present (1).

194. Meckelian groove terminates: on the inside of the dentary (0); on the ventral surface of the symphysis (1).

195. Lingual triturating shelf: absent (0); present (1).

196. Symphyseal ridges inside the tip of the beak: absent (0); present but weakly developed (1); present and well developed (2).

197. Lingual ridges inside the lateral occlusal surface of beak: absent (0); present (1).

198. Posteroventral process of dentary: straight (0); bowed ventrally (1).

199. Dentaries pneumatized: absent (0); present (1).

200. Dentary: participates in dorsal border of the external mandibular fenestra (0); excluded by anterior extension of the surangular (1).

201. Dentary: participates in ventral border of external mandibular fenestra (0); excluded by anterior extension of the angular (1).

202. Surangular and angular divided by posterior extension of the external mandibular fenestra: absent (0); present (1).

203. Posterior end of the surangular: deep (0); shallow, subequal to or shallower than angular (1).

204. Surangular: deep anteriorly (0); strap-like (1).

205. Retroarticular process extends: posteriorly (0); posteroventrally (1).

206. Metacarpal I: proportionately broad (0); long and slender, diameter 20% of

length (1).

207. Manual phalanx I-1: longer than II-2 (0); subequal to II-2 (1); shorter than II-2 (2).

208. Ischiadic peduncle of pubis with prominent medial fossa: absent (0); present (?).

209. Ischium, obturator process located: distally (0); at midshaft of ischium (1).

210. Anterior margin of obturator process: straight or convex (0); distinctly concave (1).

211. Accessory trochanter of femur: weakly developed (0); prominent, subrectangular flange or finger-like process (1).

212. Metatarsal III: with an ovoid or subtriangular cross section (0); anteroposteriorly flattened, with a concave posterior surface (1).

213. Paroccipital process: elongate and slender, with dorsal and ventral edges nearly parallel (0); short and deep with convex distal end (1).

214. Mandibular articulation surface: as long as ventral end of quadrate (0); twice or more as long as quadrate surface, allowing anteroposterior movement of mandible (1).

215. Scars for interspinous ligaments in dorsal vertebrae terminate: at apex of neural spine (0); ventral to apex of neural spine (1)

216. Sternum, distinct lateral xiphoid process posterior to costal margin: absent (0); present (1)

217. Anterior edge of sternum: grooved for reception of coracoids (0); without grooves (1)

218. Deltopectoral crest: large and distinct, proximal end of humerus quadrangular

in anterior view (0); less pronounced, forming an arc rather than being quadrangular (1).

219. Ischium: more than two-thirds of pubis length (0); two-thirds or less of pubis length (1)

220. Lateral ridge of femur: absent or represented only by faint rugosity (0); distinctly raised from shaft, mound-like (1)

221. Surangular, distinct groove on dorsal surface: present (0); absent (1).

222. Vomer, position: level with other palatal elements (0); ventral to other palatal elements (1)

223. Calcaneum: excludes astragalus from reaching lateral margin of tarsus (0); small process of astragalus protrudes through a circular opening in edge of calcaneum to reach lateral margin of tarsus (1).

224. Depression on lateral surface of dentary immediately anterior to external mandibular fenestra: absent (0); present (1).

225. Groove on ventrolateral edge of angular to receive posteroventral branch of dentary: absent (0); present (1).

226. Posteroventral branch of dentary twisted so that lateral surface of branch faces somewhat ventrally: absent (0); present (1).

227. Premaxilla, large, presumably pneumatic foramen at anteroventral corner of narial fossa: absent (0); present (1).

228. Accessory opening at anterodorsal extreme of snout: absent (0); present (1).

229. Development of symphyseal shelf of mandible: limited, anteroposterior length of mandibular symphysis (as measured on midline) less than 20% total anteroposterior length of mandible (0); intermediate, length of symphysis greater

than 20% but less than 25% length of mandible (1); extensive, length of symphysis greater than 25% mandibular length (2) (ORDERED).

230. Prominent flange or shelf arising from lateral surface of dentary: absent (0); present (1).

231. Base of retroarticular process: considerably wider mediolaterally than tall dorsoventrally (0); approximately as wide as tall (1); considerably taller than wide (2). (ORDERED)

232. Posteriormost caudal vertebrae fused, forming a pygostyle-like structure: absent (0); present (1).

233. Humeral shaft: straight or nearly straight (0); strongly bowed laterally (1).

234. Proximodorsal extensor 'lip' on manual unguals: weak (i.e., continuous or nearly continuous with remainder of dorsal surface of ungual) and/or absent (0); prominent ('set off' from remainder of dorsal surface by distinct change in slope immediately distal to 'lip') (1).

235. Pubic process of ischium, 'hooked' anterodistal extension: absent (0); present (1).

236. Distal margin of obturator process: straight (0); distinctly concave, apex of obturator process angled distally (1).

237. Proximolateral edge of metatarsal IV attenuated into pointed process: absent (0); present (1).

238. Frontal anteriorly divided by slot for nasal and possibly lacrimal: absent (0); present (1).

239. Infradiapophyseal infraprezygapophyseal and infrapostzygapophyseal fossae on cervical and dorsocervical vertebrae: one or more absent (0); all three present

(1).

240. Ratio of minimum shaft diameter of manual phalanx II-1 to minimum shaft diameter of metacarpal II: greater than 1 (0); smaller than 1 (1).

241. Ratio of minimum shaft diameter to length of manual phalanx II-2: greater than 0.10 (0); smaller than 0.10 (1).

242. Ratio of the length of the metatarsus to the length of the tibia: <0.5 (0); >0.5 (1).

243. Tibia ratio of the transverse width of the distal condyles to the length: 0.20 or greater (0); <0.20 (1).

244. Ratio of minimum transverse width to length of tarsometatarsus: >0.20 (0); <0.20 (1)

245. Fusion of distal tarsals III and IV at maturity: absent (0); present (1).

246. 'Hook-like' posterodorsal process of distal tarsal IV: absent (0); present (1).

247. Posterior protuberance on proximal end of tarsometatarsus caused by coossification of distal tarsals III and IV, plus MT II, III and IV: absent (0); present (1).

248. Anterior margin of metatarsal V in lateral view: straight or slightly curved (0); tightly curved (1).

249. Concavity on posterior surface of tarsometatarsus in cross section: absent or shallow (0); prominent and deep (1).

250. Sharp cruciate ridges on posterior surface of metatarsal III: only one sharp longitudinal ridge or no ridges (0); sharp medial longitudinal ridge continuous with lateral postcondylar ridge and sharp lateral longitudinal ridge continuous with medial postcondylar ridge forming a chiasma. Ridges are separated from each other

by longitudinal sulcus (1).

251. Posteromedial and posterolateral ridges of mt II and IV respectively: weakly developed do not extend past posterior extent of distal condyle (0); well developed extend posteriorly past distal condyle (1).

252. Distal ends of shafts of metatarsals II and IV: both straight (0); metatarsal II medially deflected metatarsal IV straight (1); metatarsal II straight metatarsal IV laterally deflected (2).

253. Ratio of transverse width to anteroposterior length of distal condyle of metatarsal III: <1 (0); >1 (1).

254. External mandibular fenestra: expanded anteriorly (0); anteriorly constricted by posteroventral ramus of dentary (1).

255. Articular ridge of mandible: low, less than 25% as tall as long (0); high, more than 25% as tall as long (1).

256. Transverse groove between flexor tubercle and proximal articular surface of manual ungual I-2: absent (0); present (1)

257. Cnemial crest of tibia greatly enlarged such that the proximal articular surface of the tibia is longer anteroposteriorly than wide mediolaterally: absent (0); present (1).

APPENDIX 3. Data Matrix for the Phylogenetic Analysis of *Gobiraptor minutus* gen. et sp. nov.

Herrerasaurus_ischigualastensis

000100-

000000000000000000000000000000000000000000000000000000000000000000

00000000001000000000000000000000000010?0000000000100?0000101??0001000

00000-

0000101000000000000100000?000?0000110010100??000??0000101??00??0000?

??00?1000?000000?00000???????000?0000?000?

Velociraptor_mongoliensis

000200-

000000101001010010100010000000000010000000000100001000000000000000000

000000000000000110000000000000100101101111101101011111-

1101011120211000011011112020011100010010000000000?0000000011000?0000

??00100001000000000110011?000?000000000000000?????00000000?000?

Archaeopteryx_lithographica

000?10-0000001011010011000100001?1000-

1110??0?1??0020????000????0000001?1???1000010-10000011-01000000-

10100??0101?00?110110010111001111111111011010-

111020201?0100?1101200?0000?0?0?00000001000?0000??001?000000?010010?

0?111??00?00000?0000?00??????00000000?000?

Incisivosaurus_gauthieri

100210-

10100001?01112100?1?01?00?00000?100010?0??200111?10?10?01??111?0101?

2101110020??00011??11?1110011??

??????????????????00000000100??????????0010000000000000???????1???????

00???01000???????0?????????????????000?

Caudipteryx_zoui

10?210-?01??0?1110?0?21?01?10???0110000111001000?????????????????????0????

????0??1111??2???0001??????11??0220?????010????0?1??11???1011?101020?0

012110110?021100???1000121??0???0??0?00?001000?000?00000000?01000?001

0???0101????0?00000?0000000?0??????000000?000?

Avimimus_portentosus

???????????0?????????????????10110??1?-1121-

101??00?101111?10?????????????????0?1??111???01?????11000???-

11?21000110?110??0???2?12100111?1?????00000?1110?10020101001111222100

010000?0????????00??00?00????0??0000??0??10110??11110????????0?0?000010?

????1000000?00??

Microvenator_celer

??

?1111?2?????11001?????????????2???0??1?????????0????1?1011??1????0???1111

?11?112???11101????????0101???001{01}?????00??0000000?0??????0?1??1???0

??1?0???1?????0??00?????????????????????

Oviraptor_philoceratops

1???????????1?11?????21????????1??10000????0?????????????????????????1????

?????1?121022??10011???1??1???22???0??1?????????????2???101101?212???????

??????????????????????0???00100100000??0??1??????????????0??????????0

??11?0?0???0??00???0???????????????000?

Rinchenia_mongoliensis

11102??01111101111???121111111?1111010011100011111?11111-

11?1111111121111111111112102?01100111111111-

1122111001 1?10100101 02?2210100 0??????0110111111101????111111??????1101

?001011????????00111??????0000000 1????????1?10???1110?0?0?0?????????????

??????????000?

Citipati_osmolskae

11202111111110110111121111111111111110011101 11?1??11111??101111?111112

1?1111111121022011001111111111 0122????????1??????????????????0?101?1?????

??????????????????????????1101100101 1?01010?0??1100000000000000100?????

010100?01110?00100010 0?0?0??????00?0??00?000?

Zamyn_Khondt_oviraptorid

11202111111110111111121111111111111110011101111111111111-

1111111111121111111111121022011001111111 11-

1122111011 1?10100101021021010110111121010012101001112111111110001111

01?001011?0000010??110?000000000?0100???00?1?100??11???001?0??00??00

??????????????000?

Khaan_mckennai

10201101?1111011?11212111111111 1?110000111000?111?111111???0??1?????1?

?????1111112102101100111111111???1221110??1????00?0102??210??1101011210

?0001100001?1211111?1100011100110010010010100111110?000?001000001000

000?01?1100?1?10101000?0000{01}00??????00000000?000?

Conchoraptor_gracilis

10101101111110111112121111111111111000011100?1111111?1111-

11111111112111111111111?102?01100111111111-

11221110111?2010010101122101111001112101000210000111211111110001110

1?????????110???1??11?????????????????0??????11?00?011?0?0000011?0??000??

???00000000?000?

Machairasaurus_leptonychus

??

????????????????????????????2?????????????????????????????0011?????????????

????????????????????????????????111110?????????????????????00???????????????

??????????1?????????????????????????

Nemegtomaia_barsboldi

11100101111110111111121011111111?1100001010101l?111111?1???11?11111112

11111111112102?11100111111?11-

11221110{02}11?201?????????????????????????10002???00?1????11?????????101

1110101l?12?11??111100000001000000l000??0??1???1??11?1?1?0001?000??00

???????????????000?

Heyuannia_huangi

????????????????????????????????????1????????????????????????????????????

???1??21021??1001????1???????21???21-

12????1?????221?11000001?20???01?10100111?1?????????????????1?1?101111?2?2

101?1?????????0?00000100?0?0?0101?00?1?11?0???0?00001????????000000000

000?

Heyuannia_yanshini

????????1??????????????11?????1?110000111O?0111111???111???11?1??111?1?

??1111111210 2?01100110111111-

1122?110011?2010010101022101100001100001001210000111211111111000 11?0

11?10101111212101111100000000000000100?0000?1?10000 1?1??0???0?000010

?000000000000000?000?

Gigantoraptor_erlianensis

??1

12111120020111001111112?????1?2???????????0010?0??10?00000?11?1??1??????

??????1??1111111000?1???000101000??????????0???100100111010 0???0??????

1?????110??112?10??????????010?000??011?

Caenagnathasia_martinsoni

??

?2101?1?????120??????????????2?1002?1?0?1????????????????????????????????

???????10?1????????????0001???0????????????011?111?1????????????????????

????????0????????0?????????????????

Leptorhynchos_elegans

??

12111?1?????1200???????1?????2??

????????????1111????0001???0???????0????0111121?10???????????1??????????

?0?????0??????1?????111100111111??1

Leptorhynchos_gaddisi

??

?21?1?{12}?????1{12}???????????????2????????????????????????????????????

??????????????????101??????0??????????????????0111121?1?????????????????

??????????????????1??????????????????

Chirostenotes_pergracilis

??1

12111110020112001111121111-

1??2????????111?????????10?????0????1??11??111101???111?1?1100111???000

10100?100101000??01111211111111112?1111????????1??010???01??1000??1111

00001100100110

Caenagnathus_collinsi

??1

02101110020112001111111111-

1??2????????????1????????????????????????????????????111101?001?????0001

0101?1?????????1101121011111111?????1????????01?0010??201??1????????????

0???0??000?

Anzu_wyliei

?1??10-

1100?1100?????????????????0?0000???????1011??100?10??1??0?011?????1121

011?002011200111111?1-

1122111021 1?1?10010?02?12100010????1210???1?11?1?1102111111115?????1?00

0010100000??01?0??0?10112111011111??1111?11010110 1?0010102120111 0????

??1????0?????0000

Hagryphus_giganteus

??

??0010?????????????

????????????????????????????000010?????????????????????2???????????????

??????????1?????00??????????????1?

Elmisaurus_rarus

????????????????????????????????0??

????????????????????????????????????0??10?????????2????1?????012????????????

??????11?1???1111??0?????????000?10?0??????????????????11????1??????????

???????????1??1111111111011120??11

Nomingia_gobiensis

??

????????????????????????????????????00?1?01?00101020??????????????????11101100

1111111111111??????????????????????????1?00??????????????????????111???0???1??

?1????????1??10????????????????????

Epichirostenotes_curriei

??????????01?010??????1?????????????????????????????????110?10?1??0?????????

??2?1?111??1???2????????????????????????

?????021?????????????????????????????????1?????????????????????111??0?0???1??

?????????????10??0??????????????????

Banji_long

11?010-

111???01111021211111111011??111001?????0??11?1111?????????1111121?0111??

11?21021??000110??1?11??122?1??

??????????????????1111100101?????????110??????0?00000?????????????????00?0

?000?0???????0????????????????????

Caudipteryx_dongi

??

??????????????????????????????????????01?0?????????????0010?1?10200?011?110

11000211?????100012????????????00?001000??????????????????01?10?????0??1?

????????????00000??????000000000????

Ganzhousaurus_nankangensis

??

1{01}111?210?{12}011001????111????2????????????0???0??????????????????

??????????????????????0001????1?001?11???????1????????0?001?10?0???????0??

????????111???0?????????????000000000????

Jiangxisaurus_ganzhouensis

1??????????1?????????????11???????1?0001????????112?????1-

1?????1?01121??0111111121021111001111111?????122??10??11??1??1?????221?1

110?0120????0?????1?????????????????????1??110010111?2?????????111??2?0100

000100??????1?1?0?????0011?00??00?????????????????????????

Nankangia_jiangxiensis

??

11101?2??????100?????????????2??????1???1??1??0?0111001?????????01110110

1111112110011111????????1101??0???????1?00??11?????0?1???1????11???????01

???11?0???0??0?00?????????????????????

Shixinggia_oblita

??

????????????????????????????????????1?2?1??1?????????????????????110000-

000?????1????1?????????????????????????????01????????????????????????????????

????????????????????????????????????

Similicaudipteryx_yixianensis

??

??????????????????????????????????0?11?0?1?0??1?2???????1????????0?001?111

110?????????0??0?12????????????????????00????????????????????????0??????????

?????????10?????0?????000?0000?????

Wulatelong_gobiensis

11?02101?11?1?1???02121?111?1??1?1110001???00??11?????????????????1111??

??????????????101????1??11?????12???????1???100????2??????????1??????1100

?111111112 1???????000?11???????????0??????011????????????000????1????1?1

0?101?????????????0??0??0????????00000????

Yulong_mini

102110-

11101101101111210101110 10?0100011100 10?11111011 0???0????????0?????111

1111210220110011{01}1111?1-

1122?100??1????001?10??{12}??0000101?11110?110?100??0??1?1?0??11?00111

0?11001011?11000?100110??????0?0000010???????1??????1110?01000??00???0

??????000?00000????

Huanansaurus_ganzhouensis

11202111111110110 1?112111111111111?110001110111?11100111?????1???11?11?

????111111121022011001111111?????122?110211?????????????????001101?112???

??????????????????????????1101100001 1?01000????1?1?0????0100000110?????0

1???0??1??011??101?01????0?????????0000?1100

Tongtianlong_limosus

10202111111110 1?011212111111101111110001100001111?21110?????011?????1?

????111101121021011001101 1??????122111020 1??01?01??0?02?1001?0???????0

1??????????1121?????1000?1110100010010?????11??111?????01000001???10?

101?010??1?10001000 1?0??0000??0??0??00??2?1??0

Corythoraptor_jacobsi

1121111111111001???2121111?1??01?11000????????????2?1?????????????????1???

??111111?2102???0001??????1???122111021 1?111??1???2????001101?11100110

1111101111211111111?1001111?1101101100101010001110000000100 0?0?00?1000

?????110???0110110??01010?0000?100000002?10?0

Apatoraptor_pennatus

??0?1???

121111100201110011111111 1-

1??2110021111?????????2?1111001001120211???1010???????????101?????????00

010100010?10??????01?11?111111111110??????1?101?11??011??101?01????111??

??????????1001

Gobiraptor_minutus

??2??11?1?1???11?????????????????????????????000??110?????????????1?11?21??

1?11111?210??0?10011?11111?10122??????????1??1??????2?0?????????????0?02

10?0?111?1001101?00011???10101011???????1????000010101000 00???11010?1?

????0?0?011??001?????0??????0?000000210 0??

APPENDIX 4. Character List for the Phylogenetic Analysis of *Nemegtonykus citus* gen. et sp. nov.

1. "Protofeathers": (0) absent, (1) present

2. Contour feathers: (0) absent, (1) present

3. Vaned feathers on forelimb: (0) symmetric, (1) asymmetric

4. Shape of premaxillary body (portion in front of the external naris): (0) wider than high, or approx. as wide as high, (1) significantly higher than wide

5. Premaxillary body in front of external nares: (0) rostrocaudally shorter than body below nares and angle between anterior margin and alveolar margin more than 75 degrees, (1) rostrocaudally longer than body below the nares and angle less than 70 degrees

6. Ventral process at the posterior end of premaxillary body (gives the posterior process a forked appearance in lateral view): (0) absent, (1) present

7. Maxillary process of premaxilla: (0) contacts nasal to form posterior border of nares, (1) reduced so that maxilla participates broadly in external naris, (2) extends posteriorly to separate maxilla from nasal posterior to nares

8. Internarial bar: (0) dorsoventrally rounded, (1) dorsoventrally flat

9. Crenulate margin on buccal edge of premaxilla: (0) absent, (1) present

10. Caudal margin of naris: (0) farther rostral than the rostral border of the antorbital fossa, (1) nearly reaching or overlapping the rostral border of the antorbital fossa

11. Premaxillary symphysis: (0) acute, V-shaped, (1) rounded, U-shaped

12. Subnarial foramen: (0) absent, (1) present

13. Pronounced maxillary fenestra: (0) absent. (1) present

14. Accessory antorbital (maxillary) fenestra recessed within a shallow, caudally or caudodorsally open fossa, which is itself located within the maxillary antorbital fossa:

(0) absent, (1) present

15. Longitudinal position of maxillary fenestra: (0) situated at rostral border of antorbital fossa, (1) situated posterior to rostral border of antorbital fossa

16. Latitudinal position of maxillary fenestra: (0) situated approximately mid-height of the antorbital fossa, (1) displaced dorsally in antorbital fossa

17. Foramen perforates ventral margin of interfenestral bar between the maxillary and antorbital fenestrae: (0) absent, (1) present, pierces ventral portion of bar

18. Promaxillary fenestra (fenestra promaxillaris, also listed as ‘promaxillary foramen’): (0) absent, (1) present

19. Secondary palate formed by (0) premaxilla only (1) premaxilla, maxilla and vomer

20. Palatal shelf of maxilla: (0) flat, (1) with midline ventral "tooth-like" projection

21. Anteroposterior length of palatal shelf of maxilla: (0) short, (1) long, with extensive palatal shelves

22. Orientation of the maxillae towards each other as seen in dorsal view: (0) acutely angled, (1) subparallel

23. Ascending process of the maxilla: (0) confluent with anterior rim of maxillary body and gently sloping posterodorsally. (1) offset from anterior rim of maxillary body, with anterior projection of maxillary body shorter than high, (2) offset from

anterior rim of maxillary body, with anterior projection of maxillary body as long as high or longer

24. Nasal process of maxilla, dorsal ramus (ascending ramus of maxilla): (0) prominent, exposed laterally and medially, (1) weakly developed, lacking lateral exposure and only slight medial exposure.

25. Anterior margin of maxillary antorbital fossa: (0) rounded or pointed, (1) squared

26. Dorsal border of the internal antorbital fenestra, lateral view: (0) formed by lacrimal and maxilla, (1) formed by nasal and lacrimal

27. Dorsal border of the antorbital fossa, lateral view: (0) formed by lacrimal and Maxilla, (1) formed by nasal and lacrimal, (2) formed by maxilla, premaxilla and lacrimal

28. In lateral view, lateral lamina of the ventral ramus of nasal process of maxilla: (0) present, large broad exposure, (1) present, reduced to small triangular exposure

29. Maxillary antorbital fossa in front of the internal antorbital fenestra: (0) 40% or less of the length of the external antorbital fenestra, (1) more than 40% of the length of the external antorbital fenestra

30. Horizontal ridge on the lateral surface of maxilla at the ventral border of the antorbital fossa: (0) absent, (1) present

31. Constriction between articulated premaxillae and maxillae: (0) absent,

(1) present

32. Subnarial gap between maxilla and premaxilla at the alveolar margin: (0) absent,

(1) present

33. Nasals: (0) unfused, (1) fused

34. Dorsal surface of the nasals: (0) smooth, (1) rugose

35. Pneumatic foramen in the nasals: (0) absent, (1) present

36. Narial region (particularly anterior end of the nasals): (0) apneumatic or poorly pneumatized, (1) with extensive pneumatic fossae, especially along posterodorsal rim of fossa

37. Dorsal extent of antorbital fossa: (0) dorsal rim of antorbital fossa below nasomaxillary suture or formed by this suture, (1) antorbital fossa extending onto the lateroventral side of the nasals

38. Shape of nasals: (0) expanding posteriorly, (1) of subequal width throughout their length

39. Pronounced lateral rims of the nasals, sometimes bearing lateral cranial crests: (0) absent, (1) present

40. External nares: (0) facing laterally, (1) facing strongly anterolaterally

41. Jugal pneumatic recess in posteroventral corner of antorbital fossa (0) present, (1) absent

42. Medial jugal foramen: (0) present on medial surface ventral to postorbital bar, (1) absent

43. Sublacrimal part of jugal: (0) tapering, (1) bluntly squared anteriorly, (2) expanded

44. Anterior end of jugal: (0) posterior to internal antorbital fenestra, but reaching its posterior rim, (1) excluded from the internal antorbital fenestra, (2) expressed at the rim of the internal antorbital fenestra and with a distinct process that extends anteriorly underneath it

45. Jugal antorbital fossa: (0) absent or developed as a slight depression, (1) large, crescentic depression on the anterior end of the jugal

46. Jugal: (0) broad, plate-like, (1) very slender, rod-like

47. Jugal: (0) tall beneath lower temporal fenestra, twice or more as tall dorsoventrally as it is wide transversely, (1) rod-like

48. Jugal and postorbital: (0) contribute equally to postorbital bar, (1) ascending process of jugal reduced and descending process of postorbital ventrally elongate

49. Jugal and quadratojugal: (0) separate, (1) fused and not distinguishable from one another

50. Quadratojugal: (0) hook-shaped, without posterior process, (1) with broad, short posterior process that wraps around the lateroventral edge of the quadrate

51. Supraorbital crests on lacrimal in adult individuals: (0) absent, (1) dorsal crest above orbit, (2) lateral expansion anterior and dorsal to orbit

52. Enlarged foramen or foramina opening laterally at the angle of the lacrimal: (0) absent, (1) present

53. Height of the lacrimal: (0) significantly less than height of the orbit, and usually fails to reach the ventral margin of the orbit, (1) as high as the orbit, and contacts jugal at the level of the ventral margin of orbit

54. Lacrimal posterodorsal process: (0) absent, (1) present

55. Morphology of posterodorsal prcess of lacrimal: (0) Lacrimal T-shaped, (1) anterodorsal process much longer than posterior process, (2) posterodorsal process subvertical

56. Passage of the nasolacrimal duct: (0) leading through the body of the ventral process of the lacrimal, (1) ventral process of lacrimal not pierced, lateral side

depressed below the level of the surrounding bones, and nasolacrimal duct passes lateral to the process

57. Ventral ramus of lacrimal: (0) broadly triangular, articular end nearly twice as wide anteroposteriorly as lacrimal body at lacrimal, angle, (1) bar- or strut-like, roughly same width anteroposteriorly throughout ventral ramus

58. Prefrontal: (0) absent, (1) present

59. Prefrontal: (0) exposed dorsally on the anterior rim of the orbit in lateral view and with a slender ventral process along the posteromedial rim of the lacrimal, (1) excluded from the anterior rim of the orbit in lateral view, being displaced posteriorly and/or

medially; ventral process absent

60. Configuration of lacrimal and frontal: (0) lacrimal separated from frontal by prefrontal, (1) lacrimal contacts frontal

61. Frontals: (0) narrow anteriorly as a wedge between nasals, (1) end abruptly anteriorly, suture with nasal transversely oriented

62. Frontal supratemporal fossa: (0) limited extension of supratemporal fossa onto frontal, (1) supratemporal fossa coovers most of frontal process of the postorbital and extends anteriorly onto the dorsal surface of the frontal

63. Anterior emargination of supratemporal fossa on frontal: (0) straight or slightly curved, (1) strongly sinusoidal and reaching onto postorbital process

64. Frontal postorbital process (dorsal view): (0) smooth transition from orbital margin,

(1) sharply demarcated from orbital margin

65. Frontal edge: (0) smooth in region of lacrimal suture, (1) edge notched

66. Postorbital in lateral view: (0) with straight anterior (frontal) process, (1) frontal process curves anterodorsally and dorsal border of temporal bar is dorsally concave

67. Postorbital bar: (0) parallels quadrate, lower temporal fenestra rectangular in shape,

(1) jugal and postorbital approach or contact quadratojugal to constrict lower temporal fenesta

68. Contact between lacrimal and postorbital: (0) absent, (1) present

69. Cross-section of the ventral process of the postorbital: (0) triangular, (1) U-shaped

70. Jugal process of the postorbital: (0) ventrally directed and tapering, (1) with a small anterior spur indicating the lower delimitation of the eyeball

71. Orbit: (0) round in lateral or dorsolateral view, (1) dorsoventrally elongate

72. Parietals: (0) separate, (1) fused

73. Parietal supratemporal fenestra: (0) separated by a horizontal plate formed by the parietals, (1) contact each other posteriorly, but separated anteriorly by an anteriorly widening triangular plate formed by the parietals, (2) confluent over parietals, parietals form a sagittal crest

74. Sagittal crest: (0) dorsal surface of parietals smooth with no sagittal crest, (1) parietals dorsally convex with very low sagittal crest along midline, (2) dorsally convex with well-developed sagittal crest

75. Posteriorly placed, knob-like dorsal projection of the parietals: (0) absent, (1) present

76. Descending process of squamosal: (0) contacts quadratojugal, (1) does not

contact quadratojugal

77. Quadratojugal process of the squamosal: (0) tapering, (1) broad, and usually somewhat expanded

78. Posterolateral shelf on squamosal overhanging quadrate head: (0) absent (1) present

79. Descending process of squamosal: (0) parallels quadrate shaft, (1) nearly perpendicular to quadrate shaft

80. Supratemporal fenestra: (0) bounded laterally and posteriorly by the squamosal (1) supratemporal fenestra extended as a fossa on to the dorsal surface of the squamosal

81. Quadrate head: (0) covered by squamosal in lateral view, (1) quadrate cotyle of squamosal open laterally exposing quadrate head

82. Quadrate: (0) solid, (1) hollow

83. Mandibular joint: (0) approximately straight below quadrate head, (1) significantly posterior to quadrate head, (2) significantly anterior to quadrate head

84. Dorsal end of the quadrate: (0) with a single head that fits into a slot on the ventral side of the squamosal, (1) double-headed, medial head contacts the braincase

85. Quadrate foramen: (0) absent, (1) present

86. Quadrate foramen: (0) developed as a distinct opening between the quadrate and quadratojugal, (1) almost entirely closed in the quadrate

87. Ectopterygoid: (0) slender, without ventral fossa, (1) expanded, with a ventral depression medially, (2) expanded, with a deep groove leading into the ectopterygoid body medially, (3) deeply excavated and medial opening constricted

into a foramen

88. Dorsal recess on ectopterygoid: (0) absent, (1) present

89. Ectopterygoid: (0) posterior to palatine, (1) lateral to palatine

90. Palatine and ectopterygoid: (0) separated by pterygoid, (1) contact

91. Contact between pterygoid and palatine: (0) continuous, (1) discontinuous in the mid-region, resulting in a subsidiary palatal fenestra

92. Flange of pterygoid: (0) well developed, (1) reduced in size or absent

93. Shape of palatine in ventral view: (0) plate-like trapezoidal or subrectangular, (1) tetraradiate, (2) jugal process strongly reduced or absent

94. Suborbital fenestra: (0) similar in length to orbit, (1) reduced in size or absent

95. Infratemporal fenestra: (0) smaller than or subequal in size to orbit, (1) strongly enlarged, more than 1.5 times the size of the orbit

96. Postorbital part of the skull roof: (0) as high as orbital region, (1) deflected ventrally in adult individuals

97. Preorbital region of the skull in post-hatchling individuals: (0) elongate, nasals considerably longer than frontals, maxilla at least twice the length of the premaxilla,

(1) shortened, nasals subequal in length to frontals or shorter, maxillary length less than twice the length of the premaxillary body

98. Basipterygoid processes: (0) well-developed, extending as a distinct process from the base of the basisphenoid, (1) abbreviated or absent

99. Basipterygoid processes well developed and (0) anteroposteriorly short and finger-like (approximately as long as wide), (1) longer than wide, (2) significantly elongated and tapering (Alvarezsauroids have extremely long, thin basipterygoid

processes.

100. Basipterygoid processes: (0) ventral or anteroventrally projecting, (1) lateroventrally projecting, (2) caudally projecting.

101. Basipterygoid processes: (0) solid, (1) hollow

102. Basipterygoid recesses on dorsolateral surfaces of basipterygoid processes: (0) absent, (1) present

103. Basisphenoid recess: (0) absent or poorly developed, (1) deep and well-developed

104. Basisphenoid recess position: (0) between basisphenoid and basioccipital, (1) entirely within basisphenoid

105. Posterior opening of basisphenoid recess: (0) single, (1) divided into two small, circular foramina by a thin bar of bone

106. Basisphenoid between basal tubera and basipterygoid processes: (0) approximately as wide as long, or wider, (1) significantly elongated, at least 1.5 times longer than wide

107. Basisphenoid in lateral view: (0) oriented subhorizontally, (1) anterior portion located much more ventrally than posterior portion, recess visible in posterior view

108. Base of cultriform process: (0) not highly pneumatised, (1) expanded and pneumatic (parasphenoid bulba)

109. Exits of CN X-XII: (0) flush with surface of exoccipital, (1) located together in a bowl-like basisphenoid depression

110. Exits of CN X and XI: (0) laterally through the jugular foramen, (1) posteriorly through a foramen (metotic foramen) lateral to the exit of cranial nerve XII and the

occipital condyle

111. Paroccipital process: (0) elongate and slender, with dorsal and ventral edges nearly parallel, (1) short, deep with convex distal end

112. Paroccipital process: (0) straight, projects laterally or posterolaterally, (1) distal end curves ventrally, pendant

113. Paroccipital process: (0) with straight dorsal edge, (1) distal end twists rostrally, distal ends of the processes oriented transversely rather than vertically

114. Base of paroccipital processes: (0) solid, (1) hollowed anteriorly by diverticulum of posterior tympanic recess

115. Ventral rim of the basis of the paroccipital processes: (0) above or level with the dorsal border of the occipital condyle, (1) situated at mid-height of occipital condyle or lower

116. Foramen magnum: (0) subcircular, slightly wider than tall, (1) oval, taller than wide

117. Occipital condyle: (0) without constricted neck, (1) subspherical with constricted neck

118. Basal tubera: (0) equally formed by basioccipital and basisphenoid and not subdivided, (1) subdivided by a lateral longitudinal groove into a medial part entriely formed by the basioccipital, and a lateral part, entirely formed by the basisphenoid

119. Basal tubera: (0) set far apart, level with or beyond lateral edge of occipital condyle and/or foramen magnum (may be connected by a web of bone or separated by a large notch), (1) tubera small, directly below condyle and foramen magnum, and separated by a narrow notch

120. Subcondylar recess: (0) absent, (1) present in basioccipital/exoccipital lateral and ventral to occipital condyle

121. Exit of mid-cerebral vein: (0) included in trigeminal foramen, (1) vein exits braincase through a separate foramen anterodorsal to the trigeminal foramen

122. Brain proportions: (0) forebrain small and narrow, (1) forebrain significantly enlarged and triangular

123. Anterior tympanic recess in the braincase: (0) absent, (1) present

124. Depression for pneumatic recess on prootic: (0) absent, (1) present as dorsally open fossa on prootic/opisthotic, (2) present as deep, posterolaterally directed concavity

125. Crista interfenestralis: (0) confluent with lateral surface of prootic and opisthotic, (1) distinctly depressed within middle ear opening

126. Dorsal tympanic recess (dorsal to crista interfenestralis): (0) absent, (1) small pocket present, (2) extensive with indirect pneumatisation

127. Caudal (posterior) tympanic recess: (0) absent, (1) present as opening on anterior surface of paroccipital process, (2) extends into opisthotic posterodorsal to fenestra ovalis, confluent with this fenestra

128. Otosphenoidal crest: (0) vertical on basisphenoid and prootic, and does not border an enlarged pneumatic recess, (1) well-developed, crescent-shaped, thin crest forms anterior edge of enlarged pneumatic recess

129. Subotic recess (pneumatic fossa ventral to fenestra ovalis): (0) absent, (1) present

130. Depression (possibly pneumatic) on ventral surface of postorbital process of laterosphenoid: (0) absent, (1) present

131. Symphyseal region of dentary: (0) Broad and straight, paralleling lateral margin, (1) medially recurved slightly, (2) strongly recurved medially

132. Dentary symphyseal region in medial view: (0) in line with main part of buccal edge, (1) end downturned

133. Posterior end of dentary: (0) without posterodorsal process dorsal to mandibular fenestra, (1) with dorsal process above anterior end of mandibular fenestra, (2) with elongate dorsal process extending over most of fenestra

134. Jaws (0) occlude for their full length, (1) diverge rostrally due to kink and downward deflection in dentary buccal margin

135. Labial face of dentary: (0) flat, (1) with lateral ridge and inset tooth row

136. Nutrient foramina on external surface of dentary: (0) superficial, (1) descend strongly posteriorly within a deep groove, (2) descend posteriorly within triangular groove, caudal end of this groove is dorsoventrally expanded

137. Dentary shape: (0) subtriangular in lateral view, (1) with subparallel dorsal and ventral edges, (2) high triangular in lateral view (as in Citipati)

138. Ventral surface of dentary: (0) straight or nearly straight, (1) descends strongly posteriorly

139. Pronounced coronoid eminence on the surangular: (0) absent, (1) present

140. Foramen in lateral surface of surangular rostral to mandibular articulation: (0) absent, (1) present

141. Laterally inclined flange along dorsal edge of surangular for articulation with lateral process of lateral quadrate condyle: (0) absent, (1) present

142. Anterior portion of the surangular: (0) less than half the height of the mandible above the mandibular fenestra, (1) more than half the height of the mandible at the

level of the mandibular fenestra

143. Retroarticular process of the mandible: (0) narrow, rod-like, (1) broadened, with groove posteriorly for the attachment of the m. depressor mandibulae

144. Attachment of the m. depressor mandibulae on retroarticular process of mandible: (0) facing dorsally, (1) facing posterodorsally

145. Retroarticular process: (0) points caudally, (1) curves gently dorsocaudally

146. Articular: (0) without elongate, slender medial, posteromedial, or mediodorsal process from retroarticular process, (1) with process

147. Angular: (0) exposed almost to end of mandible in lateral view, reaches or almost reaches articular, (1) excluded from posterior end angular suture turns ventrally and meets ventral border of mandible rostral to glenoid

148. Coronoid ossification: (0) large, (1) thin splint, (2) absent

149. Splenial: (0) not widely exposed on lateral surface of mandible, (1) exposed as a broad triangle between dentary and angular on lateral surface of mandible

150. Foramen in the ventral part of the splenial (mylohyal foramen): (0) absent (1) present

151. Form of mylohyal foramen: (0) completely enclosed in the splenial, (1) opened anteroventrally

152. Posterior end of splenial: (0) straight, (1) forked

153. Mandibular articulation surface: (0) as long as distal end of quadrate, (1) twice or more as long as quadrate surface, allowing anteroposterior movement of mandible

154. Mandibular foramen: (0) large, (1) absent or reduced

155. Shape of mandibular foramen: (0) oval, (1) subdivided by a spinous rostral

process of the surangular

156. Internal mandibular fenestra: (0) small and slit-like, (1) large and rounded

157. Palatal teeth: (0) present, (1) absent

158. Premaxillary teeth: (0) present, (1) absent

159. Number of premaxillary teeth: (0) three, (1) four, (2) five, (3) more than five

160. First premaxillary tooth size: (0) slightly smaller or the same size as 2 and 3, (1) much smaller than 2 and 3, (2) much larger than 2 and 3

161. Second premaxillary tooth: (0) approximately equivalent in size to other premaxillary teeth, (1) markedly larger than third and fourth premaxillary teeth

162. Serrations on premaxillary teeth: (0) present, (1) absent

163. In cross section, premaxillary tooth crowns: (0) sub-oval to sub-circular, (1) asymmetrical (D-shaped in cross section) with flat lingual surface

164. Maxillary teeth: (0) present, (1) absent

165. Maxillary and dentary teeth: (0) serrated, (1) some without serrations anteriorly, (2) all without serrations

166. Serration denticles: (0) large, (1) small

167. Serrations: (0) simple, denticles convex, (1) distal and often mesial edges of teeth with large, hooked denticles that point toward the tip of the crown

168. Maxillary tooth row: (0) extends posteriorly to approximately half the length of the orbit, (1) ends at the anterior rim of the orbit, (2) completely antorbital, tooth row ends anterior to the vertical strut of the lacrimal

169. Constriction between tooth crown and root: (0) absent, (1) present

170. Dentary: (0) fully toothed, (1) only teeth rostrally, (2) edentulous

171. Dentary teeth: (0) homodont, (1) increasing in size anteriorly, becoming more

conical in shape, (2) Decreasing in size anteriorly, becoming more densely packed

172. Roots of dentary and maxillary teeth: (0) mediolaterally compressed, (1) circular in cross-section

173. Maxillary teeth: (0) mediolaterally flattened and recurved, (1) lanceolate and subsymmetrical, (2) simple, conical, incisive crowns, (3) labiolingually flattened and recurved, with crown in middle of tooth row less than twice as high as the basal mesiolateral width (fore-aft basal length)

174. Maxillary tooth implantation: (0) separate alveoli, (1) set in an open groove

175. Dentary tooth implantation: (0) separate alveoli, (1) set in an open groove

176. Dentary teeth: (0) mediolaterally flattened and recurved, (1) lanceolate and subsymmetrical

177. Dentary tooth size and number: (0) large, fewer than 25 in dentary, (1) moderate number of small teeth (25-30 in dentary), (2) relatively small and numerous (more than 30 in dentary)

178. Dentaries: (0) lack interdental plates, (1) with interdental plates medially between teeth

179. Axial neural spine: (0) flared transversely and sheet-like, (1) compressed mediolaterally, anteroposteriorly reduced, and rodlike

180. Epipophyses on axis: (0) absent, (1) present as small ridges, (2) strongly pronounced (overhanging the zygapophyses)

181. Pleurocoel in axis: (0) absent, (1) present

182. Epipophyses in anterior cervical vertebrae: (0) absent or poorly developed, (1) well-developed, proximal to postzygapophyseal facets, (2) pronounced, strongly overhanging the postzygapophyses

183. Postzygapophyses of cervical vertebrae 2-4: (0) well-separated, or connected only at the base, (1) medially connected along their length by a web of bone that is dorsally concave for attachment of the interspinous ligaments

184. Anterior articular facet of anterior cervical vertebrae: (0) approximately as high as wide or higher, (1) significantly wider than high, (2) wider than high and higher laterally than medially (kidney-shaped), with neural canal emarginating dorsal aspect

185. Cervical vertebral centra: (0) amphi- to platycoelous, (1) opisthocoelous, (2) heterocoelous (state added from Turner et al., 2007)

186. Anterior cervical centra: (0) level with or shorter than posterior extent of neural arch, (1) centra extending beyond posterior limit of neural arch

187. Carotid process on posterior cervical vertebrae: (0) absent, (1) present

188. Cervical neural spines: (0) anteroposteriorly long, (1) anteroposteriorly short and centered on neural arch, giving arch an "X" shape in dorsal view, (2) extremely short anteroposteriorly, less than 1/3 length of neural arch

189. Number of cervical vertebrae: (0) 10, (1) 12 or more

190. Pleurocoels in cervical vertebrae: (0) absent, (1) present

191. Number of pleurocoels in cervicals: (0) two, arranged horizontally, (1) one

192. Pleurocoels developed as (0) deep depressions, (1) foramina

193. Interior pneumatic spaces in cervicals: (0) Structure camerate (few chambers), (1) Structure camellate (many chambers separated by delicate lamellae)

194. Ventral keel in anterior cervicals: (0) present, (1) absent

195. Broad ridge from the diapophyses to the ventral rim of the posterior end of the vertebral centra in cervical vertebrae: (0) absent, (1) present

196. Prezygapophyses in anterior cervicals: (0) transverse distance between prezygapophyses less than width of neural canal, (1) prezygapophyses situated lateral to the neural canal

197. Prezygapophyses in anterior postaxial cervicals: (0) straight, (1) anteroposteriorly convex, flexed ventrally anteriorly

198. Hypapophyses in anterior dorsals: (0) absent or poorly developed, (1) pronounced

199. Hyposphene-hypantrum articulation in dorsal vertebrae: (0) absent, (1) present

200. Postzygapophyses of trunk vertebrae: (0) abutting one another above neural canal, opposite hyposphenes meet to form lamina, (1) zygapophyses placed lateral to neural canal and separated by groove for interspinous ligaments, hyposphens separated

201. Neural spines on posterior dorsal vertebrae in lateral view: (0) rectangular or square, (1) anteroposteriorly expanded distally, fan-shaped

202. Neural spines of dorsal vertebrae in dorsal view: (0) not expanded distally, (1) expanded laterally in dorsal view to form "spine table"

203. Scars for interspinous ligaments: (0) terminate at apex of neural spine in dorsal vertebrae, (1) terminate below apex of neural spine

204. Neural spine of posterior dorsals: (0) broadly rectangular and approximately as dorsoventrally high as anteroposteriorly long, (1) high rectangular, significantly higher than long

205. Hook-like extension on anterior end of dorsal neural spines in lateral view: (0) absent, (1) present (with associated depression immediately caudal to the projection for spinous ligament attachment)

206. Parapophyses of posterior trunk vertebrae: (0) flush with neural arch, (1) distinctly projected on pedicels

207. Parapophyses in posteriormost dorsals: (0) on same level as transverse process, (1) distinctly below transverse process

208. Pleurocoels in dorsal vertebrae: (0) absent, (1) present in anterior dorsals ('pectorals'), (2) present in all dorsals

209. Transverse processes of anterior dorsal vertebrae: (0) long and thin, (1) short, wide and only slightly inclined

210. Dorsal centra articular surfaces: (0) amphiplatyan, (1) opisthocoelous

211. Ventral keel in anterior dorsals: (0) absent or very poorly developed, (1) pronounced

212. Shape of dorsal centra in anterior view: (0) subcircular or oval, (1) significantly wider than high, (2) triangular

213. Posterior dorsal vertebrae: (0) strongly shortened, centra much shorter than high, (1) relatively short, centra approximately as high as long, or only slightly longer, (2) significantly elongated, much longer than high

214. Number of sacral vertebrae: (0) two, (1) three, (2) four, (3) five, (4) six, (5) seven, (6) eight, (7) nine

215. Pleurocoels in sacral vertebrae: (0) absent, (1) present on anterior sacrals only, (2) present on all sacrals

216. Ventral surface of posterior sacral centra: (0) gently rounded, convex, (1) flattened ventrally, sometimes with shallow sulcus, (2) centrum strongly constricted transversely, ventral surface keeled.

217. Sacral ribs: (0) slender and well-separated, (1) forming a more or less

continuous sheet in ventral or dorsal view, (2) very massive and strongly expanded

218. Sacral vertebrae: (0) with unfused zygapophyses, (1) with fused zygapophyses forming a sinuous ridge in dorsal view

219. Last sacral centrum: (0) with flat posterior articular surface, (1) convex articulation surface

220. Ventral surface of posterior sacral centra: (0) rounded or flat, (1) strong ventral keel

221. Number of caudal vertebrae: (0) more than 40, (1) 25-40, (2) fewer than 25, (3) tail short and fused into a pygostyle

222. Caudal vertebrae: (0) with distinct transition point, from shorter centra with long transverse processes proximally to longer centra with small or no transverse processes distally, (1) homogeneous in shape, with no transition point

223. Caudal vertebral centra: (0) amphiplatyan, (1) procoelous

224. Position of transition point: (0) distal to the tenth caudal vertebra, (1) between the 7th and 10th caudal vertebrae, (2) proximal to the 7th caudal vertebra

225. Location of transverse processes of proximal caudals: (0) centrally positioned on centrum, (1) posteriorly displaced.

226. Shape of anterior caudal centra: (0) oval, (1) subrectangular and box-like, (2) laterally compressed with a ventral keel

227. Ventral groove in anterior caudals: (0) absent, (1) present

228. Ventral surface of anterior caudals: (0) Rounded, (1) with a distinct keel bearing a narrow, shallow groove on its midline

229. Neural spines on distal caudals: (0) form a low ridge, (1) spine absent, (2) midline sulcus in center of the neural arch

230. Neural spines of caudal vertebrae: (0) simple, undivided, (1) separated into anterior and posterior alae throughout much of caudal sequence

231. Neural spines of mid-caudals: (0) rod-like and posteriorly inclined, (1) subrectangular and sheet-like, (2) rod-like and vertical

232. Prezygapophyses of distal caudal vertebrae: (0) between 1/3 and whole centrum length, (1) with extremely long extensions of the prezygapophyses, (2) strongly reduced

233. Anterior margin of neural spines of anterior mid-caudal vertebrae: (0) straight, (1) with distinct kink, dorsal part of anterior margin more strongly inclined posteriorly than ventral part

234. Relative length of distal caudal centra: (0) significantly elongated in relation to centrum height, (1) not elongated in relation to centrum height

235. Cranial process at base of chevrons: (0) absent, (1) present

236. Distal chevrons: (0) rod-like or L-shaped, (1) skid-like

237. Mid-caudal chevrons: (0) rod-like or only slightly expanded ventrally, (1) L-shaped

238. Proximal end of chevrons of proximal caudals: (0) short anteroposteriorly, shaft cylindrical, (1) proximal end elongate anteroposteriorly, flattened and plate-like

239. Distal caudal chevrons: (0) simple, (1) anteriorly bifurcate, (2) bifurcate at both ends

240. Long, hair-like cervical ribs: (0) absent, (1) present

241. Shaft of cervical ribs: (0) slender and longer than vertebra to which they articulate, (1) broad and shorter than vertebra

242. Ossified uncinate processes: (0) absent, (1) present

243. Lateral gastral segment: (0) shorter than medial one in each arch, (1) distal segment longer than proximal segment

244. Ossified sternal plates: (0) separate in adults, (1) fused, (2) fused with ventral keel

245. Sternum: (0) without distinct lateral xiphoid process posterior to costal margin, (1) with lateral xiphoid process

246. Furcula: (0) absent, (1) present

247. Hypocleidium on furcula: (0) absent, (1) present

248. Articular facet of coracoid on sternum: (0) anterolateral or more lateral than anterior, (1) almost anterior

249. Anterior edge of sternum: (0) grooved for reception of coracoids, (1) without grooves

250. Coracoid in lateral view: (0) subcircular, with shallow ventral blade, (1) subquadrangular with extensive ventral blade, (2) shallow ventral blade with elongate posteroventral process, (3) strut-like

251. Posterior edge of coracoid (Kirkland et al., 2005, character #218)

(0) not or shallowly indented below glenoid, (1) posterior edge of coracoid deeply notched just ventral to glenoid, glenoid lip everted

252. Anterior surface of coracoid ventral to glenoid fossa: (0) unexpanded, (1) expanded, forms triangular subglenoid fossa bounded laterally by coracoid tuber

253. Coracoid tubercle: (0) absent, (1) present

254. Coracoid tubercle form: (0) anteroposteriorly short, mound-like, (1) anteroposteriorly elongated, ridge-like

255. Scapula shape: (0) short and broad (ratio length/minimal height of shaft <9), (1) slender and elongate (ratio >10)

256. Acromion margin of scapula: (0) continuous with blade, (1) anterior edge laterally everted

257. Flange on supraglenoid buttress on scapula: (0) absent, (1) present

258. Distal end of scapula: (0) expanded, (1) not expanded

259. Glenoid fossa: (0) faces posteriorly or posterolaterally, (1) faces laterally

260. Scapula and coracoid: (0) separate, (1) fused into scapulocoracoid

261. Scapula and coracoid angle: (0) continuous arc in posterior and anterior views, (1) coracoid inflected medially, scapulocoracoid L shaped in lateral view

262. Scapular length: (0) longer than humerus, (1) shorter than humerus

263. Deltopectoral crest: (0) large and distinct, proximal end of humerus quadrangular in anterior view, (1) less pronounced, forming an arc rather than being quadrangular, (2) very weakly developed, proximal end of humerus with rounded edges, (3) extremely long, (4) proximal end of humerus extremely broad, triangular in anterior view

264. Anterior surface of deltopectoral crest: (0) smooth, (1) with distinct muscle scar near lateral edge along distal end of crest for insertion of biceps muscle

265. Ratio femur/humerus: (0) more than 2.5, (1) between 1.2 and 2.2, (2) less than 1

266. Outline of proximal articular facet of humerus: (0) broadly oval (more than twice as broad transversely than anteroposteriorly), (1) distinctly rounded, often globular (less than twice as broad anteroposteriorly than transversely)

267. Internal tuberosity of humerus: (0) small and confluent with humeral head, (1)

offset from humeral head by distinct notch, often projects proximally above humeral head, (2) hypertrophied but not distinct from humeral head (as in Suchomimus)

268. Shape of internal tuberosity on humerus in anterior view: (0) triangular, often rounded, (1) rectangular

269. Humerus in lateral view: (0) sigmoidal, (1) straight

270. Ectepicondyle of humerus (lateral epicondyle): (0) small, often rectangular and does not form articular surface, (1) large, rounded and forms articular surface

271. Entepicondyle of humerus (medial epicondyle): (0) absent or small and tabular,

(1) large, projects medially from ulnar condyle as a distinct process and is distally separated from ulnar condyle by a groove

272. Distal humeral condyles: (0) primarily developed on distal end of humerus, but may also have some articular surface extending to anterior edge, (1) limited to anterior surface, condylar surfaces not present on distal end

273. Olecranon process of ulna: (0) well-developed, (1) strongly reduced or absent

274. Proximal surface of ulna: (0) single continuous articular facet, (1) divided into two distinct fossae

275. Distal articular surface of ulna: (0) flat, (1) convex, semilunate surface

276. Distal condyle articular surface of ulna: (0) unexpanded or spatulate, articular surface limited to distal end, (1) bulbous, trochlear articular surface extends onto dorsal surface of ulna

277. Radius: (0) more than half the length of humerus, (1) less than half the length of humerus

278. Radius and ulna: (0) well-separated, (1) with distinct adherence or syndesmosis distally

279. Distal end of radius: (0) unexpanded, distal end is round or elliptical, (1) expanded dorsoventrally, flange projects ventrally from elliptical distal end

280. Ossified carpals: (0) absent, (1) present

281. Lateral proximal carpal (ulnare?): (0) quadrangular, (1) triangular in proximal view

282. "Semilunate" distal carpal: (0) absent, (1) present

283. Two distal carpals: (0) in contact with metacarpals, one covering the base of Mc I (and perhaps contacting Mc II), the other covering the base of Mc II, (1) two distal carpals not present, single distal carpal capping Mc I and II

284. Distal carpals: (0) not fused to metacarpals, (1) fused to metacarpals, forming carpometacarpus

285. Rectangular buttress on the proximal surface of Mc II: (0) absent, (1) present

286. Length of Mc II: (0) half or less than half the length of Mc III, (1) subequal in length to Mc III

287. Shape of Mc II: (0) significantly longer than broad, (1) very stout, approximately as long as broad

288. Contact between Mc II and Mc III: (0) metacarpals contact each other at their bases only, (1) Mc II closely appressed to Mc III, at least the proximal half of McI flattened

289. Distal end of Mc II: (0) condyles more or less symmetrical, (1) condyles strongly asymmetrical, the medial condyle being positioned more proximally than the lateral

290. Distal articular end of metacarpal II: (0) ginglymoid, (1) rounded and smooth

291. Medial side of Mc III: (0) expanded proximally, (1) not expanded

292. Distal articular end of Mc III: (0) ginglymoid, (1) rounded and smooth

293. Shaft of Mc IV: (0) subequal in width to Mc III, (1) considerably more slender than Mc III (less than 70% of the width of Mc III)

294. Proximal articular end of Mc IV: (0) expanded and similar in width to Mc II and III, (1) not expanded, very slender when compared to Mc II and III

295. Proximal outline of Mc IV: (0) subrectangular, (1) triangular, apex dorsal

296. Shaft of Mc IV: (0) straight, (1) bowed laterally

297. Extensor pits on the dorsal surface of the distal end of metacarpals: (0) absent or poorly developed, (1) deep, well-developed

298. Number of fingers: (0) five, (1) fifth finger absent and fourth finger reduced to a metacarpal with only one phalanx, (2) fourth finger absent, (3) two fingers, third finger either strongly reduced or absent

299. Flexor surface of manual phalanx II-1: (0) convex or flat, (1) concave, 'axial furrow' along proximodistal axis

300. Shaft diameter of phalanx II-1: (0) less than shaft diameter of radius, (1) greater than shaft diameter of radius

301. Ratio phalanx II-1/Mc II: (0) 1 or less, (1) between 1 and 1.5, (2) more than 1.5

302. Penultimate phalanx of the third finger: (0) shorter than first phalanx, (1) longer than first phalanx

303. Penultimate phalanx of the fourth finger: (0) as long as, or shorter than, more proximal phalanges, (1) longer than each of the more proximal phalanges, (2)

longer than both proximal phalanges taken together

304. Length of fourth manual digit: (0) longer than second finger, (1) shorter than second finger

305. Proximal articular surface of manual ungual II-2: (0) dorsoventrally much taller than mediolaterally wide, (1) mediolaterally as broad as tall

306. Unguals on all manual digits: (0) generally similar in size, (1) digit II bearing large ungual and unguals of other digits distinctly smaller

307. Proximodorsal lip on some manual unguals - a transverse ridge immediately dorsal to the articulating surface: (0) absent, (1) present

308. Flexor tubercle placement: (0) proximal, (1) distal, (2) absent, (3) reduced to pyramidal nubbins

309. Curvature of manual ungual II: (0) strongly curved, (1) weakly curved, (2) straight

310. Curvature of manual unguals III and IV: (0) strongly curved, (1) weakly curved, (2) straight

311. Flexor tubercle size: (0) large (>1/3 articular facet height), (1) small (<1/3 articular facet height)

312. Lateral grooves of manual ungual II-2 in ventral view: (0) unenclosed, (1) proximal end of grooves partially enclosed by lateral notches, (2) proximal end of grooves passes through foramina on ventral surface of ungual

313. Ilium: (0) brachyiliac, (1) dolichoiliac

314. Ventral edge of anterior ala of ilium: (0) straight or gently curved, (1) ventral edge hooked anteriorly, (2) very strongly hooked

315. Preacetabular part of ilium: (0) significantly shorter than postacetabular part,

(1) subequal in length to postacetabular part, (2) significantly longer than postacetabular process

316. Anterior rim of ilium: (0) gently convex or straight, (1) distinctly concave dorsally, (2) anterior end strongly curved, (3) pointed at the anterodorsal corner

317. Preacetabular part of ilium (height): (0) approximately as high as postacetabular part (excluding the ventral expansion), (1) significantly higher than postacetabular part

318. Cuppedicus fossa: (0) deep, ventrally concave, (1) fossa shallow or flat, with no lateral overhang, (2) absent

319. Cuppedicus fossa position: (0) ridge bounding fossa terminates rostral to acetabulum or curves ventrally onto anterior end of pubic peduncle; (1) rim extends far posteriorly and is confluent or almost confluent with acetabular rim

320. Preacetabular portion of ilium: (0) parasagittal, (1) moderately laterally flaring

321. Brevis fossa shape: (0) shelf-like, narrow with subparallel margins, (1) deeply concave, expanded posteriorly with lateral overhang

322. Brevis fossa lateral view: (0) Poorly developed adjacent to ischial peduncle, without lateral overhang and medial edge of the brevis fossa is visible, (1) well developed fossa along full length of postacetabular blade, lateral overhang extends along full length of fossa, medial edge of brevis fossa covered in lateral view

323. Medial brevis shelf: (0) strongly developed, projects medially, (1) low ridge on medial surface of postacetabular ala

324. Postacetabular ala of ilium in lateral view: (0) squared, (1) acuminate

325. Articulation of iliac blades with sacrum: (0) vertical, well-separated above sacrum,

(1) strongly inclined mediodorsally, almost contacting each other or sacral neural spines at midline

326. Vertical ridge on iliac blade above acetabulum: (0) absent or poorly developed, (1) well-developed

327. Pubic peduncle of ilium: (0) transversely broad and roughly triangular in outline,

(1) anteroposteriorly elongated and narrow

328. Pubic peduncle: (0) subequal in length to ischial peduncle, (1) significantly longer than ischial peduncle, ischial peduncle tapering ventrally and without clearly defined articular facet, (2) craniocaudally shorter than the ischial peduncle.

329. Articulation facet of pubic peduncle of ilium: (0) facing more ventrally than anteriorly, and without a pronounced kink, (1) with pronounced kink and anterior part facing almost entirely anteriorly

330. Anterior margin of pubic peduncle: (0) straight or convex, (1) concave

331. Supraacetabular crest: (0) absent, (1) present

332. Supraacetabular crest on ilium: (0) separate process from antitrochanter, forms hood over femoral head, (1) reduced, not forming hood

333. Antitrochanter posterior to acetabulum: (0) absent or poorly developed, (1) prominent

334. Postacetabular blades of ilia in dorsal view: (0) parallel, (1) diverge posteriorly

335. Tuber along dorsal edge of ilium, dorsal or slightly posterior to acetabulum: (0) absent, (1) present

336. Dorsal margin of postacetabular ala in lateral view: (0) convex or straight, (1)

concave, brevis shelf extends caudal to lateral ilium making it appear concave in lateral view

337. Caudal end of postacetabular ala in dorsal view: (0) rounded or squared in dorsal view, (1) lobate, with brevis shelf extending caudally beyond caudal terminus of the postacetabular ala

338. Ilium and ischium articulation: (0) flat or slightly concavo-convex, (1) with process projecting into socket in ischium

339. Pubic orientation: (0) propubic, (1) vertical, (2) moderately posteriorly oriented,

(3) opisthopubic

340. Strongly expanded pubic boot: (0) absent, (1) present

341. Pubic boot projects: (0) anteriorly and posteriorly, (1) with little or no anterior process, (2) only expanded anteriorly

342. Pubic apron: (0) extends medially from middle of cylindrical pubic shaft, (1) shelf extends medially from anterior edge of anteroposterioly flattened shaft, (2) absent

343. Pubic apron: (0) about half of pubic shaft length, (1) less than 1/3 of shaft length

344. Pubic apron: (0) completely closed, (1) with medial opening distally above the pubic boot

345. Obturator foramen in pubis: (0) completely enclosed, (1) open ventrally (obturator notch), (2) absent

346. Pubic fenestra below obturator foramen: (0) absent, (1) present

347. Pubic shafts in lateral view: (0) straight, (1) anteriorly convex, (2) anteriorly

concave

348. Lateral face of pubic shafts: (0) smooth, (1) with prominent lateral tubercle about halfway down the shaft

349. Length of ischium: (0) more than two-thirds pubis length, (1) two thirds or less of pubic length

350. Obturator process of ischium: (0) absent, (1) proximal in position, (2) located near middle of ischiadic shaft, (3) located at distal end of ischium

351. Ischiac shaft: (0) rodlike, (1) anteroposteriorly wide and plate like

352. Lateral blade of ischium: (0) flat, (1) laterally concave, (2) with longitudinal ridge subdividing lateral surface into anterior (including obturator process) and posterior parts

353. Ischium: (0) straight, (1) ventrodistally curved anteriorly, (2) twisted at midshaft and with flexure of obturator process toward midline so that distal end is horizontal, (3) with laterally concave curvature in anterior view, (4) distal portion curved posteriorly

354. Contact of obturator process of ischium: (0) does not contact pubis, (1) contact pubis

355. Ventral notch at distal edge of ischial obturator process: (0) absent, grades smoothly into ischial shafts, (1) present, makes obturator process triangular in lateral view

356. Obturator process on ischium: (0) confluent with pubic peduncle, (1) offset from pubic peduncle by a distinct notch

357. Morphology of offset triangular obturator process of ischium: (0) wide base along ischiac shaft, rostral process short, (1) narrow base, rostral process elongate

358. Distal end of ischium: (0) slightly expanded, (1) strongly expanded, forming ischial "boot", (2) tapering

359. Distal ends of ischia: (0) form symphysis, (1) approach one another but do not form symphysis, (2) widely separated

360. Distally placed process on caudal margin of ischium: (0) absent, (1) present

361. Tubercle on anterior edge of ischium: (0) absent, (1) present

362. Posterior process (ischial tuberosity) on posteroproximal part of ischium: (0) absent, (1) well-developed

363. Form of posteroproximal ischial process (ischial tuberosity): (0) small, tablike, (1) large, proximodorsally hooked and separated from the iliac peduncle by a notch

364. Semicircular scar on posterior part of the proximal end of the ischium: (0) absent, (1) present

365. Femoral length: (0) longer than tibia, (1) shorter than tibia

366. Femoral head (0) without fovea capitalis, (1) circular fovea present in center of medial surface of head

367. Oblique ligament groove on the posterior surface of femoral head: (0) absent or very shallow, (1) deep, bound medially by a well-developed posterior lip

368. Femoral head: (0) confluent with greater trochanter, (1) separated from greater trochanter by a distinct cleft

369. Femoral head: (0) directed anteromedially, (1) directed strictly medially

370. Greater trochanter: (0) anteroposteriorly narrow and narrowing from medial to lateral, (1) anteroposteriorly expanded, forming a trochanteric crest

371. Lesser trochanter: (0) separated from greater trochanter by a deep cleft, (1)

trochanters separated by small groove, (2) completely fused (or absent) to form crista trochanteris.

372. Lesser trochanter shape: (0) alariform, (1) cylindrical in cross section

373. Placement of lesser trochanter: (0) at distal end of femoral head, (1) more proximally placed, but distal to greater trochanter, (2) as proximal or more proximal than greater trochanter

374. Vertical ridge on lesser trochanter: (0) present, (1) absent

375. Posterolateral trochanter: (0) absent or represented only by rugose area, (1) posterior trochanter distinctly raised from shaft, mound-like

376. Fourth trochanter on femur: (0) present, (1) absent

377. Accessory trochanteric crest distal to lesser trochanter: (0) absent, (1) present

378. Broad groove on cranial surface of distal femur: (0) absent or poorly developed,

(1) well developed and bounded medially by an expanded medial lamella

379. Popliteal fossa on distal end of femur: (0) open distally, (1) closed off distally by contact between distal condyles

380. Distal end of femur: (0) anteroposteriorly broad and distally flattened, (1) less broad and well rounded

381. Lateral femoral distal condyle: (0) distally rounded, projects only slightly more distally than medial condyle, (1) distally conical, projects considerably further distally than medial condyle

382. Lateral accessory cnemial crest: (0) absent, (1) present

383. Medial cnemial crest: (0) absent, (1) present on proximal end of tibia

384. Fibular condyle on proximal end of tibia: (0) confluent with cnemial crest

anteriorly in proximal view, (1) strongly offset from cnemial crest

385. Medial proximal condyle on tibia: (0) round in proximal view, (1) arcuate and posteriorly angular in proximal view

386. Posterior cleft between medial part of the proximal end of the tibia and fibular condyle: (0) absent, (1) present

387. Fibular crest: (0) absent, (1) present, extending from proximal articular surface distally, (2) present, clearly separated from proximal articular surface

388. Shape of fibular crest: (0) quadrangular, (1) low and rounded

389. Bracing for ascending process of astragalus on anterior side of distal tibia: (0) distinct 'step' running obliquely from mediodistal to lateroproximal, (1) bluntly rounded vertical ridge on medial side, (2) anterior side of tibia flat

390. Fibula: (0) reaches proximal tarsals, (1) short, tapering distally, and not in contact with proximal tarsals

391. Insertion of m. iliofibularis on fibular shaft: (0) not especially marked, (1) present as a well-developed anterolateral tubercle

392. Ridge on medial side of proximal end of fibula, that runs anterodistally from the posteroproximal end: (0) absent, (1) present

393. Medial surface of proximal end of fibula: (0) concave along long axis, (1) flat

394. Deep oval fossa on medial surface of fibula near proximal end: (0) absent, (1) present

395. Astragalus and Calcaneum: (0) condyles indistinct or poorly separated, (1) distinct condyles separated by prominent vertical tendinal groove on anterior surface

396. Astragalus and calcaneum: (0) separate from tibia, (1) fused to each other and

to the tibia in late ontogeny

397. Fibular facet on astragalus: (0) large and facing partially proximally, (1) reduced and facing laterally or absent

398. Height of ascending process of the astragalus: (0) lower than astragalar body, (1) higher than astragalar body, (2) more than twice the height of astragalar body

399. Shape of ascending process of the astragalus: (0) tall and broad, covering most of anterior surface of distal end of tibia, (1) short and slender, covering only lateral half of anterior surface of tibia, (2) tall with a medial notch that restricts it to lateral side of anterior face of distal tibia

400. Ascending process of astragalus: (0) confluent or only slightly offset from astragalar body, (1) offset from astragalar body by a pronounced groove

401. Astragalar condyles: (0) almost entirely below tibia and face distally, (1) significantly expanded proximally on anterior side of tibia and face anterodistally

402. Horizontal groove across astragalar condyles anteriorly: (0) absent, (1) present

403. Calcaneum: (0) without facet for tibia, (1) well-developed facet for tibia present

404. Distal tarsals: (0) separate, not fused to metatarsals, (1) form metatarsal cap with intercondylar prominence that fuses to metatarsal early in postnatal ontogeny

405. Metatarsals: (0) not co-ossified, (1) co-ossification of metatarsals begins proximally, (2) begins distally

406. Metatarsal I: (0) present, (1) absent

407. Metatarsal I: (0) attenuates proximally, without proximal articulating surface, (1) proximal end of Mt I similar to that of Mt II-IV

408. Metatarsal I: (0) contacts the ankle joint, (1) reduced, elongated and splint-

like, articulates in the middle of the medial surface of Mt II, (2) broadly triangular and attached to the distal quarter of Mt II, (3) absent

409. Distal end of metatarsal II: (0) smooth, not ginglymoid, (1) with developed ginglymus

410. Tuber along extensor surface of MtII: (0) absent, (1) present

411. Posteromedial margin MtII diaphysis (this seems to be developed independently of the ridge on MtIV): (0) well-developed flange absent or area rugose, (1) with flange projecting caudally or medially

412. Distal end of metatarsal III: (0) smooth, not ginglymoid, (1) with developed ginglymus

413. Metatarsal III: (0) subequal in width to Mt II and IV proximally, (1) pinched between II and IV and not visible in anterior view proximally, (2) does not reach the proximal end of the metatarsus

414. Shaft of MT IV: (0) round or thicker dorsoventrally than wide in cross section, (1) shaft of Mt IV mediolaterally widened and flat in cross section

415. Length of MtIV: (0) subequal to Mt II, (1) markedly longer than Mt II

416. Posterolateral margin of MtIV diaphysis: (0) well-developed flange absent or area rugose, (1) with flange projecting caudally or laterally

417. Metatarsal V: (0) with rounded distal articular facet, (1) strongly reduced and lacking distal articular facet, (2) short, without articular surface, transversely flattened and bowed anteriorly distally

418. Pedal digit IV: (0) significantly shorter than III and subequal in length to II, foot is symmetrical, (1) significantly longer than II and only slightly shorter than III, foot is asymmetrical

419. Ungual and penultimate phalanx of pedal digit II: (0) similar to those of III, (1) highly modified for extreme hyper-extension, ugual more strongly curved and about 50% larger than that of III

420. Pedal phalanges of digit IV: (0) anteroposteriorly short, with proximal and distal articular surfaces very close together, particularly in distal elements, (1) anteroposteriorly long, proximal and distal articular surfaces well-separated

421. Extensor ligament pits on dorsal surface of pedal phalanges: (0) shallow, extensor ridges not sharp, (1) deep and extensive proximally, corresponding extensor ridges sharply defined in dorsal view

422. Lateral surface of coracoid: (0) flat, (1) bearing a longitudinal ridge.

423. Lateral surface of coracoid: (0) smooth, (1) ventral half decorated with deep and narrow grooves and bumps.

APPENDIX 5. Data Matrix for the Phylogenetic Analysis of *Nemegtonykus citus* gen. et sp. nov.

Eoraptor

???0000?00?00---00?0?0101000010000000001?010010000010-001001?0?-
000?00???0000000?0?10???0???0000?????????????????????????????00?0001
00??0??0????????00?00100000011O?0?000??0???01??0????0??????00??0??0???0
???0?1?????????0?0??0???0??00????????????0????0??00?0???10?0????????0????
????10?1???0??011??0100???0????000?0??????000?000?????????0-??0000?01???
?00-0???0-????0??????0??0?0??????0???0?????????????????0????0????????00

Herrerasaurus

???000?????10---0???0100000000000?00?00001?220000000000-
0010000??-??0?00?0?001????01?11??000?0?000?0???0??000???1??0??0????0???
????0?2?????0??000????????????1010?00?0??00?0?000???0101000????0???0000
01?0??1??00?0000000?2???0??0?000?00000?00?????????????0??0-
01010?00??100000??0??00????0???1000?1?0000110?11100000???0000?0???00?0
000000?????00??10??0000?011???00-
0?1?0-??01000??0?00?00000?0000?0?10????0010000??0?0?00?0?000?0?000
Coelophysis

???011????00---?????000101001?1?00?00101???000?000010-00100????-
0?0?01?0?0?0?????0?????0?????000?0???1????0??????0??0????????????0?2???0
?0??000?????????1??1010?10?0??00???000???0101??0????1000?0000??0??00?0{
01}?00023?01???0??0?010100?00?00????????????0????01?00?0???10000???0???

0????1?000001?0??0?0?1??111100?0???010000???10?0000010????000??0-??001

10110???10-

0?0?0-??11000??0?00?000???0?11?0?11????0010000????1????0???100??00

Dilophosaurus

???010?1???00---

01????0000?00011?00???101?22000?00?01??0010?0????0?0001?0??11????00011

????????000?0???1??000?1?1?00??0??101???????0?????0?0???01??????????0??10

10?00?0??10?1?000???0202010????101?000?1100??11?01?00023000???0??0?01

0?000001????0?????????0??0-

01?00?0???100000??0???0???01?00?001?0?1000110?1?11000?????1???0???0??0

000010?????10??0-??1??00?10???10-????0-??1100001 0?00?000???0?11?0?10???

?0010000??0?1?0??0?0?2001000

Syntarsus

????11?????00-??0???0000101001 11?00?00101?1{01}000?000010-

0010010??-??0000?0?010????00010??00??1?000?0???1??100?0?1?00??0??001??

?????0?2???1?0??000?????????????1010?10?0??00?1?000???0?010?0????100?00?

00100??0??01?00023011???0??0?010?00000100????????????0??0?01000?0???10

0000??0???0????1??00001?0?1000110?11110000???010000???10?0000010????00

0??0-??00110100???10-

0?0?0-??11000??0?00?10000?{01}011?0?11???10010000?10?1?0??0???1001?00

Abelisaurus

???1001?0010????0??0??1000?00000?1??0101??????00??2?????1??11?000001?1

11111100001?100-????????100???

?????????????1???

??

??

??

Carnotaurus

???1000?00100---0??0?01000100000?1000111??2000000?0000-?10-

110000001?1110110000010000-???0????100??2??????0???00??101?????????????

?0100010010??0?1101000001101??0???1?00?00?00?011200?0?20101?101001

00111?1100?00140??1???????000???????????000??00-0?0000-

0001010?2?01?0?0000?0010?100?001000?1?00?0?1??????????????10000??????0

00??00??0?0000010??10000010?00?0-

10000-??000?0000?01?101??00?11?????????????????????????????????00

Ceratosaurus

???1001000100---00?0?0100000000?11?010111011000002110-

00100100000000111111010001010 0-

0?00?0??100?02??1??000???1??1??0???0????????0?????1?0??0?0?????100????10

0??00?0??10?0??0????0212?00000?10110000010001101110?0014001?0?00?0?01

0?020001000?000???????0000-

0101000???100010??0???0??1?????1001?0??0?011?????????2????10000???0??00

000001000000000-101001001000010-10000-

0?110000000100?1010001?11?00100???0010011?????????0????????00

Majungasaurus

???1001?00100--??10000100010000?1100101112200000101?0-010-

110000001?1111111000010100-

0000001?100012??1000001?????????????????????????????1?????????????????????

10???????????000???????0????2?????????0?????????????????????????????????

??1?????????????????0-???????0????0??0?????????????????????????????????????

2????????????10????????????000??????????0??0?????-??0?????????????????????0

0??1?????????????1??????0???00????0?????00

Masiakasaurus

?????????????0-

-??100??000???00??????0?????????????????????0-?????????????????????????????

??0121001O???????????0-???????????

?0010?00?0??0001???0??00?2?101-?0100100010?01????01????1??1????01?0??0

?0?????0?????????00010000010???10?1001????????????????????????????????????

????????????????????????????????????1110000?????????????????010000010000

0010?01011?10?????1??1111100???00?0?0?????????

Afrovenator

???????????101001????20001000?0????????0???10?????11??00???????????0101?

????1??????0??????????0?0?0??

??????????????????????0??20???0?????0202?11????111?0010?10???????{01}???01??

????????0?????100?010????????????????????????????0?00????????????1???011

1?0?????1???2?????0?????1?0?0???00?0000100?????00??0-??1??00010???1100?

0?0-????010?01?00???10????????0??0????0???111??0?2????0???2??????

Allosaurus

???0?0100101?0000?000?10?010?0??0??0????11??0000011?0-?11001000-

00??010???0?00010001120?00010??00100110O?0011000??011001?10?00000000

00010010?1?0000010101001020000001020000000001021200100001110001011O

000100110010030000?00?0?01101001010100O0?1??10??0001011000000000000

0000100000??0100?011100?10101200211100000000111000000?0000100100000
000100?1100001000011000000-
000101000100011010001012?0?100000011011 0?002000000?02000000

Cryolophosaurus

??????????????????????????????????0?0?1???0?2??????011?0??01000????0?0001?0
?1010?0?0??10?0?0?????????????????????010?1??00???????0?????????????0110?
?0?????????????????0??{12}??????????????????00?0?111{01}?????110??1?10?????
????0?????????????00?0?0?00??0?????????????????????????0??????00????????????
??????????????????????????????????????00??0??10?????00?????0???????0????00?
?????0100?010??0?1???????????0??????0011000?????????????????????

Monolophosaurus

???000100101100 00?00012000100000?111101000221010002110-001000000-
000?01100001?00001010????????000?????1??00???010?10?010??????????00000
0100101????000211?10110100000010200000000011112??10?0?111?101001000?
101110010130 0??0??????010???????????0?????????????????????????????????????
??????????????????????????????????????1000000100?00001001000000000-
10100100 10?01?0-
000?0-??

Neovenator

???010??????10000???0?2000100000?0??1??0??????????????????????????????
??0?????1??????????
??????????020????0???0???00??????????????1???????????????????2?????????????
????0?????0???0???
??????????????????1??????????????1???????????1????{12}0???1?????101????????

10?0?01??0?1?100?????????????????1??????????00?0?0???00000

Piatnitzkysaurus

????????????1?????????100????0?0????????????????????????????????0?????????????

????????????????????????????????1??0?????1??1??0???01???????0???????????????????

???????????????????0???0?0???????1202?10????1110?0100100??1??01??101?0?0???

?????0????????????????????????????0????01?00?0???10?00???0???0???????????????????

??????????????????????1?0?????????000000?????????1????000?01????10-

0???0-??11000?01?00???10??1?12?0??0?????????????????????0????????00

Sinraptor

???000000000100000000100001100000010100000200000011110-?11001100-

000?011000010000000113000001000000000110000012000?100100??10?000?0000

000100100100000?0101000110100000010000000000010212001000011101010110

0001?010001013300?00??0?0?000???????????00??1???00?????100100?0?????????

????????????????????0??111012?????1000000101110l??000?0?0000010000000011

?1110000100000?1000000-

00010?000110001010001012?000?000000100110000200000?0100?0??

Torvosaurus

???010??????0-????????200????000????????1?2?100???011??00???????????100?

????????0?0?0???0?????????????

???????????00?????0???0?????????????2?11????111000100100??1????2??101?????

?????0?011??0?0?1?????????????????0-???????????0?01???0???1????????0111?0

?10?01?????????0????0120?0???00?0000100?????00??0-??00000010???00-

0?0?0-?????????????????????1?12?0??0????01?0111?????????0????????00

Acrocanthosaurus

????000?????1?0??10??10?????00000?1?1???112?1????011?0??1110?????0?1?11

?0?1010?0?0??1?20?0??1?0???????10?0????010?1??01???1?????????00??????011

???0?0?????????1??00?0??2????????0?1?12?010?0?1012??10?11?00??01???1????

??????????0???10?1?10?0??0????????0????11?10?0?00?0??0???00??0???0?0??01

11?0?10100200???100?0???0?????????????0???????????01??0?{01}0??0???0?11

?00?00???0?01?100??0?1???????1?????????0??1????000000??0?0??2?00000

Carcharodontosaurus

????????????0?-???0???1?????00??0?1?1???1?2?1?????11?0??111??????0?1?11?0

?1?????????10?????????????????????????1?????0????1?????????????????????????

??????????????????0??2?????????????????110?0?1?11??10?????????????????????????

??

??????????????????????10?????????????????????????0?1?????????????????????01?1?

100??0???

Giganotosaurus

????????????0????10???1?????00000?1?1?????2???????11?0???110?????0?1011?

0?1??????0??10{12}?????????????????????????10?1???????1???0??????0????????

11?????????????1??00?0??2????????0?1?12?{01}1??0?101???10?110??1??1????

?????0???0????0???000??1?00???????????0?????1?10?0?????????????????????????

????????????????????????????100?10?0??00?010?11?????001??0110??0?????11

?0???????0101?100??1?1?????1?12?0?100????1?????????????????????00

Mapusaurus

????????????0?-??10???1?????0000??1?????1?2?1?????11????1110?????0?1??1??

????????1??10???0??????0?1???0

?01?1????????????0???????????0?1??2?010?0?1012??10?110001?????????????

??????0???1001??0??????????????????11??0???0?????1?????????????????????0??

0?????????????0??????100?10???????01??110????00?????????????0?1??00?00???

0?01?100??1?1?????1??2?0?100???1?1011??0??????0?0???????00

Baryonyx

????101???????????1???2?????00001???0?????2???????11?0??0100-????0?0001?

??1??????0??10?????????????????100????000?1??00???1???0?????00???????1???

???01?1??????3???1?1???????????2?1?120110?0?111???10?110001?01???1??????

????????0?????????0????0????????0????01??0?0?00?02?1???00??1?????????????

????????10????0100?????????????0?????010?????????00??0?????0???0?10????00?

??0101????????0?????????????100??0?????????????????????????00

Irritator

??????1?????0?-??????12?????00??1???0???0?2??????011?0??01001????0?0?01?

0?101???????10????????0???????100????000?1??00???1???0?????????????01??

????0?????????????????1??2???

??

?????????????0??

??

Suchomimus

????10{01}?????0?-???1??12?????0000????0?????????????0???0???100???????00?

??0???????????10????????0?????????????????????????????????????00???????1??

??????????????3??01?1??2?????????2?1?12?????0?11???????110001?01???1?????

?????????????????????0??0????????0????0?????0000?02?1???00??1????????????

?????100???????0100?????100???????00???????0?0???00??0?{12}0??0???0?1??0

0??0???0101?100??0?0?????1?12???100????1101?????????????????????

Coelurus

??

??

??????????????????????????????1?10000?111?10111100000001110001????????0

???1110010?0?????????????????????00?00??0110?00?0100??00???1?0??????0???

??0??1110110100?????????????????101

0?000110001?10?????2?2?100100??1111???????????0?0???????

Ornitholestes

???0000?010?10100?10??1000??11000??00??01?000000010010-?0101?000?10?0

0001000?000100011{23}?????00000??0????0?0??101?1?0?00??11?????0000000

10000111000101000100101011100102000000000???2?20001?111?10111110010

10110?101?0?010?10?0?01110?0?0??1?1?????????????????????01010000001100

?00?????????????????????????????????111?000000?000110110000001 1??10?10

0001?01001?00000-

0???????????1?0010??????????0???????????00???0?1000?0?0?1?00

Albertosaurus

???1?0000011?0????101????????00011?00???002??0000011?????1??0?0??00??11

1???0?010010?10???????0??0??????0???01?000??01?010?10?1?00000000010010

?1?01100???010?10??0?10010?000000000102?2000000????????010000?00??00

?0?410?00?10?0?0??0??0?????00000100?01000010?00?0000100 1??????1000?0?

10000000 1?0????????3?0??-?0000?????110?00000?0?10???1000000?010001??000

1000001020000-

1???0100110000000?0001?12?20100100?20110?0000200001 0?0?00??00

Daspletosaurus

?????01?0??1?010???0?10000001?0011100?????2?000?00111???011??1????????1

??????????10?103?????????0?????????0????????????10?10?01000?????????1?1??

?????211????1??0????????????00000??????????0??????????????????????????????

??????????????????1111??????????????1???????????01????????????????????????

??????????-????????0?????????????10??

010002????1010?01?12?2????????????????????????????????????00

Dilong

10-1000?011?10100110?1000?000100101000000122100001011O-

0010001000000000120001?10010011??0?????000010011000000???1??1?100??0??

??????000000100001111111010101?1101?00100102000000000????1?00??0?1?1?

?0100?????1?????0101????????????0????1?001????000???????0????01000?01??1

0001?????????????????????11?1?111002??21????00000?1?1?00000??0?10100100?0?

0??11?????????0?????0??0????11?110001?00??010001?12?201???00020111??0??

??0?00?0?2?0??00

Guanlong

???10000011110100110?10?0???0100101?000001221010010l1??0?10001000010

000100001010?100??30??????000010001000001100011000010010112000000000

10000111??1?0????10?10100010110 20?0000?0?????1?000000111010100100011O

0100010130001O?10?0?010??1000?11??000???????000101?0000??111000000100

0000?10100000110 1?111002002121000????01111000000?00101011001O??01100

0100000100000 1?00000-

0?1?0100011000101O?01?12?20100100010110100002000000002 10??00

Stokesosaurus_clevelandi

??

??

??

??

????????????111?000101?0?11101100102?10??????????????????????????????????

??

Stokesosaurus_langhami

??

??

????????????????????????????????10?00?0?111??0??????0??0??1?0?0130001002?

0??000??????1??

??????????????????120??00??1?0?11101100?000101100??001010?000100?0?10???

?????0??

Tyrannosaurus

???10000001110101110110000000000111001O?00221000001110-?111101000001

?11122?0101001001O3?000010000010011102?00100001101?01?010?02000000000

1001011?011001010101101000100102000000000102120000000111?010010000

100110000310?00?10?0?0?000100111100000l??11??000101000000010010012?0

0100010?1?0?000011002----030021--

00000?00111110000?011010110000001010001100001000001021000-

101101001200011010001012?20??0100020110100002000010002000000

Anserimimus

??

????????????????????????0??

??????1???????????????-??????????????????????????0????????????????????????

????????????0???????????1110??1?0???2?????????????1??0?00?101?1???????2

???????001221??110?00?11?0??????1010000?010?00??00?10010010??000-?????

?????0??????????????????????????????00???00?010???0?????

Archaeornithomimus

??

?????1??0??1???1????

?????????????????????1??-????????1?20?1100--

-?011010000??0?00????311010?10?0?01?00?000???0???????????2011110??000?2

01??01?00100000?????0?101111?1110?2?11???00?1121?100000010?000010010

0010??01000?2000001010000100 01??10?010001?01?0010?01?02?????1000??10

10?0000?00?110?0?0?????

Gallimimus

???10021000100 10??101100?000?000000000000110??000000010-

011000000010?0000000?00111200-???1?010?100?1101000010?0001100001??11

?0101000010000011?1?10020???000011-?---1-----2---??---

10?1?20101011??????010000??0??00???501??0?10?0?0??0??0?????00010???????

21110?01?010020?0????001000?1??0??00101?1????????2?0??2?000111101110?00

011?0?0????1010000?010100??0001001001000000-

110????00?000110??00?????????0100??01???001?-00?01010?00??00

Garudimimus

???1002?00011001?0101100000001000?0100000??010100000010-01100?000-

0?0?00?0-

001000??0?113??1?0100100?11???000101000110 00?1?????????00101000000101

?10020??????011-?---1-----2---??--

00?10??????????????01?00?0???0?0101401?1???????????0?????????????????????

??1?1000111?0

1000001001000?0100011000??0?????0???????10?010001??011011001?10??00??

100?20????0000200?000?02000?00

Harpymimus

???????2?0??????0???0???0?00?????????????????1????????0?????????????????0???

??????????????????????0?????????????????????????????????????0?10?0???1???0?00

00-0?10011-?---?2---

01-?-?0?0?????????????????????????????0????????4????????????????????????????

??????????????????2??0????001?00?1??0?000001?0??????0200??2?00?1021011

1????????0???????????00?????????00??0?1????00????????????????????????????

??????????????001?-00000?00?000000

Ornithomimus

???1??210001??11???0???0?000???????0????11??1?000000?0-

1110?0000001??000???0?00110101????????????00?11?110???0?000??00?0??111?

0101000010000?011?1?111?0???000011-????1?????2??-????010????20100011?1???

?010?00??0?00??0?501?00?10???0??0??0?????000101??????21111?01?01002 0??

??????1000?1??0?0001???1???????2?0??2?00012210?110?00011?0??????101000

0?01010???0001??1001000000-

110????00?00011010?0?????????0100??01???00???00?010?0?000?00

Pelecanimimus

0??????2?00?0??00???????????0????????0????????110???????0-?110????0?????00??

??????????????????????0??????????1??????????????????????0?0000?0?1?????0

??????10?103?0?102--

210??0?1?20??0?

??0???002?????????????????????????1?00?1????000101?1???????2?0????00?1121??

?????????????????????????0?????????????????????????0????????????????????????????

????????????????????????????????????

Shenzhousaurus

???0002100O0?0001?1?1??0?010????0??0????1?????????00?0-???????00?0?????0

?????001???0????????1?????????????????????????????????????000100000?1?1??

???0????10??1-????12-

-?0101-?0??????????0?????????????????0??????0?0???4????0??0?0?0??????????1?0?

??2??????000110l??

010??0010?0??????101??00?01010???0001?0000?000000-???1???00?0001?010??

??????????????????????????????????????00

Struthiomimus

???10021000?1?10?11011000000100000000010011??10?0000010-

1?100000001l0?0000-

00100111201l???1?0???1?0????110???0?000?????01??11?01010001l000?011?1?

10120???010011-????1?????2????????10??02010001l??????010000??0?000???50

1?00?10?0?0??0??1???1?000101??????21111?01?010020????????1000?1??0?000

101?1??????0200??2?0001111O?11??00011?0??????1010000?010000??00010010

01000000-110????00?00011010?0?????????0100??11???001?-00?01010?00?000

Compsognathus

0??001000???1010?1?0??201000?00?00??0000??000000000010-??10110???000?

001000???????0?????????????0?????1???????????00?????????????00000010010

-

0?000?1210?1-?10100100110200000000010??1??00?00111?00?????10001??110?

023????0?00?0?00?10000010010100???1???0001010?000000?1???????0?0000???

??0?010??0?10???2?12??10000011010100??0???0?0?1???????00?011??01000010

0000010000?0-?1?????0000?1???1??0??????0??0?0001??10?0000200?000?0200??

00

Huaxiagnathus

???0000001?010100??0??2000?????000???1??????10000?00????1???1?????0??00

??????????????????????????0??????????????????????????????????0000010???????

????????1??10??0?00110?000000?00????2?????10???????????10?01???10?01????

????0?0?????110??100001000??10??000101000000000?????????1?00?0??0100000

1?0??10?1?2?12111?000000?10100010???0?0?1??02??000?111?????0001000001

000000-?1?????0??????????????????00???00?20110?000020??00??0200????

Juravenator

00-0000?01?01010?0?0???2?0???01?000000100???0?0000???10-?10-

11???00?0?00?0?0000??????????????????0?????????????????????????????????0

000010??????0????????1-?100?0100110 2????00????1?????????0????????????1???

?????0??????????00?0????0?10?0?0000100????????????11?000??0?1??00?????00

00?????0001?????1????2?1???10000???01?????????????????10?????????????????

??????????0??????????000??1?????????????????????????????????0??????????

Sinosauropteryx

1000000001?01??0?0????00000??0?000??0?????????00??00?0-??10???????0??00

????0??00012?10??????????0??????????????0??????????????????00?00?100?????

?????????1??10100100110200000000????1??01?10111?10?????10?01??2?0??13

??????00?0?0??1110?01111010000?????000101001000000?00?00???0?0000??1100

0011101?1110?2?12111000001001010??0???0?0?101020?000?111??1??0001000

011?000?0-?1??010001??0??01??01??1??00?0?00?20110100002??00?00200??00

Albertonykus

??

??

??

??00?1?1?????????????????????1

?????1??1???2??

?????????????1?????????????????????????2??????????

Alvarezsaurus

??

??

??????????????????????????????????0??1?11?????????????????0?????2??11?01?

02?11??2???1?????????????????0????0??00?????????????????????1????????????????

??????1??1111?1?10?2-

001?1?0????11???00?????????????????????????????????1???00????1????????0??

??00???1???00???00?00?1??000100

Mononykus

??

??????????????????????????????????100??????????1012?0????????????????????

??????????????????2???1?0?2??0????????1?11?0???101?10101???1?011?0??????11?

01?12?1?????????????1??20??002000??00?0000300010?1?00011?1?1?1?10111101

101100211???111011112?0?????0??????????111??00?3????1??00?00?0????????0?

?1????121?101001?101????1?1??1011??21???0000200102000?000100

Parvicursor

??

??

??0??????10??1????????1???1?

1??

??????????????????????????????????????30?2??????????????????????????1???

?????1?1?1?1?1??1?1???????22?????????????201??0?????

Patagonykus

??

??

???0??????????????????????????????2??????????????110????1?0?0?0?322?111?01

??20?????????????????????????200?-????001?30?01011100011?0??-1?10???10????-

-??112????1011?1??????????10???0200101????0110?111000??????010??0???????

1?1111?00?00111011111?????0?010?010?1?0???????0??????1?11

Xixianykus

??

??

??0???010011?02502011??1

?1201??

??????????????????????0???11?1100200111?00?03002112000000000??1022000-

1100111211101?01110011111211?000112211001107????1?20?0???????

Ceratonykus

??????????????????????0??????????000??0??1?00?11?1?10111?1100000001?0?00?

???10?00?0010?????????0?00211010001???10??1?001??1????????00100010000?

100??00??????????????????????????????????21??1?0????0?????????????????????

??????1?120110?????????????2?????2000-????????30??????????????1?1010?111

0???1??021?2???

???????1????1?????????????????????1122110?11????0?02010???0100

Albinykus

??

??

??

??

????????????1???????11?1?0?????11?00?????????????000????2?????????????????

??????????????????????0112211O?1100200102010?0001??

Shuvuuia

1??0?0110000101O1?1010200000?000000000001100?1111?101110110010O0?100

000100010000000010???01?120000021101000100110??100010??11012100001000

100000100111O??0000?1??0???02??210012?1?2010?1121111?1110101010100??0

1?011?0?502??1120111211100200?1110010?20??002000?100000003000101l?00

01100???1?10111?0???1??02112???1101111?010?2??111????2??111?000?30?2?

1??00000?0????22000?01??11121?1010011??1???1121??10111221l0?000020010

2000?001100

Linhenykus

??

??

????????????????????????????????????11?1110?0???0100??01?011?0???????????0

?120110?????????????20??002000?1000010?????????????????????1???1011110?????

?031?2???11011?12?????2????????0??010????????????????????????????????????

????????0011?1???11211?1010?2211??000??00102000???1100

Bonapartenykus

??

??

??100????1?????0????????????

??????????????????????????2000-

100?011??1??????????

?0????????110211??00??????????????????0????11???0??????10?1?1?2??????0?????

??????????????????????11

Haplocheirus_sollers

???000110111101011101110001001000011100??00100001??111?11001000-

110000????000101?0?10?00110100002 1??10?0100110111?0011?????????00010

011001101001 1?02100001101 0?10011010 0?000?01????11?00?000--

-?011111?????100101013000?0??0010????00?001?10?000?????????01011000010

????10?11000110001?100000010111110021121210100 01?11????1-?01????01001

00???00011100?00002000011001 0?0-

0???0101011000001110111 1?201????0?2??1??00???0??000??2001100

Alxasaurus

??

??21??10010??????????

??????????????????01?10111?0121??????0?????????????10000??0??00???4?1??0??

0?1????00?2???000001?????????0?????0????000?0????011?00?0??10001000000?

111012?02???00100000?110?11101?0??????0-??000?2????1????021101?1?220?0-

???????01??????0?0?????????????????????????001?00?000?0?001???

Beipiaosaurus

??

??1??1??1????????????

??????????????001?1??1???121?????????1??

????????????????????????0??1??10??????????????????01??????????00100??????????

2????1?00?0000???1????????1?????????????????????0?????????????????????1?????

00???0??????0?????????10?0??0????00?????????????????00

Erlikosaurus

???10010011000?0??10110000011000?0?0????1???10000100?0-?110?100001000

0010?000000100??0???101210001---

00????00?0001000?00??????1?00211010010001 1?00020100000011-?---

000021011100111???1??????????

????????????????????????????0????????01??

??

????????????????????0????0??0??????000??

Falcarius

????????????????????0??00?????00???

???????1?010?????????????????1??00?001?000??00?01?11011200??0??0001???????

??????????????????????0010?10111??110???1110001?101?111111101 0?00120010241

1010?10?1?1111100001111101????110?10010110100??01?00100011100?0101100

1001100?11110200211100100000111011010???000100110 10??11101011 00?13?0

3001?22?00-

010?0100010001001 0?01?12?20?0100001011010000 10??000???00????

Nothronychus

??

????????????????????????????????0??00??00??0??1?1?110?????????????????

??????????????0000?10?11??11????2100101?10??????1?1?00?0??200?0?????????

????0????????????????????????????0??10??41???10?010000?0???????????0????

????????????0000?????????????????????????12??????????3?101?1?21?00-

00??????????0??????0?????????10??????????????0????????????00

Segnosaurus

??

??1??1?01?00?1?000?0

???0100????????000?10111?0111????????????????????????????????????0???

??????????????????????????1?????????1??00?0????01?????????????????????

?2??????00???????110??0201?0??????0-

0?000?210?????00021101?1?2?001??0?????????????01?0????????????0??100????

001?0??00?10?0?????

Avimimus

????????1?1?????????????????????????????????11?1????????????000??0??001??

???0?0000?11???????????1?1?0110?0001110??00?00?110?????02?????2?100?0?0

0??????110?11-?????2-

-??2????-???11?1?00011?101?001?1100000?010?01?2?01??0????????????????????

????????????????????0????01010?10?001????0???1?????????????????????????????

??01????001?1?0????0-11?00?110??020001210300l0?0000-

010?111002?100001??01?02?2?10??01120110111O?200?01?10100????

Caudipteryx_zoui

010???0?111??0000??????0?0?0???????0????1????00001???12?10-?1000010??00

????0???0?000?????????????1?????????????????????????????????????21200000l?0???

0?0????0?0??10???1012-

-??2??-?0??????????0?0?0?1???????????????{01}?0???4????0?21???????0??0111

10?????0?10??00???100??0?0??1??10???1???00???110?00??0??11???2?021-?00?

0110010101??0?1?1?0?100?????00?????01??201210?00102?0?0-?1???111111??

??1????????2??????012011?100?0??0??1??0?00??00

Chirostenotes

???1?????1?0??????111???

??????????????????????????1?010?01?1?0?110??01?001?11???1??21200000100?0??

00?0????100???????1?????2????-??????????0??1?10??????111?????????????521??

???????0?????????????????????????10?????0?10?????????????????????????????0??

?????20???????10000??010??1?0??????????0-??000??120????20121030010210 00-

01?????0??????????0?0???????????00???1???0??0?00?010?0?00????

Citipati

???10000101010l?0?11100000201000?011?0011?0201100001112?10-

11100010 0?0012000?00000001 0?0110111111l?0??10101001110?000?00??12121

000212000201001010001 00-0111011-?---1-----2---?----

10?1?20101111??????111000??0??10?1?52???0?11??????0??2?????00011?01?111

100???00?110001?????001?00?0??1?10?00??0???????2?0????0010000??010???0

01?1??????0-01000?110110??20?2103001 02?000-

01?????21?10100010?0?????????0000??0????00?0?00?000?0?00??00

Conchoraptor

??????001110?0?00??1???0?020???????1????1???111?000??12?10-?1000010??00

1?????0000000?????????1??1?????????0????1??????00??11?????0212000201?0?0

?000?0???101011-????1?????2????-?????????0????????????1???01??0????????11

??0??????1?????????????0???????1?11?01??0??010001??????001???????????????

0????????0?????00101100?010?1?001?1??????0-

10000?1100?1??20??1???010??000-

0??????11?1010?010?0????????????0????????0?0?00?00??0?0?????

Incisivosaurus

???10000011111?000?10110000010000001110001100001010011O-?????01000100?

001??000000012010?01101210?11-

0??11110?1?1100010000?????????2110000000?0?0?010??0?10110120?002-

-?11?010011???

??

????0??????????????????0??

??????????????????????????1????????

Heyuannia yanshini (= “Ingenia” yanshini)

????????1?1?1?????????????????????????1?????????????????12???????????0??00???

??0???????????212?00??100?0?000

?0???111011-????1?????2????-?????????????????????????????????????5????0??

1?????????2?????00???001?1112001O?00??1?000??????001?00?0????10?00??0??

?????2????0?0110010??010???0?1?1?0????0-???00?110?11??20021030010110O0-

010????11?101?001000?????????0?00?201????000200?00010?0001??

Oviraptor_philoceratops

??????0?11????1????1???0?0?0?0?????1????1???0?10??0??12?????1??0??0??001

????????000?10???1?1?1??11?0?1?????????????0?00??????????2120002010O?0?

00??0????11?11-????1?????2??-?-?????????????????????????0???????????1??????

0?????????????????????????????11????????0??1???0??????001????0????1??????0??

???????0????00?0000??01?????0??1??

?????????????010?0?????????????????????0??????????????????

Achillobator

???????????????1???0???0???0??

??

?????????????0010?0?0???000????2?20?01??1???????110????1??0????????????

0??????1??2?????11??????????10110?????0????????????????????????????????????

??2??????????0000??113?11011?0??????0-

1??000110?01??0001000001021000-?0?????21??110?0??10????????????0??0????

00????0?10?????1??00

Adasaurus

??10?????????????????????

????????????????????????????????????00??0?0????????????????0??????????????

????????0???0002-

-??10???0020????????????????????????????????????40101?????????????1????????

?????????10110100100??11

?3?000???10001000-

111??120110010001210?00102?0?0-?1??

????????0????01????

Buitreraptor

???????0000?1?10???01??0???????????0???????????0?????????????110010??001

??????0??1001????????????????????????????????0?????????????00??010?????????

??????????????????02???0?0?0000101l?1?20111011?????11??0???1?01????01??

0??0?1?1??10?2?????1201?????0??1?1???1??101101????????11?????1?110??????

???????2?????????????????????????01?1??????111?111?1??10???201??2??0?1??0?10

01??????1??1?0?????????????1????11?201????000210??10?1?01??00

Deinonychus

???0002000011111010O?000000000000010100011O?10000100110?11???1???10??

00????101000?011031?110100?0???????1?????00???0??0???????1???00?0001001

1?1001??1101010110110000110200000000001212020001?1100101101101110112

00100?????0??0?1?11010?100?1?1201??????1?11110?10?101001?0???000110O?0

??1110000110l?1111120021Z?00100000101310000l?1?0?1000-

1110012101012?0012120001021010-

0101011111111000101011l2?201?000002011010000010?101101011000

Dromaeosaurus

??????2?0??1?1?1??10???0???0?0??????????11??10000l???????0-

111111?????0????????0?0001031???0?0??0010001000?00?00101?1010111010100

000000010010111010111010101l0?00110010?0000000000?????????????0?????

??????0??

??1????????????????????

??1????

Mahakala

??10?00?????????

????????????????????????????????????001??????????1?01????????????????????

??401??0??0

?1?1??10?2?????1????????????????????????????????????1??????1110?0??????????

?2????????10?????00??2??11?1??????0-

11100??????????????????????????????????11??110??????????????????00??01????0

00?10?10??0?01????

Microraptor

0100?01000??1??????0??00????????00?0????????1??0??????????????????????0??

??????????????????????0??????????????????????????????????????0?00010??????01?

?1??????010???1?01--

210?0000?0????2???011?????????0?100?0?1?00??014???1??10?1?1??1--1-

0?1??2011?01101??0????1??1111011???0??11???00??11000000101?0??0?2?02??

100100000?111?11??1?1??????0-

011?1?21110?2001131?0?01111101O?1?????11?1111??10?0?????????0?0???01???

1000010?11?01?11?000

Saurornitholestes

??1?????????????????1111?????????

????????????1?????????????????????????????????0??????????00??0???0??0????????

??1???????1??0?110?00000?000012121200010111?10101110111011 20??0041101

0??0???1??1??2?????1101????????10?????????????????1?00101?00???1?0000?10

??111102002???00100000112310100??100110111001 00???????????0??1???0?0??0

??????????????????????10111 2?2010010011011001001210?101?0?011?00

Sinornithosaurus

??00001?000?1111?100??000001???0?0?0?10???0000000100110??11111001?0?

00102010???00?010??????????0??????????0????????????????????00000010011

0??0?0?1????00?10101000110?00000?0000?????????1?????????1??????????????

4????0??0???1?????2???????????01??1110110?10?10110?????????1????0?????0?

00??1???????2?0??2?00?0000??01??1??01?0??????0-

11??0?211??1??01131???01121101O?1?????????1?????????????????????0??11???0

000?10??1??1?01??00

Tsaagan

???10020000?11010?101100000000000000001001?00100001001????0-

11110110O?0012000010000000103????0?0000010011010?01100001100O0??12101

000000000100101110101110?010?10101000110200000000000????1??0?1????????

??1??????????

??

??

??

Unenlagia_plus_Neuquenraptor

??

??

??????????????????????????0?????????????????????????1101110112?0?01?010?0????

???????????1?????????????????????10?110?00110?11?????????????????????????????

??????????00???10200110O1?1?011000-??111?2111012000121O?0011????11010?

01111210100010?????2?2?????????????????????0?????1???????

Utahraptor

???000?10?01???????0?????????000????????????????????????????????1??10???

??

?????????01?0000010???????0??????20200?1?111?1010?1100?10??2???00?00?1?

???????1010?100?????????????????111??

??????????????????1????00???????1?00???????1???????????2?0??01??2??1?000

?0101011010001??01?12?2??????????????????????????????????

Velociraptor

???00020000?1111011011000000000000001100110000?000100110?10-

11111010000?000???0?1?0000010?1?1?0100?0??001?01??01?001??00?00??121010

000000001001O?1?0?01110101011O?11000110?000000000012???2000101l??????

111011?01??0??1?501010?10?1?1??1??????1?12011001?01010110?10?111001?0?

?0?001100?0??1?10?00??0???????200??2?00100000101301100l?100?0000-

011000211101100012102001021010-

0111???11?11?0001010?1???????0000?201???1000?10010111?011000

Byronosaurus

???000110000100011?10110000001000000000100??000?????20111O?0-?0?????????

??????????????????????????00?11?????0?01100111?010??1101011?00000020001?

??????????????101?01002--

2102000101?10????0??????????10111?????0??????????????0??????2??????????

??

??????????????????????????????1?????????????????????????1??????????01??2?

????0?????????????????????????1????

EK_troodontid

??

??????1??11??????????0?????0?????????????0?1???1?0??01??????????10???0???

1?????????????????1???0?????????0??

??10?001?0??????

?20?????0000?????????????????????????????????????0????????????????????????

??????????????????????????????????00?00?1?0???11????

Mei

???0001101l?0?-??0?0?1200000?00000000100??01-111?000111O?0-

110?00??0??01000??????10?11??????????0?????????????110?????????????????00

?00210????100???1???????10?0??002--1????00????1101?2011100---

10101??00?0011?10?1140?01??10?1??002--0-

001??20?????111?10110100110100010?11?011????????????????????????????????

??000001????2-00??10010000-

0110000??10020101?10??0??20??10?10?01?11111100011???????2110??01120110

?00002??1?10112111???

Microvenator

??

??212?00?????????????

??????????????2-

-??2????-???11110?0?01?10???01?011000??0?21??11?0??????1???1??0??2?1????

???????????0001??00?0?0?1110??0?00100000????????0??0???????????2???0010?

000101010100l??1011000-

0??00??10101??20??????0?????????1??111012101100l000???2?2?100000120110

1??00???????????????00

Saurornithoides_mongoliensis

???1??11000???10??1????0???0???????0????????1?????????????????????????00??

??????????????????1?01????0?11??????1???????????0??????011?10?002000???????

??1????10??0?00??0101?10003?101??????????1?????????????????0?0??????01??

0??????1??

???????????0????????????????????????????????????1?1??0??2103001020000-

0??????11?1110?????????????????????????????0???????10???11????

Sinornithoides

??????1?000?????????1??0?00????????0?????????????00???????0-???????0???0??

??1???????0??1??00?00200?????????

??????10??0?00??010??100???101???????011??11??????1?????????????????????0

?10?1?1??1??0???1?12?10?????1?10110?00?1??01???????0?1?????????10?001?0

????????2?0?????0?0000????????001?1??????0-

1???0?0???01??00?310?00?0210?0-?1??????1??110?????????????????0?????????

000?0?10?011?111?00

Sinovenator

???10001010?0010?11011100??1?000?0?01???11????0?0????????0-????00?????0

1????????012011??????????00?0010???000?100??10?1???11011001?0?002000?0

?1?0?0?????00??101?0??0110??00?001?1????1?201?0??0??????01100???0?01???

?401?00?10?1?1??2??0??????1??????????10110?10?101?????????????????0????10

?001?????????????????????0000??????11????1??????0-

11?00?21110???001310?00112100l0?10?011111111000l1?11?12?21100?10??01?

??00???00?101?1?11??00

“Troodon”

???0001?0?0?10?01110?100000?10?????0?????????????20?11??0-?000001??000

1?00??00??1?01030??1?11??0001100??00101100100101011101001111?00210??

?????0???????0??101?0?00101?10203010?1?2110201l1?1111101011101l??0?010

10150101 0??0???10120?0??????2?1?????????????100110??01?0?10?011????0???

??0?001?0????????2??????001??????0?????????????????????????010001??0??2??3?

?1?21000-0?0001111211100l?001101?2?10100012011 0?00???0011101l?11????

Epidendrosaurus

??0100?0??????1??00?????0???

??????????????????????????????????????0?????????????????????2100000100?1?00?

10???0?????????????????1?????????????????????????????0?00?0?0?01???13???0??

10?1????10?0???1?1????1??????101?????1?0110?2????00?0?0??1?1?110???0?1?

1?????2?0?????000001?????0??0?1?????1???????0?000??????0?00??2????2?0?0?

?1?????2?2?0100????0??????0?????????????1020??00??0?00????

Epidexipteryx

??-??????????????????????????????0???????????0000???????0?0??00?????01?1

???????00?0??1??00??00????1?00??

????0????0??11002???011?2???00??????????0????????0??00?0???0????14????1?

20?2????1??2????????10?1?????1?1???0?100?1002????0000????1?????????0????

?????2?0??????00001?????0??????????1???????0??00??????0?00102????210?0??

1????????1?????????????????0?????1??01???11102????0??0?????00

Apsaravis

?????0????0??????????????????0??

??????????????????????0????????????????????????????????????002???1?0??????????0

?????0?1?????????????????????????1??21?1111??????0???????0?0???0?501010?30

?2?100???2???????0???1???103?10-

1101101040????????111??0??1111?0????????????2?????????????100012?????10?

??????1?????312???2000000000?1?22000???1?1?12???010???1???????????0??11?

??1???1{12}10-00?100?0?00??00

Archeopteryx

011??0100100??10???0???0?010?0??0??0????11??110?0000?0-

1?0-?1000??0??000???0?0?000000-?1???12???00?0???????00?100???????????101

200?000000?10000?1?0?020??0010010?00?002-

-?10012?00011?????01??0?1?????????00???0?????0?4????0?20?1?1??1??2???1?1

1000?1??01?1010-?10?11111020????001?0??0??1?10?00??0????????2?0???2??0000

000?002??1001?1?0????0-

01100?2?1?11??00131000010?2101001?????11?111000?0?0????????00?00??0???

?11?0?00?00??0?01????

Confuciusornis

011???1?0000???????0???0?110???????0????1???1?00??0?????10-??0?0?10??000

?????0?00001?????????0??0?????????????1?????0?????????????0010000010?1?

000?0???000?11-????1?????2?????????????????????0?????????0100???1?????0?5???

?0?21?-?1?????????????011?21?010?0?????0?1111402O????1111???0??1?11?00??

0???????2?0?????000000??002???0?1?1??????0-??100?30-?1???00101????1?2110

11?11????2??1?10???0?1????????01??1??20???11?0?01?10??0?00????

Jeholornis

??????????0?????????????????????????0????????????????????????????????????

??????1??0??10?????00?????????????????

????????1?????1????????2?????????????????????????????0?????2?????3???1???0?

2?2???1???????????0???????1?????1??1011{04}0????????1?1??????110?0???????

????2???????000000??012?0??0??1?????????????????????????????????????1??1?

???

Rahonavis

?1???0??0??????????0?????????????????????????1?????????????????????????????

?????????????????????0???

???????1?????????????????0?????????0????????????1110???????????510?1??20?

1?11010?2?0?1?12?????????????????????1?????2???????111?00?????????????????

????????00??????10201110 01?10011000-0111002110112-

0013100?011?2101101 0?01121--

1100010?01?12?2110100012011 0?0000?11?10110?0110??

Sapeornis

??????0?010?1?1??0?????0???????????0???????????00?0??????0??1??0?1???000

0???????????0??00?001??0??1??0

??0??00????0??0?002???????????0???????2???0????????????????????????6???1?

?3????0??00???????????0????1??0?1???0??101141????????110?????1111?0?????

??????2???????010000??012?2?????1??????0-

0?10??3111102?1?10100????1?001101?????????????0??????????1????11??11???1

1?01?0?100?0?00??00

Yixianornis

1??????2?0?0?????????1?????????????0??????????1?????????????????????00???

?????????1?????????????????0?????????????????????????00??00??0???1??0??

?????????0????012???1?0?????0???????0???111??????0???0???0?2?????7???0??3

1?-????00?2?????????1?11?0003?1???1??10114????????110?????0111?0???????

????2???????01000???000?2?????1??????0-

1?1???312????2?1?031000???20?01?010????21??1?0????????????1?????1?1?????

1{12}?01????0????00??00

Nemegtonykus

??

??

??01???????0?1?01?02?1???01{

01}02110010?001?00??0???????1000-

100?010??111??012

0?111?0???3?????????????????????????????1??0112?{12}?0100010011?1212111??11

1{12}?110?1{12}???001??000????00

국문초록

마니랍토라(Maniraptora)는 현생 조류를 포함하는 다양한 수각류 공룡이 속한 계통군(clade)이다. 오늘날의 매우 높은 다양성과 비교하면 마니랍토라류의 화석 기록은 그만큼 많지 않다. 그럼에도 불구하고 현대의 이 계통군에 대한 이해는 중생대의 마니랍토라류 화석에 의해서 획기적으로 깊어질 수 있었다. 백악기에는 마니랍토라에 속하는 주요 계통군들이 수많은 종으로 분기하였는데, 고비사막은 이러한 공룡들이 산출되는 대표적인 지역 중 하나이다. 2008년 한국-몽골 국제 공룡탐사팀은 몽골 남부 고비사막의 알탄울(Altan Uul) III 지역에 노출되어 있는 후기 백악기(마스트리히트세) 지층인 네메겟층(Nemegt Formation)에서 수각류 공룡의 화석 여러점을 발굴하였다. 이 화석은 여러 수각류 공룡 개체들이 모여있는 표본으로, 그 중 두 개체에 대한 연구 결과가 본 학위논문에 수록되어있다. 이 두 개체의 여러 해부학적 특징을 기존에 알려진 다른 분류군(taxon)들과 비교하여 이들이 각각 오비랍토르과(Oviraptoridae)와 알바레즈사우루스과(Alvarezsauridae) 안에 속하며 아직 알려지지 않은 분류군이라는 것을 밝혀내었다. 그중 오비랍토르과에 해당하는 새로운 분류군에는 *Gobiraptor minutus*, 알바레즈사우루스과의 새로운 분류군에는 *Nemegtonykus citus*라는 학명을 붙였다. 지난 수십년 간 몽골 고비사막의 후기 백악기 지층에서 산출된 여러 오비랍토르과와 알바레즈사우루스과 공룡들이 보고되었지만

네메겟층에서는 단 한 분류군의 알바레즈사우루스과만 알려져 있었다. 게다가 알탄울III에서는 과(family) 수준까지만 분류된 두 오비랍토르과 표본을 제외하면, 오비랍토르과나 알바레즈사우루스과에 속하는 속 또는 종 수준의 분류군이 전혀 보고되지 않았다. 따라서, *Gobiraptor*와 *Nemegtonykus*는 각각 알탄울III에서 처음으로 보고되는 오비랍토르과와 알바레즈사우루스과의 분류군이라고 할 수 있다.

본 학위논문에는 *Gobiraptor*와 *Nemegtonykus*의 자세한 기재와 함께 이 분류군들과 가까운 유연관계의 분류군들과 비교 내용이 포함되어 있다. *Gobiraptor minutus*의 완전모식표본(MPC-D 102/111)은 불완전한 머리와 몸뼈 일부로 이루어져 있다. *Gobiraptor*는 고유의 해부학적 특징 조합(주로 아래턱과 미추의 특징)을 갖고 있어 다른 오비랍토르과의 공룡들과 구분된다. *Gobiraptor*의 가장 두드러지는 특징은 아래턱에 있다. 아래턱 앞쪽에 두껍게 발달한 symphyseal shelf와 이에 후방으로 연결되는 두 lingual shelf, 그리고 각각의 lingual shelf에 발달한 여러개의 작은 occlusal groove와 하나의 긴 lingual ridge는 다른 오비랍토르과 공룡에서는 이전에 보고된 바가 없는 특징이다. 먹이 활동과 직접적인 관련이 있는 턱의 구조가 독특하다는 점은 *Gobiraptor*가 다른 오비랍토르과 공룡들과는 다른 섭식전략을 갖고 있었을 가능성이 높다는 것을 보여준다. 위의 특징을 고려했을 때, *Gobiraptor*의 아래턱이 단단한 음식을 부수는데 적합한 구조임을 유추할 수 있었고, 이러한 음식에는 씨앗이나 이매패류가 포함되었을

것으로 추정된다. 또한 오른쪽 대퇴골 중앙 부분을 잘라 만든 뼈박편 시료는 이 개체가 사망 당시에도 빠르게 성장 중인 어린 나이였음을 보여주었다. 한편, *Gobiraptor*의 계통 분석 결과에 따르면 이 분류군은 오비랍토르과 공룡 중에서도 상당히 분화되었으며 네메겟 지역의 다른 오비랍토르과 분류군들보다 중국 남부의 감주(Ganzhou)지방에서 보고된 세 종의 오비랍토르과 분류군들과 더 가까운 유연관계에 있다. 게다가 이 계통 분석 결과는 네메겟 분지에서 일어난 오비랍토르과의 분화가 동소적 종분화과정(sympatric speciation)을 나타내지 않는다는 이전 연구의 가설을 뒷받침해주기도 한다. 또한, *Gobiraptor*가 네메겟층에서 산출되어 최소 세 오비랍토르과 분류군이 습한 환경에서 퇴적된 네메겟층에 존재하게 됨에 따라 네메겟 분지의 오비랍토르과 분류군들이 메마른 환경을 선호한다는 이전의 가설이 맞지 않다는 것이 더욱 분명해졌다고 할 수 있다. 그리고 *Gobiraptor*가 새로 명명되면서 네메겟 분지의 오비랍토르과 다양성이 한층 증가하였다.

*Nemegtonykus citus*의 완전모식표본(MPC-D 100/203)은 불완전한 몸뼈들로 이루어져있다. *Nemegtonykus*의 전체적인 해부학적 형태는 다른 알바레즈사우루스과에 속하는 분류군들, 특히 그중에서도 파르비쿠르소르아과(Parvicursorinae)에 속한 분류군들과 유사하다. 하지만 *Nemegtonykus*는 다른 알바레즈사우루스과 분류군들과 구분되는 고유의 특징 조합을 갖고 있는데, 주로 골반과 뒷다리의 특징이 포함된다. *Nemegtonykus*의 가늘고 긴 뒷다리는 이 분류군이

다른 파르비쿠르소르아과 분류군들과 같이 빠르게 달릴 수 있었음을 암시한다. 특이하게도 *Nemegtonykus*의 대퇴골 비율은 다른 비조류 수각류 공룡들보다는 땅 위에서 서식하는 조류에 더 가까운데, 이를 통해 *Nemegtonykus*의 대퇴골이 조류와 비슷하게 수직보다 수평에 가까운 방향을 향했다고 추정해볼 수 있다. 이와 함께 미추와 장골, 그리고 뒷다리 뼈들의 특징들은 *Nemegtonykus*의 보행이 원시조류에서 나타났을 법한 초기 형태의 조류형 보행 방식(골반보다 무릎을 주로 이용하는 보행 방식)과 닮았을 가능성이 크다는 것을 시사한다.

*Nemegtonykus*의 계통 분석 결과는 이 분류군이 파르비쿠르소르아과 내의 계통군들 중 하나인 모노니키니(Mononykini)에 속하며, 알바레즈사우루스과에서 가장 분화된 분류군들 중 하나임을 보여준다. 또한, 같은 계통 분석 결과에 따르면 *Nemegtonykus*가 중국 북부의 내몽골에서 발견된 *Linhenykus*와 자매분류군(sister taxon)이며 같은 네메겟층에서 산출된 *Mononykus*보다 *Linhenykus*나 자독타층(Djadochta Formation)의 *Shuvuuia*와 더 가까운 유연관계에 있다. 이러한 결과는 *Mononykus*와 북미에서 산출된 *Albertonykus*가 자매분류군이라는 결과와 함께 모노니키니 분류군들의 관계를 해석하는데 어려움을 준다. 지금까지 네메겟 분지에서 알바레즈사우루스과 분류군들의 분포는 대부분 건조한 환경을 나타내는 두 풍성퇴적층에 국한되었고, *Mononykus*의 완전모식표본 한 개체만이 하성퇴적층인 네메겟층에서 발견되었다. 하지만 *Nemegtonykus*가

네메겟층에서 발견됨으로써 습한 환경에서도 알바레즈사우루스과 분류군들이 다양하게 존재했을 가능성이 높아졌다. 또한, 이 학위논문에서 *Nemegtonykus*가 새로 명명됨으로 인해 네메겟 분지가 알바레즈사우루스과의 다양성이 세계에서 가장 높은 지역이 되었다.

주요어: 공룡, 마니랍토라, 오비랍토르과, 알바레즈사우루스과, 백악기, 네메겟층, 고비사막, 몽골

학 번: 2016-29125